February 2013

Geographical, Geological, and Hydrogeological Attributes of Formations in the Footprint of the Eagle Ford Shale

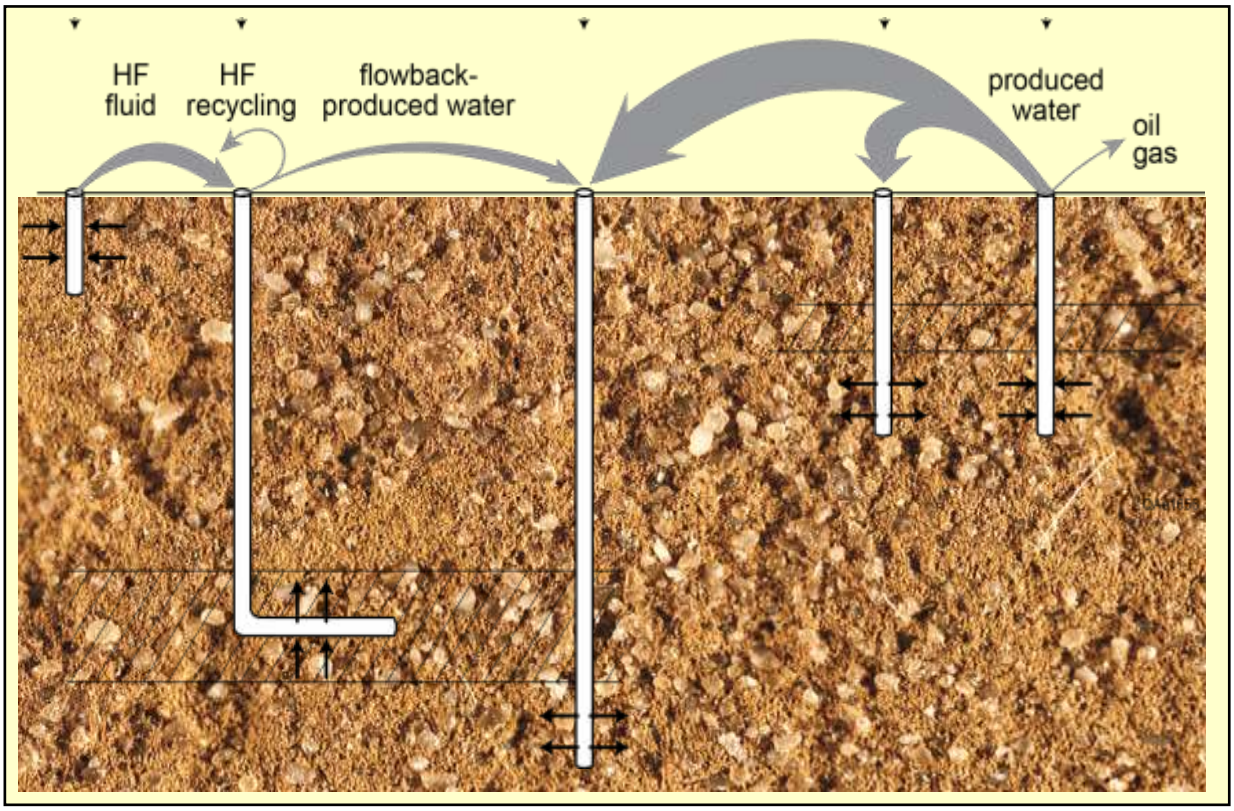

Prepared for:
Houston Advanced Research Center
Houston, Texas

by
Jean-Philippe Nicot, Ruth A. Costley, and Yun Huang

Bureau of Economic Geology
John A. and Katherine G. Jackson School of Geosciences
The University of Texas at Austin
Austin, Texas 78713-8924

Cover page photo credit: David M. Stephens; hand sample of Carrizo Fm. sandstone (Bexar County)

Geographical, Geological, and Hydrogeological Attributes of Formations in the Footprint of the Eagle Ford Shale

Jean-Philippe Nicot, Ruth A. Costley, and Yun Huang*
*** currently at Schlumberger Water Resources, Tucson, AZ**

Bureau of Economic Geology
John A. and Katherine G. Jackson School of Geosciences
The University of Texas at Austin
Austin, Texas 78713-8924

Executive Summary

This document presents an overview of mostly geological characteristics of formations in the footprint of the South Texas Eagle Ford (EF) Shale play with a focus on water. The ~25-county EF play has seen a dramatic development in the past few years and it keeps expanding to additional counties towards the north of the play. However, the EF area is not new to oil and gas exploration and production. At least 110,000 wells, not including the ~5000 EF wells (as of March 2013), has been drilled in the EF footprint during the past century, many of them still active. The EF shale is actually a source rock and has supplied oil and gas to reservoirs such as the Big Well and Pearsall fields and the very large Giddings field. Most of the EF lies in rural areas but several large cities (San Antonio, Laredo) are located at its edges. The document focuses on those two key aspects of hydraulic fracturing (HF): water use and water disposal. The South Texas location of the play with its scarcity of surface water resources exacerbates perceived conflicts with other water users.

The large depth of the folded Paleozoic basement below the EF (>15,000 ft) allows for a thick sediment sequence of Jurassic and younger age. The EF shale is positioned towards the middle of the sequence (~4000 to 11,000 ft deep) leaving many formations between it and the ground surface, particularly the thick Midway Clay, and providing several horizons for disposal of fluids. EF's thickness varies from ~100 ft East of Austin to >500 ft at the Mexican border. The sedimentary sequence on top of the basement is initially carbonate-rich with platform carbonate formations such as the Edwards or Glenrose formations or the Austin Chalk , including the EF which is a carbonate mudrock. Toward the end of the Cretaceous the succession turned siliciclastic with alternating sandstones and claystones deposited in mostly fluvial and/or deltaic environments. Some of the sand-rich intervals of the succession compose the fresh water aquifers in the EF footprint such as the Carrizo aquifer and other aquifers of lesser water quality such as the Wilcox and Yegua-Jackson aquifers. Shallow subsurface water tends to be brackish outside of the outcrop area and of the Carrizo aquifer.

Water use was ~24 thousand acre-feet (AF) in the EF play in 2011. In the same year, the top HF users in the EF consisted of Webb (4.6 kAF), Karnes (3.9 kAF), Dimmit (3.7 kAF), and La Salle (2.9 kAF) counties. Although overall water use has increased, water use per well has decreased. The change is related to the switch by most operating companies from the gas to oil and condensate windows and the use of gelled rather than slick-water HF jobs. Currently operators recycle very little of the flowback / produced water but use brackish water (likely in the vicinity of 20% of total water use). One reason why recycling is minor to negligible is that flowback volumes are far from providing enough water for a subsequent HF operation, especially at early times. The median well produces ~25% of the injected volume after 6 months and ~40% and plateauing after 1 year. Flowback / produced water is actually disposed of in injection wells. Approximately 2500 Class II injection wells were active at least part of one year during the 2008-2012 period. Many are related to waterflood operations and not to disposal. Preferred horizons for disposal are the formations of the Navarro-Taylor Groups in the Maverick Basin, a multi-county area next to the Mexican border as well as the Wilcox and Edwards formations.

Table of Contents

List of Figures

List of Tables

Acknowledgments

Funding for this project is provided by RPSEA through the "Ultra-Deepwater and Unconventional Natural Gas and Other Petroleum Resources" program authorized by the U.S. Energy Policy Act of 2005. RPSEA (www.rpsea.org) is a nonprofit corporation whose mission is to provide a stewardship role in ensuring the focused research, development and deployment of safe and environmentally responsible technology that can effectively deliver hydrocarbons from domestic resources to the citizens of the United States. RPSEA, operating as a consortium of premier U.S. energy research universities, industry, and independent research organizations, manages the program under a contract with the U.S. Department of Energy's National Energy Technology Laboratory.

In addition, the authors would like to thank IHS Energy for access to the Enerdeq database.

Acronyms

AF	Acre-foot (1 AF = 325,851 gallons or 1 million gallons ~ 3 AF)
bbl	Barrel (42 gallons)
BEG	Bureau of Economic Geology
EF	Eagle Ford
EFF	Eagle Ford Formation
Fm., Fms.	Formation, formations
gal	Gallons
GAT	Geological Atlas of Texas
GCD	Groundwater Conservation District
GIS	Geographic Information System
HF	Hydraulic Fracturing
MGD	Million gallons a day
PBSN	Powell Barnett Shale Newsletter (now Powell Shale Digest)
RRC	Texas Railroad Commission
STEFF	Eagle Ford Formation in South Texas
TCEQ	Texas Commission on Environmental Quality
TDS	Total Dissolved Solids
TWDB	Texas Water Development Board
USDW	Underground Source of Drinking Water
USGS	United States Geological Survey

I. Introduction

The present document is mostly a desktop study and represents a small component of a much larger project, the Environmentally Friendly Drilling Technology Integration Program (EFD TIP) headed by the Houston Advanced Research Center (HARC), Houston, TX (http://www.efdsystems.org/AppliedTechnology/TechnologyIntegrationProgram/tabid/2347/Default.aspx). One of the goals of the EFD TIP program is to improve the water footprint of unconventional shale development. Following the decision to perform field tests in the Eagle Ford (EF) Shale area, this report compiles information useful to site the testing area. The two major issues discussed in this document concern water availability and disposal. Developing shale formations for oil and gas production requires a significant amount of water (Nicot et al., 2011; Nicot and Scanlon, 2012; Nicot et al., 2012) through the process of hydraulic fracturing (HF). Once HF has been performed and while readying the well for production, some of the injected water flows back to the wellhead and need to be recycled or dispose of (Figure 1). This initial flowback period is followed by production of the so-called *produced water* which bears the characteristics of resident brines. Produced water is generally thought of as the water produced with hydrocarbons from conventional reservoirs. In this document we did not try to distinguish between flowback and produced water because their exact definition has not been settled yet and because, often times, we do not have the means to discriminate between the two as defined above. The document focuses on those two key aspects of HF: water use and water disposal. The ongoing drought and recent increased activity for shale gas/oil production in the Eagle Ford play of South Texas (~25 counties) have highlighted the need for better information on water resources. We collected available information on formation and water resources in the footprint of the Eagle Ford Shale. We also provide background information about geographical features such as topography, rivers, lakes, and other surface water sources (treatment plants, waste water…), as well as other factors that would impact oil and gas development. This is mostly a desktop study but we added synergetic information from other projects and results from discussion with operators as appropriate. Area of interest includes all or part of the following 42 counties (alphabetical order): Atascosa, Austin, Bastrop, Bee, Bexar, Brazos, Burleson, Caldwell, Colorado, Comal, De Witt, Dimmit, Duval, Fayette, Frio, Goliad, Gonzales, Grimes, Guadalupe, Hayes, Jim Wells, Karnes, Kinney, La Salle, Lavaca, Lee, Live Oak, Madison, Maverick, McMullen, Medina, Milam, Robertson, Travis, Uvalde, Victoria, Waller, Washington, Webb, Williamson, Wilson, and Zavala counties (Table 1).

The report is organized in the following way. We first present a short introduction to the Eagle Ford play and HF followed by a description of cultural attributes. Section II documents surface features and climate characteristics followed by a discussion of the geology and hydrostratigraphy (Section III) and of aquifers and their chemistry (Section IV). Next, we examine oil and gas production, current water use and fate related to production in the Eagle Ford (Sections V and VI). From a practical standpoint, figures in this report fall into two categories: those specifically developed for this report, mostly in ArcGIS, and those gleaned from outside sources—a judicious choice of maps and figures scanned (and referenced) from several public-domain and published reports and then adapted to suit this document.

South Texas has been the focus of oil and gas exploration for decades and its geology is relatively well-known. Many publications, peer-reviewed papers and reports, have been produced in the same time interval. We also made use of Nicot et al. (2010), a report on the

uranium geology of South Texas which somewhat overlaps with the topic of this document. The agreed-upon general scope of work is as follows:

- provide a general description of the stratigraphic column in the footprint of the Eagle Ford in terms of nature of the sediments, their depositional environment, and likely groundwater flow behavior. The work will not entail well-correlation efforts specific to the study.
- provide a description of water-bearing zones: alluvial aquifers if any of significance (fresh water), Carrizo Fm. (mostly fresh water), Wilcox/Indio, Queen City/Bigford, and Yegua-Jackson Fms. (mostly brackish), in particular in terms of capacity, salinity, and yield. Rely on published data (BEG, TCEQ, TWDB, USGS) and other data possibly available to us (operators, GCD's). GIS mapping of aquifers footprint and other attributes if relevant such as pump tests results. We will not undertake a specific study of geophysical logs to map salinity isolines.
- GIS-mapping of water samples showing likely formation, depth, salinity, ionic makeup, their use (domestic, municipal, irrigation, hydraulic fracturing) if known.
- GIS mapping of all oil and gas wells in the Eagle Ford with available attributes
- GIS mapping of disposal wells with available attributes

An ArcGIS data file is provided with the report, a summary of which is presented in Appendix A.

I-1. The Eagle Ford Formation

A subsequent section will present more details on the Eagle Ford Formation but we introduce it in this section. The formation of Late Cretaceous age forms a broad band along the coast of the Gulf of Mexico, extending across the Mexican border. It covers a large section of South Texas all the way to East Texas, where it meets the deltaic deposits of the Woodbine Formation of equivalent age (Hentz and Ruppel, 2010, Fig. 9). It lies below the Austin Chalk and is very likely the source of its well-known hydrocarbon accumulation. Located at a depth of 4,000–11,000 ft, the play is slightly overpressured (pressure gradient of 0.43 to 0.65 psi/ft; Vassilellis et al., 2010), making it more attractive because of the higher initial production rates. Most current interest is focused on the South Texas section of the Eagle Ford. The discovery well was drilled by Petrohawk in 2008 in La Salle County (PBSN, Sept 20, 2010). The EF formation produces natural gas, condensate, and oil. Earlier wells were vertical, located in Central Texas (Brazos, Burleson Counties), and looking for oil. The Central Texas play is somewhat disconnected from the South Texas play (from the Mexican border to Gonzales and DeWitt Counties) by the San Marcos Arch, a persistent higher-elevation structural feature. The Eagle Ford Shale contains oil updip, gas downdip, and gas and condensates in between. The "shale" is carbonate rich, up to 70% calcite (Cusack et al., 2010, p. 171), much higher than that, for example, of the Barnett Shale. Figure 2 illustrates the fact that the Eagle Ford outcrop total surface area is rather small. To enhance visual effects, in all maps produced for and presented in this document, we used the formation immediately on top of the EF, the Austin Chalk Group.

I-2. Hydraulic Fracturing

The past five years have seen an explosion of oil and gas production thanks to the combination of two technologies: (1) high-volume or massive HF and (2) horizontal drilling. HF was

developed several decades but until recently had been used only in tight formations (that is, with a very low permeability) to enhance the permeability of the (vertical) wells. The volumes used were less than 100,000 gal (~2400 bbls) (Nicot et al., 2011; Nicot, 2012). Commercial horizontal drilling debuted in the 1980's and by 1990, 85% of the 1000 horizontal wells drilled in the US were in the Austin Chalk in Central Texas (EIA, 1993). This formation with a low matrix permeability benefited from horizontal wells because they could intersect many more productive fractures than vertical wells. Then in the 1980's, the attention of some operators, in particular Mitchell Energy, now absorbed by Devon, turned to source rocks of the Fort Worth Basin. Tight formations, although with very low permeability, are still conventional reservoirs in the sense that oil or gas migrated from the source rock to accumulate in a trap. For example, the Eagle Ford shale sourced the overlying Austin Chalk and the numerous oil and gas reservoirs in the Fort Worth Basin including the Bend Conglomerate Fm. originated from the underlying Barnett Shale (Pollastro et al., 2003). In the 1990's, many Barnett (still mostly vertical) wells were completed with high-volume HF soon complemented by horizontal drilling the early 2000's. Then the technology spread to the Fayetteville Shale in Arkansas and the Haynesville Shale at the Texas-Louisiana state line, very soon followed by the Eagle Ford Shale in South Texas and the Marcellus Shale in Pennsylvania and West Virginia, then by the Bakken Fm. in North Dakota and Permian Basin Formations, which both include shale strata and tight intervals and actually represent new prospects for HF. The latter two areas produce oil in addition to gas and have become the current (early 2013) center of drilling activity along with the Eagle Ford Shale.

The focus of this work is on water. Millions of gallons of water are needed to perform HF. The water is sourced from surface water or groundwater but flowback / produced water from previous HF operations and used waters from industrial or municipal plants can also be used. In general, most of the flowback is injected into the deep subsurface through injection wells. The amount flowing back to the surface is variable but relatively small in the case of the Eagle Ford (Nicot, 2013). It follows that recycling is not sufficient in itself to sustain HF and that a significant amount of makeup water is needed.

I-3. Cultural Attributes

The South Texas Eagle Ford Shale play is located between several major cities and urbanized areas (San Antonio, Corpus Christi, Laredo, and the Rio Grande Valley), and, according to the 2010 U.S. census, the total population in the active areas of the play is approximately ½ million residents, not counting large cities. Population density ranges from very low (fewer than one inhabitant per square mile) in McMullen County (Figure 3) to that of large cities on the periphery of the study area. However, population density remains low along the main producing zones with no large cities but many small towns well connected through the road network (Figure 4). Population density, along with land use, can be used as a proxy for domestic and industrial water use and for groundwater well density in rural and suburban areas (they generally tap the shallowest aquifer).

Administrative divisions of interest include groundwater conservation districts (GCD) (Figure 5), regional water planning groups (RWPG) (Figure 6), and groundwater management districts (GMA) (Figure 6). Most of the EF footprint is within a GCD except Webb and Maverick counties and a small fraction of Gonzales County (as of January 2013) and includes two large multi-counties and active GCD's: Wintergarden GCD and Evergreen Underground Water Conservation District (UWCD) (http://evergreenuwcd.org/). The South Central Texas Water

Planning Group Region L (http://regionltexas.org/index.php) includes most of the Eagle Ford footprint in South Texas. So does GMA 13 which corresponds to the Carrizo-Wilcox aquifer and allied minor aquifers.

Table 1. Area and population of counties within the Eagle Ford Footprint in South Texas

County	Area (mi^2)	Pop. (2010)	Pop. Density /mi^2 (2010)	Pop. 2012 (Estimate)
Atascosa	1221.47	44,911	37	45,579
Austin	656.38	28,417	43	28,665
Bastrop	895.55	74,171	83	75,115
Bee	880.33	31,861	36	32,095
Bexar	1256.09	1,714,773	1,365	1,756,153
Brazos	591.24	194,851	330	197,632
Burleson	676.81	17,817	26	17,251
Caldwell	547.16	38,066	70	38,442
Colorado	973.69	20,874	21	20,816
Comal	574.88	10,842	19	111,963
DeWitt	910.49	2,444	3	20,255
Dimmit	1334.51	9,996	7	10,118
Duval	1795.60	11,782	7	11,669
Fayette	959.81	24,554	26	24,732
Frio	1134.35	17,217	15	17,400
Goliad	859.37	7,210	8	7,243
Gonzales	1069.85	19,807	19	19,904
Grimes	801.60	26,604	33	26,887
Guadalupe	714.78	131,533	184	135,757
Hays	679.92	157,107	231	164,050
Jim Wells	868.34	40,838	47	41,339
Karnes	753.55	14,824	20	14,946
Kinney	1365.12	3,598	3	3,630
La Salle	1494.23	6,886	5	7,001
Lavaca	970.44	19,263	20	19,347
Lee	634.10	16,612	26	16,666
Live Oak	1078.88	11,531	11	11,447
Madison	472.43	13,664	29	690
Maverick	1291.78	54,258	42	13,747
McMullen	1156.78	707	1	55,405
Medina	1334.53	46,006	34	46,367
Milam	1021.77	24,757	24	24,699
Robertson	865.35	16,622	19	16,740
Travis	1023.01	1,024,266	1,001	1,063,130
Uvalde	1558.63	26,405	17	26,535
Victoria	888.84	86,793	98	87,545
Waller	517.82	43,205	83	44,013
Washington	621.75	33,718	54	33,791
Webb	3375.59	250,304	74	256,496
Williamson	1134.44	422,679	373	442,782
Wilson	808.41	42,918	53	43,789
Zavala	1301.73	11,677	9	11,849
Total	43,071.42	4,796,368	111	5,043,680

Source: U.S. Census Bureau, http://quickfacts.census.gov/qfd/states/48000.html, last accessed February 2013

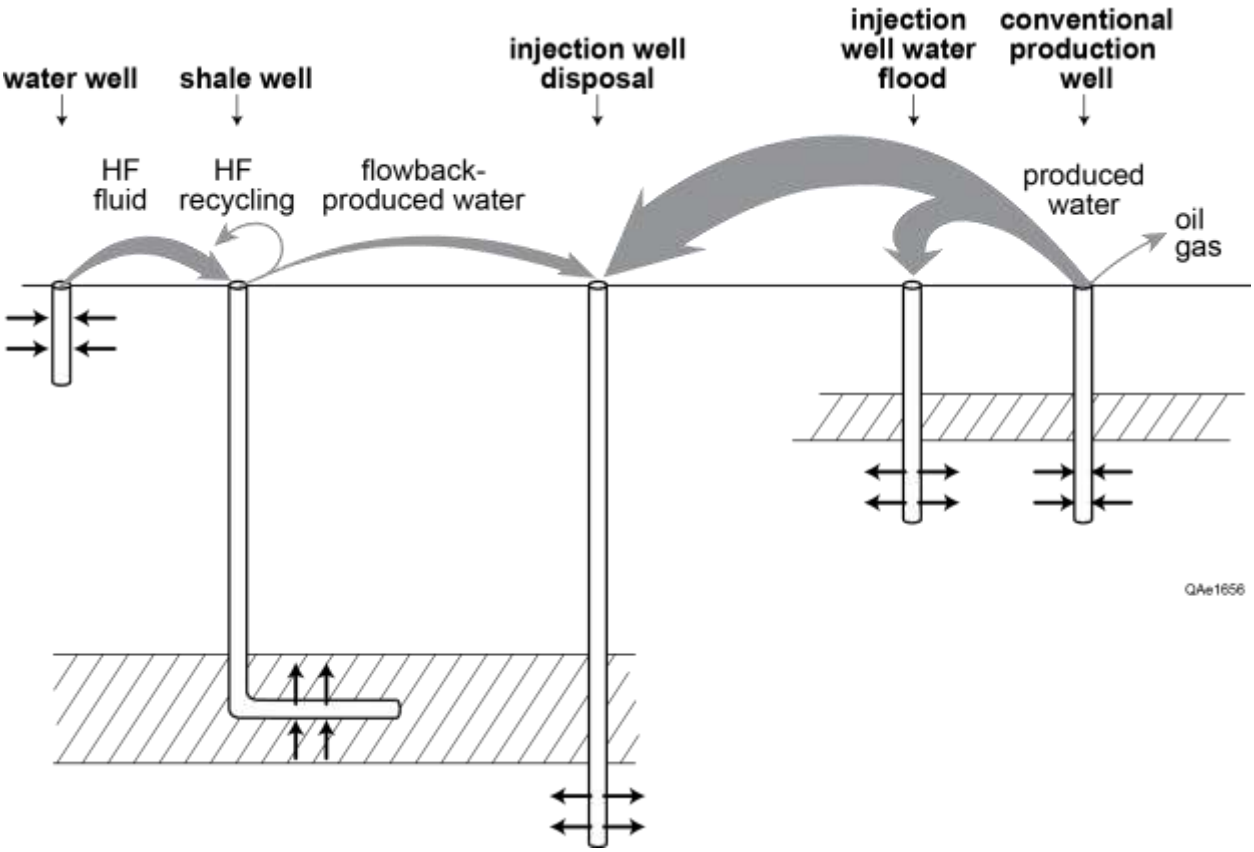

Figure 1. Schematics of water life cycle subsurface component

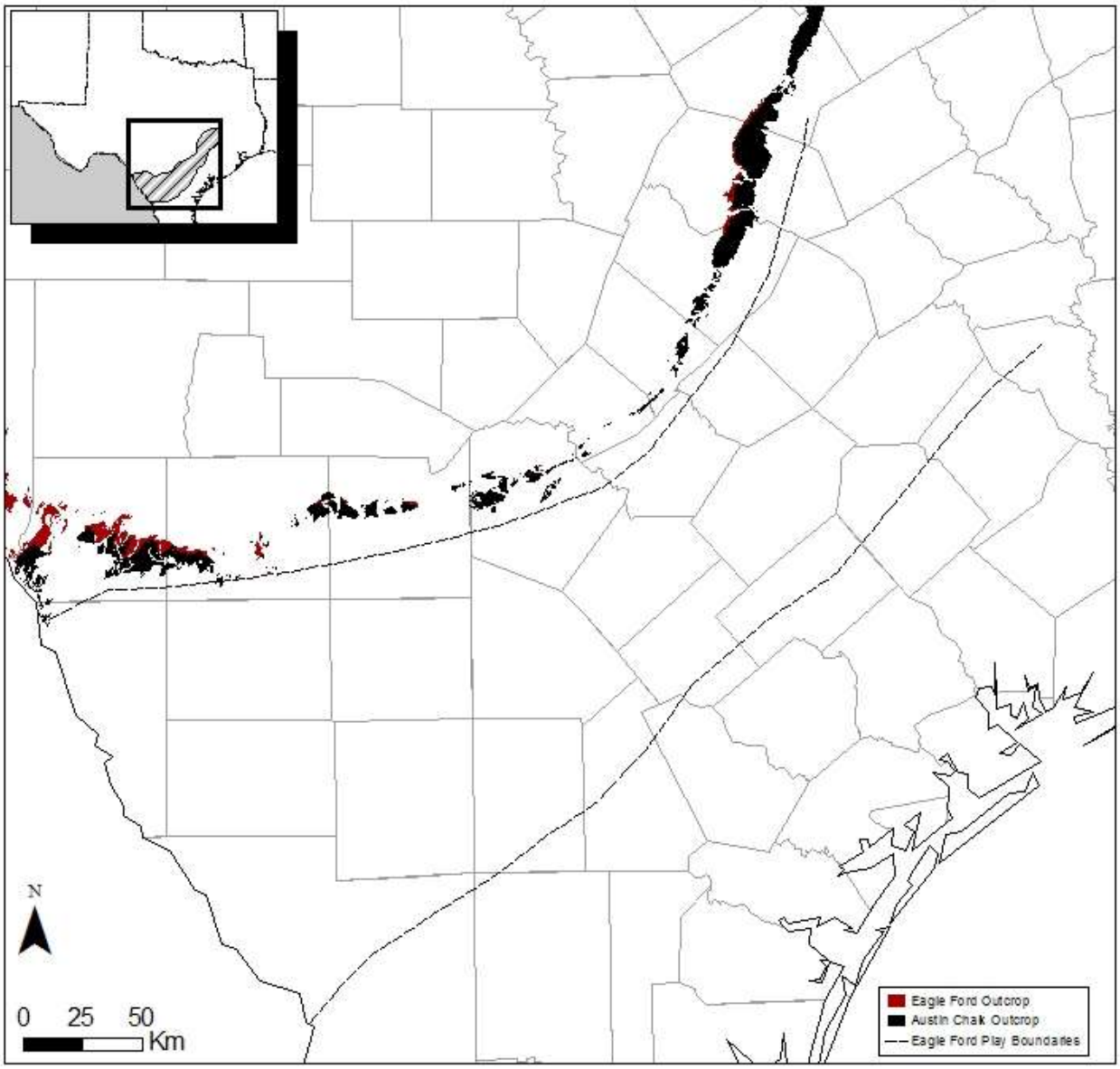

Source of outcrop outlines: GAT sheets
Note: Outcrop of the Austin Chalk group is also shown

Figure 2. Map illustrating EF footprint and outcrop.

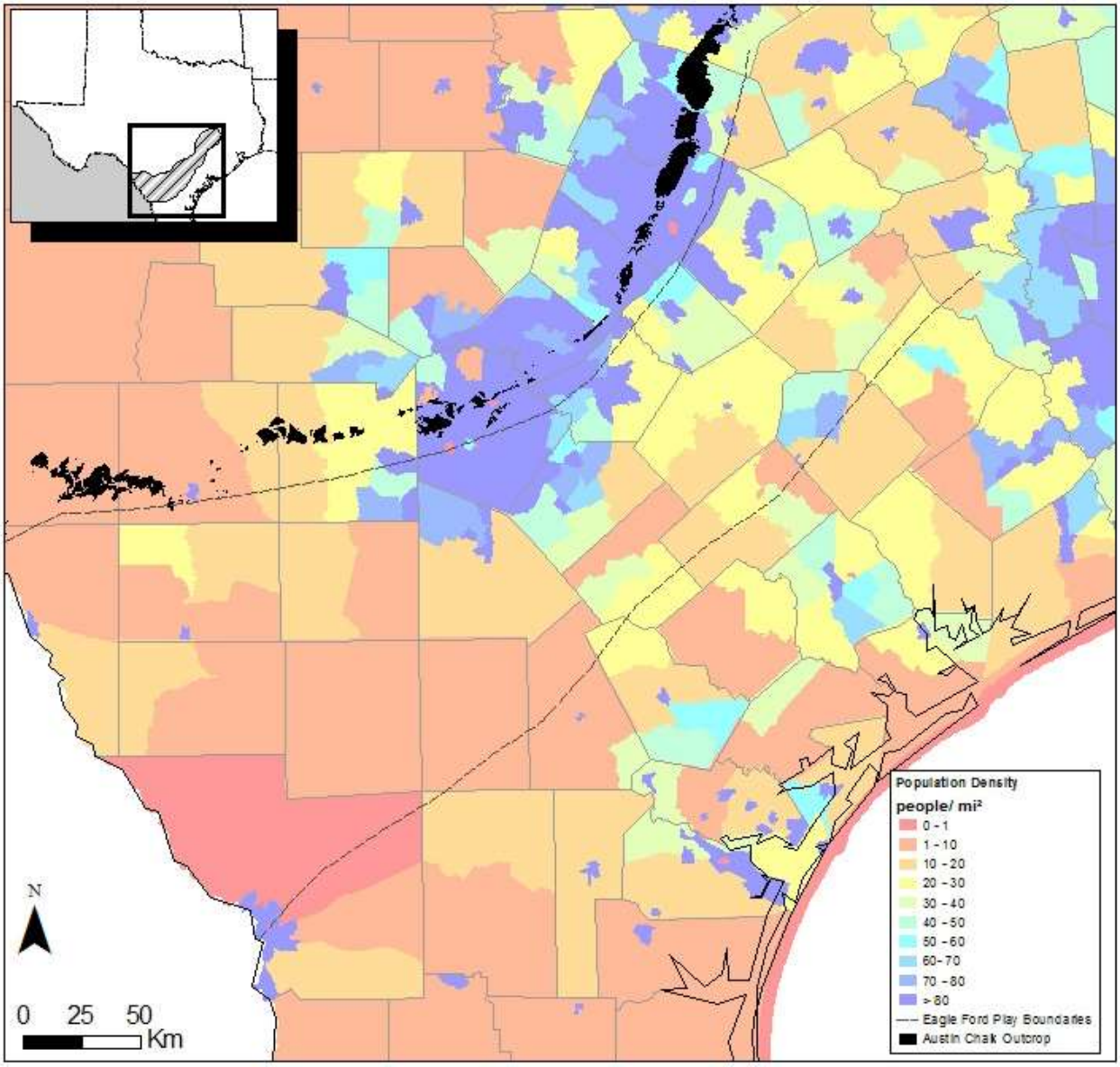

Source: U.S. Census Bureau (http://www.census.gov/) —data for 2010.

Figure 3. Population density for census tracts in Texas in 2010

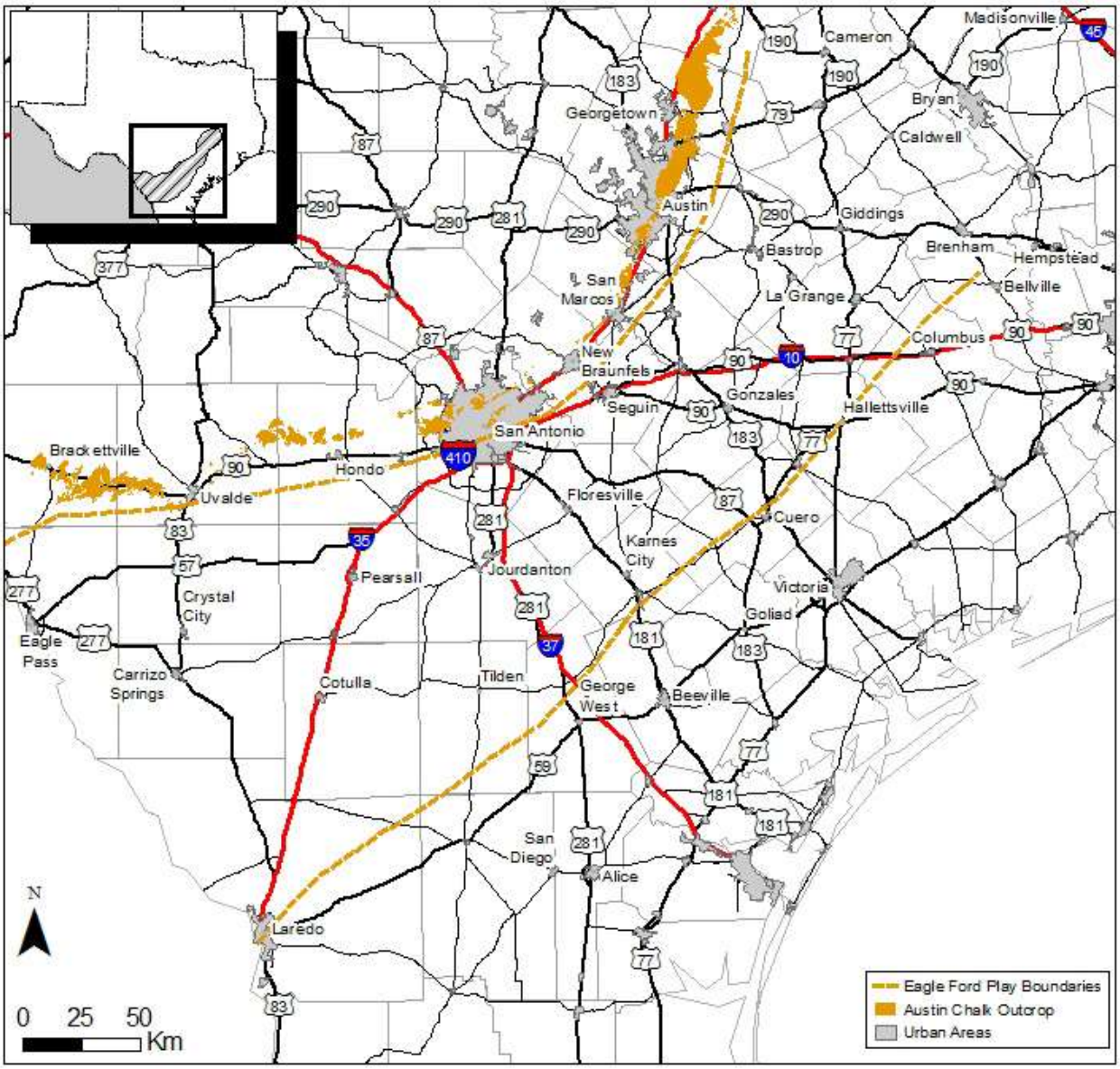

Source: TXDOT, http://www.tnris.org/get-data?quicktabs_maps_data=1

Figure 4. Major roadways and urban areas in south Texas

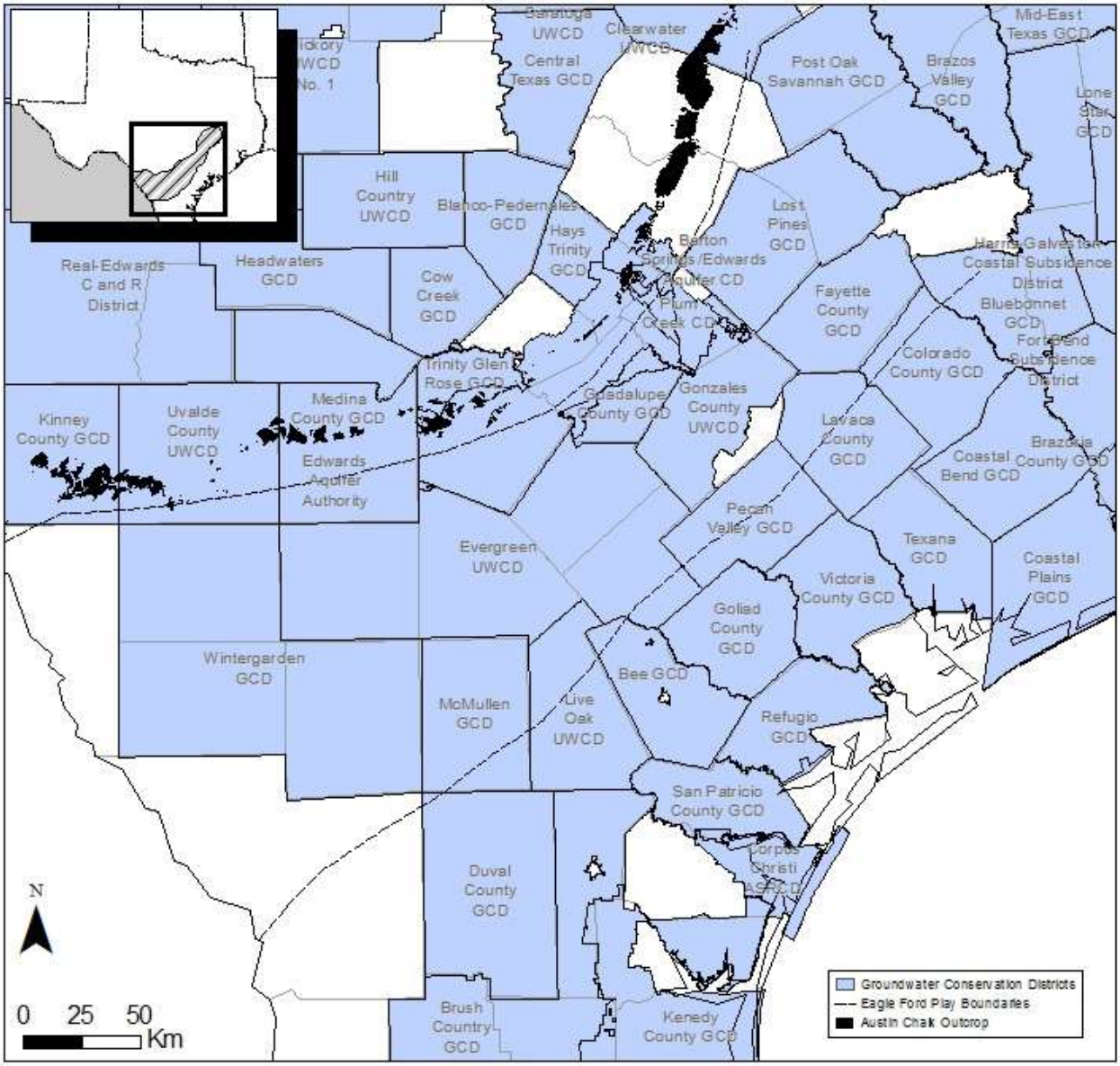

Source: Texas Commission on Environmental Quality (TECQ), http://www.twdb.state.tx.us/mapping/gisdata.asp

Figure 5. Locations of groundwater conservation districts in south Texas

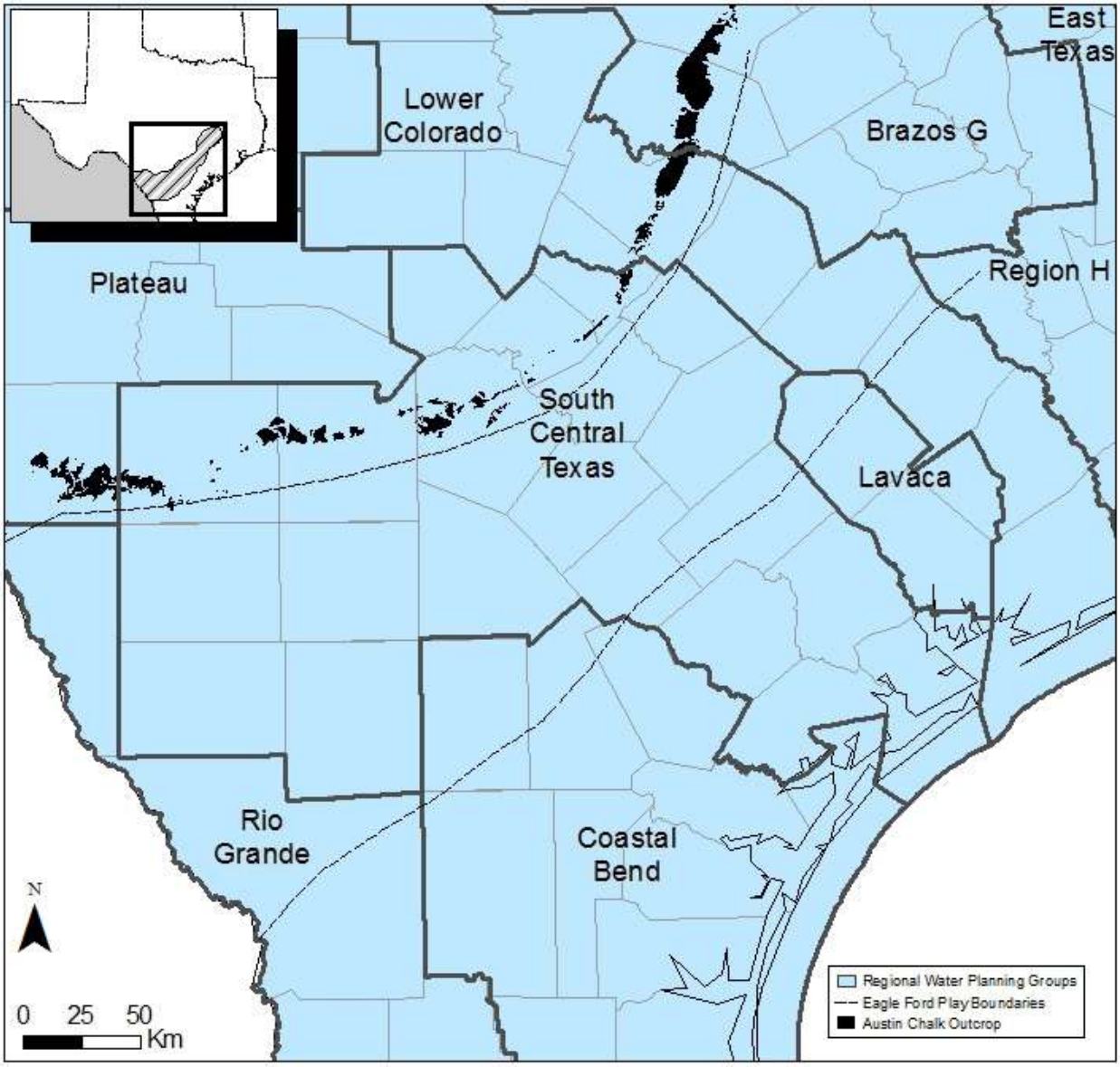

Source: Texas Board of Water Development (TWDB), http://www.twdb.state.tx.us/mapping/gisdata.asp

Figure 6. Location of regional water planning groups in south Texas

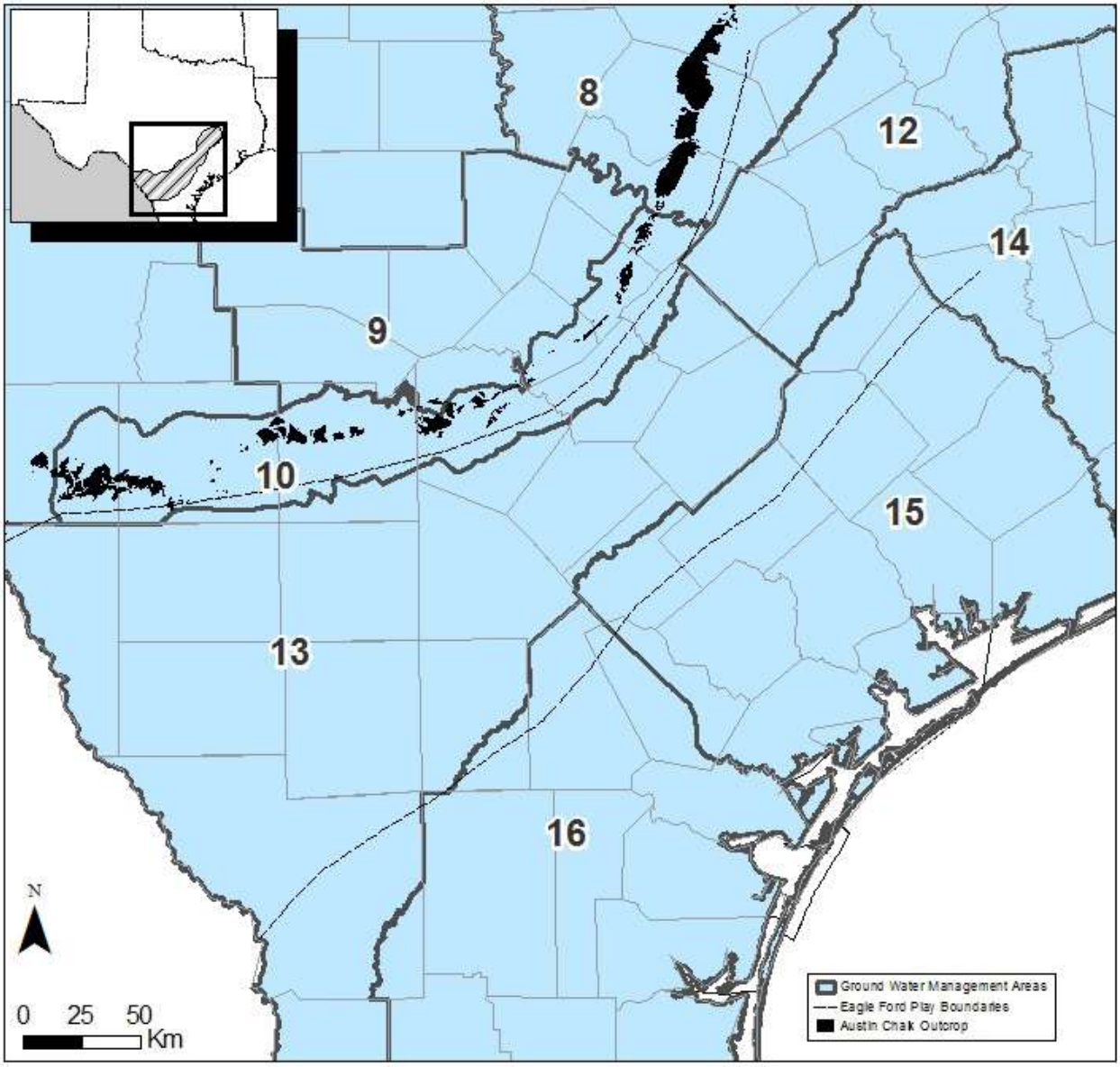

Source: Texas Board of Water Development (TWDB), http://www.twdb.state.tx.us/groundwater/management_areas/index.asp

Figure 7. Location of groundwater management areas in south Texas

II. Physiography and Climate

Physiography and climate do more than just set the stage. A discussion of the physical geography is important because it helps in understanding infiltration and recharge to these aquifers used by the industry and other users (are precipitations spread out during the year or concentrated in a few summer or winter months? what is the interannual variability?) and evapotranspiration (what is the natural landscape? What is the native vegetation? What is the current land use?). For example, recharge to aquifers is impacted by precipitation and the time of the year it takes place. Vegetation through evapotranspiration, in particular, and parameters such as rooting depth, perennial character, and leaf area index also make an important impact on recharge and shallow subsurface processes. Topography and river network are two factors controlling rejected recharge, i.e., groundwater that discharges to streams and does not move downdip into the confined parts of the aquifers (Figure 8).

The coast of the Gulf of Mexico forms a flat, low-lying, wide arc from Florida to Mexico. Topography of the lower Gulf Coast is relatively flat, whereas the upper Gulf Coast, including the EF footprint, generally has low relief (rolling plains) except where it is locally dissected by rivers and streams (Figure 9 and Figure 10; note the difference in scale and coverage). Elevations range from sea level to about 800 ft in the southwest of the study area. Ground surface elevations gently decrease from the southwest to the northeast and southeast. The gentle elevation decrease towards the Gulf coast is interrupted by resistant Tertiary sandstone outcrops, most prominently the Carrizo and the Catahoula-Oakville outcrops (Hamlin, 1988). The river valleys are broadly incised with terraced valleys that are hundreds of feet lower than the surface basin divide elevations (Hamlin, 1988). Three major rivers from south to north are: the Nueces River, which flows into Corpus Christi Bay, and the San Antonio and Guadalupe Rivers, which flow into San Antonio Bay southeast of the city of Victoria. The Rio Grande in the west and the Lavaca River in the northeast bound the study area. Rivers and river basins are shown in Figure 11. Knowledge of the river and stream network is important (1) because of permanent interaction between surface water and groundwater and typically alternating losing and gaining sections; (2) because rivers and reservoirs can provide water to operators for HF; and (3) because, conversely, they can also be contaminated by HF and other oil and gas activities.

The South Texas EF region encompasses many climatic regions, and its climate ranges from semiarid in the southwest to semi-humid in the northeast, with temperature and precipitation both varying significantly across this gradient. The climate there is classified as subtropical humid across most of the region whereas the northern and southern ends are classified as subtropical humid and subtropical steppe, respectively (Larkin and Bomar 1983). Overall the climate is warm and dry, with hot summers and relatively mild winters and subject to periodic droughts. However, the region is strongly influenced by its proximity to the Gulf of Mexico and, as a result, has a much more marine-type climate than the rest of Texas, which is more typically continental. A network of weather stations provides data to develop the interpolated maps that follow (Figure 12).

Mean annual precipitation across the region varies from less than 20 inches/yr at the U.S.-Mexico border to slightly more than 35 inches/yr toward the northeast of the study area (Figure 13). On average the wettest months are May and September, which tend to see more than 4 inches per month, and the driest months are January, February, and March, with approximately 2 inches per month. Most of the remainder of the study area follows the same relative trends

(Figure 14). USGS has published data summaries on extreme events (e.g., Lanning-Rush et al., 1998). The NCDC (National Climatic Data Center) publishes maps showing precipitation intensity during a given time period at a given recurrence interval (NCDC, 2009). A recurrence interval of 25 yr seems a good compromise for future activity in the EF. Across the EF footprint, precipitation intensity with a return interval of about 25 yr is 7 to 8 inches during a 24-h period, 5 to 6 inches (6 h period), 4 to 4.5 inches (2 h period), 3.2 to 3.5 inches (1 h period), and about 3 inches for 30 min period (Figure 15). Similar maps have also been published by the USGS (Asquith and Roussel, 2004).

Monthly mean temperatures range from 55ºF (mean daily minimum temperature of 42ºF) in January to 84ºF (mean daily maximum temperature of 96ºF) in August. Mean annual temperatures are between those two extremes and vary from 68ºF to 74ºF (Figure 16, Figure 17, and Figure 18). Pan evaporation ranges from 85 inches/yr in the southwest to 45 inches/yr in the northeast (Larkin and Bomar, 1983; Williamson and Grubb, 2001), implying a general excess of evapotranspiration over precipitation over much of the south Gulf Coast region. Average gross lake evaporation varies from 40+ to 70+ inches/yr (Figure 19). Net lake annual evaporation (evaporation–precipitation) is always positive and varies from a small value in the northeast of the study area to 40+ inches/yr in Webb County (Figure 20).

Major natural regions (Figure 21) depend on topography, lithology, and climate. The Gulf Coast prairies of the lower Gulf Coast run along the Gulf of Mexico. Trees are uncommon except along streams and locally on coarser sediments. Most of the EF footprint belongs to the so-called South Texas brush country. The region is blanketed with low-growing, mostly thorny vegetation. Where conditions allow, a dense understory of small trees and shrubs develops (TPWD, 2010). North and East of Wilson County into Bexar, Guadalupe, and Gonzales counties, the South Texas brush country transitions to oak woods and prairies and blackland prairies natural regions. The former consists of a cover of Oak and Hickory trees and savanna. The latter includes juniper-oak savanna and prairies. Both natural systems have been extensively modified .and changed to agricultural crops on about 75 percent of the area. These physiographic provinces are further subdivided into ecological regions (Figure 22). Outside of large cities, the EF footprint is mostly sparsely populated, and the land use / land cover map reflects mostly natural regions (Figure 23).

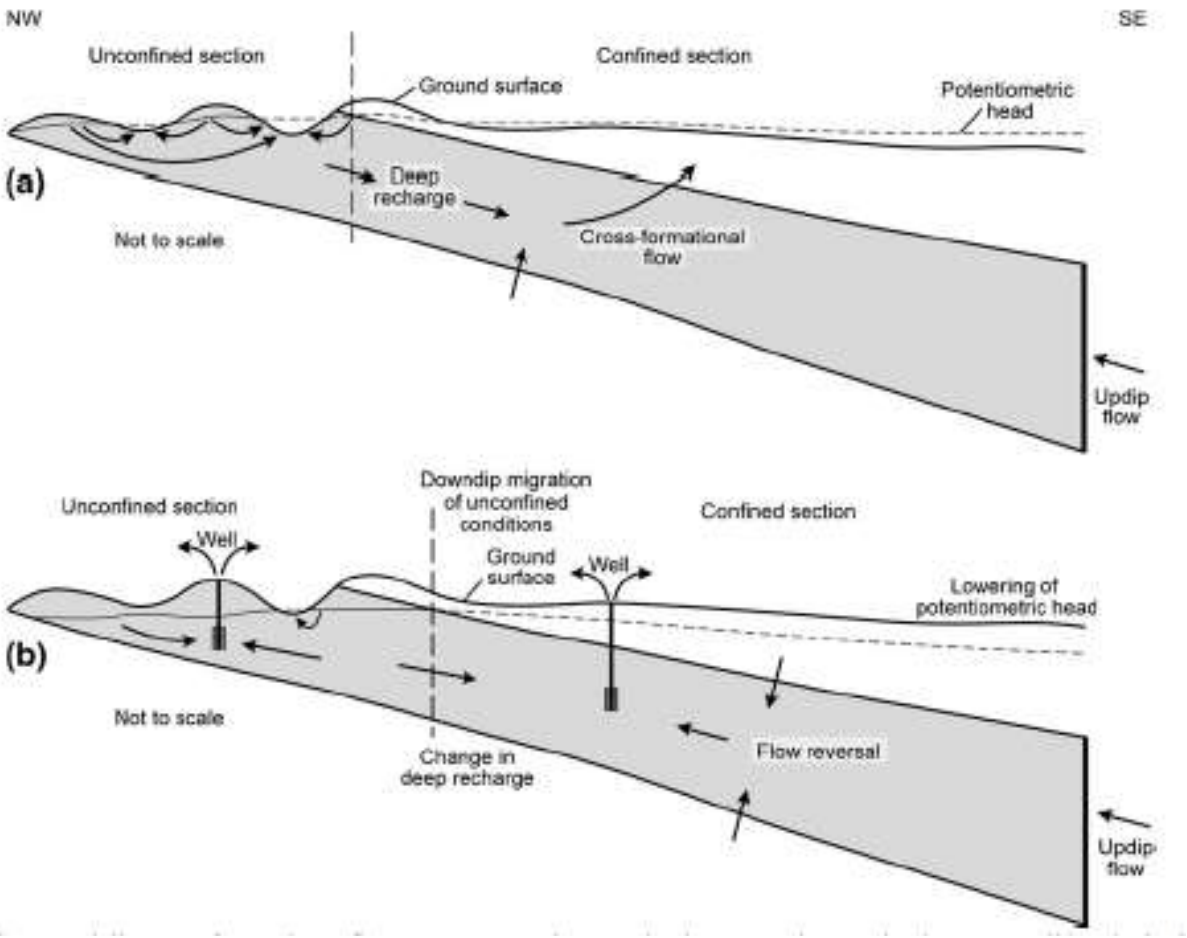

Source: Huang et al. (2012, Fig.3), Reedy et al. (2009, Fig.1)

Figure 8. Conceptual diagrams of groundwater flow components under (a) pre-development and (b) post-development conditions in the Carrizo-Wilcox Aquifer and other aquifers of the Gulf Coast

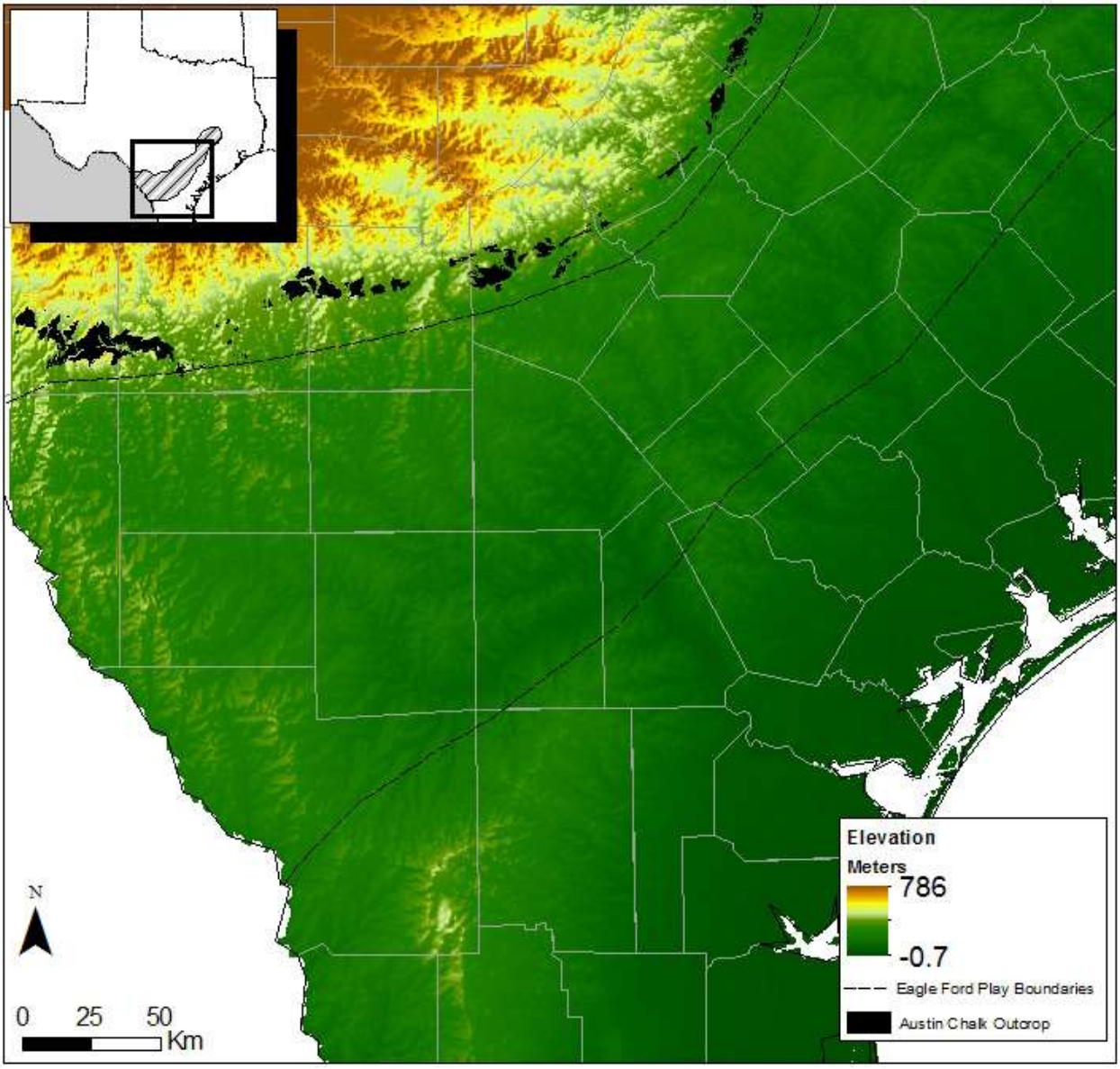

Source: USGS, http://ned.usgs.gov/

Figure 9. Topographic map of south Texas

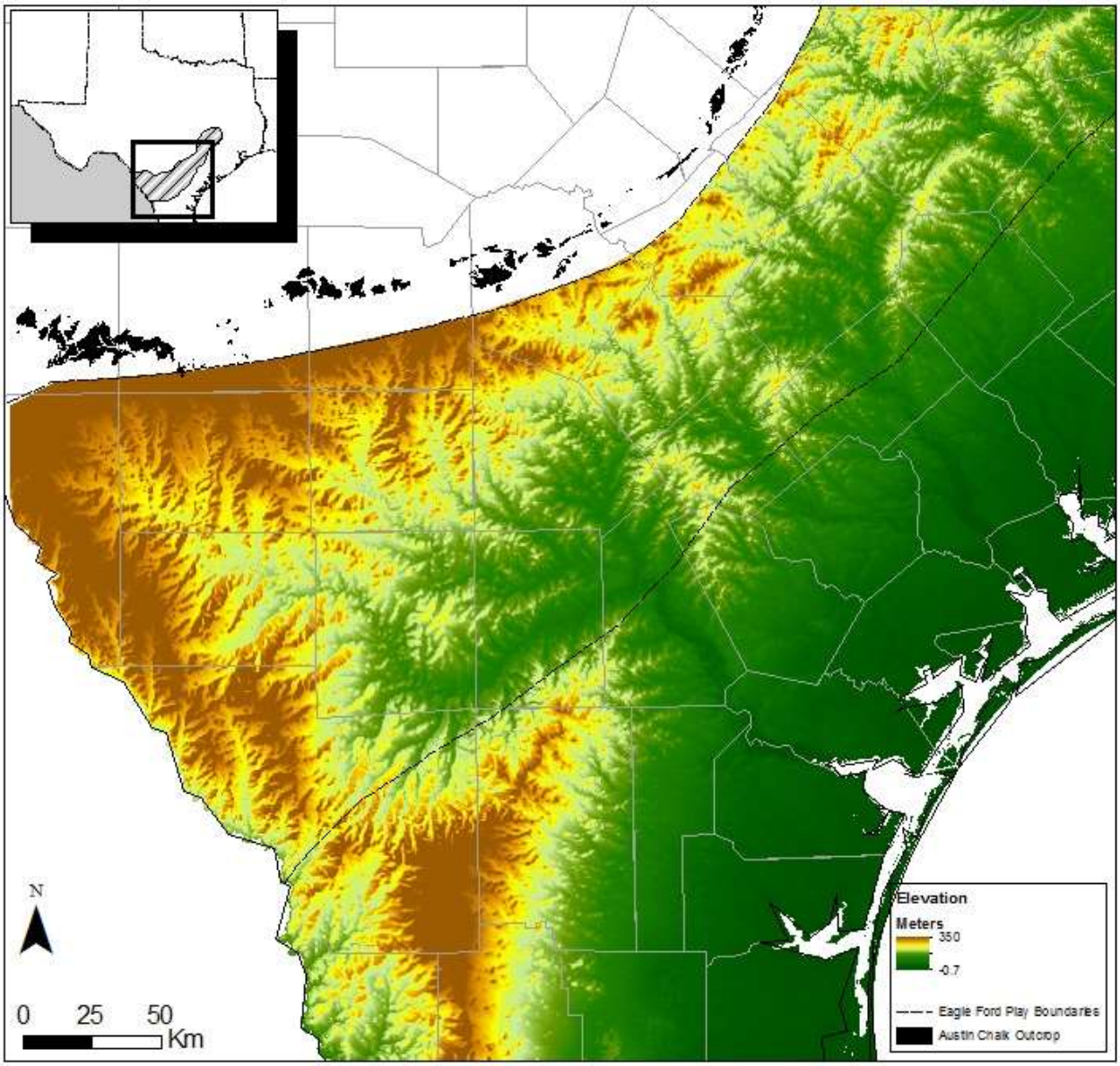

Source: USGS, http://ned.usgs.gov/

Figure 10. Topographic map of the Eagle Ford footprint

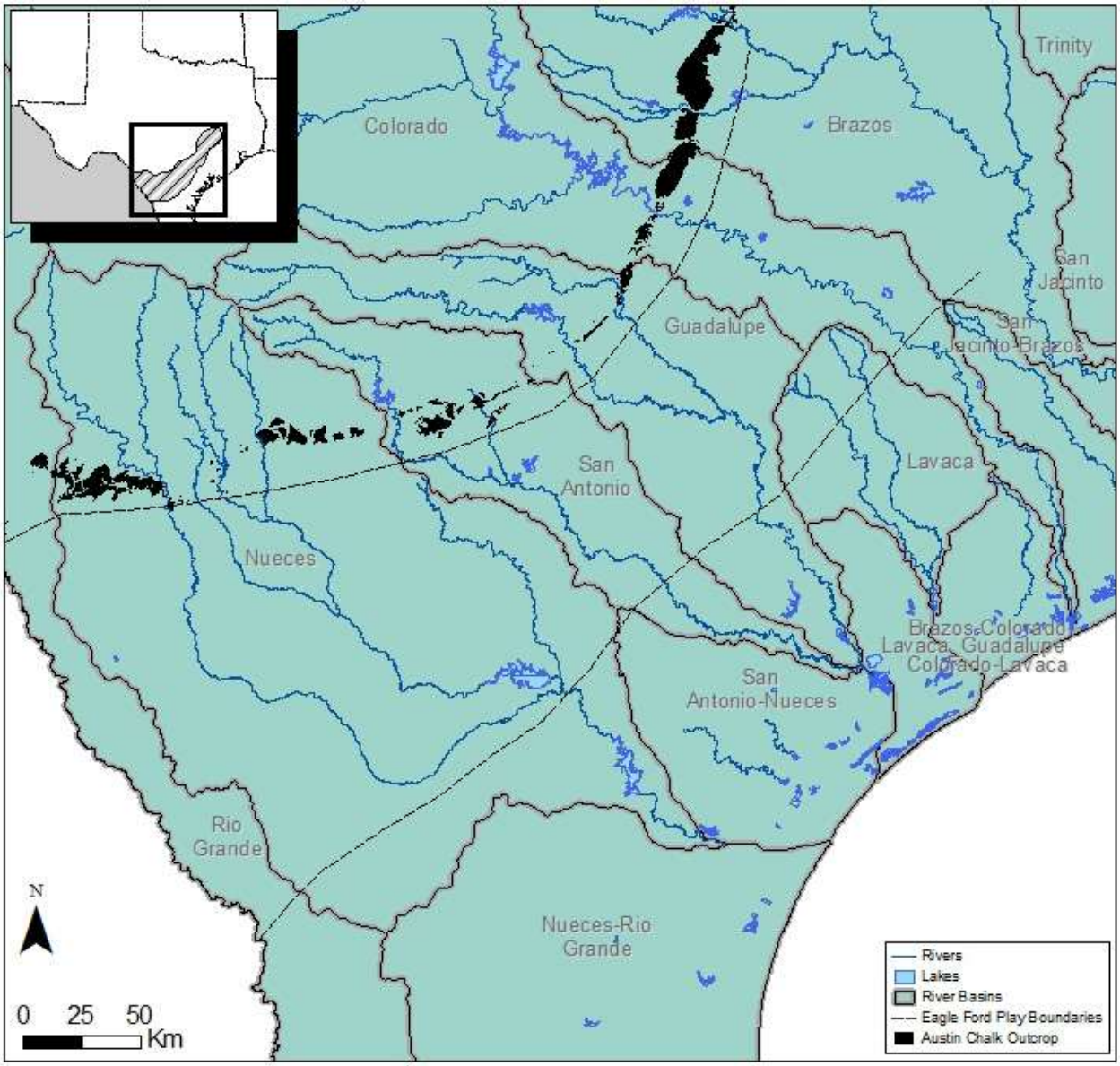

Source: http://www.twdb.state.tx.us/mapping/maps.asp

Figure 11. River basins of South and Central Texas

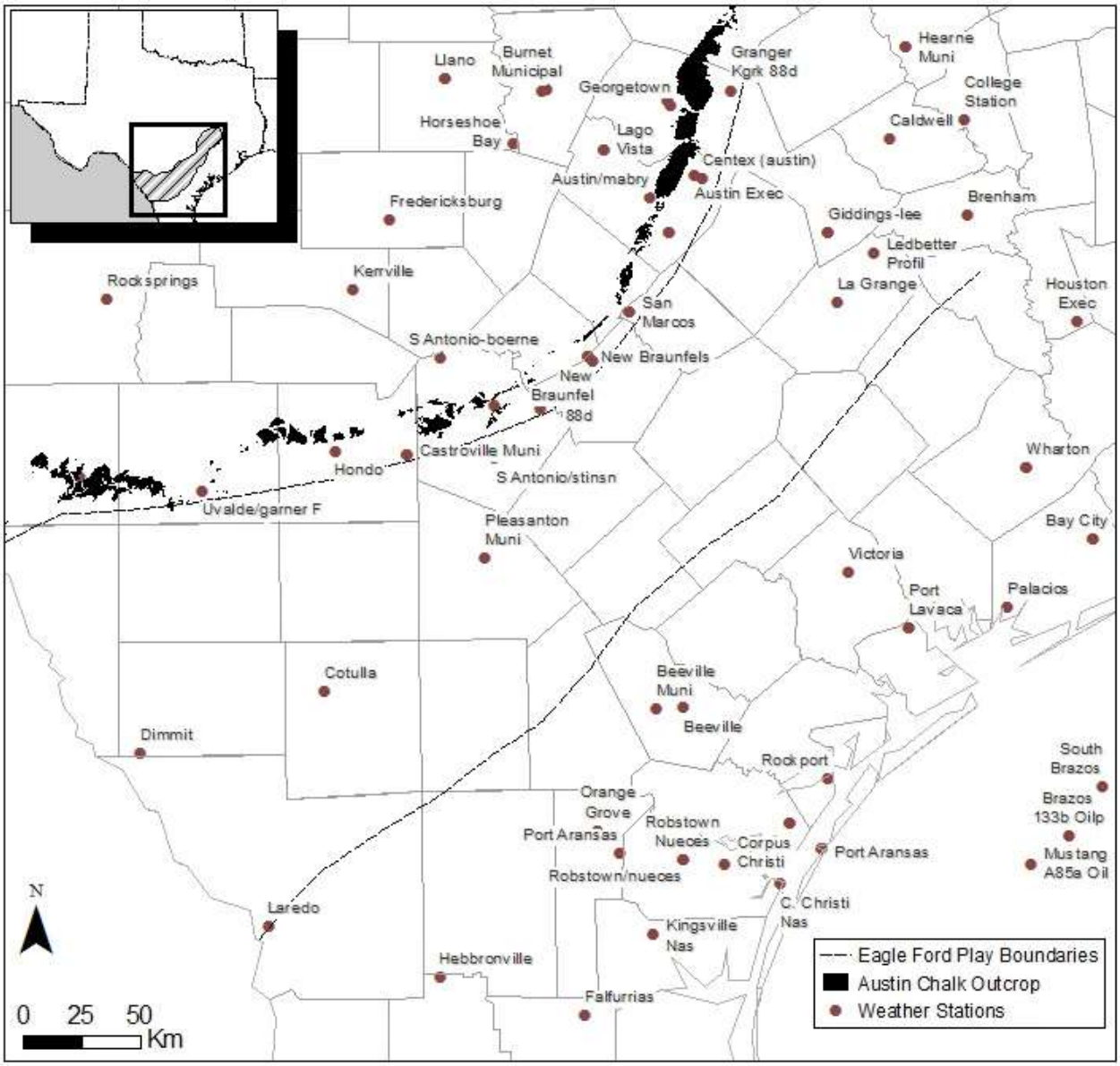

Source: National Center for Atmospheric Research http://www.rap.ucar.edu/weather/surface

Figure 12. Weather station locations in South and Central Texas

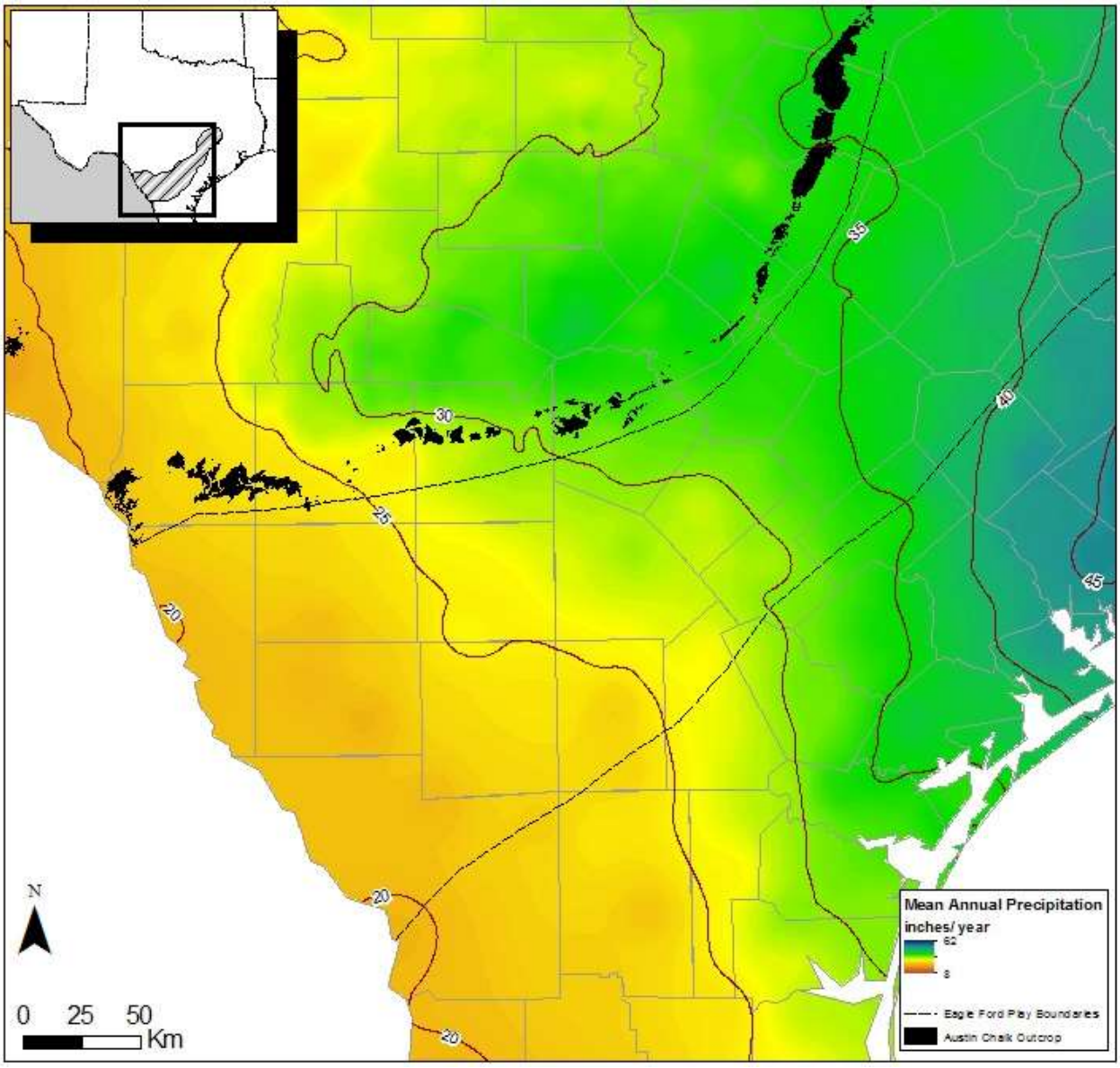

Source: Oregon State University, PRISM Climate Group, http://www.prism.oregonstate.edu/

Figure 13. Mean annual precipitation in South and Central Texas

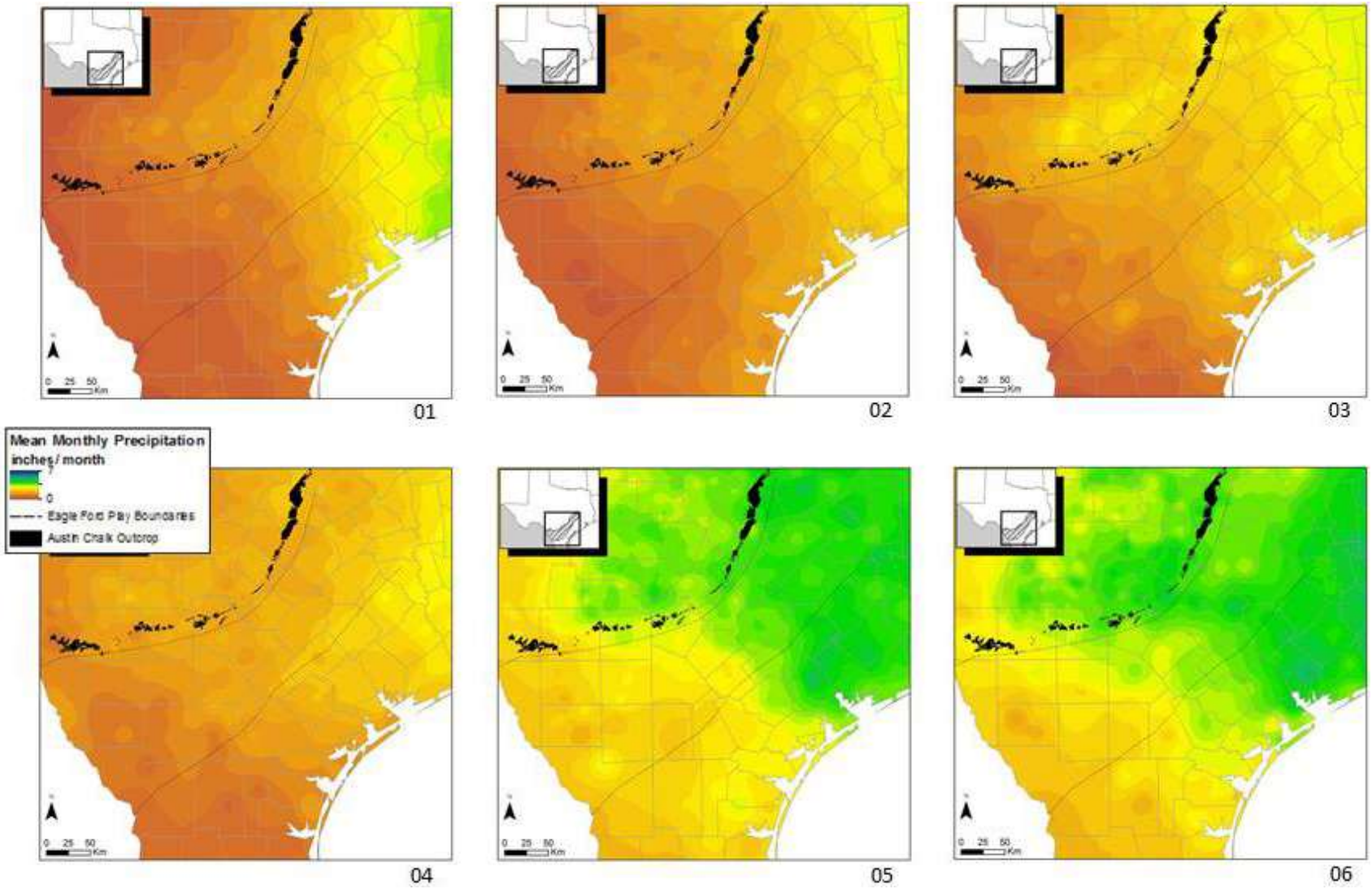

Source: Oregon State University, PRISM Climate Group, http://www.prism.oregonstate.edu/

Figure 14. Average monthly precipitation in South and Central Texas

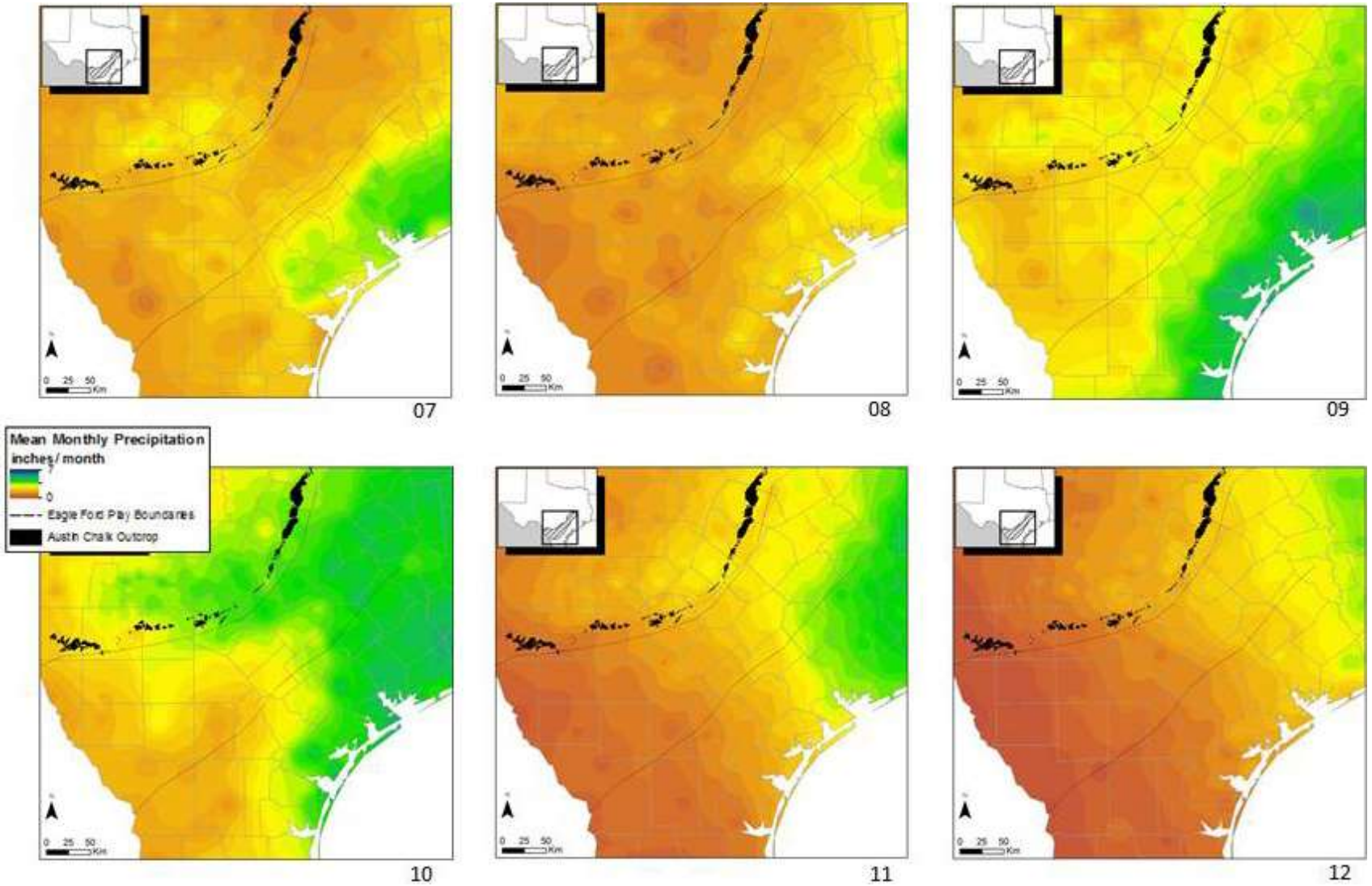

Source: Oregon State University, PRISM Climate Group, http://www.prism.oregonstate.edu/

Figure 14. Average monthly precipitation in South and Central Texas (continued)

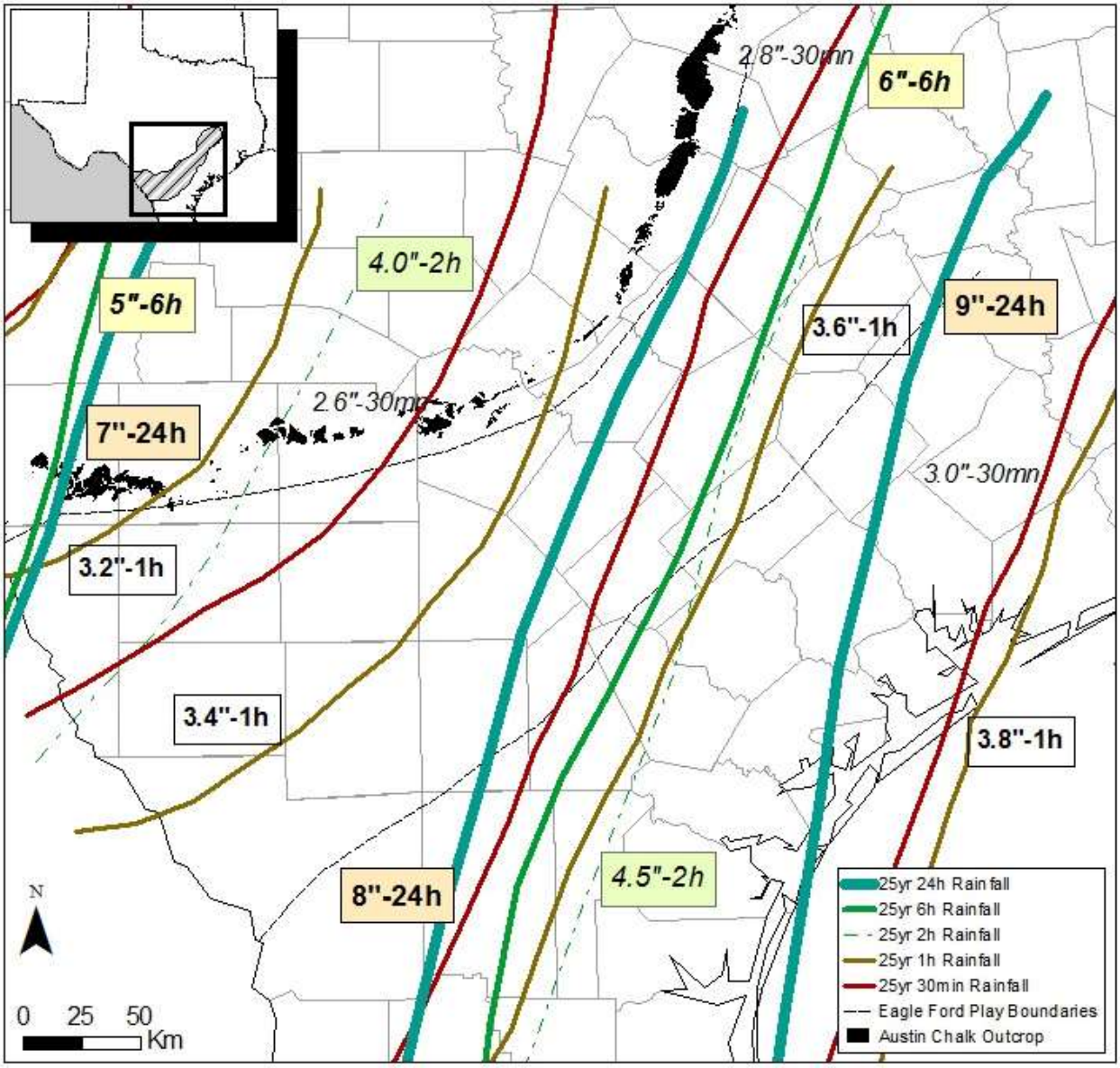

Source: NOAA, http://www.ncdc.noaa.gov/oa/documentlibrary/rainfall.html and Hershfield (1961)

Figure 15. Iso-maximum precipitation contour lines with a 25-year recurrence time in South and Central Texas

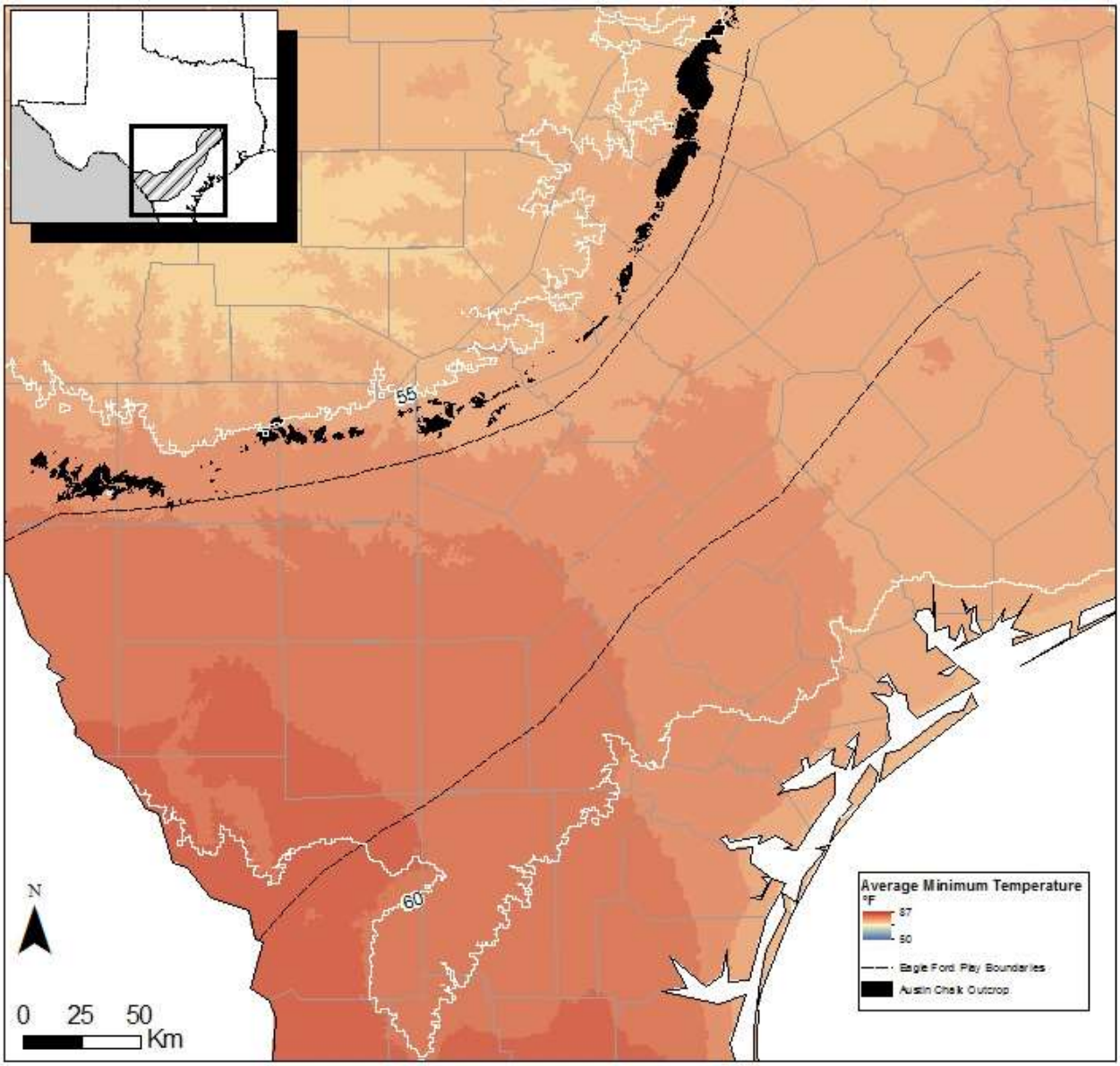

Source: Oregon State University, PRISM Climate Group, http://www.prism.oregonstate.edu/

Figure 16. Average maximum temperature in South and Central Texas

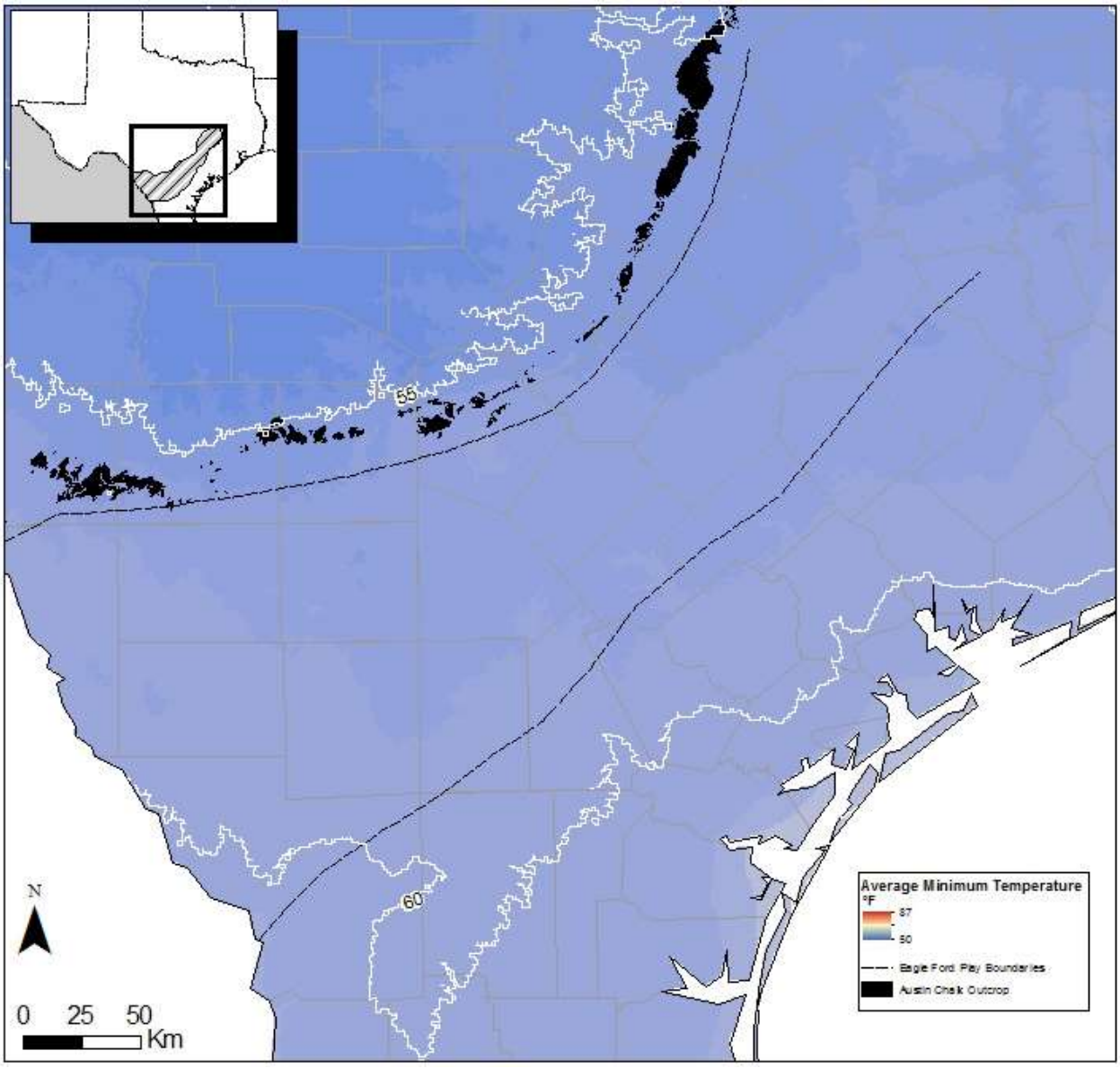

Source: Oregon State University, PRISM Climate Group, http://www.prism.oregonstate.edu/

Figure 17. Average minimum temperature in South and Central Texas

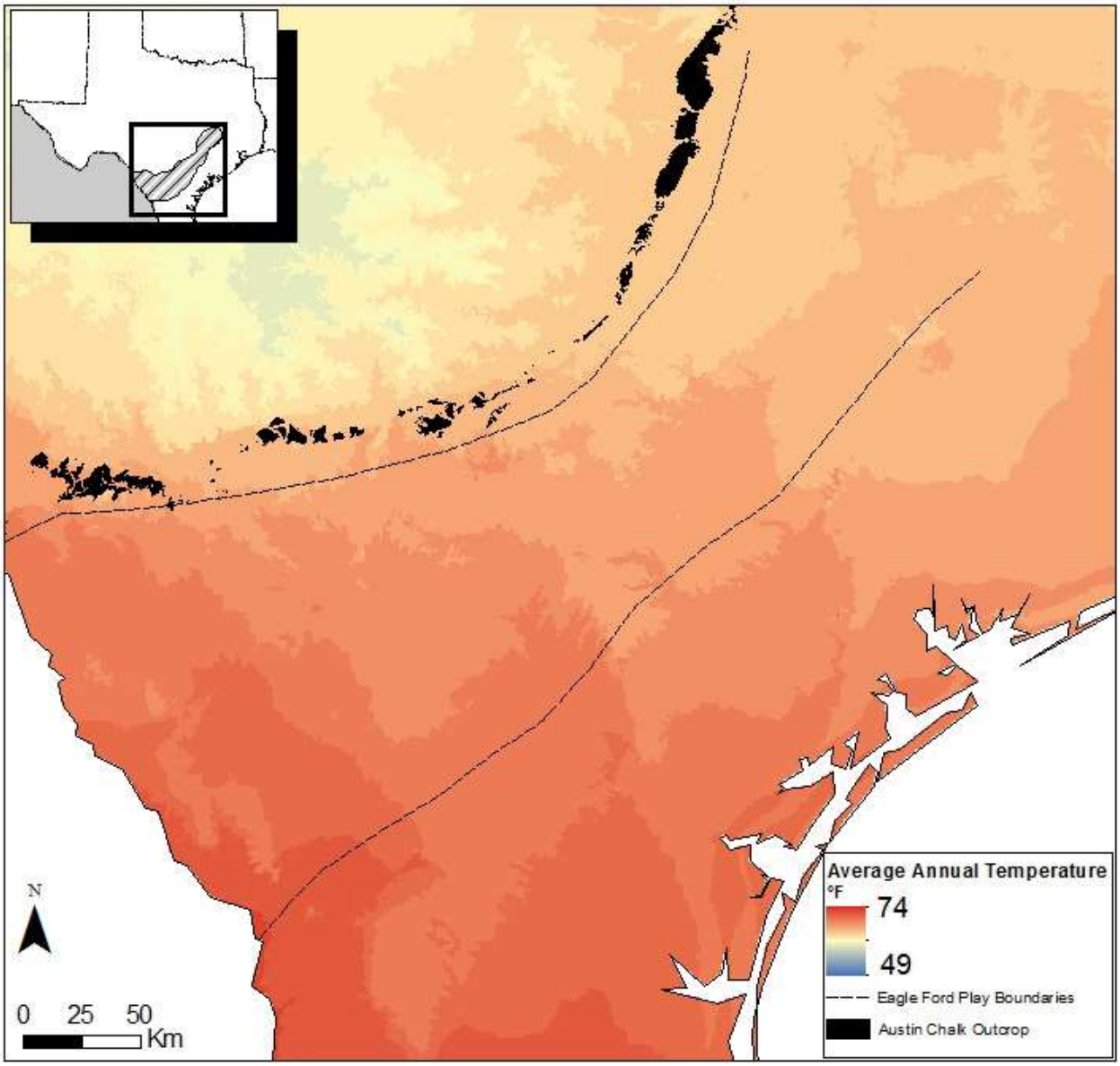

Source: Oregon State University, PRISM Climate Group, http://www.prism.oregonstate.edu/
Note: avergae annual temperature was computed as the mean of min and max annual temperature. The prism site does not provide average annual temperature.

Figure 18. Approximate average annual temperature in South and Central Texas

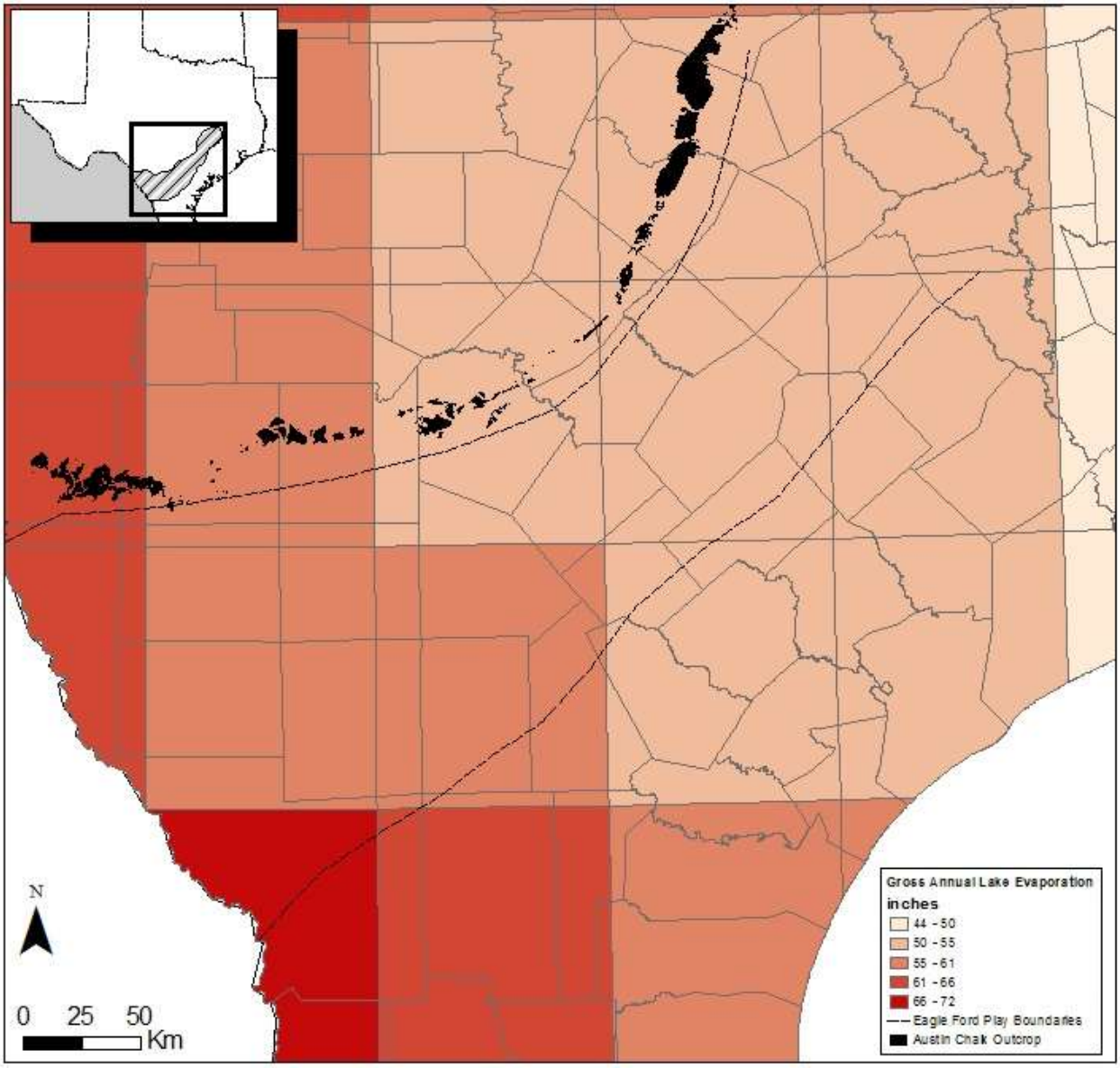

Source: TWDB, evaporation/precipitation data for Texas

Figure 19. Gross annual lake evaporation rate in South and Central Texas

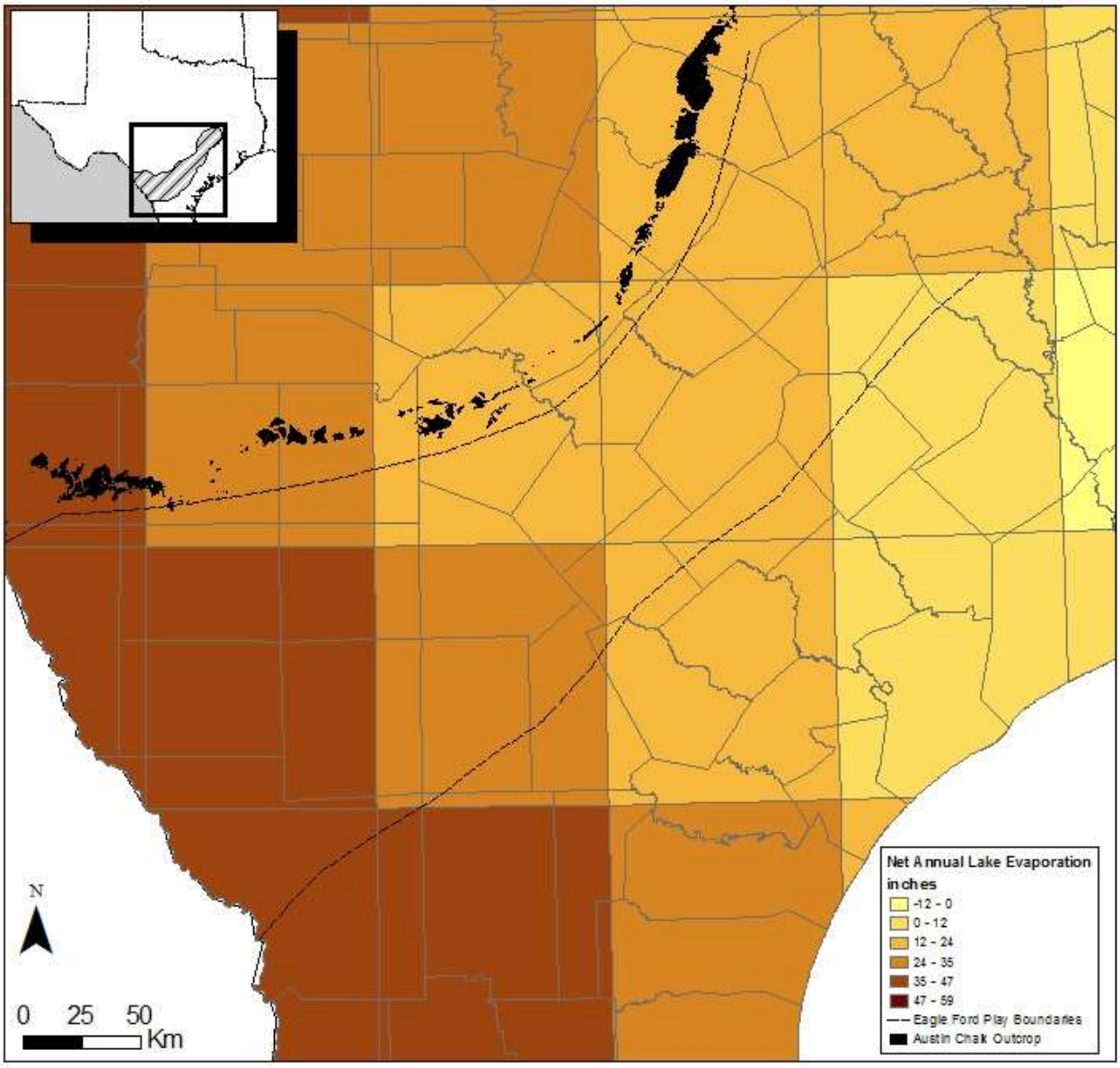

Source: TWDB, evaporation/precipitation data for Texas

Figure 20. Net annual lake evaporation rate in South and Central Texas

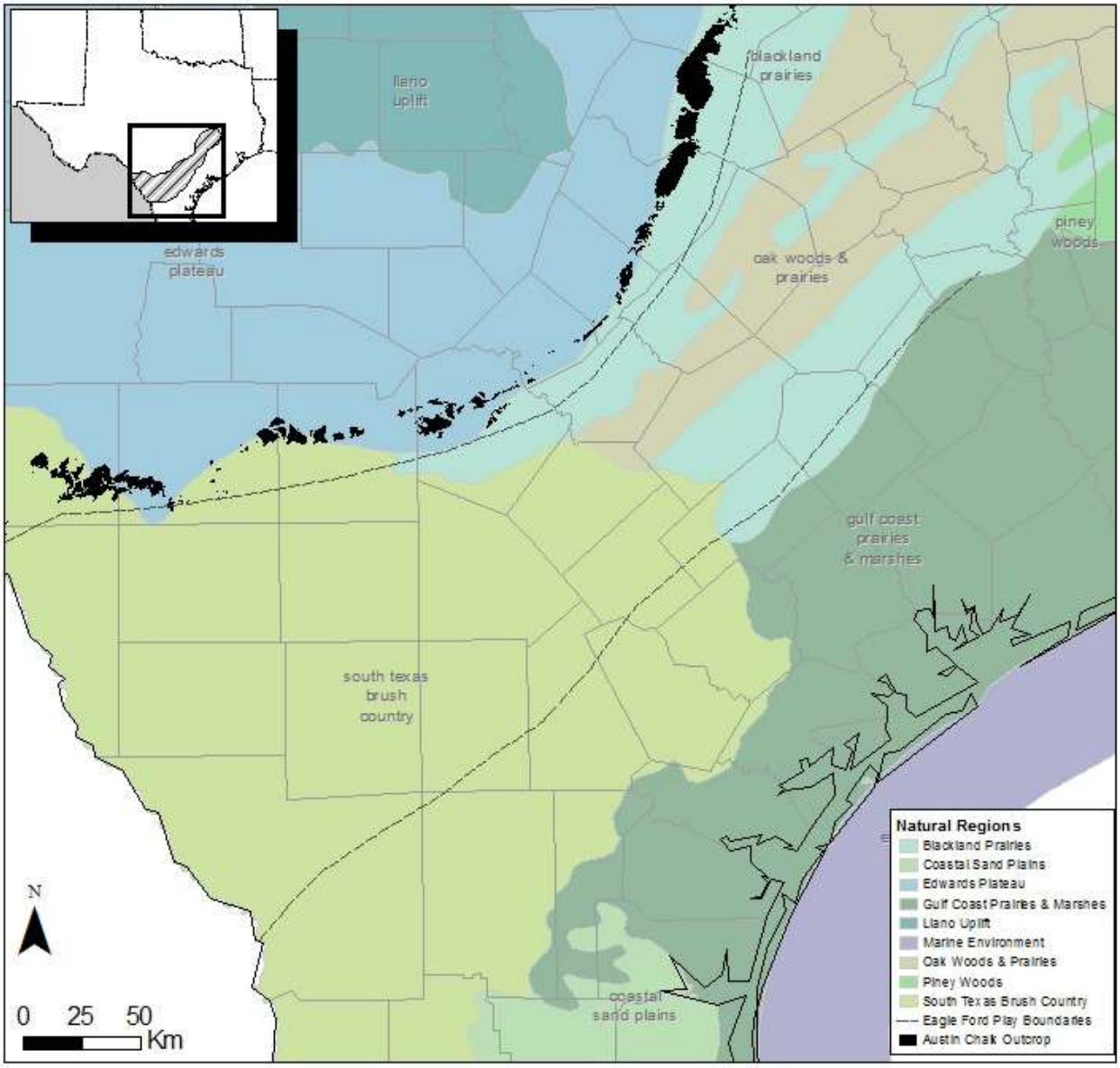

Source: Texas Parks and Wildlife, http://www.tpwd.state.tx.us/landwater/land/maps/gis/data_downloads/

Figure 21. Major natural regions in South and Central Texas

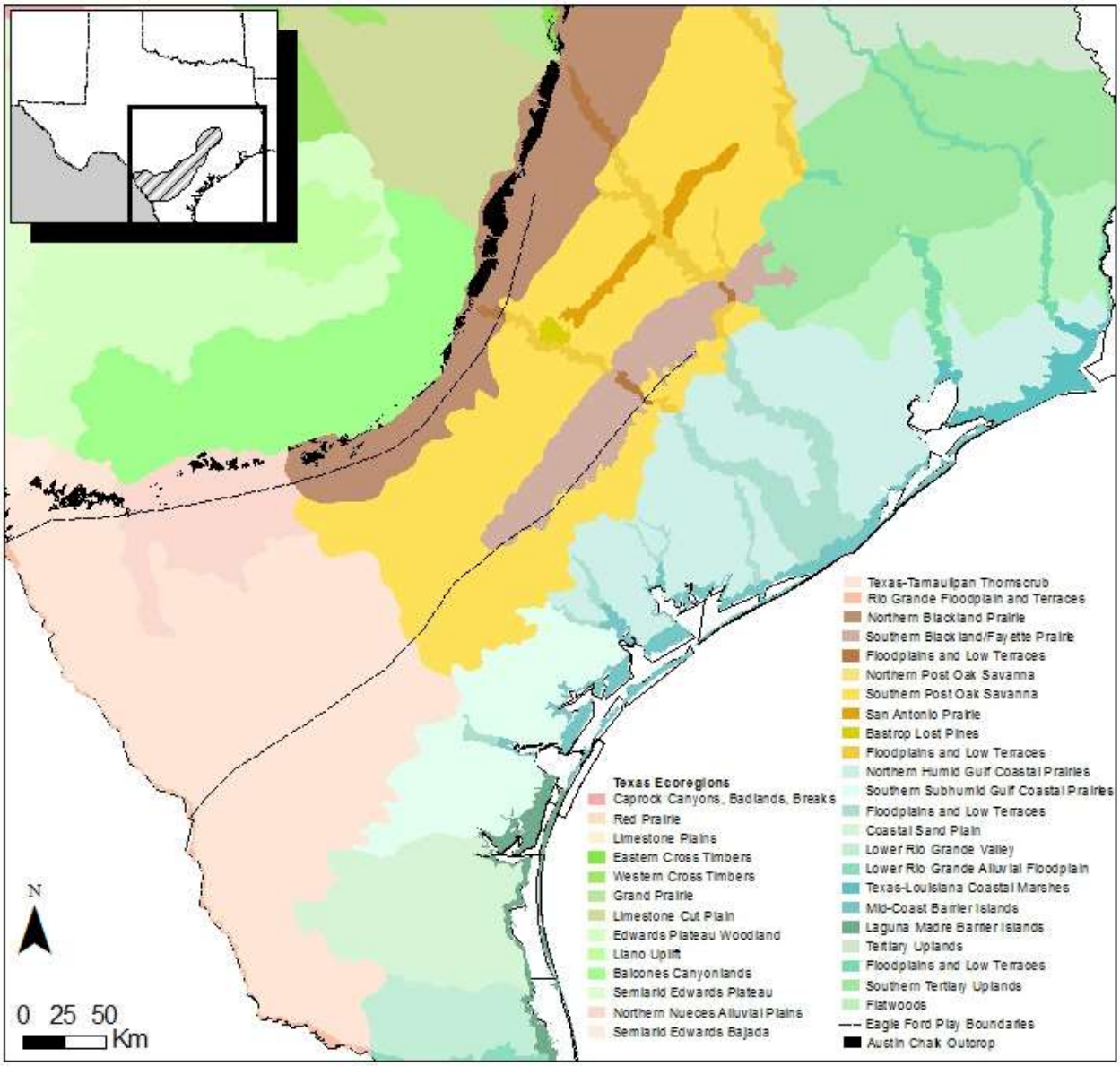

Source: Griffith et al. (2004) ; http://www.epa.gov/wed/pages/ecoregions/tx_eco.htm

Figure 22. Ecoregions of South and Central Texas

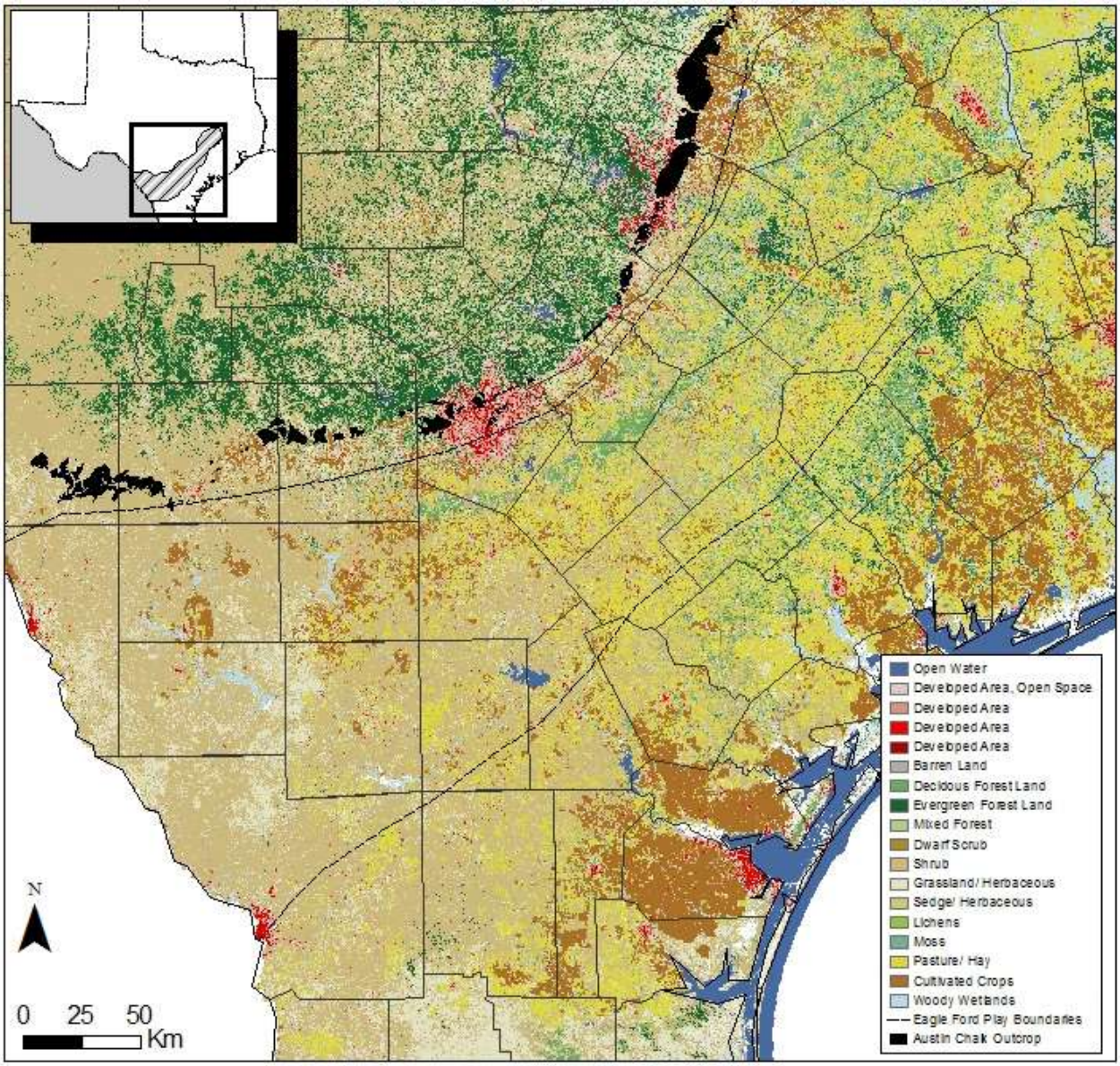

Source: USGS, http://www.usgs.gov/pubprod/data.html#data

Figure 23. Land use/ land cover for South and Central Texas

III. Geology and Hydrostratigraphy

Most information presented in this section was obtained from large projects undertaken at the BEG in the 1970's and 1980's in support of oil and gas and uranium exploration. The methodology was always the same: gather numerous (hundreds to thousands) of geophysical oil and gas or water well logs (generally resistivity and spontaneous potential) and correlate them in dip- and strike-oriented cross sections. Resistivity logs measure salinity of water near the wellbore. Salinity is generally higher and resistivity lower in less permeable rocks such as clays. Complications arise because of the presence of drilling mud, and generally long- and short-range resistivity tools are used in combination. Spontaneous potential measurements detect differences in electrical potential between formation water and drilling mud. Deflection toward lower potential (to the left) suggests that salinity of the formation is lower than that of drilling mud, suggesting a sandy layer ("sand line"). On the other hand, deflection to the right (higher potential) suggests a less-well-flushed, clayey layer ("shale line").

From the well logs, regional maps of lithofacies and inferred depositional systems and total sand thickness were produced. Many reports that document the process and general results related to the Gulf Coast have been published in several publications (Galloway et al., 1982a; Galloway and Hobday, 1996; Galloway et al., 2000). Fisher and McGowen (1967) introduced the concept of depositional systems in the Gulf Coast area. They defined it as "a three-dimensional, genetically defined physical stratigraphic unit that consists of contiguous, process-related sedimentary facies." The overarching concept of depositional systems has become a powerful tool for correlating formation properties in a sophisticated way between well log locations. Depositional systems are made up of various depositional environments that are genetically related in a predictive way. Once a depositional environment is characterized, it becomes more straightforward to project its flow properties be it an aquifer or a disposal interval. The importance of describing formations' depositional environments lies in their control of fluid flow, as has been well described in Knox et al. (2007) in a report for the TWDB on the structure of the Yegua-Jackson aquifer. A particular powerful tool is to build net sand maps consisting in contouring total thickness of sand strata above some thickness threshold. Simple principles can be applied to yield high-level conclusions. For example, sand bodies deposited in fluvial or deltaic environments will tend to be dip-aligned facilitating communications between outcrop areas and deep subsurface. This means recharge can reach deeper levels of the aquifer but also that injected fluids have a pathway to the surface. On the other hand, strandplain deposits would be along strike and would favor flow in that direction. If lagoons happen to have existed behind the beach deposits and are still preserved, the high permeability sands could be isolated form the ground surface supplying good reservoirs for hydrocarbon accumulation or ideal injection intervals. Many different scenarios can be deduced form the various spatial distributions of the different depositional environments. Similarly, knowledge of how long a carbonate formation has been exposed to aerial conditions gives a clue towards its ability to transfer fluids. Many carbonate intervals begun as mudstones or mudstone-cemented clastic rocks with limited intrinsic permeability. Actually several tight carbonate formations can be considered aquitards. However, long exposure to surface and shallow subsurface conditions tend to create karsts and generate a sharp increase in permeability and possibly in effective porosity. The Cretaceous Edwards Fm. and Ellenburger Fm. of Ordovician age are two examples of such a process whereas the Glenrose limestone is generally considered an aquitard.

In this Section III we examine the general stratigraphy of all layers above the folded Paleozoic basement (observed at depth >15,000 ft) including that of the Eagle Ford Fm. Before presenting stratigraphic details, we offer a simplified geological history of what is now the State of Texas to set the stage. We then discuss structural information in a shorter Subsection III-2. We conclude Section III by summarizing the hydrostratigraphy in the EF footprint. Intervals defined by the stratigraphy and fresh, brackish, or saline water-bearing formations do not necessarily coincide.

III-1. Stratigraphy

III-1-1 General Geology

III-1-1.1Background

The section gives an overview of the relevant Texas geology summarized from Ewing (1991). Most of West and Central Texas is underlain by Precambrian rocks that crop out mostly in the Llano Uplift in Central Texas and locally in the Trans-Pecos area. Starting in the Cambrian period, about 550 million years ago, failed continental rifting resulted in widespread deposition of shelf sediments on a stable craton (e.g., Cambrian sediments, Ellenburger Group). Carbonate and clastic deposition continued until late Devonian, 350 million years ago. Thickness of the deposits varies, with a maximum in the ancestral Anadarko Basin and total removal by erosion of some formations along a broad arch oriented NW-SE on the Amarillo-Llano Uplift axis (Concho Arch). Beginning in the Mississippian period (starting 350 million years ago), the passive-margin history of rifting and subsidence was replaced by extensive deep marine sedimentation and tectonic convergence on the eastern flank of the continental margin. This convergence episode yielded the so-called Ouachita Mountains, now eroded and buried, whose trace approximately follows the current Balcones Fault Zone that runs west from San Antonio and northeast through Austin to the east of Dallas and continues through the related Mexia-Talco Fault Zone in East Texas. Behind the orogenic belt, north and west of the current Balcones Fault Zone, during and after the compressive event, sedimentation continued in and around several inland marine basins. Sedimentation was thicker in the basins and thinner or absent on platforms and arches. During these Pennsylvanian and Permian times (320 to 270 million years ago) major subsidence and sediment accumulation, partially fed by the erosion of the Ouachita Mountains, occurred in the Permian Basin. Farther north, the Anadarko Basin is separated from the Midland Basin by another basin and two structural highs. The Anadarko Basin also underwent abundant sedimentation during the Pennsylvanian and Permian and included coarse granitic detritus (“granite wash”) from the Amarillo Uplift. The Fort Worth Basin is similarly filled with Pennsylvanian and Permian sediments.

Beginning in Triassic time (250 million years ago), Texas was again subject to extension and volcanism, leading to Jurassic rifting of the continental margin and creation of the Gulf of Mexico and Atlantic Ocean. The focus of major geologic events shifted to the eastern part of the state. The small rift basins that initially formed were buried under abundant salt accumulation (Louann Salt). At later times, as the weight of sediments continued to increase, the salt became unstable and started locally to move upward in diapirs. During the Cretaceous, sediments deposited from shallow inland seas formed broad continental shelves that covered most of Texas. Abundant sedimentation in the East Texas Basin and Maverick Basin (in South Texas) occurred during the Cretaceous. In the Tertiary era (starting 65 million years ago), as the Rocky Mountains to the west started rising (Laramide orogeny), large river systems flowed toward the

Gulf of Mexico, carrying an abundant sediment load, in the fashion of today's Mississippi River. All the area west of the old Ouachita Mountain range was also lifted, generating a local sediment source, including erosional detritus from the multiple Tertiary volcanic centers in West Texas and Mexico. Figure 24 illustrates the relative amount of sediments across the state. Figure 25 depicts the major geologic regions of the state. The EF footprint is entirely included in the Gulf Coast region.

The geology of the Texas Gulf Coast is complex because of cyclic deposition of various sedimentary facies (Figure 26) but has been the subject of a large number of publications because of its relevance to the oil and gas industry. For example, a summary of the depositional history in the Gulf of Mexico, including South Texas is provided by Galloway et al. (2000) and includes an overview of the lithologic history of the Gulf of Mexico for Cenozoic age formations. In the next paragraphs, we summarize relevant points of the geological history of the Gulf Coast province.

The plains of the Gulf Coast were formed by downfaulting and downwarping of folded Paleozoic basement rocks during the breakup of the Paleozoic megacontinent, Pangaea, and the opening of the North Atlantic Ocean in the Late Triassic (Byerly, 1991; Hosman and Weiss, 1991). At the same time was deposited the thick Louann salt layer. Three main structural zones can be seen in the study area: the Balcones Fault Zone, the San Marcos Arch, and the Rio Grande Embayment. The Balcones Fault Zone is north of the study area and forms a divide between outcropping Upper Cretaceous and Eocene strata (Baker, 1979, 1995; McCoy, 1990). The Balcones Fault Zone consists of mainly normal faults that occur parallel to the trend of the buried Ouachita Orogenic Belt. Along these faults, sediments have been displaced by up to 1,500 ft, moving downward to the Gulf of Mexico. The San Marcos Arch, between the Rio Grande Embayment and East Texas Basin, is a broad area of lesser subsidence and a subsurface extension of the Llano Uplift (Chowdhury and Turco, 2006). The arch is crossed by basement-related normal faults that parallel the buried Ouachita Orogenic Belt of Paleozoic age (Ewing, 1991). The Rio Grande Embayment is a small deformed basin that lies between the El Burro Uplift in northeast Mexico and south of the basin-marginal Balcones Fault Zone (Ewing, 1991). Some data indicate that the embayment was possibly compressed during the Laramide Orogeny in the Late Cretaceous–Paleogene (Ewing, 1991).

During the Cretaceous, sediments deposited from shallow inland seas formed broad continental shelves that covered most of Texas. Summarized as early Late Jurassic carbonate deposition followed by Late Jurassic and Early Cretaceous clastic deposition and concluding with platform carbonate deposits of late Early Cretaceous (Ewing, 1991, p.20).

In the Tertiary (starting 65 million years ago), erosional debris from Laramide reliefs (Rockies) periodically surged to the Gulf Coast, changed the nature of sediments from carbonate deposits with some clastics to almost exclusively clastic, and started prograding the continental self seaward. Six major progradational events occurred in which sedimentation built out into the Gulf Coast Basin (Figure 26). These progradational sequences include, from oldest to most recent, Wilcox, Queen-City, Yegua-Jackson, Vicksburg-Catahoula-Frio, Oakville-Fleming, and Plio-Pleistocene sand-rich wedges (Galloway et al., 2000). The set of depositional systems is the same throughout the Tertiary period: fluvial, deltaic, barrier bar/strandplain, shelf, and slope/basin depositional systems. During most of the Tertiary history of the Texas coast, little variation occurred in the area of the main depocenters, resulting in individualized subbasins. Major fluvial depoaxes occupying the same structural troughs include the Rio Grande

Embayment of South Texas and the Houston Embayment, separated by the San Marcos Arch characterized by less abundant sediment influx. This variable sediment input is also true at a smaller scale explaining the lateral variations in sand content. Vertical continuity of sand in main depocenters is impacted by lateral migration of channels through time. For example, channel sand bodies vertically stack in rapidly subsiding basins, whereas in a more stable tectonic environment, distributary channels may wander more, resulting in vertically offset sand bodies. Lateral continuity can also be understood in terms of depositional systems. Wave-dominated deltaic and strandplain systems present high lateral continuity and may be thick, whereas fluvial and fluvial-deltaic systems may present abrupt lateral facies change. In addition, sediments from wave-dominated deltaic and strandplain systems are generally well sorted. In general, sand permeability is correlated with sand-body thickness—that is, transmissivity increases more than linearly with thickness.

Growth faults, resulting from sediment loading on unstable substrates, periodically develop. Intermittent movement along these growth faults accommodated accumulation of enormous masses of sediments. Growth faults are mostly syndepositional faults, and zones of growth faulting mark basinward movement of the shelf edge. Fault-bounded reservoir compartments create many structural traps for hydrocarbons in the Tertiary stratigraphic section of the southern Gulf Coast Basin.

Two generalized stratigraphic columns located at the Dimmit-Zavala county line (Figure 27) for the southern area of the EF footprint and Karnes – Gonzales county line (Figure 28) for its northern area illustrate the general stratigraphy of the area, in particular the variations in thickness of individual strata. The next sections will detail each of the intervals represented in the columns. Note that the columns show broadly alternating high (“aquifer”) and low (“aquitard”) permeability intervals. They also suggest intervals that might go through HF in the future but this aspect is not further discussed in this document. The geological map associated with the EF footprint (Figure 29, simplified from 1/250,000 GAT sheets) displays a number of formations that may or may not exist in the subsurface or that may or may not have been deposited in the same depositional environment. A number of formations especially older ones exist in the subsurface but do not crop out in the study area or do not crop out at all anywhere. As displayed in Figure 26, formations are stacked in such a way that older formations crop out further away from the coast.

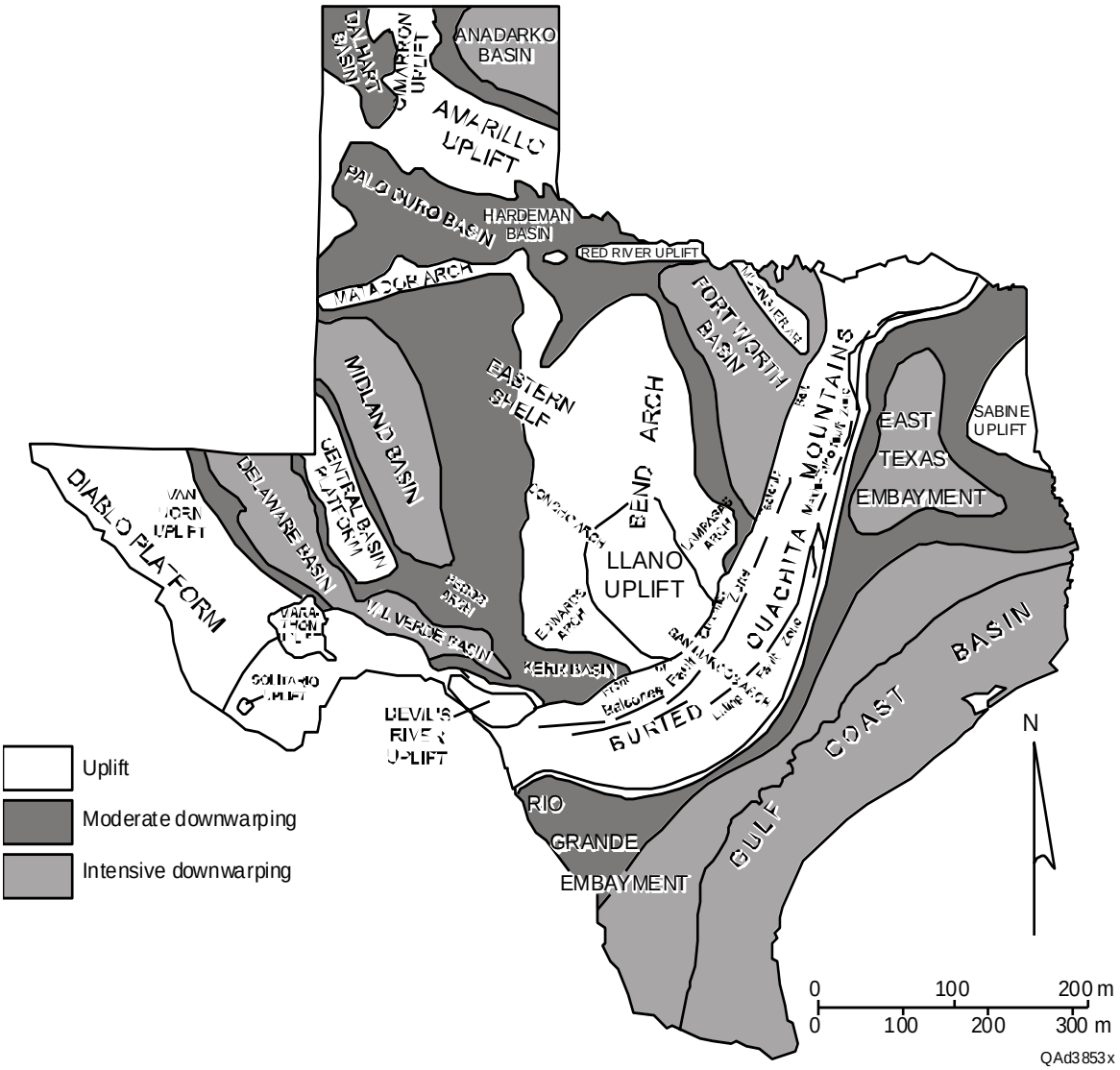

Source: modified from Kreitler, 1989
Note: amount of downwarping is a measure of the relative thickness of the sediment pile.

Figure 24. Generalized tectonic map of Texas showing location of sedimentary basins.

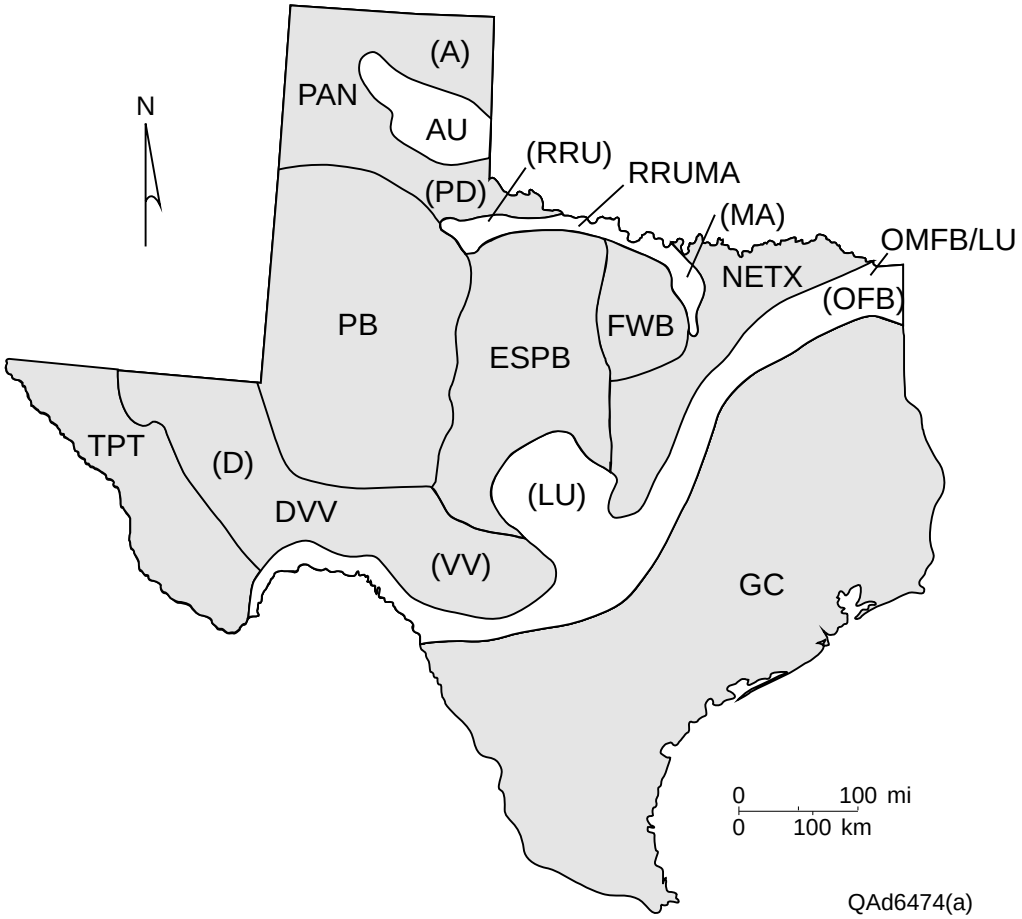

Source: Ambrose et al. (2010)
Note: Regions are: AU Amarillo Uplift, DVV Delaware (D) and Val Verde (VV) Basins, ESPB Eastern Shelf of the Permian Basin, FWB Fort Worth Basin, GC Gulf Coast, LU Llano Uplift, NETX Northeast Texas, OFB Ouachita Foldbelt, OMFB/LU Ouachita and Marathon Foldbelts and Llano Uplift, PAN Texas Panhandle, PB Permian Basin, PD Palo Duro Basin, RRUMA Red River Uplift (RRU)-Muenster Arch (MA), TPT Trans-Pecos Texas

Figure 25. Major geologic regions (basins and uplifts) in Texas

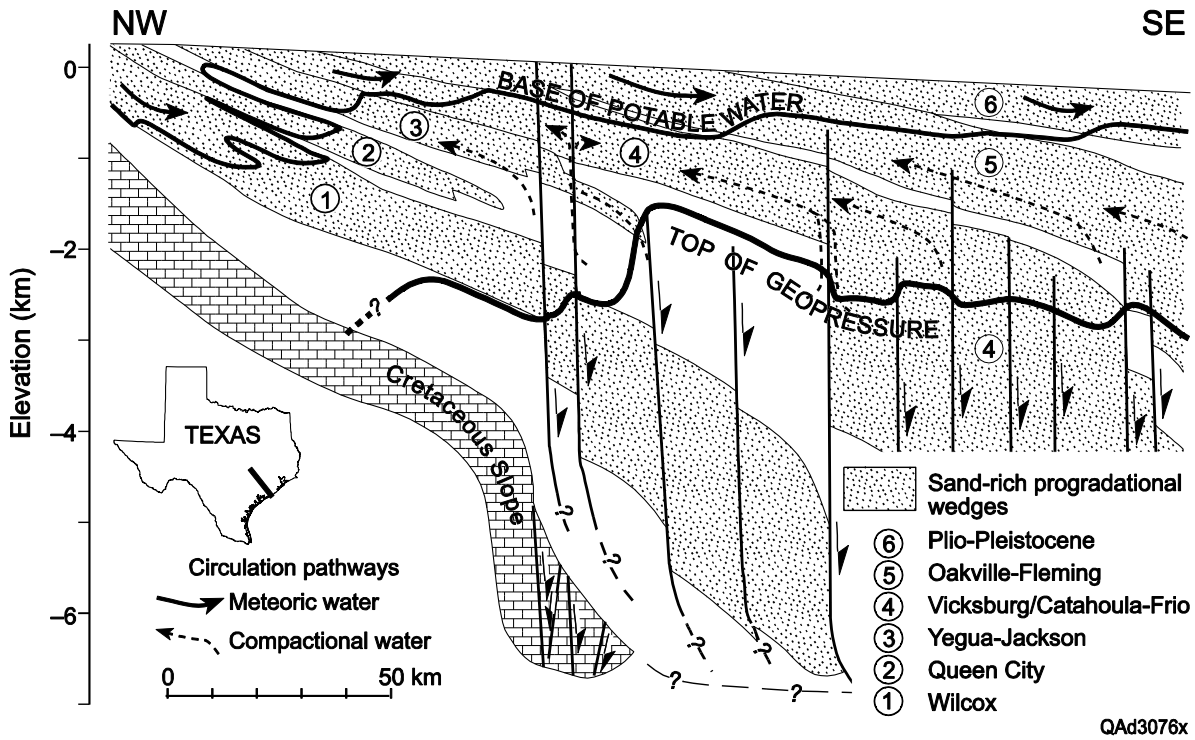

Source: Adapted from Galloway (1982a) and Galloway et al. (1982c). The last major progradation wedge of Plio-Pleistocene age (6) is still active and does not contain uranium deposits.

Figure 26. Southern Gulf Coast major sand-rich progradational packages and growth-fault zones beneath the Texas Coastal Plain

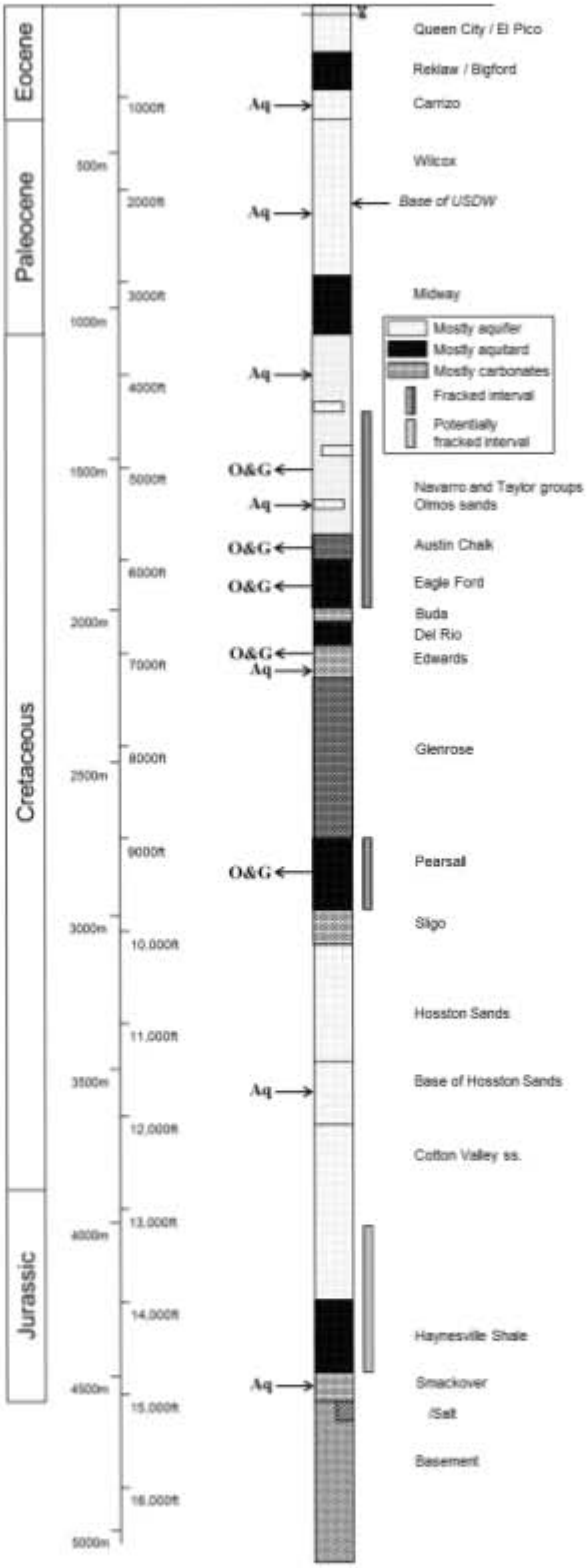

Source: Nicot and Duncan (2012)

Figure 27. Simplified stratigraphic column in the footprint of the Eagle Ford (~Dimmit-Zavala county line towards the south of EF domain in Texas)

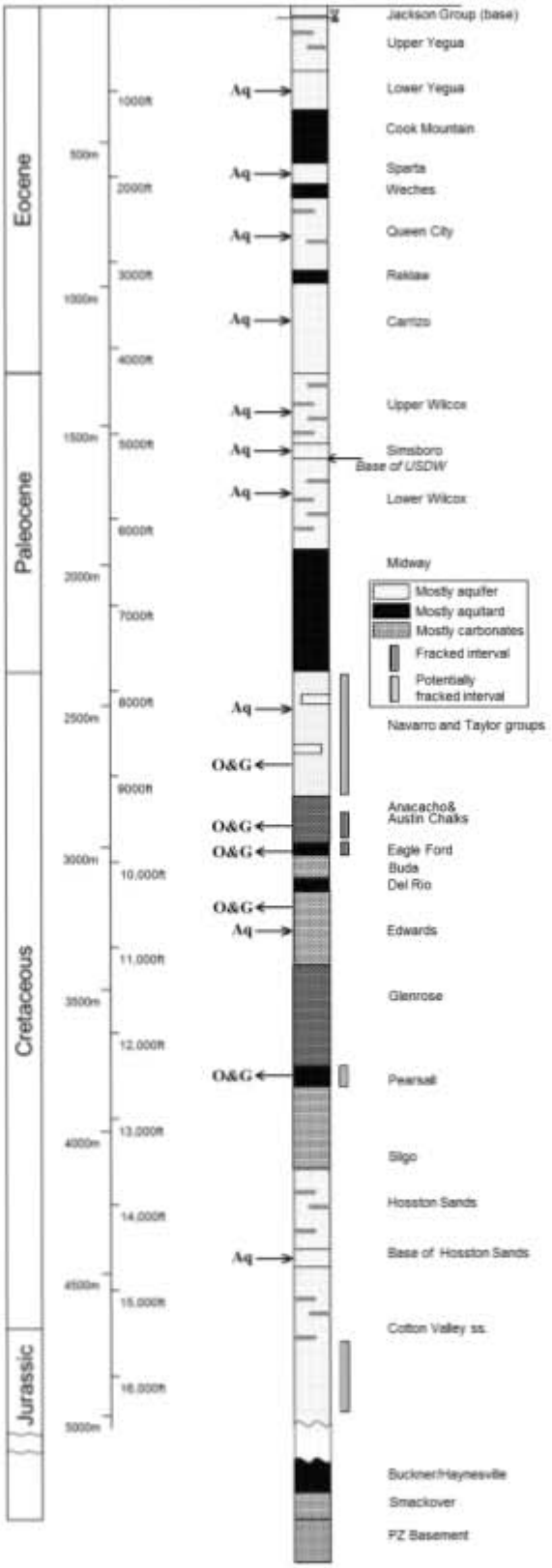

Figure 28. Simplified stratigraphic column in the footprint of the Eagle Ford (Karnes-Gonzales county line)

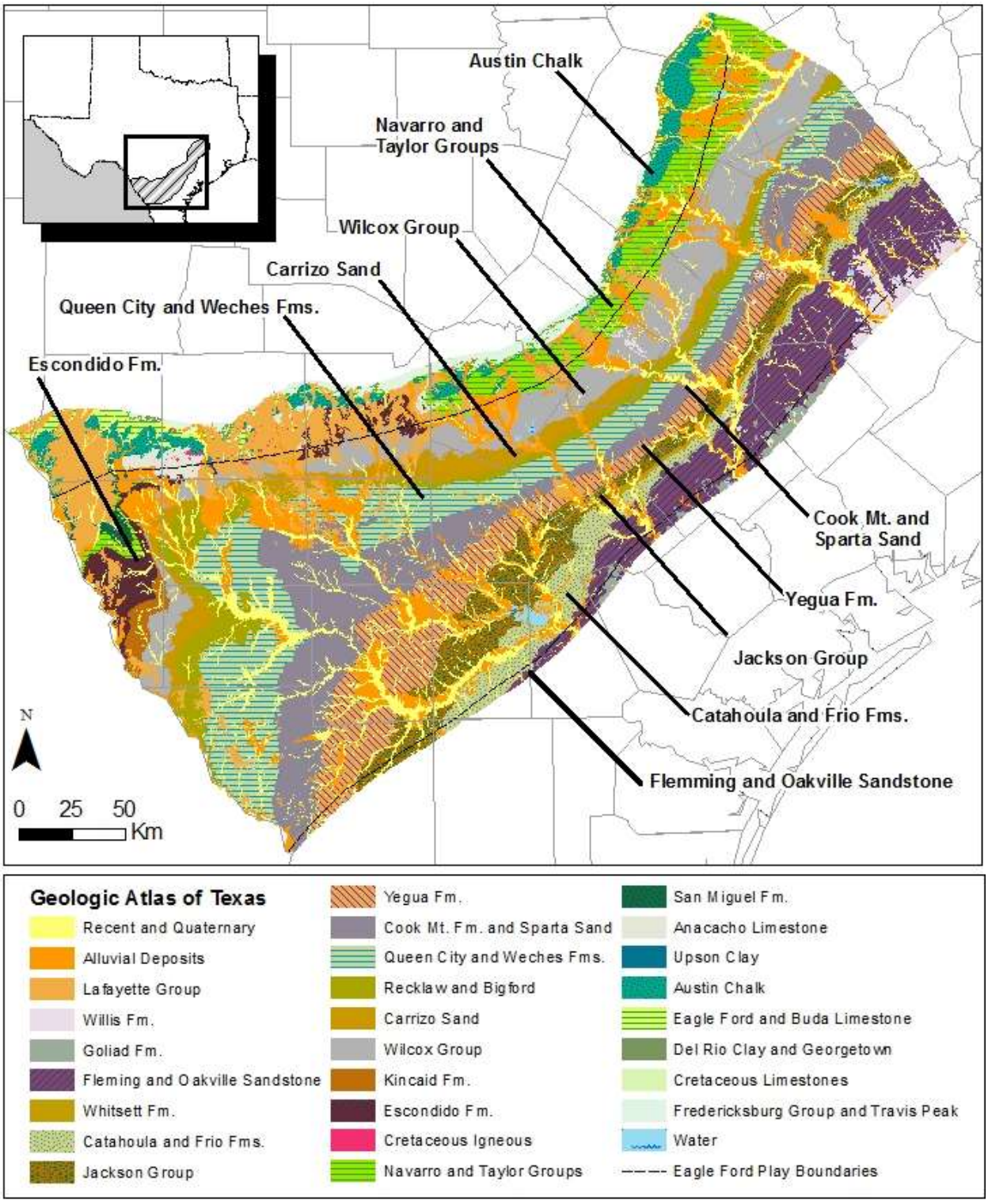

Source: TWDB, www.twdb.state.tx.us/groundwater/aquifer/GAT/Share

Figure 29. Simplified geological map of South and Central Texas

III-1-1.2Cretaceous and older Formations

The Eagle Ford Fm. is only one of the many formations of Cretaceous age (Figure 27). It is sandwiched between the younger Austin Chalk and the older Buda Limestone. In this section we examine all relevant formations to the base of the Midway Fm. The folded Paleozoic basement (Ouachita orogeny) is at a depth of ~ 15,000 ft or deeper in the EF footprint (Figure 27 and Figure 28). South Texas "basement" consists of deformed and metamorphosed Paleozoic (Ouachita) sandstone, shale, and chert, overlain by two redbed successions; the "Blum Unit" of Permian (?) age, narrow band across northern Frio and Atascosa, southern Medina, and Bexar Counties, and the fill of the "Chittim Rift" of early Mesozoic (?) age along the Rio Grande in Maverick County (Ewing, 2010). The first major deposit on the Paleozoic basement is the evaporites of the ***Louann Salt***. It is recovered unconformably by the Jurassic-age ***Norphlet Fm.*** which probably does not exceed 30 ft in South Texas (Budd and Loucks, 1981, p.3). It is composed of shales, anhydrite, dolomite and some sands deposited in a tidal flat environment. The ***Smackover Fm.*** unconformably overlies the Norphlet Fm. Its lower section consists of carbonate mudstone interpreted as deepwater deposits prograding to shallower environment (open shelf and lagoon) deposits in the upper section with sometimes high-energy oolitic facies. The formation thickness increases seaward to >1000 ft. Note that the Smackover Fm. onlaps the basement over the Louann Salt and that more generally, deposits of younger formations invade further inland the Paleozoic basement (Figure 30 and Figure 31). This clearly translates into a deep well to the basement not necessarily intersecting all the formations described in this section. Conformably overlying the Smackover Fm., the evaporitic ***Buckner Fm.*** transitions seaward to ***~Haynesville*** shales and limestone, equivalent to the Haynesville Shale of the East Texas Basin.

Cotton Valley Group includes abundant sandstone updip, but transitions into marine shale downdip. Bossier-like deep-water fans are possible (Ewing, 2010). They represent large sand bodies unconnected from their source and embedded into mudstones. Figure 32 illustrates the onlap of the Cotton Valley deposits onto the basement and a generalized stratigraphic section is given in Figure 33. The sand bodies are from fluvial to marine origin.

Hosston and ***Sligo Fms*** form two coeval (deposited at same time different depositional environment). They represent (Bebout et al., 1981) the first of three major transgressive events (Figure 33): Hosston / Sligo, Hensel / Pearsall (and equivalents formations at the outcrop), and Glenrose / Stuart City. Upper Sligo consists mostly of limestone whereas the lower Sligo includes dolomite and anhydrite. The Hosston material is siliciclastic sandstone (of fluvial, deltaic, and strandline origin) transitioning upwards to and mixed with tidal sediments such as dolomite and mudstones. Basal sandstones overlap Jurassic carbonates down dip beyond the Cotton Valley updip limit, see Figure 30) and Paleozoic rocks updip. The Basal Hosston in South Texas is an unusually sandstone-rich section that unconformably overlies the Cotton Valley Group and is conformably overlain by fairly thick and continuous shale. At the basinward edge or shelf margin (Bebout and Loucks, 1974) existed a complex of reefs and related sediments that persisted during Edwards and Glenrose times. Such reefs ringing some parts of the Gulf of Mexico existed during several periods (Sligo, Stuart City, Edwards) going across Webb County, then LaSalle, McMullen, Live Oak, Karnes, DeWitt and Lavaca Counties and beyond to the northeast. The earliest reef, the ***Sligo Trend***, is farther basinward and runs through Webb, Duval, and McMullen counties and merges with younger reef trends to the northeast. The Hosston Fm. forms the base of sediments that were deposited on the Paleozoic basement beyond the Ouachita Front. It forms the base of the Trinity Aquifer extending from Dallas to San Antonio (Mace et

al., 2000; Harden and Associates, 2004) but is present in the EF footprint only at greater depths as suggested in Figure 34 (Bexar County) and Figure 35 (cross-section located north of the study area but indicative of sections further south). Note that at deposition time, the large faults showed in the cross-sections did not exist and sediments were deposited on a relatively flat erosional surface (paleoplain). Examination of rocks on the upthrow compartment of the fault system informs well on the rocks on the downthrow side now buried at depths >4000 ft and quickly increasing gulfward (Figure 30 and Figure 31). Sligo extent and contour map of elevation of top are displayed in Figure 36 and Figure 37.

The ***Pearsall Shale*** is a dolomitic and argillaceous planktonic mudstone representing a rapid transgression over the Sligo limestone (Bebout and Loucks, 1974, p.12; Enomoto et al., 2002) and is present only south of the San Marcos Arch in the Maverick Basin (Figure 38 and Figure 39). Recall that the Rio Grande embayment to which the Maverick Basin belongs has experienced higher sediment input than the areas further north. The Pearsall has recently seen some interest as a shale gas (for example, Hull, 2011). A few wells were HF'ed in the mid 2000's. Formation is divided into three members, two clastic members with a carbonate member in between (Hull, 2011).

The shallow-water carbonates of the ***Glenrose Fm.*** were deposited on a broad shelf covering most of Texas. At the base, a sand, sometimes called Sycamore Sand, overlaps the Paleozoic basement and is seen as the outcrop equivalent of the Hosston sands. Some sands, called the Hensel sands, are also coeval of the Glenrose deposition (Figure 33 and Figure 34). A reef and associated sediments that continued on during Edwards times and called the ***Stuart City trend***, also developed at the shelf edge but slightly more inland than the Sligo Trend to the south before both merge in terms of geographic location at the level of Bee County. Its total thickness is of 2,000 to 2,500 ft.

Formations are arranged in higher-order categories called *groups*. Hosston / Sligo form the lower ***Trinity Group***, Pearsall / Hensell and associated strata from the Middle Trinity Group, and Glenrose (and Stuart City Trend) form the Upper Trinity. Georgetown, Del Rio and Buda Fms. form the ***Washita Group*** whereas Edwards and other formations from the ***Fredericksburg Group*** between the Trinity and Washita groups. Some well-known formations do not exist in South Texas. For example, the Paluxy Fm. between the Glenrose and Edwards Fms. Is well-developed in East and North Texas but not in South Texas. Similarly the Walnut Fm. present in Central and North Texas does not exist in South Texas (Hovorka et al., 1996, Fig.1).

Similarly to the Glenrose Fm., the ***Edwards Fm.*** was deposited on a shallow platform that extended to the Stuart City reef at which point deposits transitioned to deep-sea deposits in the ancestral Gulf of Mexico. The Edwards in the Maverick Basin where it consists of ~700 ft of fine-grained limestone is different from more porous sediments further north (Scott, 2004, p.608) and of lower porosity as if was deposited in a subtidal environment (Hovorka et al, 1996, p.1). The thickness of the Edwards Group increases towards the south to the open sea and to the west in the Maverick Basin (Figure 40).

The ***Georgetown Fm.*** was deposited in deeper water than the Edwards Fm. but did so on the eroded and previously aerially exposed top of the Edwards Fm. Both the Edwards and Georgetown Fms form the Edwards Aquifer. The ***Del Rio Clay*** is a thin calcareous marine shale overlying the Georgetown Fm. The ***Buda Fm.*** is a carbonate mudstone deposited on a relatively flat depositional surface (Scott, 1977, p.166).

The ***EF shale*** extends all the way to the Stuart City trend / Sligo shelf margin where its depth is >15,000 ft (see next Section III-1-2). Directly overlying the EF, the ***Austin Chalk*** is a laterally extensive open-marine micrite (fine carbonate mud) overlaid by a discontinuous carbonate bank called the Anacacho age-equivalent to downdip clays (Upson Fm.). The Austin Chalk contains some large fields and has been subjected to HF.

Formations from the ***Navarro Group*** and ***Taylor Group*** complete the Cretaceous succession leading to the Midway clay. Those two groups are considerably more developed in South Texas in the Maverick Basin. There, three terrigenous clastic wedges correspond to a large sediment influx resulting from erosion of the newly formed Rockies and related mountain ranges located closer to the basin: ***San Miguel, Olmos, and Escondido Fms*** (Tyler and Ambrose, 1986; Dutton et al., 1993).They contain mostly deltaic sandstones but the Olmos includes also strandplain and fluvial deposits. Figure 41 shows that Olmos outcrop is mostly clayey and not very thick. The San Miguel and Escondido are marine sands and shales, while the Olmos is largely non-marine and contains plant-rich shales, coal, and fluvial sediments (Scott, 2004). Deposits with significant thickness cover southern Maverick, northern Webb, Dimmit, Zavala, Frio and half of LaSalle counties. Underlying the Olmos the San Miguel formation is very similar in terms of location of the major depocenters and overall extent (Weise, 1980, p.5). The Olmos sands contain many small fields some of which are tight gas and require HF to produce gas. In addition, numerous small basaltic volcanic plugs intruded these formations in South Texas. These formations transition to the Navarro (Escondido Fm.) and Taylor (San Miguel and Olmos Fms.) groups traditionally described in Central Texas. The Navarro overlies unconformably the Taylor group. The Escondido Fm. truncate the Olmos Fm. in the outcrop and shallow subsurface.

III-1-1.3Cenozoic and Younger Formations

The ***Midway Fm.*** of Paleocene age (***Kincaid Fm.*** in the Maverick Basin) represents the first strata of Cenozoic age and is partly composed of dense marine clays. The Midway Fm. is transitional between the fully marine deposits of the Upper Cretaceous and the foredelta and lower delta floodplain deposits of the Lower Wilcox (Fisher and McGowen, 1967; Bornhauser, 1979; Roy, 1984; Ayers and Lewis, 1985; Dutton et al., 2003).

Thickness of the ***Wilcox Group*** in South Texas vary progressively from ~1000 ft at the outcrop to ~4000 ft towards the shelf edge at which point it grows quickly to >8000 ft and larger (Bebout et al., 1982, Fig.8) (Figure 42). The Wilcox is generally subdivided into lower, middle, and upper intervals. The ***Lower Wilcox*** (Figure 43) consists in a barrier bar and lagoon-bay system (Fisher and McGowen, 1967). Sand units can be as thick as 100 ft and have an aggregated thickness between 400 and 100 ft in South Texas. Mud facies occur northwest of this bar system and forms the Lower Wilcox outcrop in South Texas. Because rocks in outcrop look (and are) different, those deposits were given a different name early on: ***Indio Fm***. The sandy bar facies transition to the southwest to muddy shelf deposits (Figure 43). The delta muds at the base of the Lower Wilcox transition to the marine clays of the Midway (Figure 44). Further north, in Central Texas the (outcrop) lagoon facies disappears to leave place to strandplain deposits and the thick so-called Rockdale delta extending further north to East Texas [strike-oriented sand bodies in South Texas as opposed to dip-oriented in Rockdale Delta not good for recharge but good for confinement]. The Lower Wilcox is sometimes called the Hooper Fm. in Central Texas. Beyond the Colorado River towards the north, a thick sand package called the Simsboro Fm. corresponds to the Middle Wilcox and is the continuation of the Rockdale delta deposits (Dutton et al., 2003, p.22) (Figure 45a). The ***Middle Wilcox*** of South Texas is composed of marine and lagoonal

muds. The ***Upper Wilcox***, called the Calvert Fm. on Central and East Texas GAT sheets, contains abundant lignite resources indicative of a low-energy environment but also large sand bodies that can provide significant volumes of water. Nomenclature and interpretation are not always entirely settled or clear. The fluvial ***Carrizo Sands*** are well-characterized at the outcrop but its more deltaic and marine facies downdip equivalents are merged with the Upper Wilcox especially in South Texas (Bebout et al., 1982; Hamlin, 1988; Xue and Galloway, 1995; Dutton et al., 2003, p.19). Carrizo Sands thickness increases from Central Texas to South Texas (Figure 45b). Carrizo sands are the fluvial (continental) unit whether the marine time equivalent is included in the Upper Wilcox. The upper Wilcox subgroup consists of the South Texas Rosita delta system, the associated strand-plain and barrier-bar system, and the updip Carrizo fluvial system (Xue and Galloway, 1995) that fed the Rosita Delta. A prominent feature, the Yoakum Channel, is present mostly in Lavaca County along its boundary with De Witt County and consists in sands corresponding to an incised valley through the entire Wilcox succession.

Deposits of the ***Claiborne Group*** that overlies the Wilcox Group also reflect several episodes of fluvial and deltaic progradation, marked by thick sandstones of the Queen City and Sparta Fms, interspersed with relative marine advances marked by the marine shale of the Reklaw, Weches, and Cook Mountain Fms (Dutton et al., 2003)

The ***Recklaw Fm.*** caps Upper Wilcox deposits and consists in regionally transgressive shelf mudstones (Galloway et al., 2000). In South Texas, south of the Frio River in the Maverick Basin in the Rio Grande embayment, the fluvial-deltaic ***Bigford Fm.*** is age-equivalent to the Reklaw, consists mainly in sands, silts, and shales, and directly overlies the Carrizo sands (Figure 46 and Figure 47).

The ***Queen City Fm.*** represents another prograding event well developed in the Rio Grande embayment with lagoonal facies in what is now the outcrop of the Fm. in South Texas. repeating a pattern already seen in the Wilcox with the Indio Fm., those deposits were given a different name: ***El Pico Clay*** (Figure 47). Figure 48 illustrates the extent of the mostly lagoonal faces in the outcrop. To the East, sediments carried by the ancestral Rio Grande and other rivers accumulated in a thick fluvio-deltaic package (up to 2500 ft with >1000 ft of net sands locally) with its thickness decreasing towards the NE in Central Texas (mostly strandplain deposits) and North Texas (Figure 49).

The muddy glauconitic ***Weches Fm.*** overlies the Queen City Fm., represents another regional transgressive episode, and is traceable in subsurface throughout Texas. It is composed of shelf sediments in the lower part and prodelta fades in the upper part that are related to the overlying Sparta delta progradation (Guevara and Garcia, 1972). The Weches is a thin formation, generally less than 100 feet thick and represents a period with low sediment influx (Galloway et al., 2000).

The sand-rich Sparta Sands or ***Sparta Fm.*** represent another progradation interval but one for which the main sediment input was further north in the Houston and Mississippi embayments. Consequently, thickness of the Sparta Fm. in South Texas is less than that of the same formation in Louisiana and that of the previous progradation interval (Queen City Fm.) (Figure 50). Sands are mostly strandplain deposits with minor local influx and interspersed lagoonal facies in outcrop. In south Texas, the Sparta varies in thickness from 300 ft updip to 500 to 750 ft downdip thickening toward Mexico (Ricoy and Brown, 1977). However, sand fraction also decreases downdip, resulting in a net sand thickness decreasing downdip (Figure 50).

The Sparta F. is overlain by deposits from another marly marine transgressive event, the ***Cook Mountain Fm.***, consisting in shelf deposits transitioning to prodelta or lagoonal mudstones updip. In south Texas, west of the Frio River, the Cook Mountain Fm. is absent as such and its equivalents and the Sparta Fm. are combined under the ***Laredo Fm.*** (outcrop name).

The ***Yegua Fm.*** represents another important prograding event (Figure 51). It forms, with the Cook Mountain Fm., the Upper Clairborne Group. The Yegua Fm. was deposited during a strong influx of sediment, primarily in the Houston Embayment area (Fisher, 1969; Meckel and Galloway, 1996; Knox et al., 2007) but its thickness in South Texas can reach >2000 ft. Sand is more widespread in the downdip area but also occurs in the outcrop. They are mostly deltaic sands and their feeding fluvial systems. However, as noted by many authors, deltaic sediments show the imprint of wave energy that orients them along strike.

The ***Jackson Group*** overlies the Yegua Fm. and presents similar characteristics but occurs mostly outside (to the SE) of the EF footprint (Figure 52). Only the sections containing fresh water are of interest. Similarly outcrop expressions of formations overlying the Jackson Group are the Oligocene ***Frio Clay*** and Oligo-Miocene ***Catahoula Tuff***. Combined they form an aquitard underlying the Miocene ***Oakville Sandstone*** (locally in communication with Catahoula sandstone -Figure 53) (Figure 54 and Figure 55) separated from the Pliocene ***Goliad Sand*** by the Fleming Fm. (see, for example, Ryder and Ardis, 1992, and Nicot et al., 2010 for details). Oakville Sandstone and Goliad Sand are components of the Gulf Coast Aquifer System which provides some water to some EF HF operations.

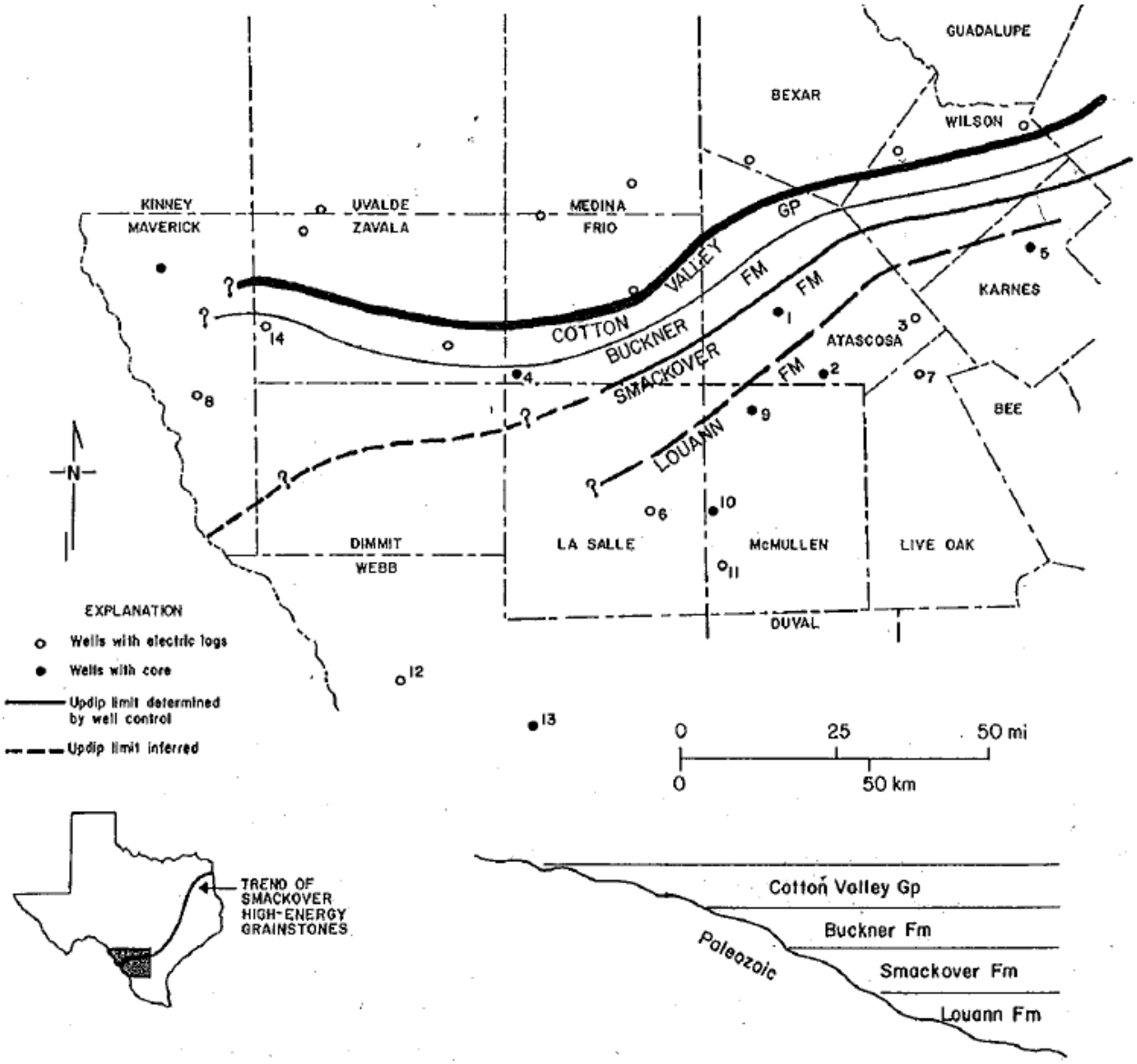

Source: Budd and Loucks (1981, Fig.3)

Figure 30. Updip limits exhibited by Jurassic strata

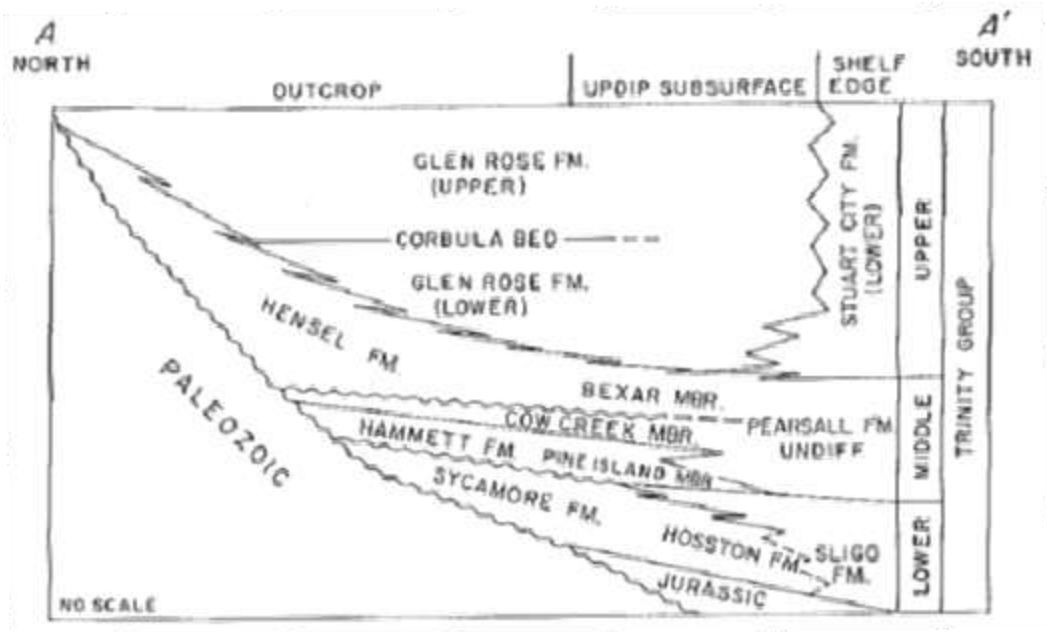

Source: Loucks (1977, Fig.4)
Note: idealized cross section through Bexar, Wilson and Karnes counties

Figure 31. Stratigraphic diagram of Trinity Group in South Texas

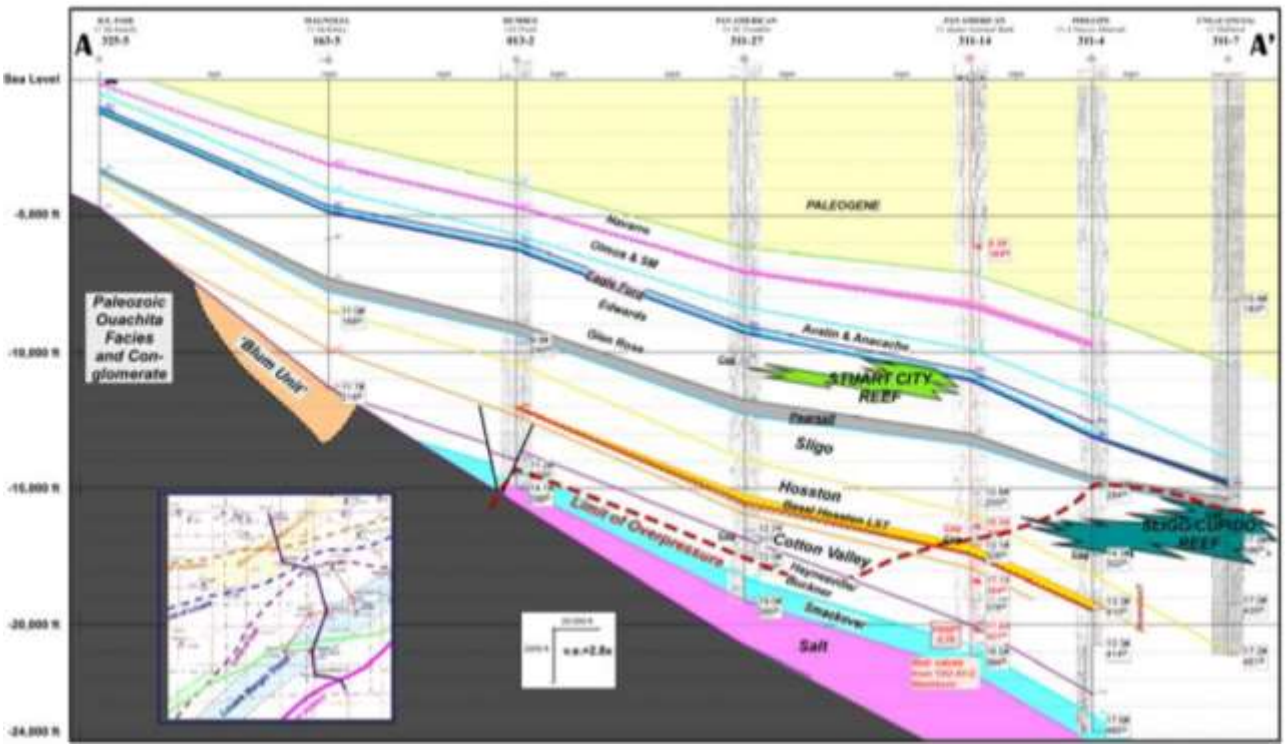

Source: unmodified from Ewing (2010, Fig.4)
Note: point A is in southern Medina County and point A' on the McMullen-Duval county line.

Figure 32. Regional north-south cross section in Atascosa and McMullen counties, Texas

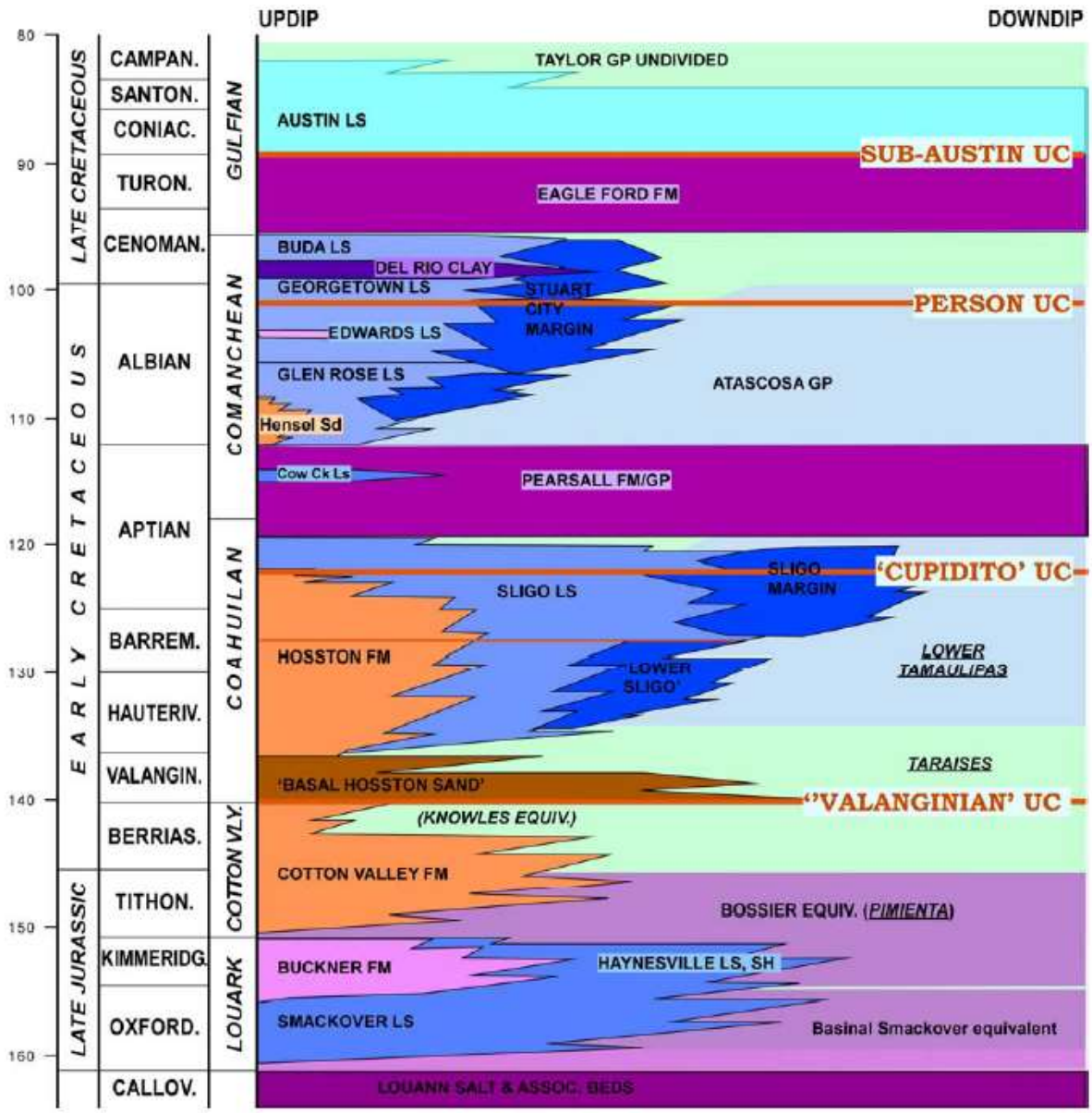

Source: unmodified from Ewing (2010, Fig.5)

Figure 33. Time-stratigraphic section of Jurassic and Cretaceous strata in South Texas.

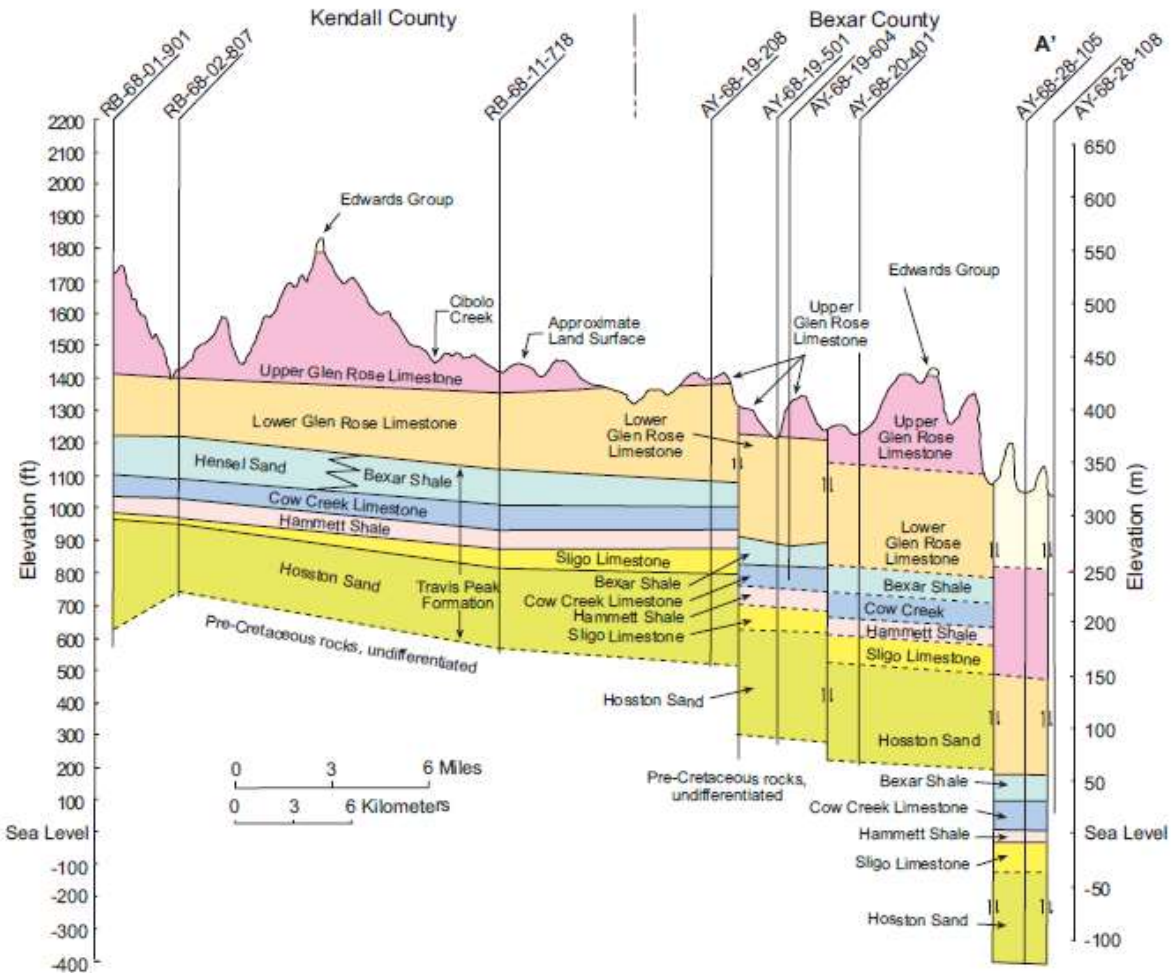

Source: Mace et al. (2000, Fig.9)

Figure 34. NW-SE cross section through Kendall and Bexar Counties

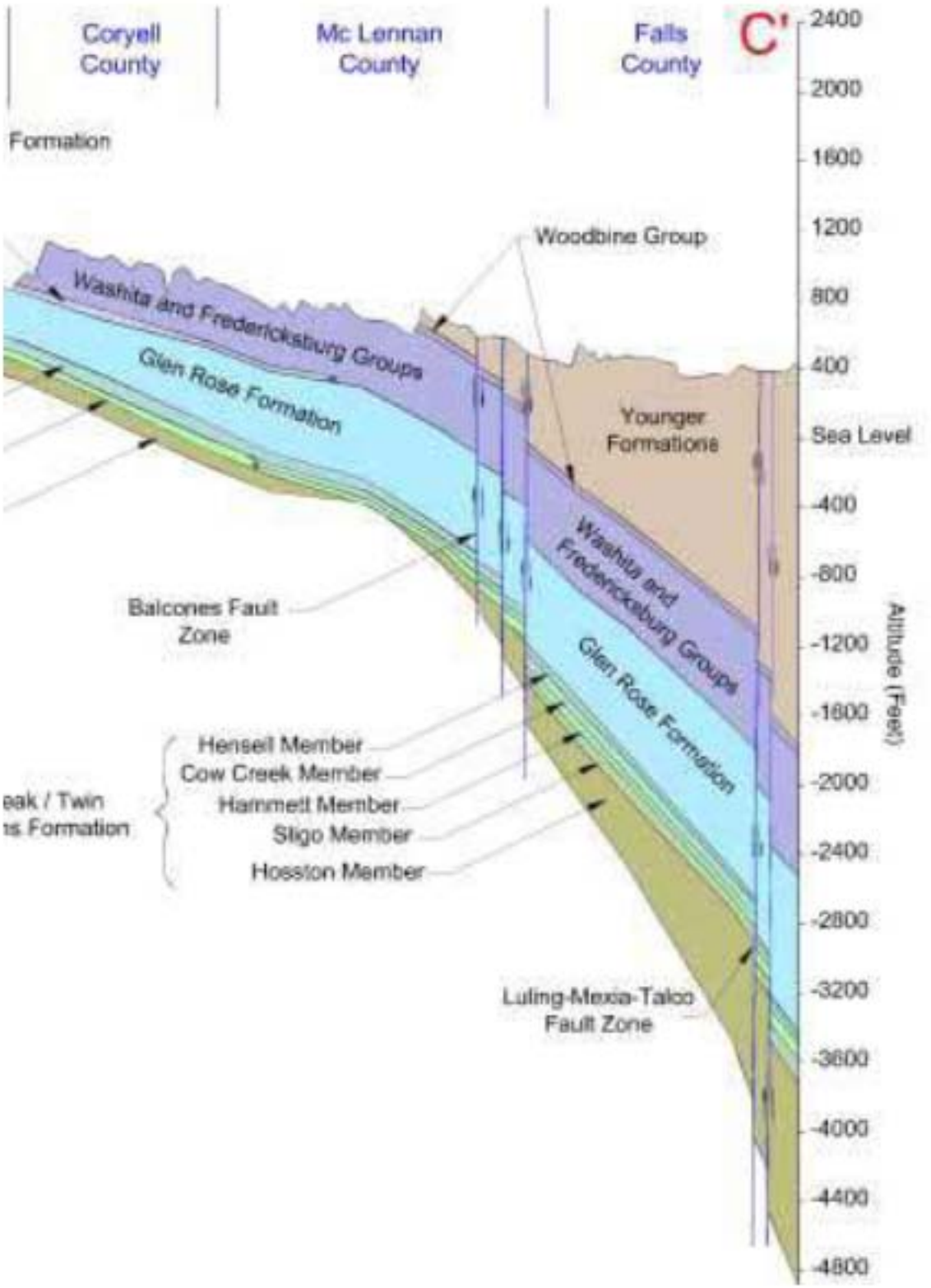

Source: Harden and Associates (2004, Fig. 2.16)

Figure 35. NW-SE cross section through McLennan and Falls Counties

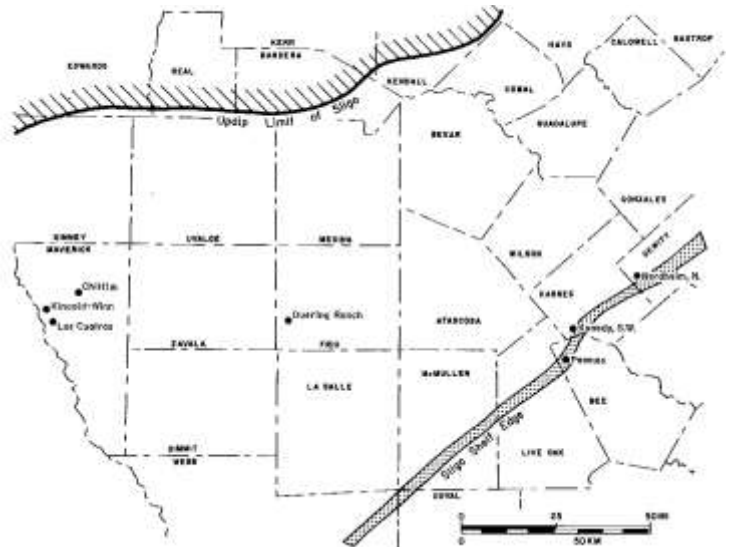

Source: Bebout et al. (1981, Fig.3)
Note: Sligo deposits exist between shelf edge and updip limit

Figure 36. Location of Sligo Formation in South Texas

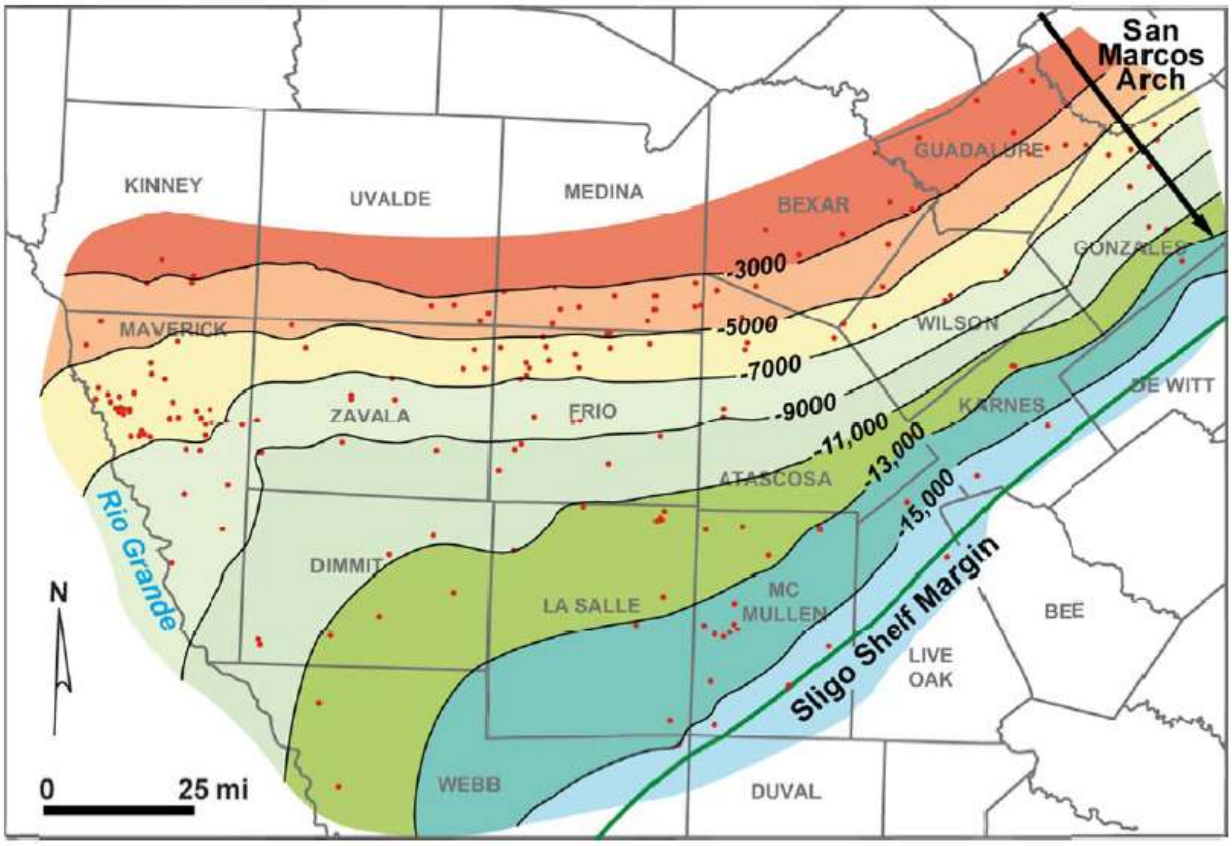

Source: Hull (2011, Fig. 2.6)

Figure 37. Structure map on top of the Sligo Formation (~bottom of the Pearsall Fm.)

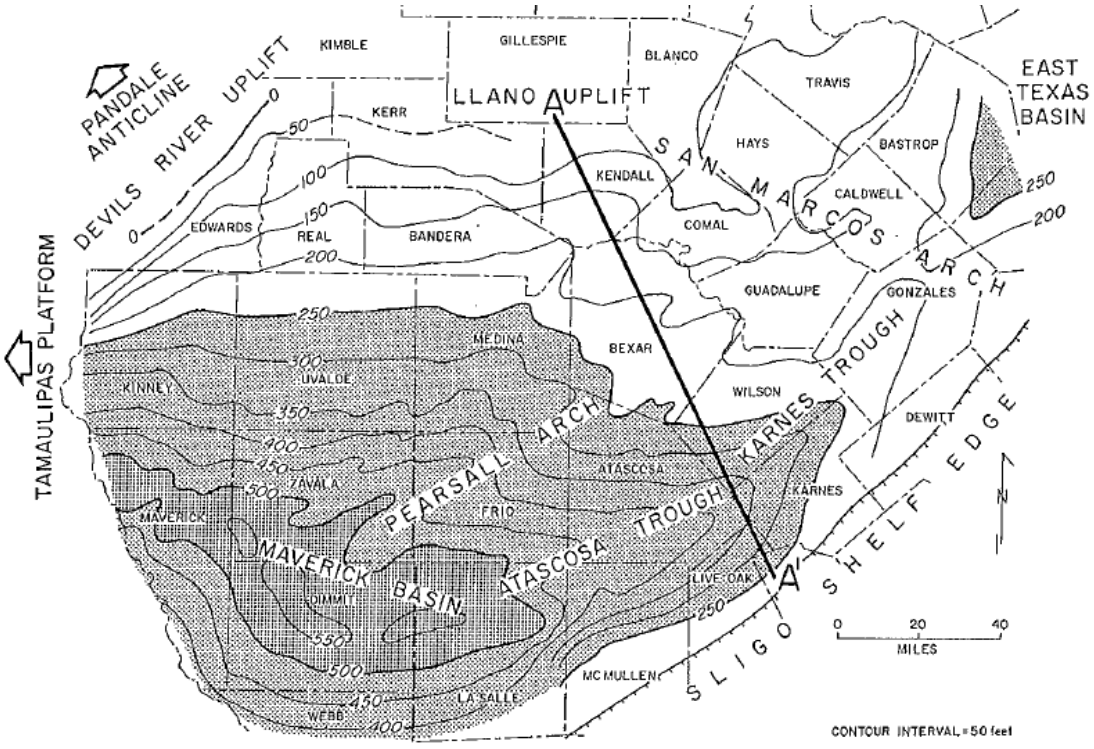

Source: Loucks (1977, Fig.3)

Figure 38. Pearsall Formation isopach

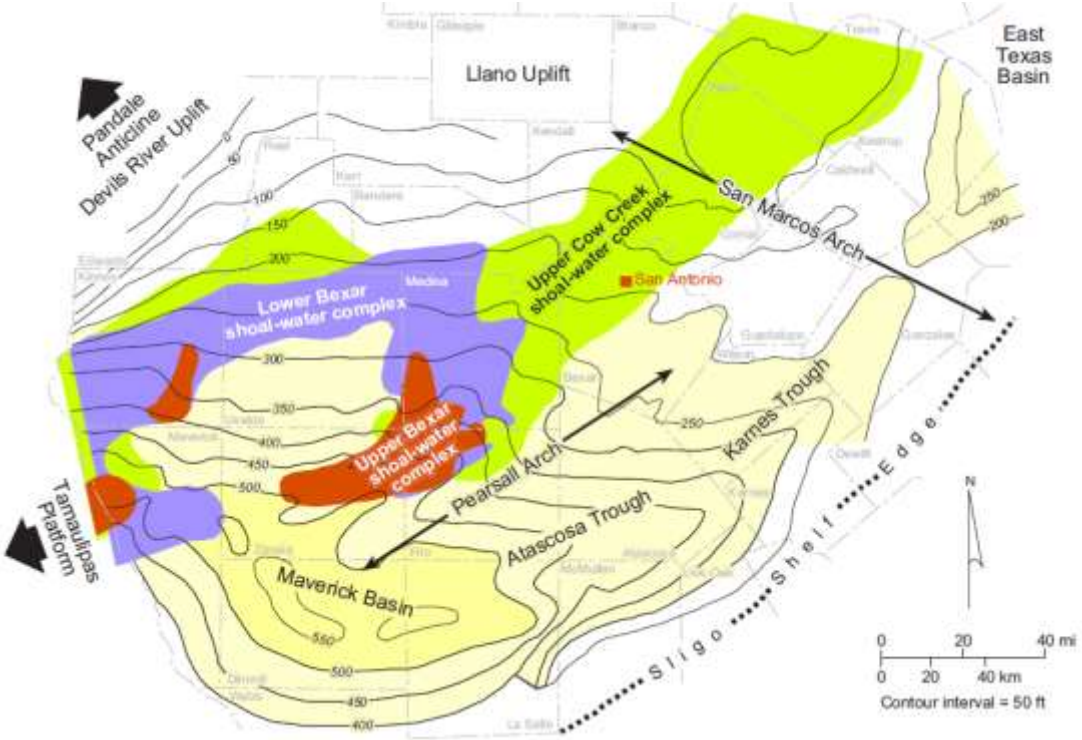

Source: Loucks (2002, Fig.2)

Figure 39. Isopach map of Pearsall Fm. with major paleogeographic features

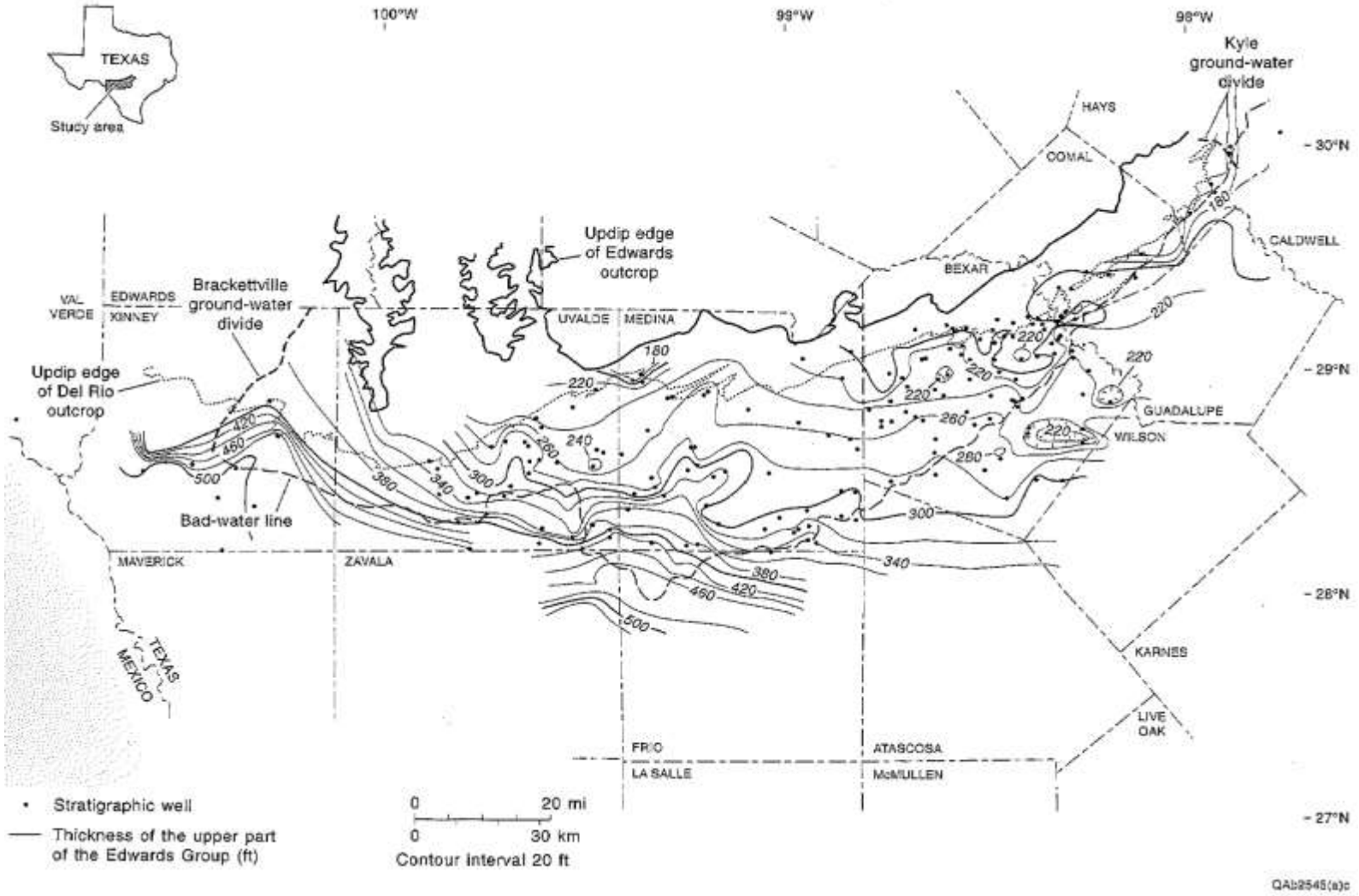

Source: Hovorka et al. (1996, Fig.25)

Figure 40. Isopach map of the Edwards Group

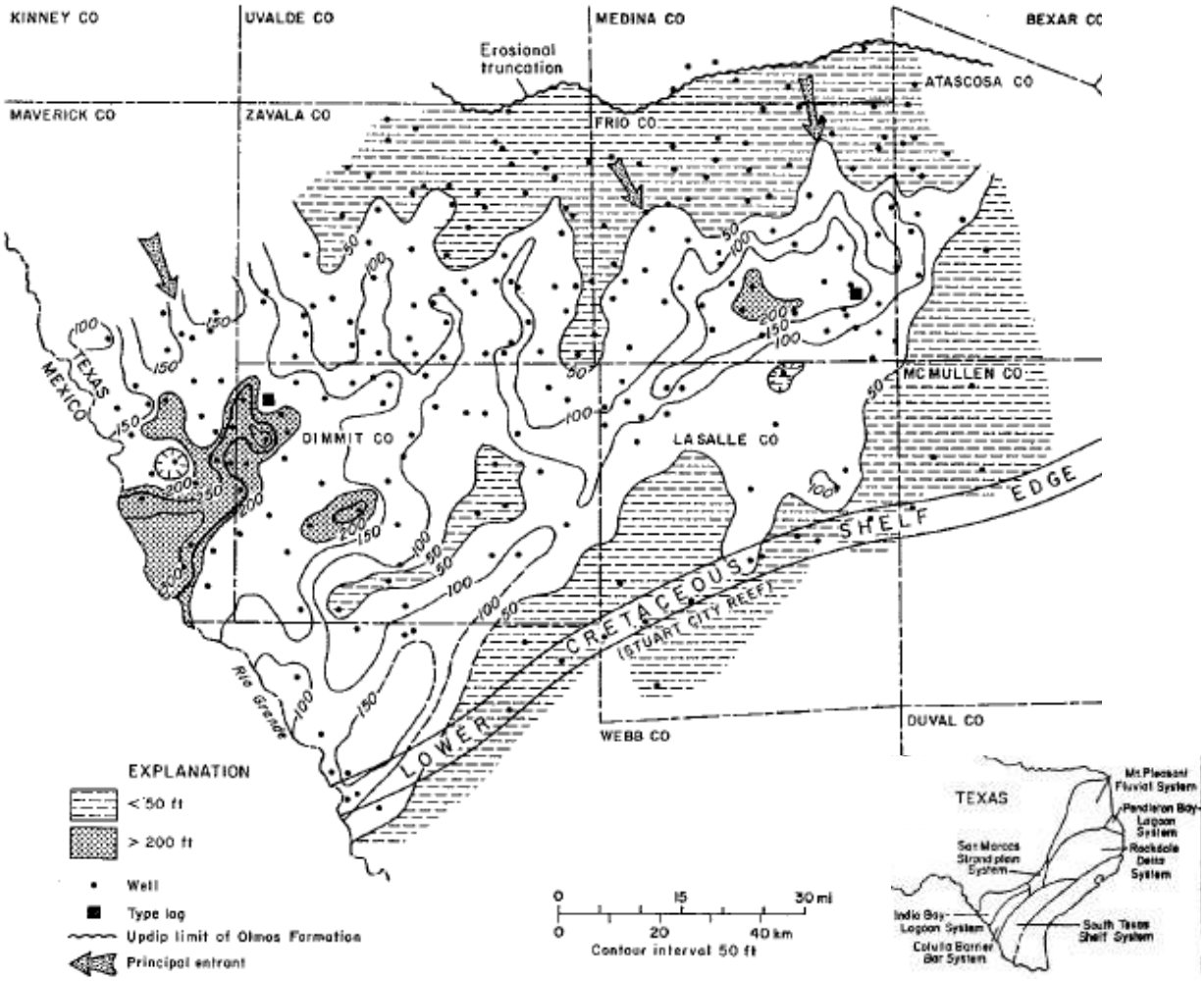

Source: Tyler and Ambrose 1986, Fig. 6)
Note: Sediments were transported from the north and northwest into an eastern depocenter in Frio County and a larger western depocenter in Maverick and western Dimmit Counties

Figure 41. Net sandstone map of the Olmos Formation

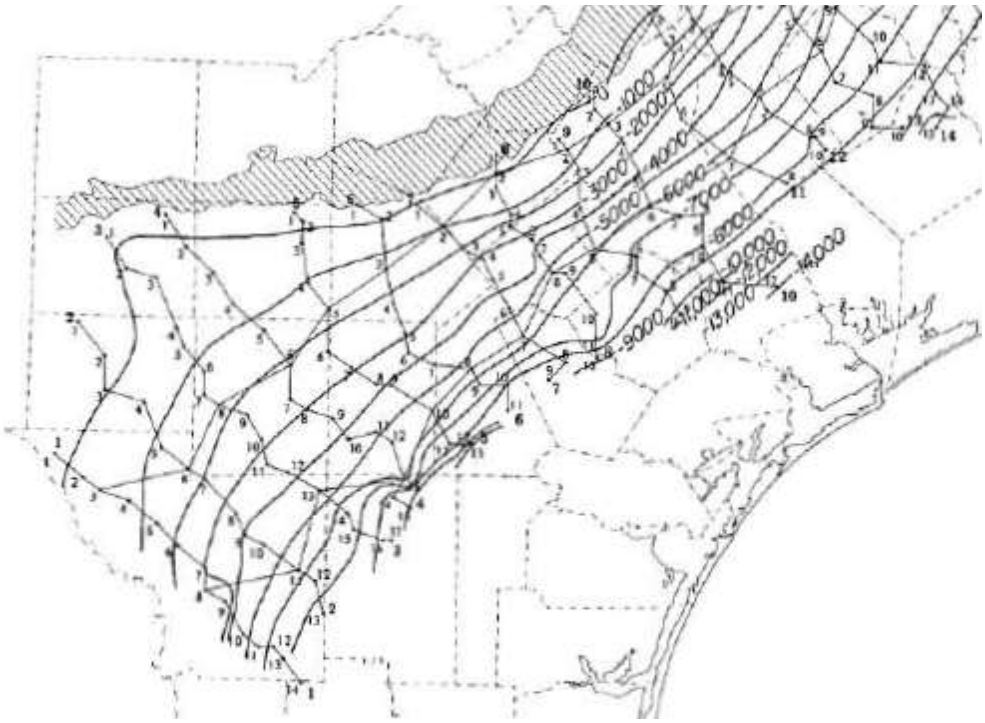

Source: Bebout et al. (1982, Fig.8)
Note: Wilcox outcrop is stippled

Figure 42. Total thickness of the Wilcox Group

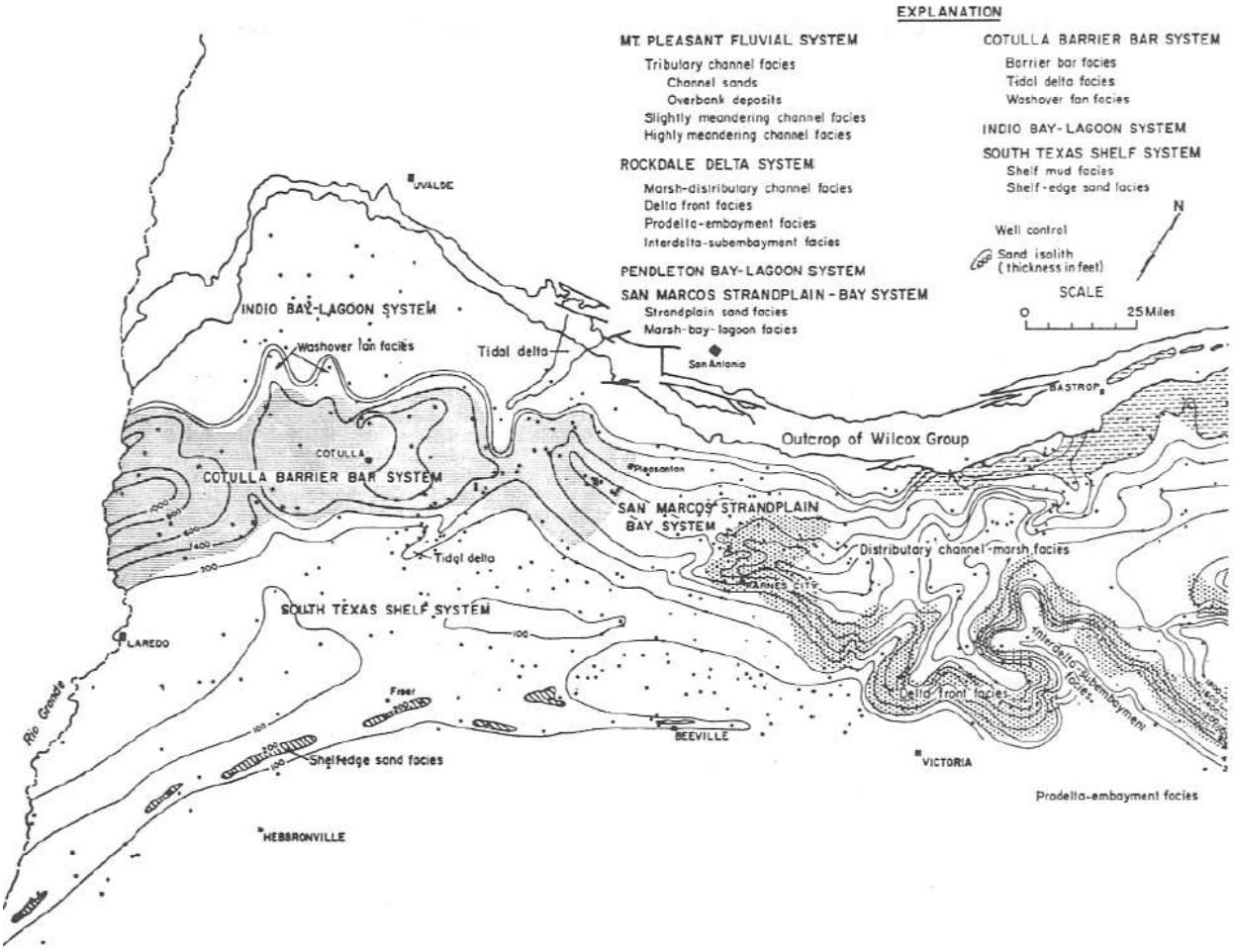

Source: Fisher and McGowen (1967, Fig.1)
Note the orientation of the north arrow

Figure 43. Lower Wilcox sand map and depositional environments.

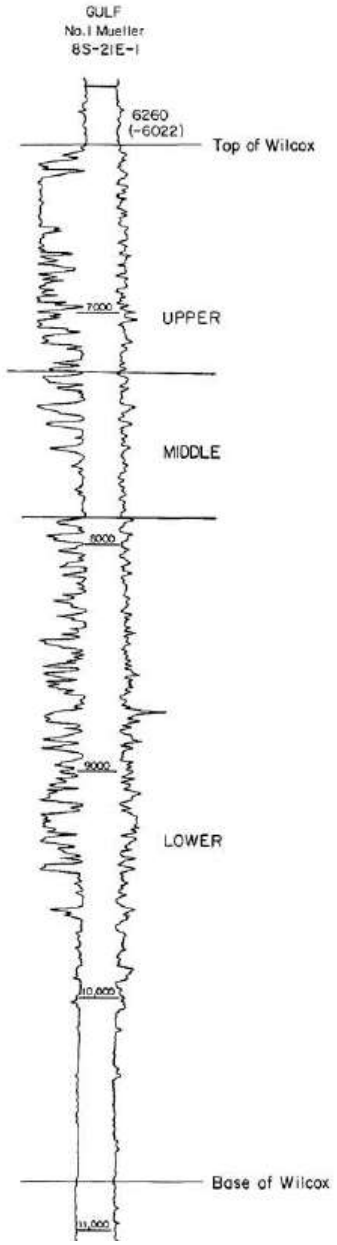

Source: Bebout et al. (1982, Fig. 10)
Note transition to Midway Clay at the bottom and to the Reklaw Fm. at top
Note: Bebout et al (1982, p.4) include Carrizo in their definition of Upper Wilcox

Figure 44. Well log in De Witt County showing ~4,500 ft of Wilcox Group and Carrizo

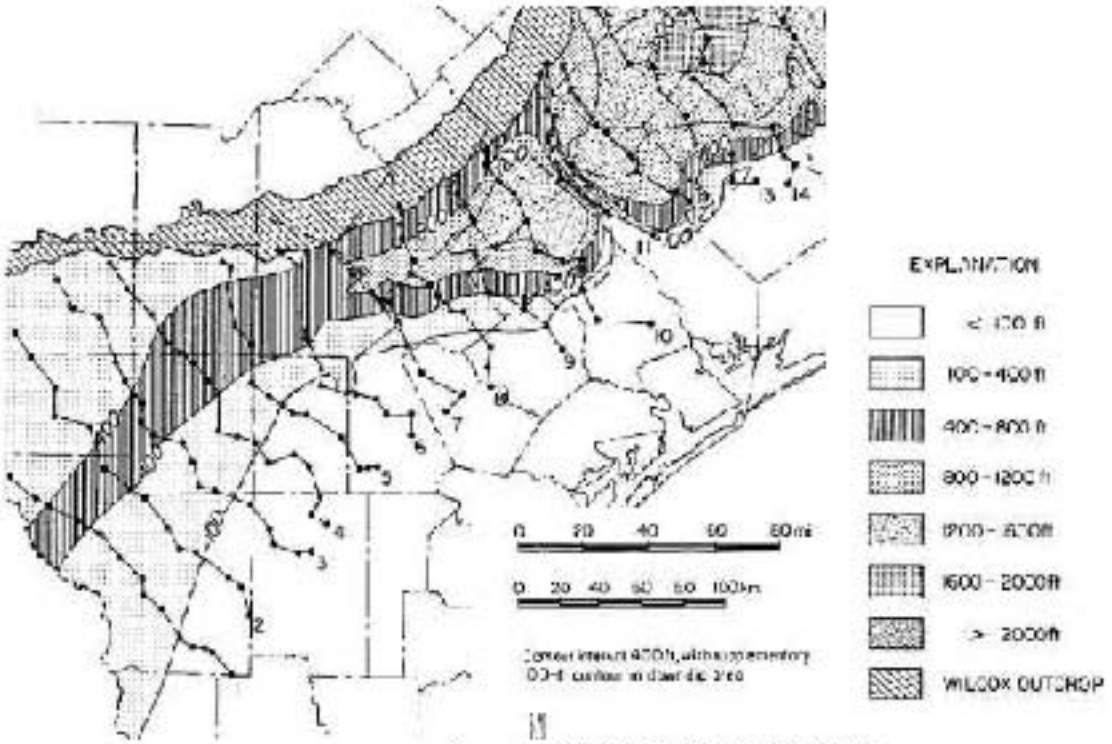

(a)

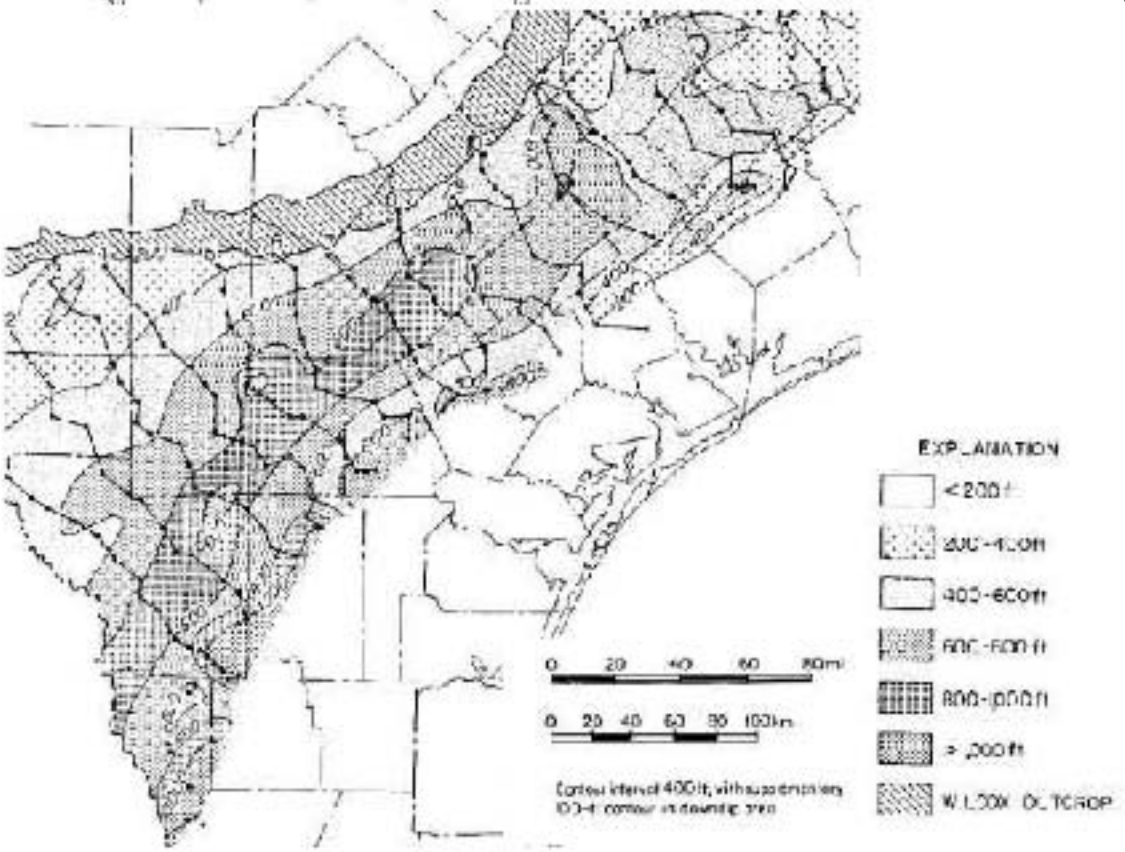

(b)

Source: Bebout et al. (1982, Fig.34 and 35)
Note : Bebout et al (1982) include Middle Wilcox in their definition of Lower Wilcox
Note : Bebout et al (1982, p.4) include Carrizo in their definition of Upper Wilcox

Figure 45. Net-sandstone map, (a) lower and (b) upper Wilcox Group

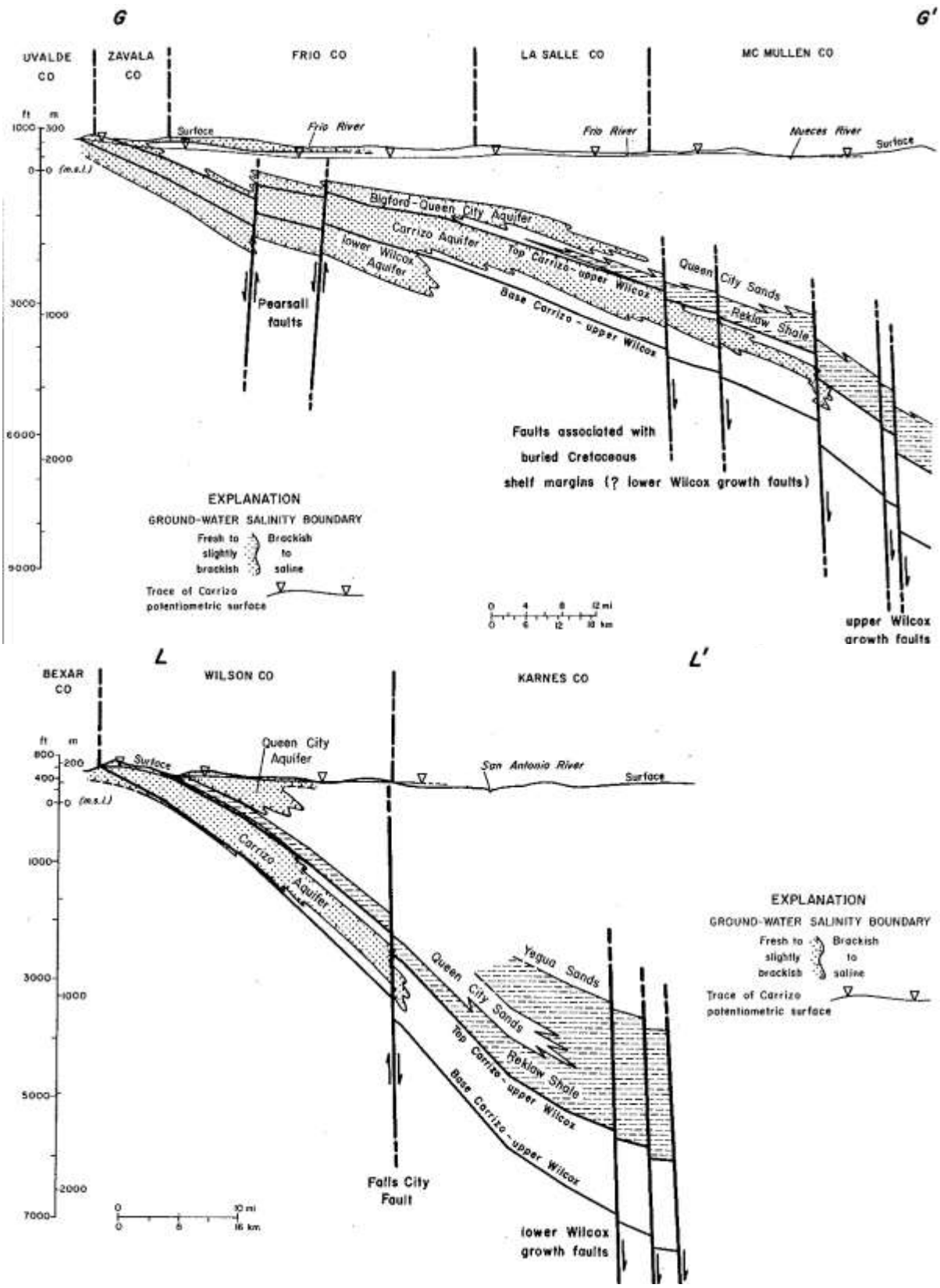

Source: Hamlin (1988, Fig.24 and 25)

Figure 46. South Texas NW-SE cross sections, Wilcox Group and Queen City Fm.

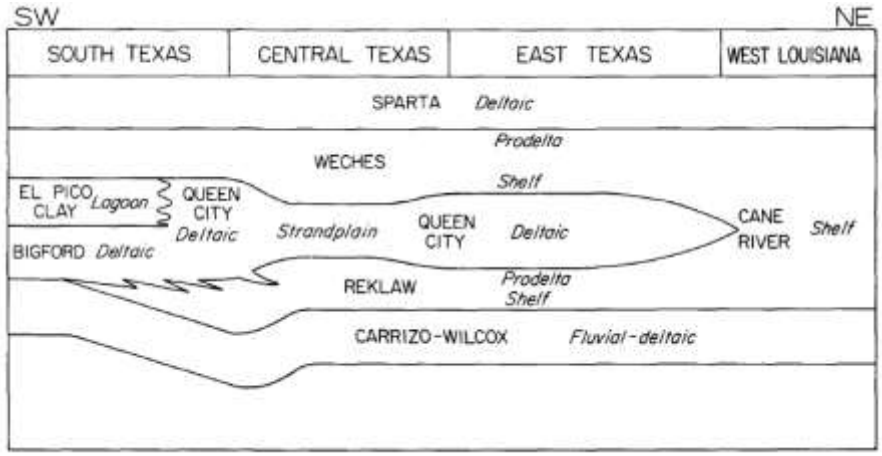

Source: Guevara and Garcia (1972, Fig.14)

Figure 47. Relationship between formal stratigraphic nomenclature and facies of the Queen City depositional systems.

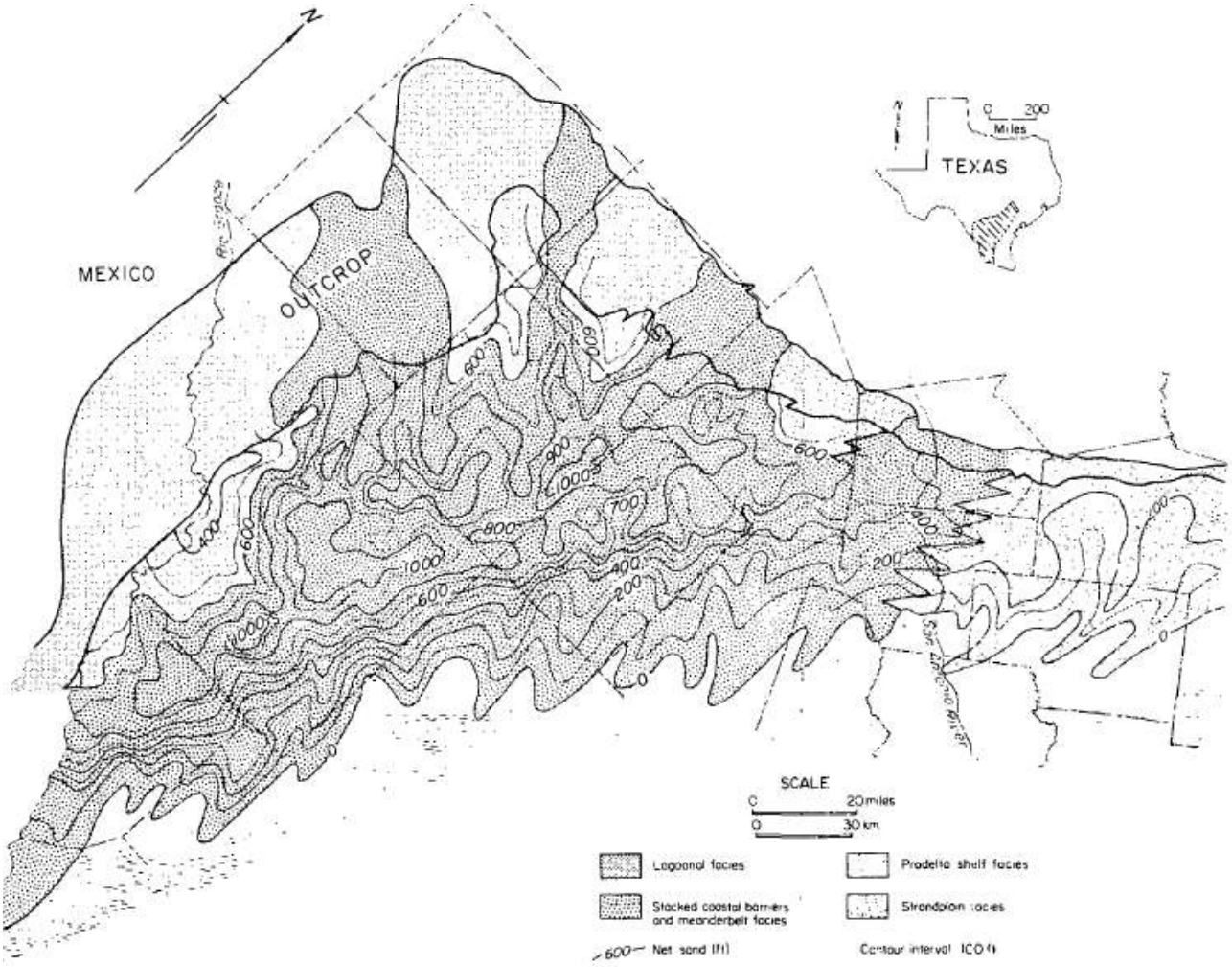

Source: Guevara and Garcia (1972, Fig.3a)

Figure 48. Net sand map and principal facies in the Queen City Formation and equivalent units, South Texas.

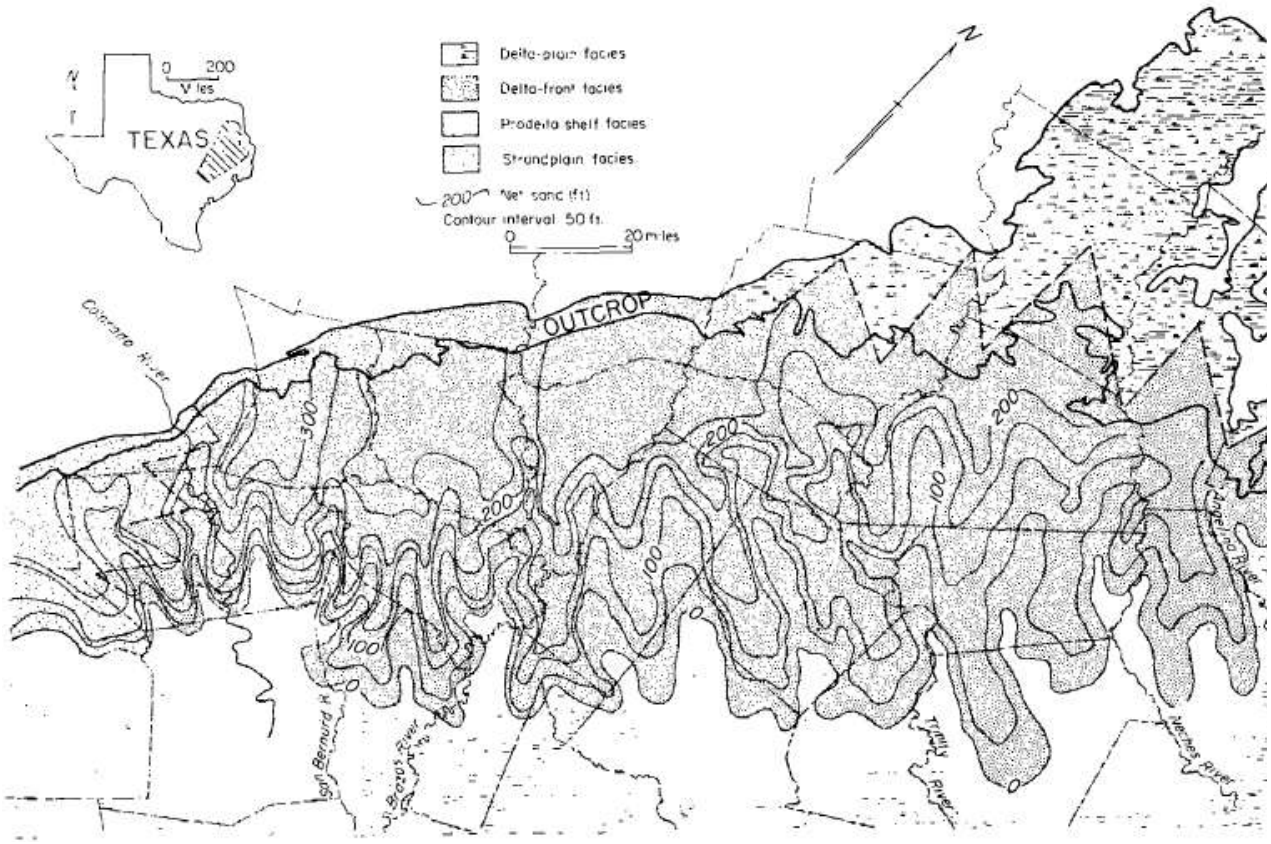

Source: Guevara and Garcia (1972, Fig.3b)
Note: continuation to the NE of Figure 48

Figure 49. Net sand map and principal facies in the Queen City Formation and equivalent units, Central and North Texas.

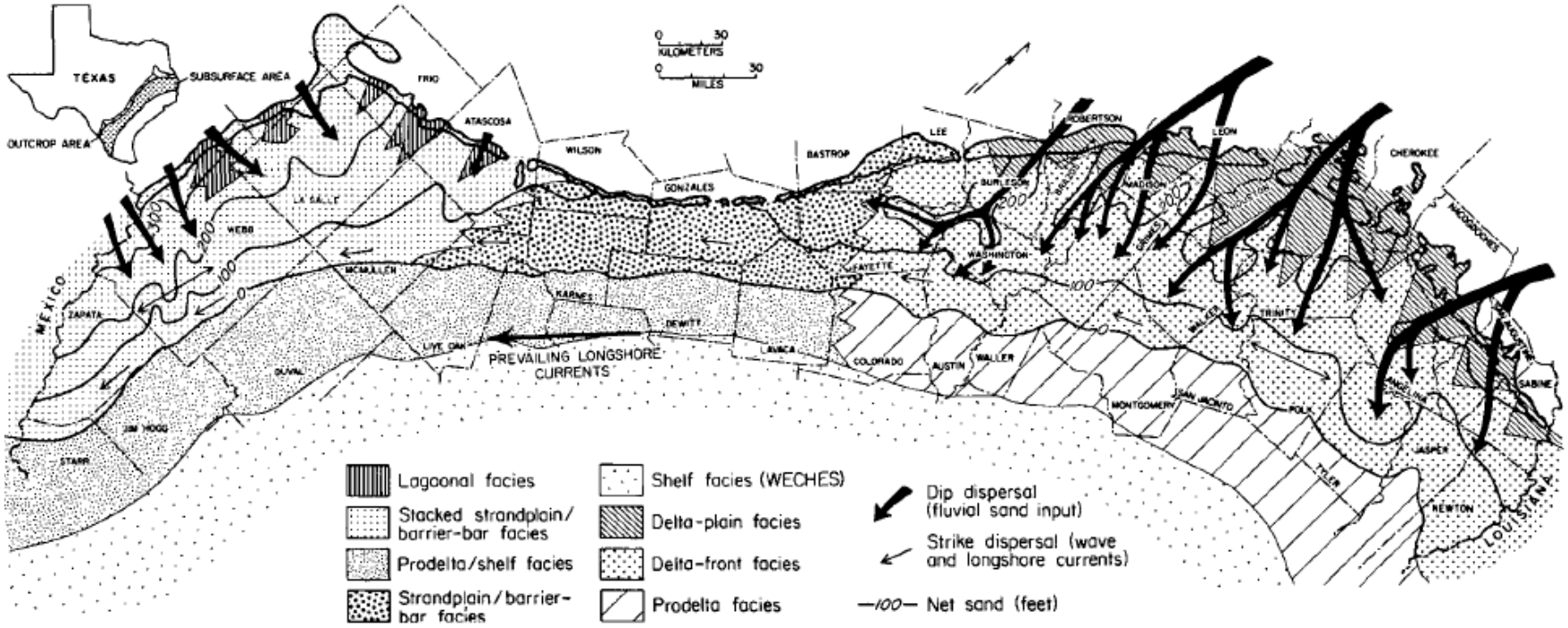

Source: Ricoy and Brown (1977, Fig. 7)

Figure 50. Net sandstone, areal distribution of principal facies, and inferred dispersal system, Sparta depositional systems, Texas Gulf Coast

Thickness Upper Yegua

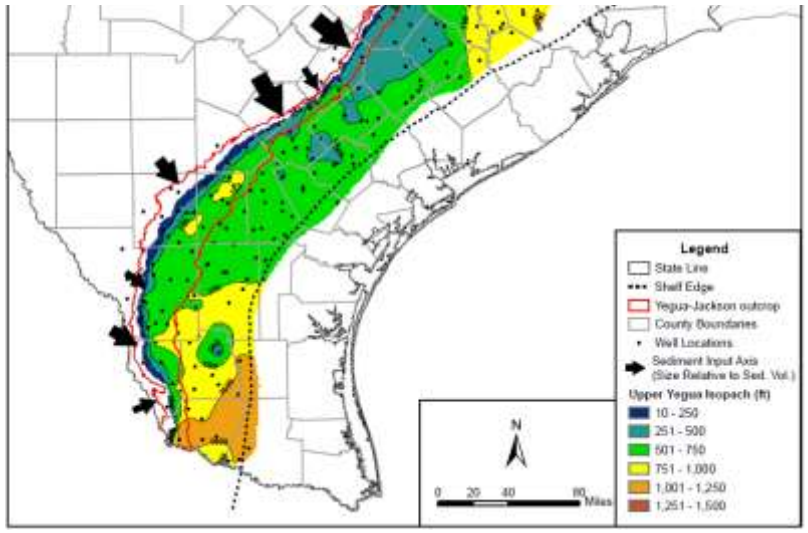

(a)

Thickness Lower Yegua

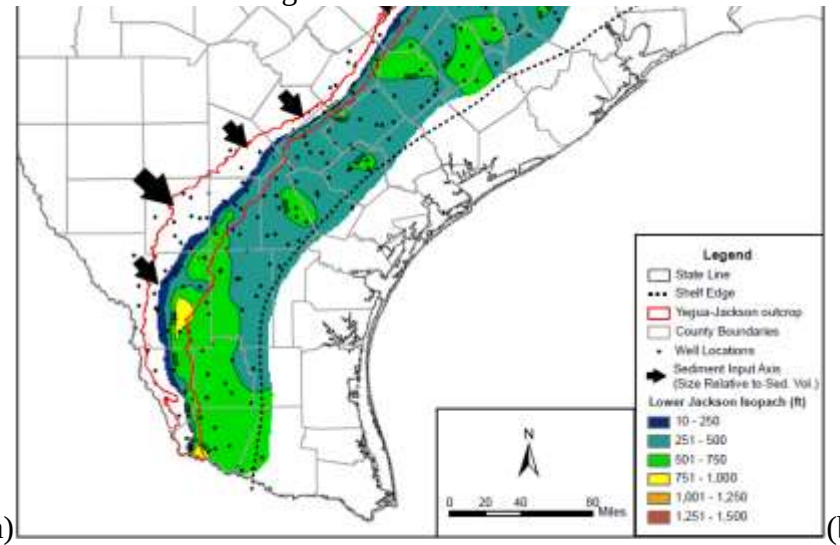

(b)

Sand fraction Upper Yegua

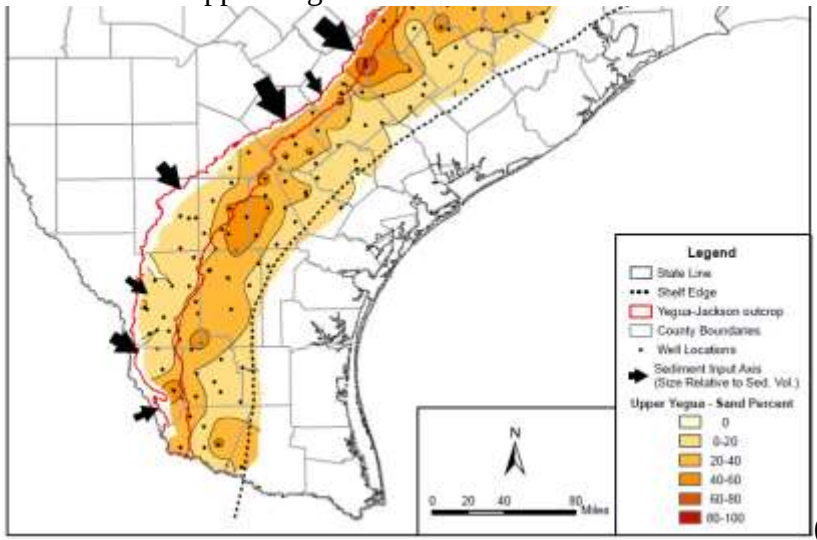

(c)

Sand Fraction Lower Yegua

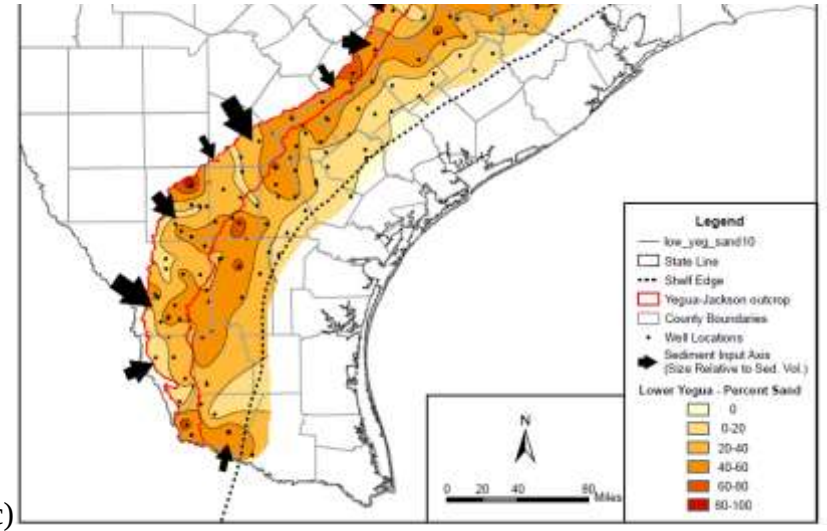

(d)

Source: Knox et al. (2007), cropped from Fig. 5.2, 5.3, 5.8, and 5.9

Figure 51. Thickness and sand fraction of the Upper and Lower Yegua

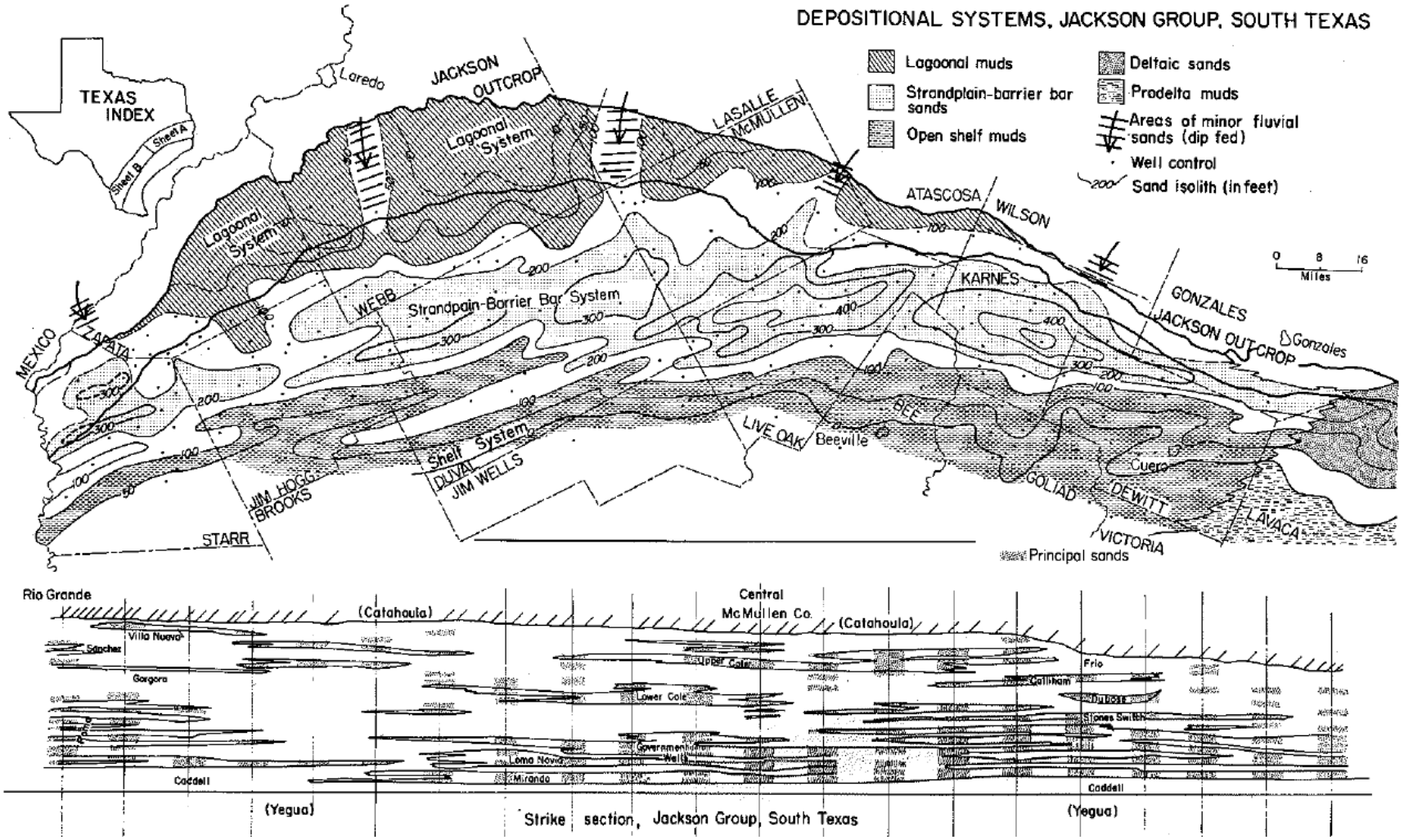

Source: Fisher et al. (1970, Fig.1b)

Figure 52. Net-sand isoliths, principal depositional systems, and strike profile (along maximum sand thickness) of the entire Jackson Group.

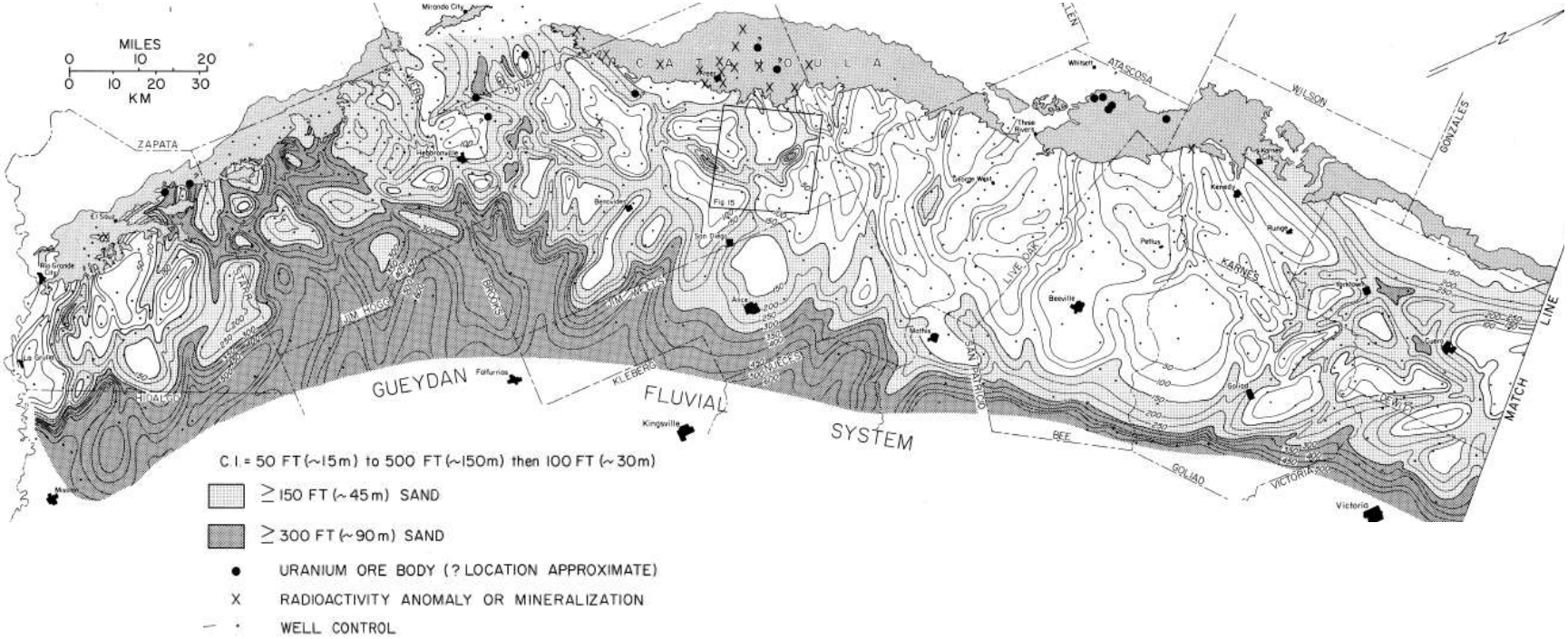

Source: Galloway (1977, Plate I)

Figure 53. Catahoula net-sand isopachs

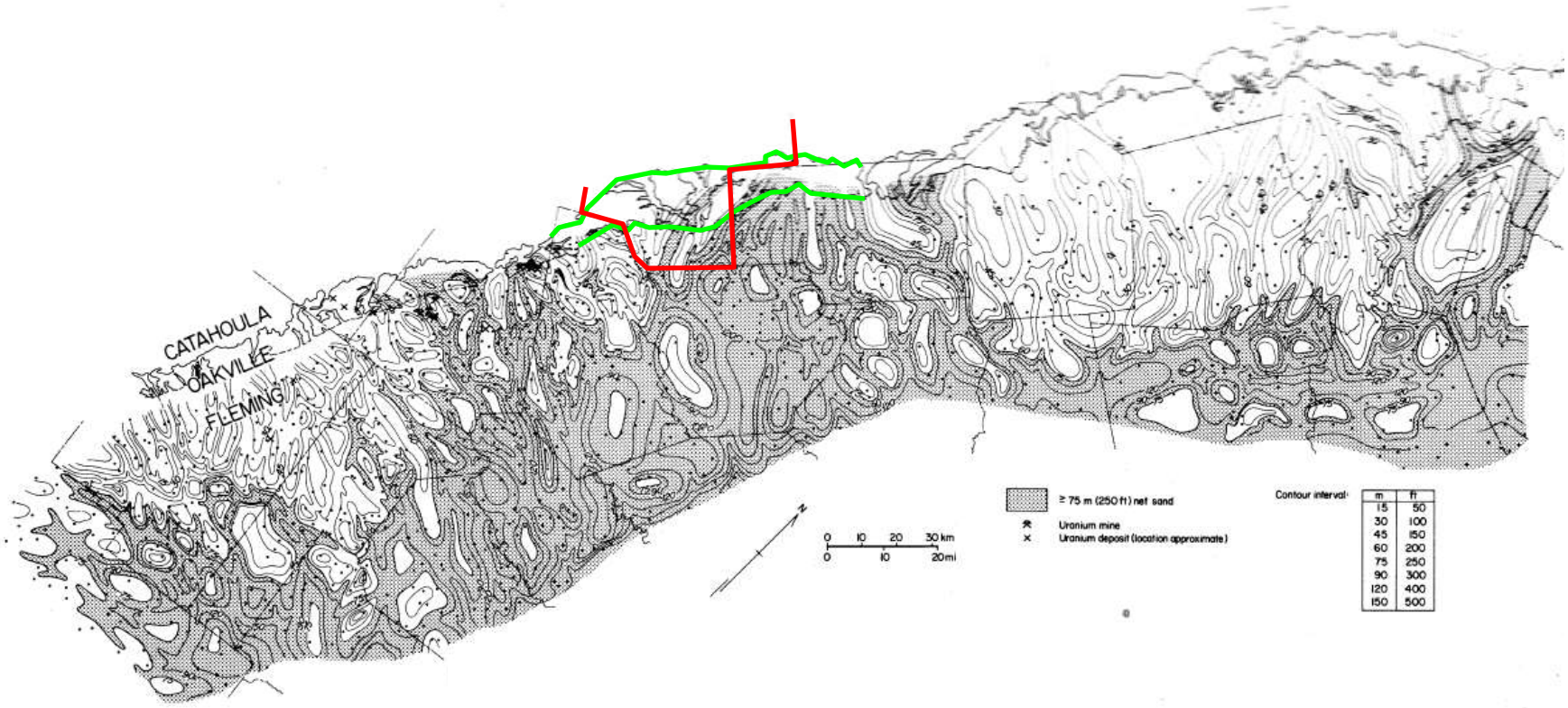

Source: Galloway et al. (1982a, Fig.5)
Note: Southeastern Karnes County boundaries are shown in red, and Oakville outcrop across Karnes County is highlighted in green.

Figure 54. Net-sand isolith map of the Oakville Sandstone

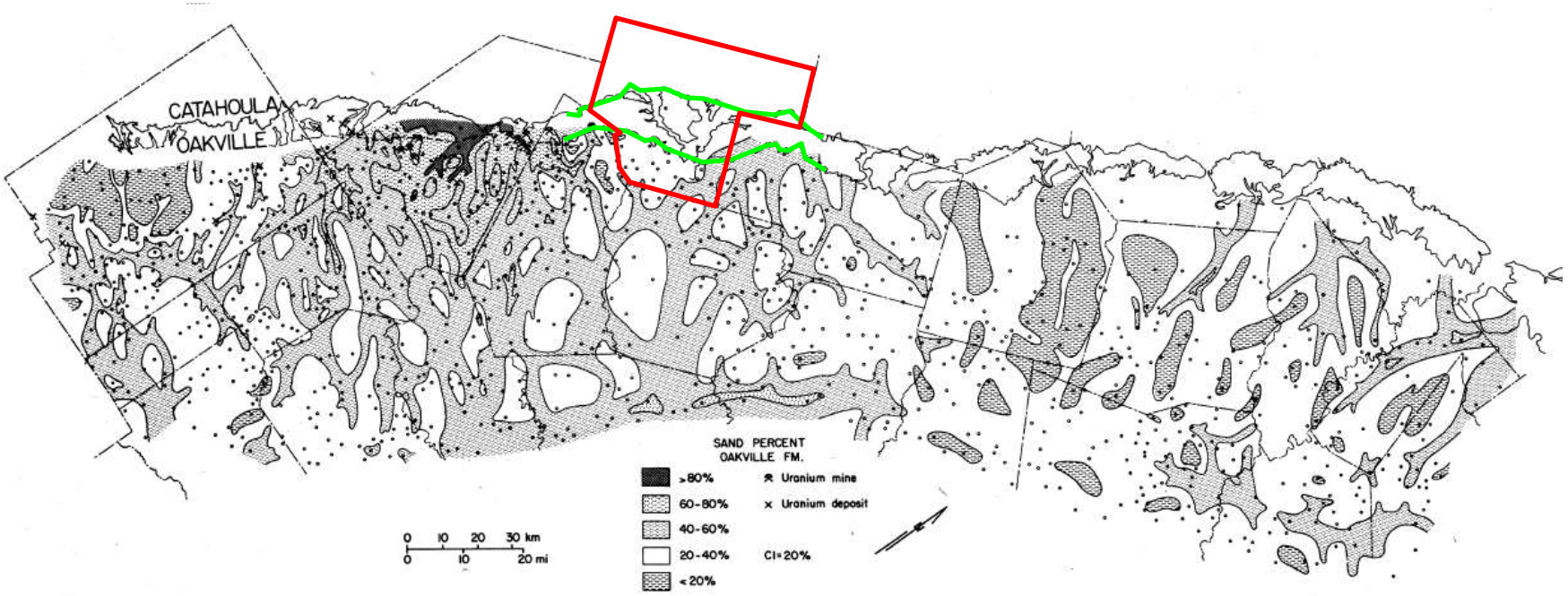

Source: Galloway et al. (1982a, Fig.6) or Galloway and Hobday (1996, Fig. 14.7)
Note: Karnes County boundaries are shown in red, and Oakville outcrop across Karnes County is highlighted in green.

Figure 55. Sand-percentage map of the Oakville Sandstone

III-1-2 Eagle Ford Formation

The Eagle Ford Formation of Late Cretaceous age covers a large section of South Texas all the way to East Texas, where it meets the deltaic deposits of the Woodbine Formation of equivalent age, as depicted in the schematic cross section of Figure 56. It lies below the Austin Chalk (Figure 57) and is probably the source of its hydrocarbon accumulation. Its thickness varies from <100 ft in Central Texas to >600ft in the Maverick Basin in Maverick County (Figure 58, Figure 59, and Figure 60). Located at a depth of 4,000–11,000 ft (Figure 61 and Figure 62), the play extends to the Sligo shelf margin (see Section III-1-1.2), and is slightly overpressured (pressure gradient of 0.43 to 0.65 psi/ft; Vassilellis et al., 2010), making it more attractive because of the higher initial production rates. Most current interest is focused on the South Texas section of the Eagle Ford (Figure 58 and Figure 59). The Central Texas play is somewhat disconnected from the South Texas play (from the Mexican border to Gonzales and DeWitt Counties) by the San Marcos Arch, a constant higher-elevation structural feature (Figure 56). The Eagle Ford Shale contains oil updip, gas downdip, and gas and condensates in between. The "shale" is carbonate-rich, up to 70% calcite (Cusack et al., 2010, p. 171; Harbor, 2011), much higher than that of the Barnett Shale, which makes it more prone to HF (Mullen, 2010).

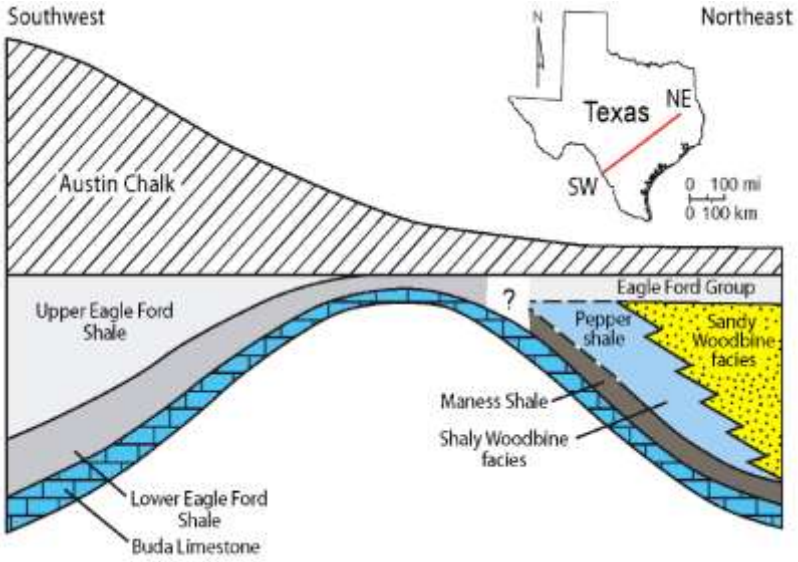

Source: Hentz and Ruppel (2010, Fig. 9)
Note: cross section hangs on top of Eagle Ford; top of Eagle Ford shallower in East Texas Basin than in Maverick Basin to the southwest

Figure 56. SW-NE schematic strike cross section illustrating regional lithostratigraphic relationships across the Eagle Ford play area

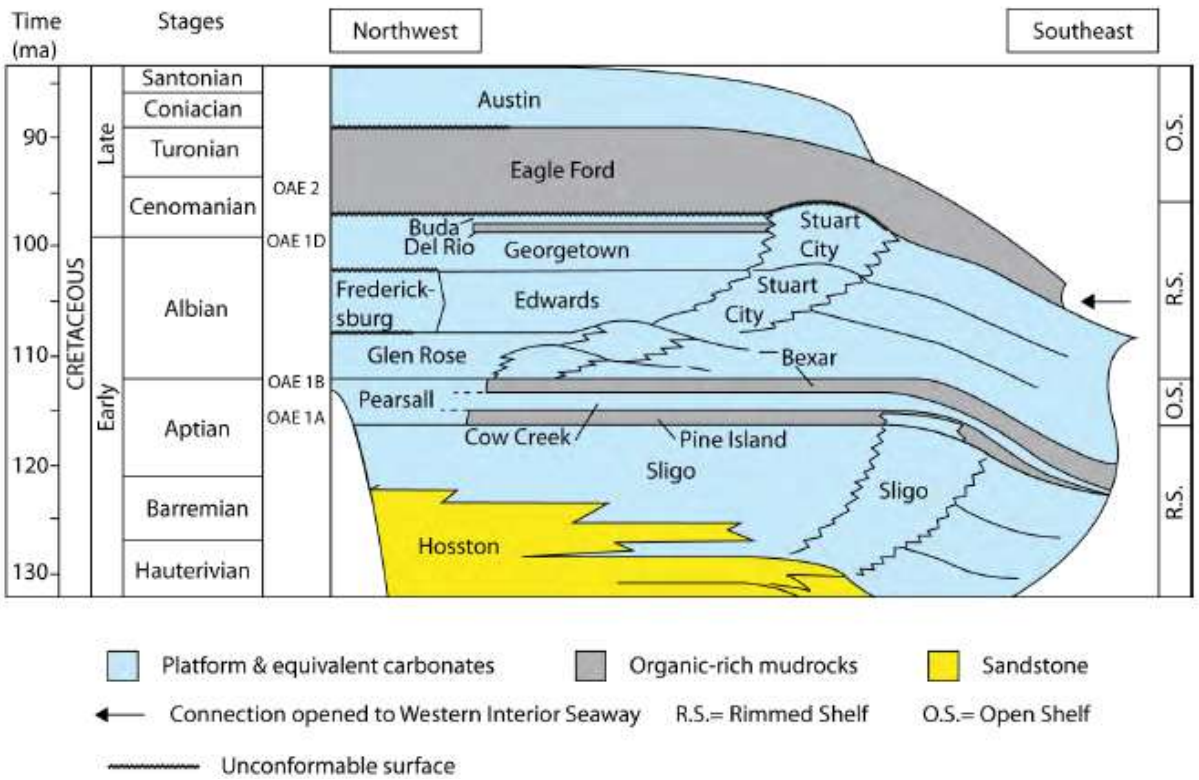

Source: Harbor (2011, Fig. 5)

Figure 57. Architecture of Gulf Coast Cretaceous depositional systems

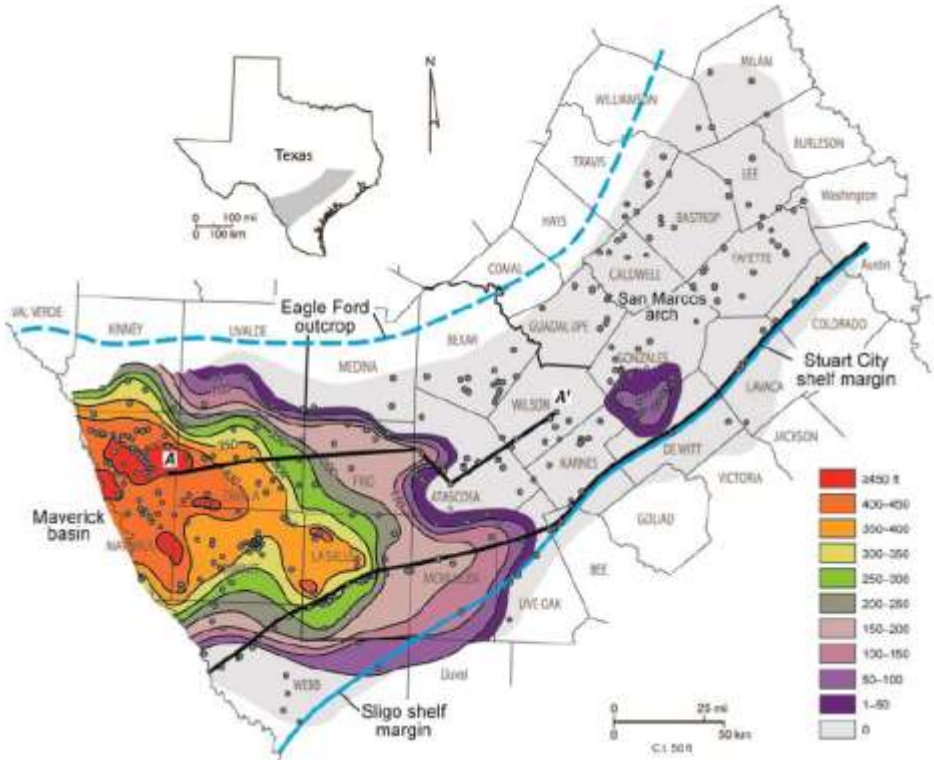

Source: Hentz and Ruppel (2010, Fig. 7)

Figure 58. Isopach map of upper Eagle Ford Shale

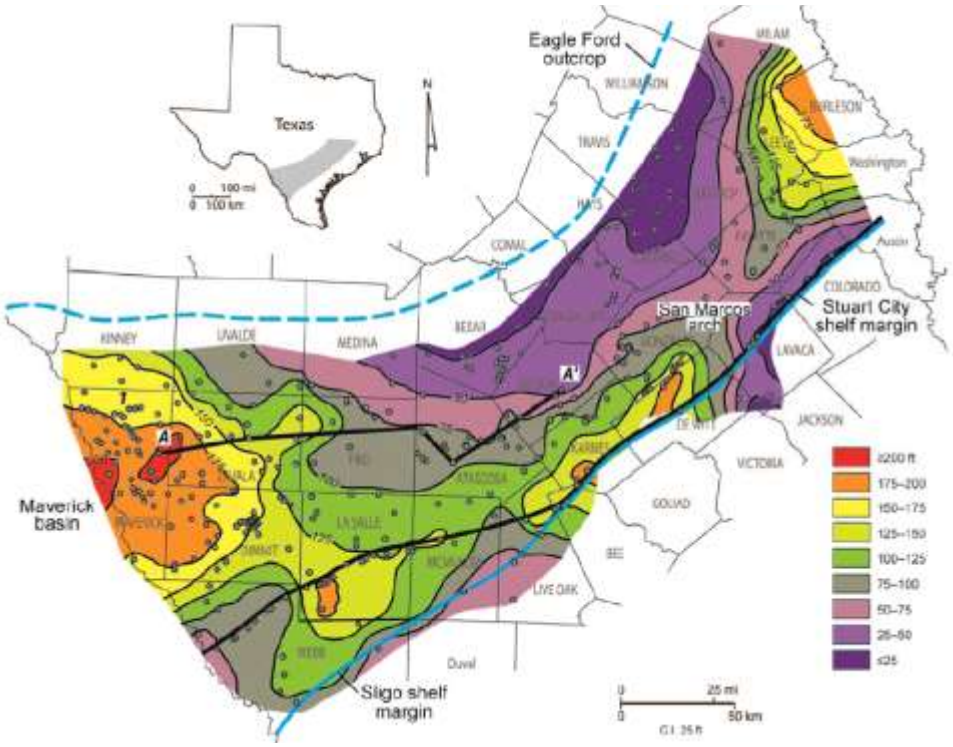

Source: Hentz and Ruppel (2010, Fig. 6)

Figure 59. Isopach map of lower Eagle Ford Shale

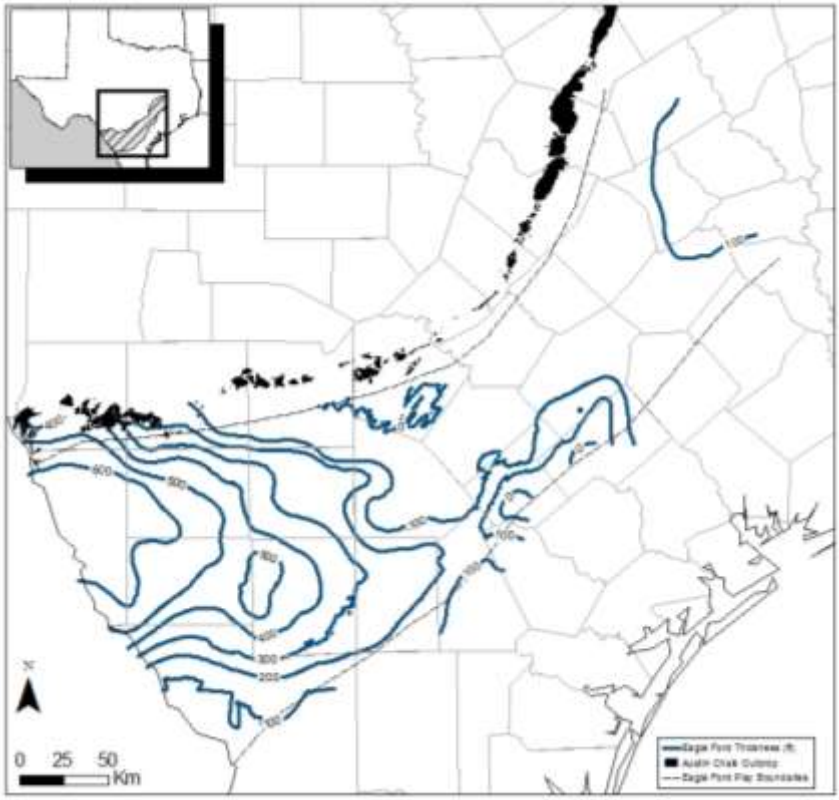

Source: modified from Hentz and Ruppel (2010)

Figure 60. Eagle Ford thickness map

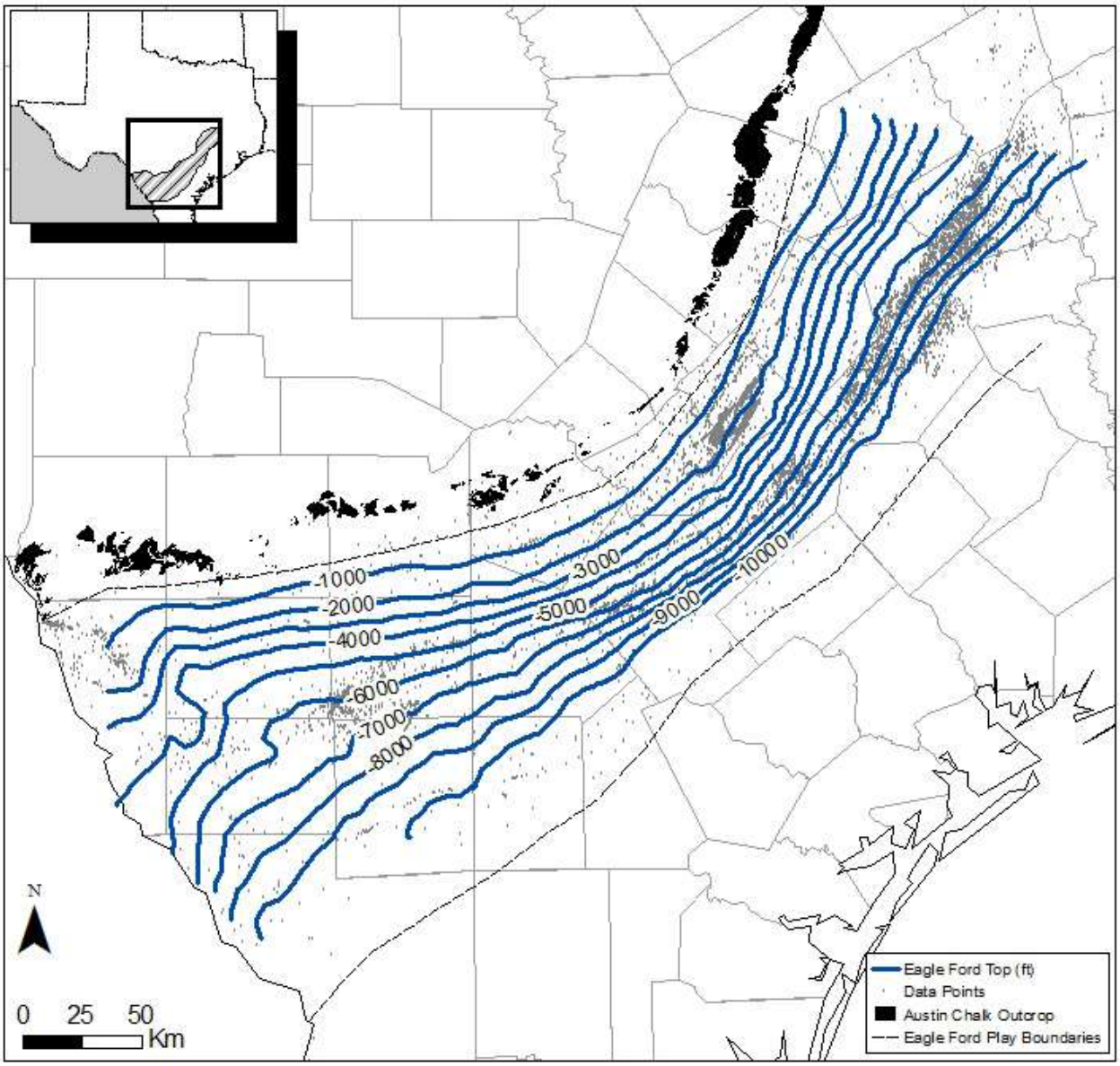

Source: IHS database

Figure 61. Eagle Ford top elevation contour map

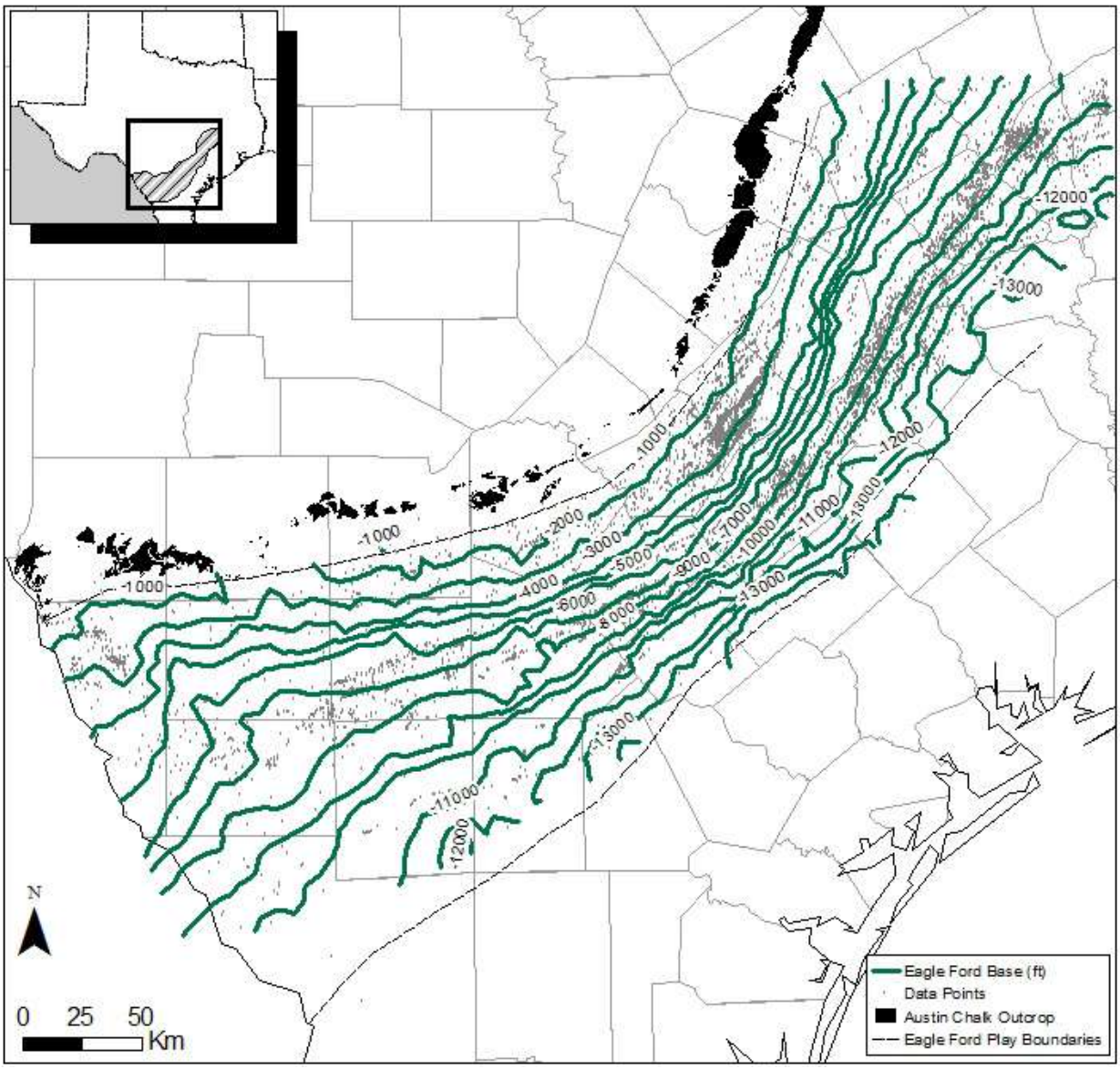

Source: IHS database

Figure 62. Eagle Ford base elevation contour map

III-2. Structural Information

The major structural feature in Texas is the fault system known as the Balcones and allied fault zones, recent surface expression of the Paleozoic Ouachita belt contrasting the folded Paleozoic basement to the east covered by thick Mesozoic and Cenozoic deposits and the relatively unperturbed Paleozoic formations to the west that are covered by relatively thin Mesozoic to present strata and that let older Precambrian rock crop out locally (Far west Texas, Llano Uplift). All deposits on the Eastern side of the Ouachita Front are generally described as Gulf Coast deposits (Figure 24 and Figure 25). The area of study of this document is entirely concerned with Jurassic, Cretaceous and Paleocene to Eocene deposits totaling >15,000 ft to the east of the Ouachita front. The sediments have been impacted by growth faults, particularly those of Cenozoic age beyond the Cretaceous shelf margin (Figure 63). The upper Gulf Coast has been impacted by normal faults such as the Luling Fault Zone continuing on the north as the Mexia-Talco Fault Zone. A cross-section shows dip and throw of faults. (Figure 64). Vertical displacement along the faults can be as much as 1000 ft (Dutton et al., 2006, p.861) and can locally exceed formation thickness.

As eluded too earlier, sediment input has been variable along the Gulf Coast; however location of major depocenters has not changed much. They are, in Texas, the Rio Grande embayment and the Houston embayment separated by the San Marcos Arch characterized by relatively smaller sediment input. The broadly-defined Rio Grande embayment contains several individualized basins including the Maverick Basin covering most of Maverick and Dimmit Counties and a portion of Zavala County. The Maverick Basin was deformed by the Laramide Orogeny in latest Cretaceous and Paleogene times (Ewing, 1991, p.20). The most prominent Laramide feature in the Basin is the Chittim/Chittum Anticline that plunges to the southeast across Maverick County into the northwest corner of Dimmit County (Scott, 2004) as visible on the geologic map (Figure 29).

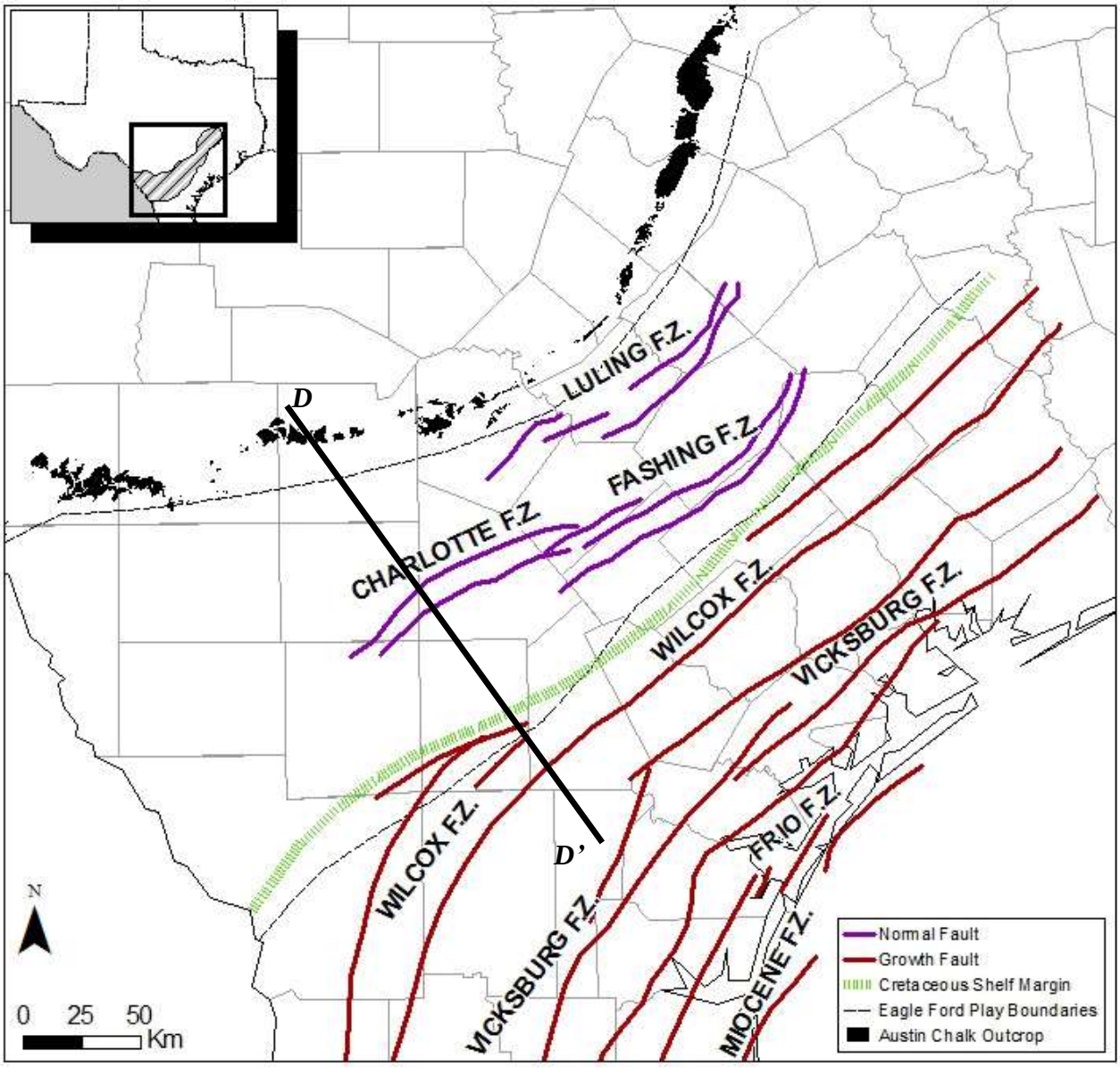

Source: Galloway et al. (1983, Plate I); Ewing (1991, Fig. 11)
Note: cross-section *DD'* of Figure 64 shown

Figure 63. Approximate location of fault zones (not necessarily all faults) in South and Central Texas

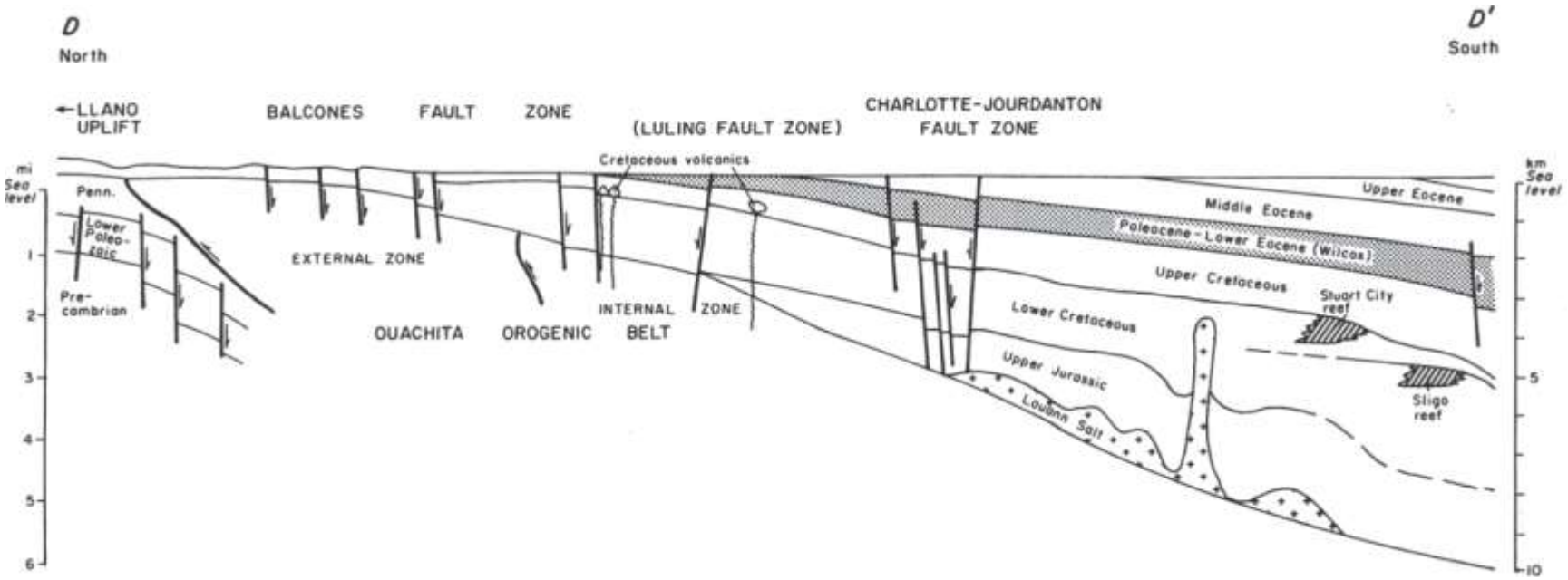

Source: Ewing (1991, Fig.12)
Note: see Figure 63 for location of cross-section

Figure 64. Structural cross section of South Texas showing faults, basin margins, and diapirs

IV. Groundwater and Aquifer Description

Hydrostratigraphic units or aquifers do not necessarily correspond to stratigraphic units. The former are defined in terms of flow (i.e., in terms of "permeable" layers vs. "impermeable" or much less "permeable" layers), whereas the latter are defined in terms of age. In this section, we examine fresh and brackish water aquifers in the EF footprint and neighboring areas. They can be binned into four categories: TWDB-sanctioned major and minor aquifers (http://www.twdb.state.tx.us/groundwater/models/gam/index.asp), non TWDB-sanctioned but named aquifers and unnamed aquifers. TWDB developed numerical models and corresponding documentation for all major aquifers in the state and for most minor aquifers. USGS also published several documents of interest, in particular Ryder and Ardis (2002) which, although dealing with the entire Gulf Coast to Florida, provides an excellent background on aquifers of South Texas.

There are tens of thousands of water wells in the area of interest. Figure 65 display >40,000wells including >10,000 in the EF footprint. Note that many wells are likely missing from the map (maybe as much as 90%). Some of the wells on the figure are municipal wells but many are irrigation wells as well as domestic wells. The map does not show well yields; irrigation and municipal wells are likely to withdraw water in volumes orders of magnitude larger than that of domestic wells. Number of domestic wells is related to population density in rural areas (Figure 3) whereas municipal well fields are generally located not too far from the city or town they provide water with (Figure 4) and irrigation wells can be matched with land use (Figure 23). Total well depth (Figure 66) is controlled by yield needs and geology. Domestic wells are generally shallower, for example, a small sand body within an otherwise low-permeability package will satisfy household needs but not much else. High volume irrigation and municipal wells generally tap the deeper confined section of aquifers (see Figure 8 and text for details).

Several salinity thresholds have practical and regulatory significance. A total dissolved solids (TDS) <500 mg/L is preferred for human consumption but the legal limit for fresh water is 1000 mg/L. The base of usable quality water (BUQW) threshold is defined at 3000 mg/L. Texas oil and gas drillers used to set surface casing to protect groundwater resources at a depth controlled by the depth at which this threshold occurs. The threshold currently used is 10,000 mg/L in accordance with EPA rules. Unless exempted, all groundwater sources with a TDS <10,000 mg/L is deemed an underground source of drinking water (USDW).

IV-1. Aquifers

TWDB defines major aquifers as those that are important water sources for large communities or those that contain large water reserves (Ashworth and Hopkins, 1995; Smith, 2004; George et al., 2011). Minor aquifers are those that are locally important but that cannot be classified as major aquifers. Note than many aquifers are described neither as major nor minor by the TWDB. The area of interest is concerned with three major aquifers from the oldest to the youngest: Edwards aquifer, Carrizo-Wilcox aquifer, and Gulf coast aquifer system (Figure 67). Minor aquifers are the Queen City aquifer, the Sparta aquifer, and the Yegua-Jackson aquifer (Figure 68). Individual county water resource reports published by the TWDB document other groundwater sources (http://www.twdb.state.tx.us/publications/reports/index.asp).

For clastic aquifers, characteristics from the previous Section III to watch for are: strike or dip orientation controlling flow direction and recharge, distribution of sand packages such as increasing mud deposits towards the shelf with river-deposited sand packages directing flow or lagoonal mudstones facies in present-day outcrop limiting recharge. For carbonate aquifers, presence of a paleokarst is a strong indication of fast subsurface flow.

IV-1-1 Major Aquifers

A summary of major aquifers in the state are presented in Ashworth and Hopkins (1995) and George et al. (2011). The Edwards aquifer is a karstic aquifer with a quick reaction time vis-à-vis external forcing. It runs from Kinney County to Hayes County though Uvalde, Median, Bexar, and Comal counties. Two small segments not connected with each other or with the main San Antonio segment from its continuation in Hayes, Travis and southern Williamson counties (Jones, 2004; Scanlon et al., 2001). The Edwards aquifer is the main water provider for the city and San Antonio and other towns in South Texas and is also used for irrigation in Uvalde and Median Counties (Lindgren et al., 2004). The aquifer is strictly regulated by the Edwards Aquifer Authority (EAA, http://www.edwardsaquifer.org/). The water quality degrades quickly past the outcrop except in Medina County (Figure 69 and Figure 70) but, beyond the "*bad water line*", the Edwards Fm. itself extend all the way to the Stuart City reef. The salinity gradient across the bad water line to TDS>10,000 mg/L is relatively steep. The Edwards Fm. (aquifer and downdip areas) has a good porosity because it was karstified before the deposition of the overlying Georgetown Fm. (Senger and Kreitler, 1984, p.6).

The Carrizo-Wilcox aquifer (Deeds et al., 2003; Dutton et al., 2003; Kelley et al., 2004) is one of the most prolific aquifer in the state. It is a composite aquifer with several water-bearing intervals. The Simsboro Fm. (Middle Wilcox) of Central Texas and the Carrizo Sands of South Texas displays the high capacity and high yield. They are clastic aquifers with mostly dip-oriented sand bodies favoring deep recharge. Note the extent of the confined section of the aquifer in Figure 67 compared to that of minor aquifers (Figure 68). Note too how much narrower the confined section of the aquifer is in Central Texas or, similarly, how quickly the TDS goes beyond 3,000 mg/L. Normal faults (Figure 63) break up the continuity of transmissive sandstones between the outcrop and the deeper part of the aquifer (Dutton et al., 2006, p.865). Where faults die out to the southwest, the width of the aquifer increases to more than 100 km (Dutton et al., 2006).

We mention the Gulf Coast aquifer system because some of the water used for HF in the EF originated from these aquifers. A quick analysis counting the number of EF wells on aquifer footprint suggest that ~1/3rd of HF groundwater could come from the Gulf Coast aquifers. Three main aquifers define the system: the Jasper, Evangeline, and Chicot aquifers, which broadly include the Oakville Sandstone, the Goliad Sand, and Quaternary units, respectively. The Fleming Formation is a confining unit between the Jasper and Evangeline aquifers and is called the Burkeville Confining Unit. Five cross-sections including Duval, Live Oak, Karnes, Gonzales, De Witt, Fayette and Lavaca Counties display groundwater occurrences in the various aquifers of the Gulf Coast aquifer system (Figure 71, Figure 72, Figure 73, Figure 74, and Figure 75). See Chowdury et al. (2004) for details about the GAM model.

Baker (1979, 1986) assigned the Miocene Oakville/Fleming geologic units to the Jasper aquifer, which has been best characterized along the northeastern Texas Gulf Coast, north of the Brazos River. The Jasper aquifer is generally composed of the Miocene-age Oakville Sandstone but

includes sections of the Fleming Formation in some places where the Fleming is relatively transmissive. The Oakville Sandstone/Fleming Formations are commonly grouped because they are both composed of varying amounts of interbedded sand and clay. In most of the central part of the Gulf Coast (Brazos River to central Duval County), they are distinguishable as stratigraphically adjacent units because the Oakville Formation is sand rich and the Fleming is relatively more clay rich. Galloway et al. (1982a) described the Oakville in the southwest Gulf Coast as a sand-rich fluvial system overlying the Catahoula Formation. They globally associated the Oakville Sandstone with the Jasper aquifer and the Fleming Formation with the Burkeville Confining System. The match is generally good only in the south part of the study area. Farther north, at intermediate depths, only the lower half of the Oakville Sandstone is part of the Jasper aquifer. The mixed-load muddier top is part of the Burkeville Confining System, whose top corresponds to the middle of the Fleming. The upper part of the Fleming is included in the Evangeline aquifer (Galloway et al., 1982a, p. 27). Farther north, in Fayette and Washington Counties, sands at the top of the Catahoula make up a significant part of the Jasper aquifer. To the northeast of the Brazos River, the Oakville Sandstone and Fleming are indistinguishable.

Delineation of the Evangeline aquifer corresponds closely with the extent of the Goliad Formation. The Goliad is entirely within the Evangeline aquifer, and the upper boundary of the Evangeline aquifer closely follows the top of the Goliad Formation where present (Baker, 1979). However, the bottom of the Evangeline aquifer can include sandy units of the Fleming (Baker, 1979, p. 40) fully hydraulically connected to the Goliad Formation.

The Evangeline aquifer is composed of water-bearing zones primarily within the Goliad Sand and secondarily in underlying parts of the Fleming Formation (Ryder and Ardis, 1991, 2002). The Goliad Sand is identified only as an aquifer unit in the TWDB well database within and to the south and west of Lavaca and Jackson Counties.

IV-1-2 Minor Aquifers

A summary of minor aquifers in the state are presented in Ashworth and Hopkins (1995) and George et al. (2011). Queen City and Sparta aquifer GAM models are detailed in Kelley et al. (2004). The Queen City aquifer is not defined by the state as a minor aquifer beyond Frio, LaSalle, and McMullen counties (Figure 77). The water-producing horizons of the equivalent Bigford Fm. are generally downdip (Figure 47 and Figure 48). Both Queen City and Sparta aquifer water tend to be brackish in South Texas except in the outcrop area (George et al., 2011, p.138 and 150).

Structure of the Yegua-Jackson aquifer is provided in Knox et al. (2007). The GAM model has not been fully completed yet. Waters of the Yegua-Jackson aquifer tend to be brackish as well.

IV-1-3 Other Aquifers

They often correspond to sand bodies, possibly large, encompassed within a so-called aquitard. They tend to be shallow and unconfined to benefit from direct recharge. This category also include alluvium and terraces deposits along major and other rivers. They are typically unconfined and tend to have good communication with the stream (when not dry).

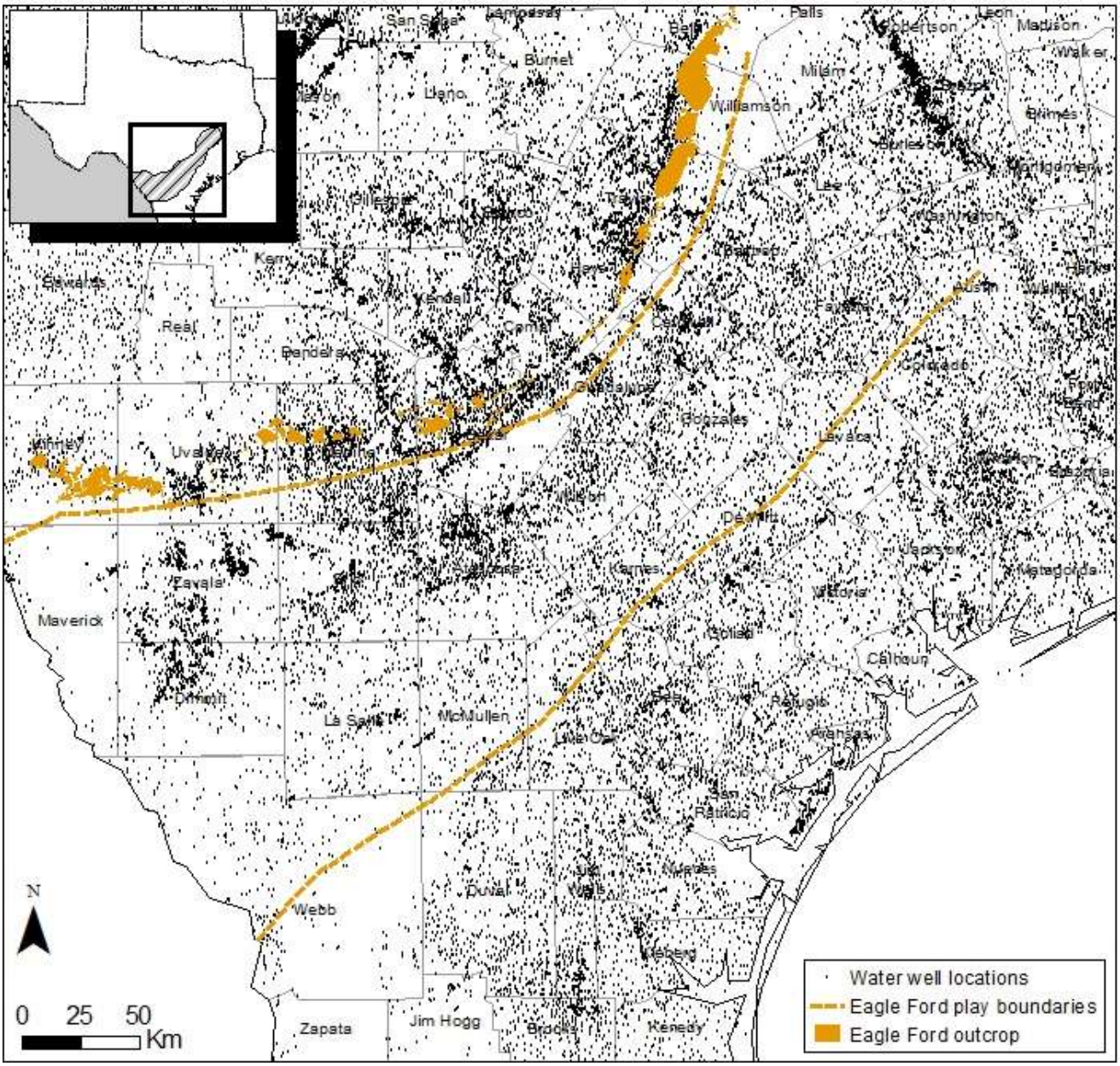

Source: TWDB, http://www.twdb.state.tx.us/mapping/gisdata.asp, September 2011
Note: 40,969 wells on the map.

Figure 65. Water well locations in south and central Texas

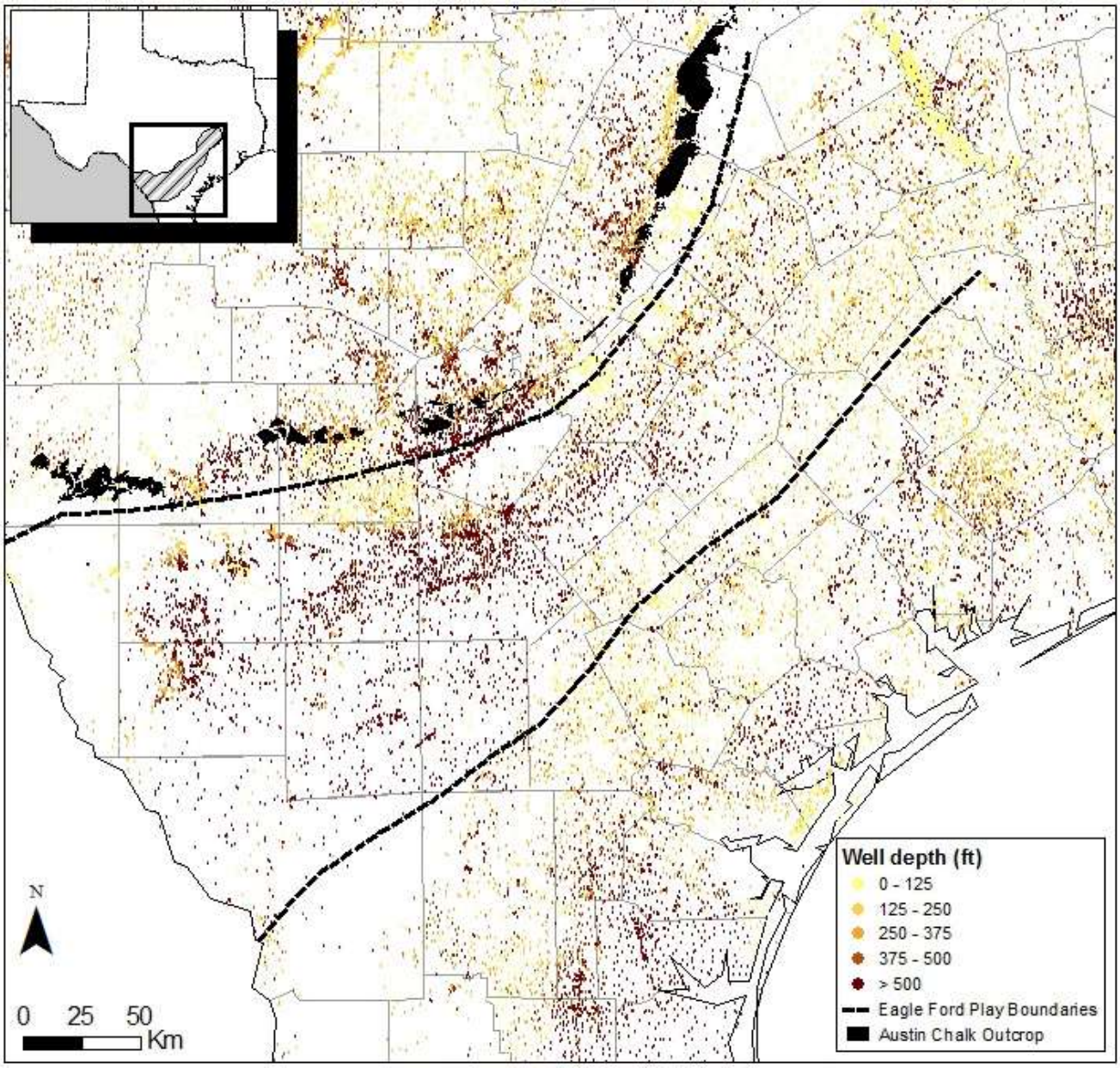

Source: TWDB, http://www.twdb.state.tx.us/mapping/gisdata.asp, September 2011

Figure 66. Depth color-coded water well locations in south and central Texas

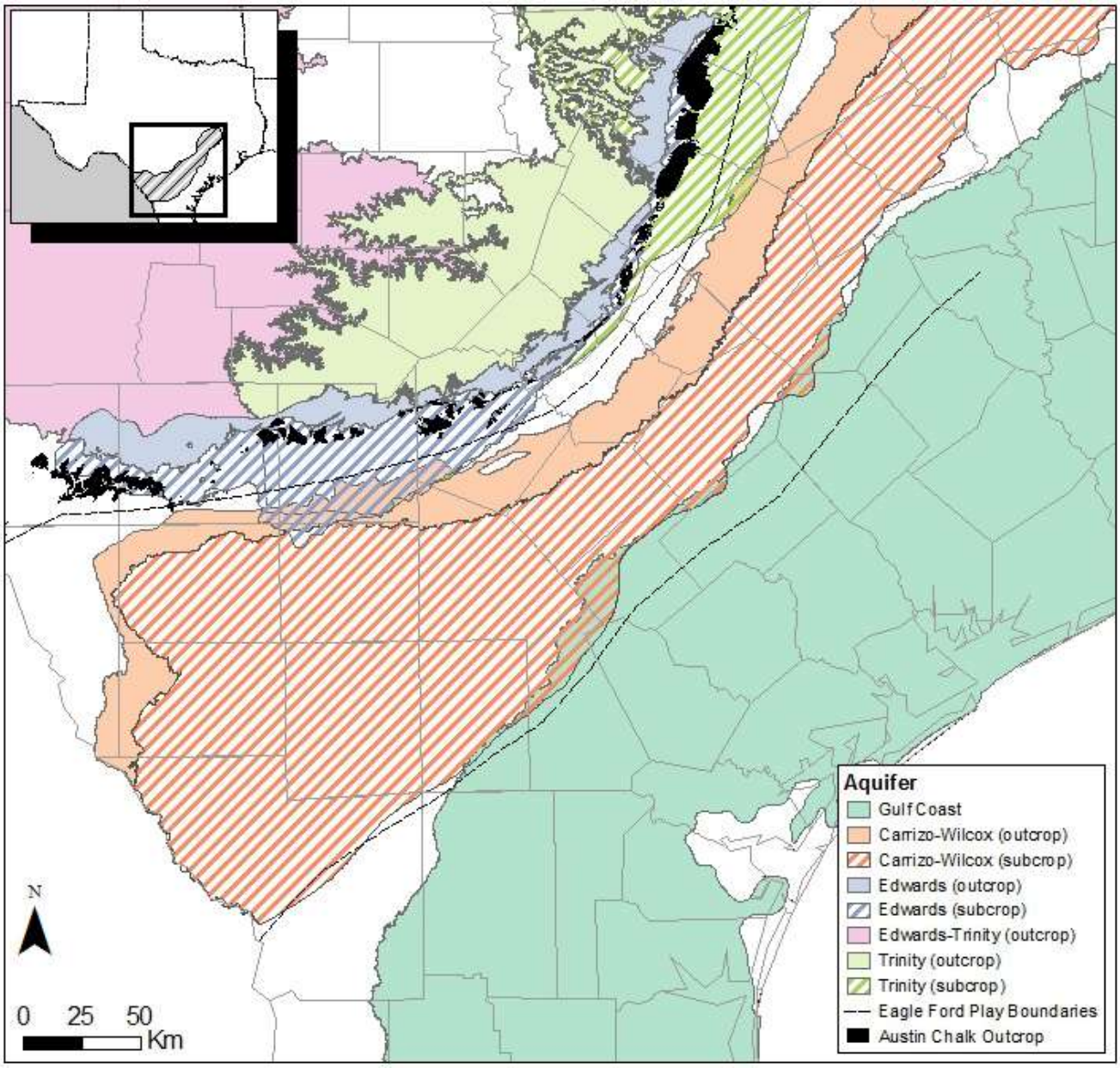

Source: TWDB, http://www.twdb.state.tx.us/mapping/gisdata.asp
Note: the downdip limits at set at 3000 mg/L for the Carrizo-Wicoz and 1000 mg/L for the Edwards aquifer (Ashworth and Hopkins, 1995, p.1)

Figure 67. Map of major aquifers in south and central Texas

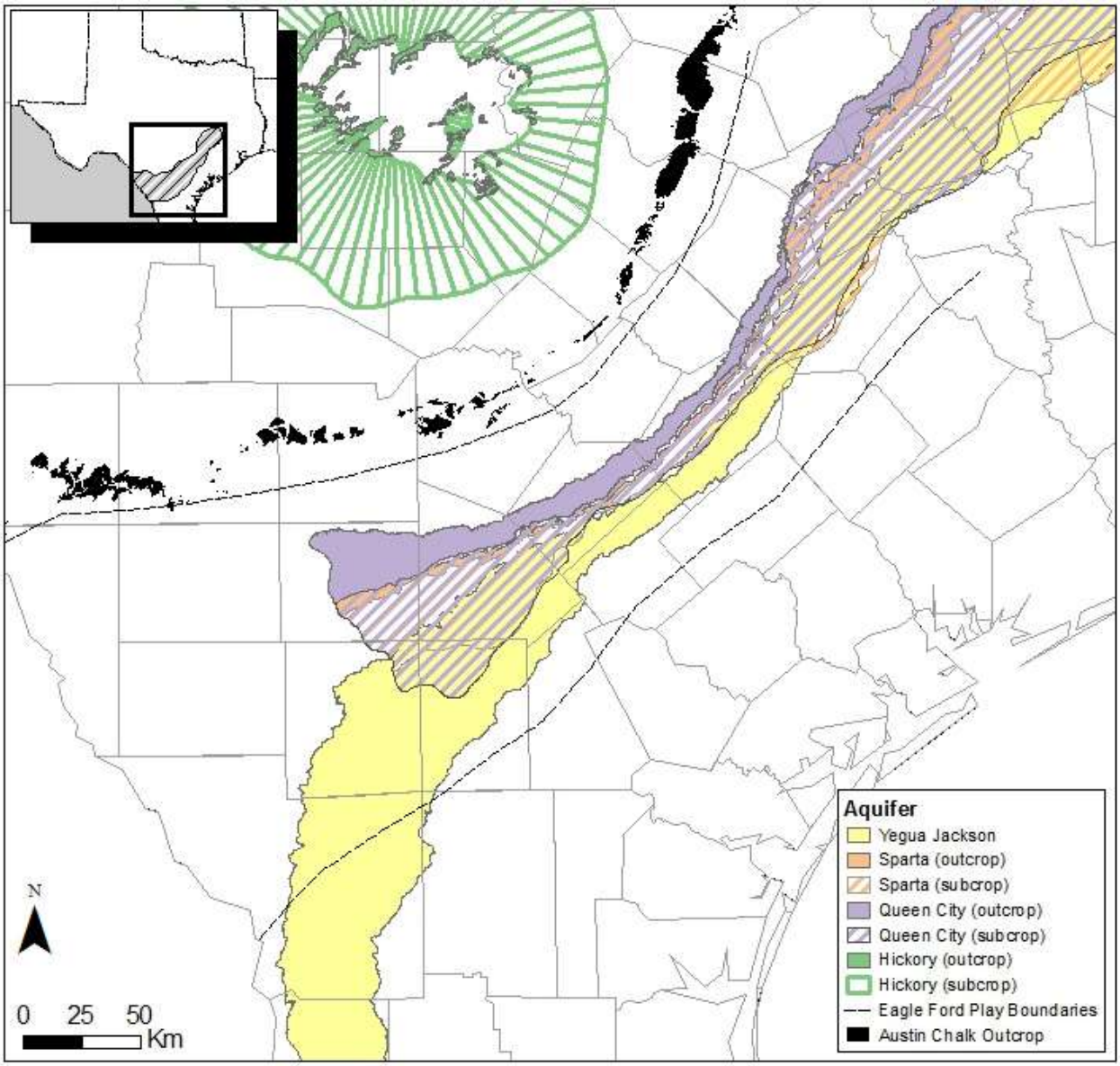

Source: TWDB, http://www.twdb.state.tx.us/mapping/gisdata.asp
Note: the downdip limits at set at 3000 mg/L

Figure 68. Map of minor aquifers in south and central Texas

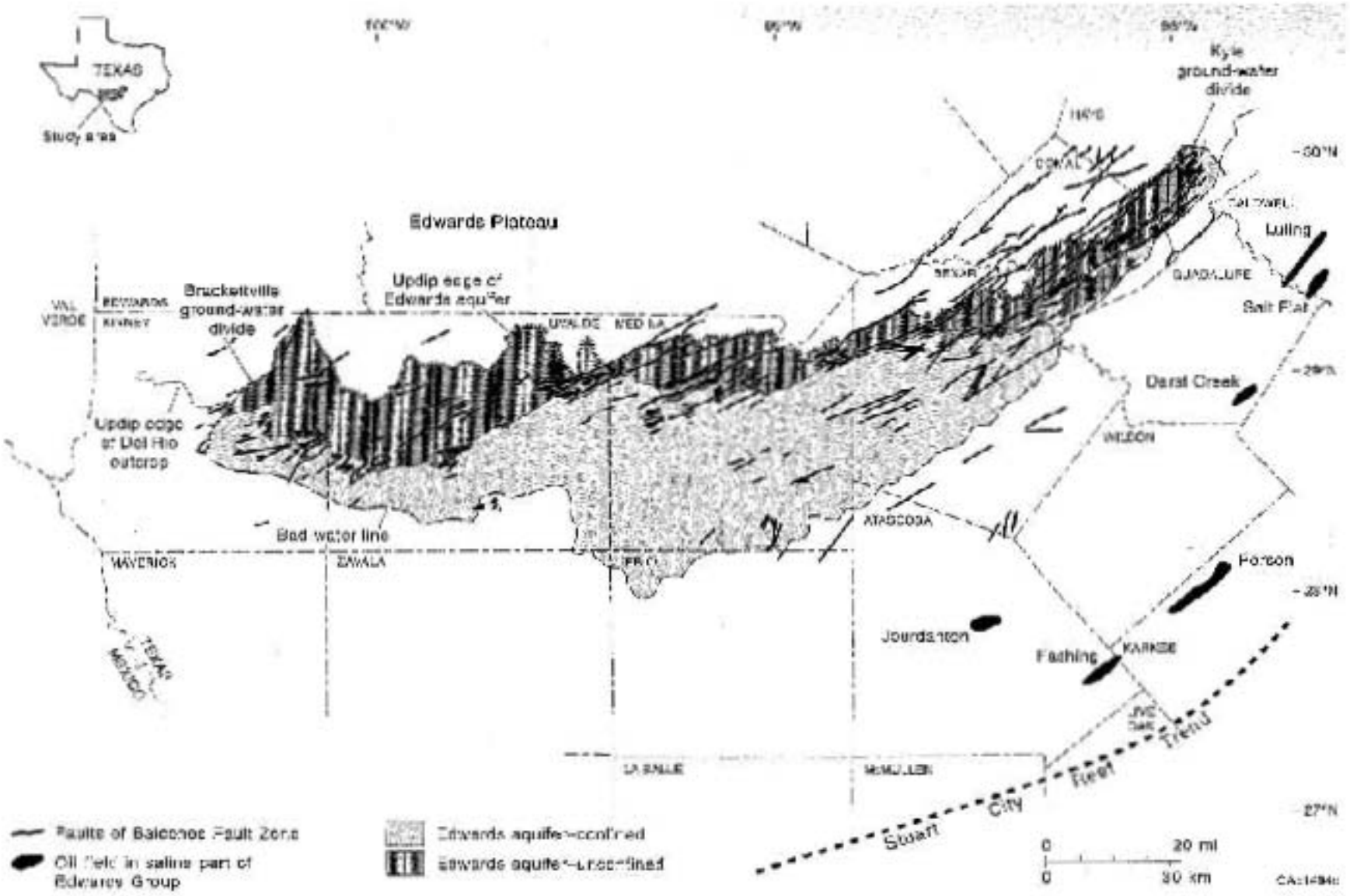

Source: Hovorka et al. (1996, Fig.4)

Figure 69. Outcrop, confined section, bad water line location of the Edwards Aquifer

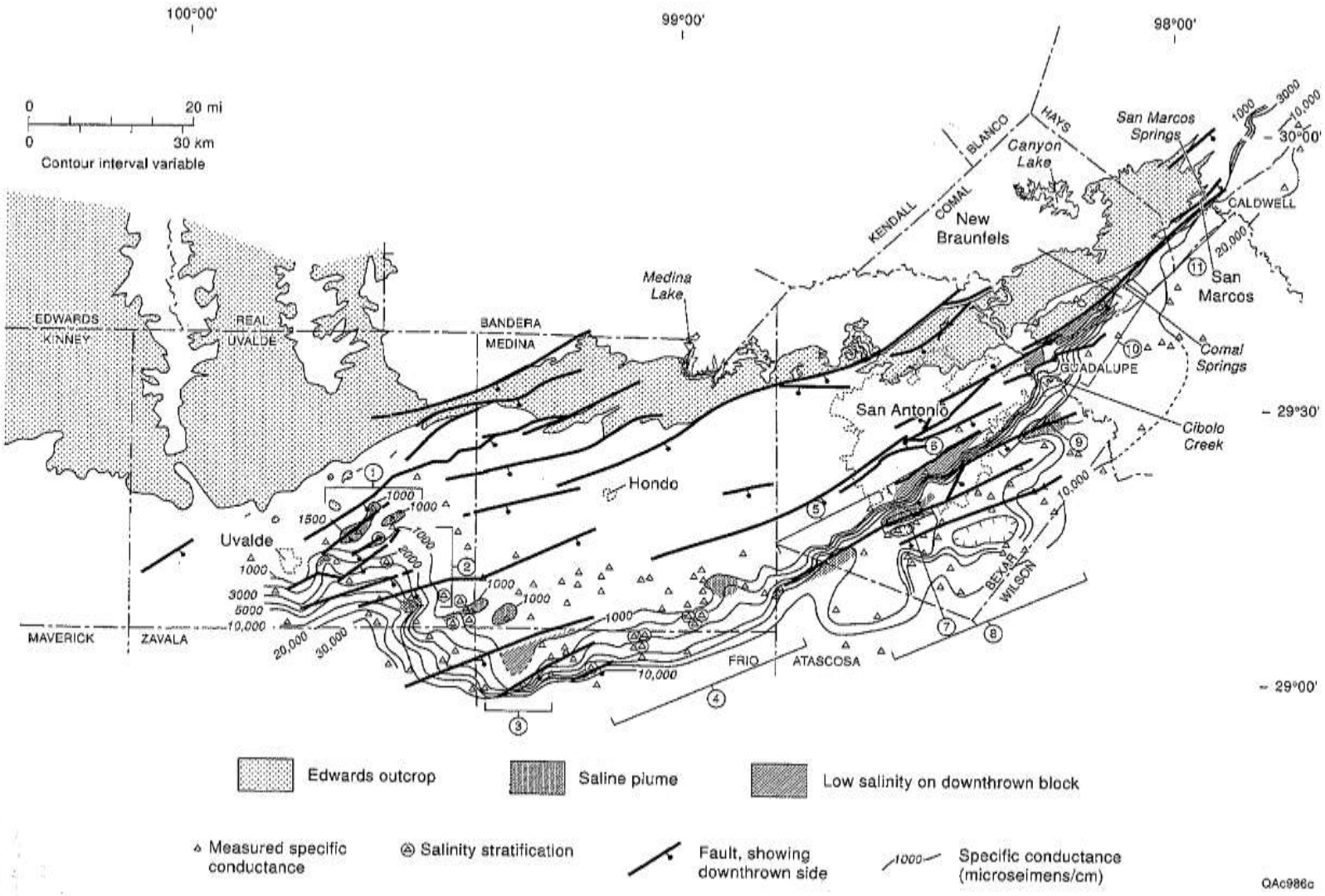

Source: Hovorka et al. (1998, Fig.4) ;

Note: Hovorka et al. (1998, p.16) notes than a rough approximation of a TDS of 1000 mg/L is a conductivity falling between 1300 and 1500 μS/cm (depending on the ionic makeup)

Figure 70. Edwards Aquifer conductivity map

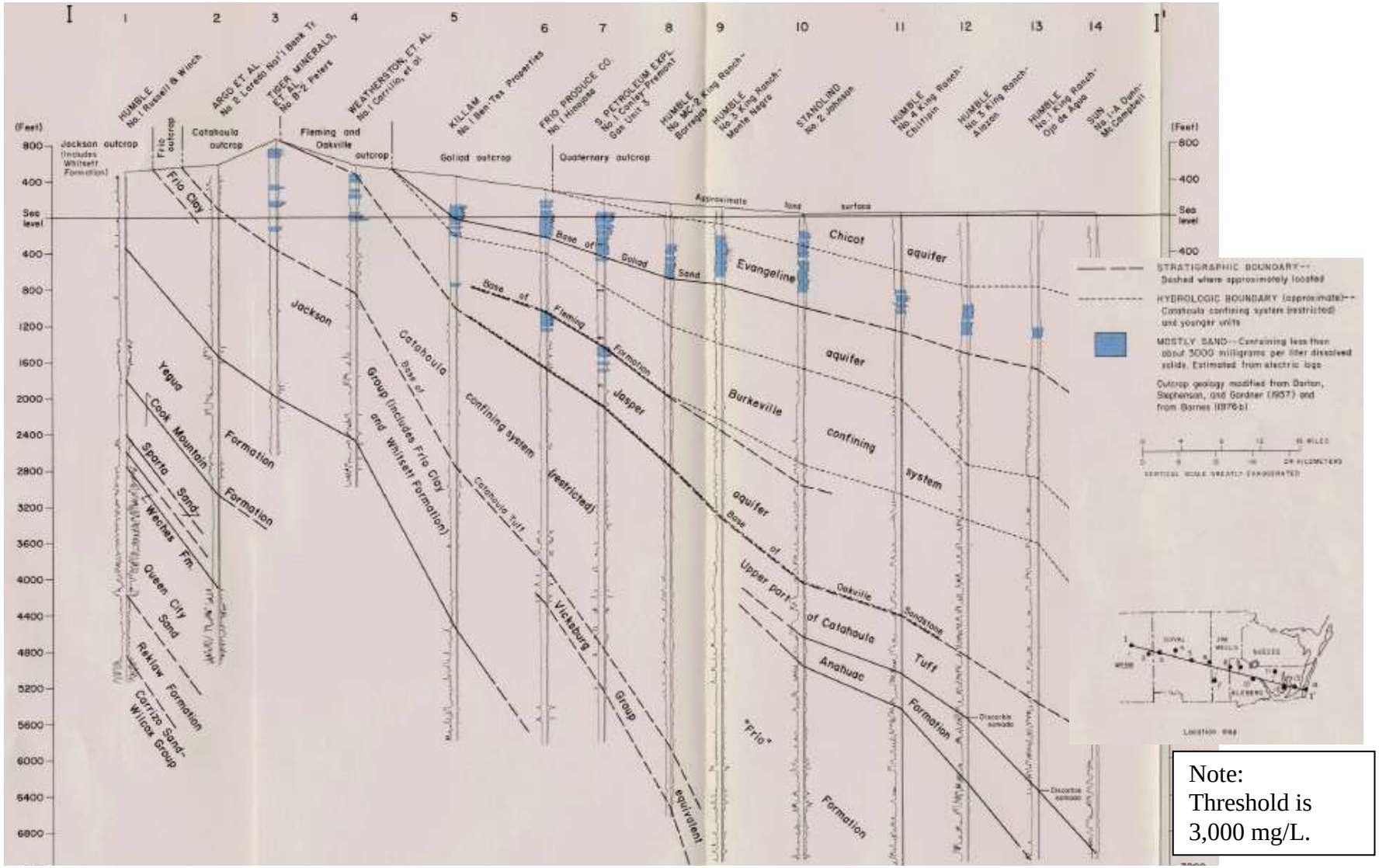

Source: Baker (1979, Fig.10)

Figure 71. Stratigraphic and hydrogeologic cross section of Duval County and part of Webb County

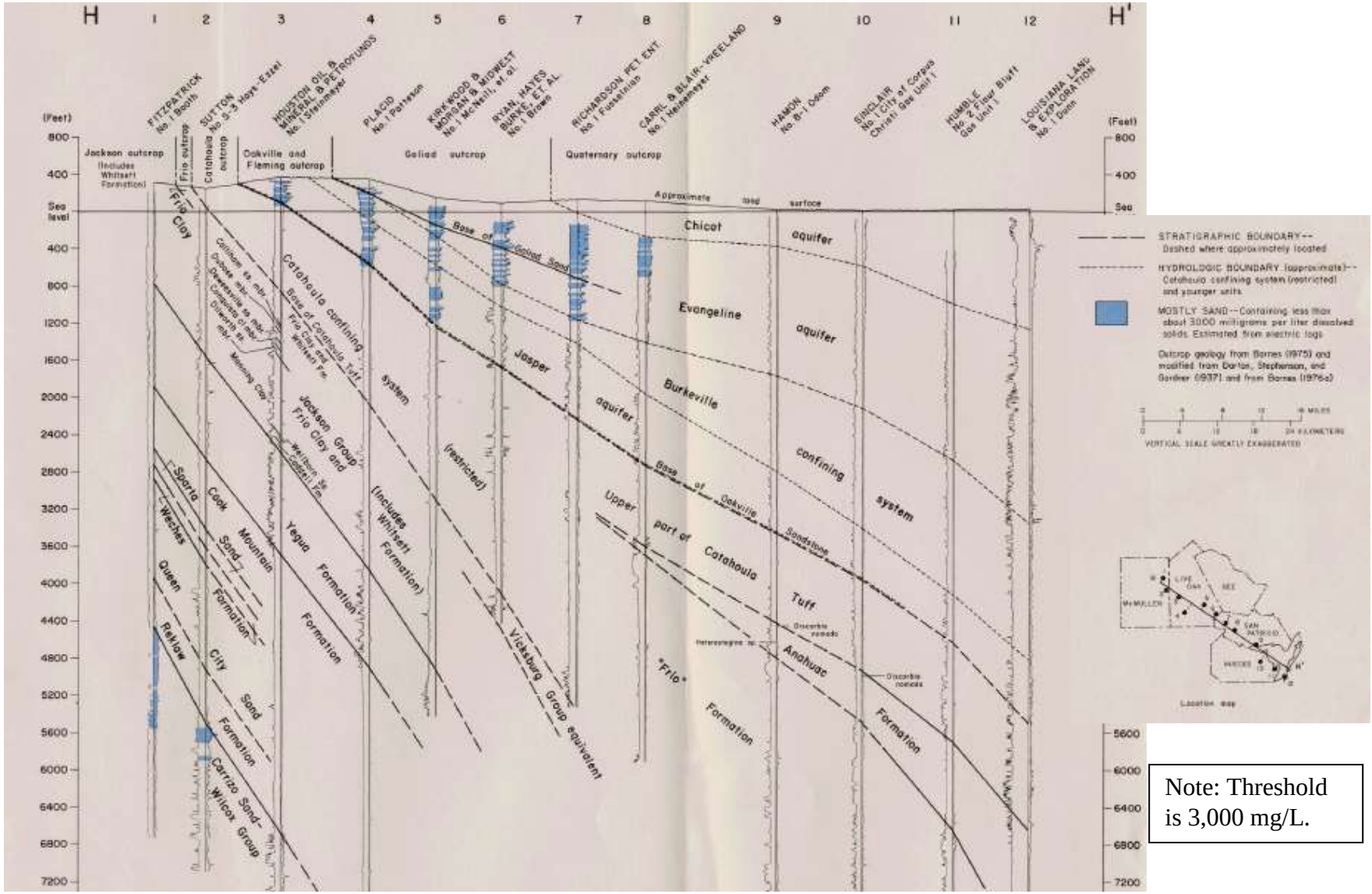

Source: Baker (1979, Fig.9)

Figure 72. Stratigraphic and hydrogeologic cross section of Live Oak County

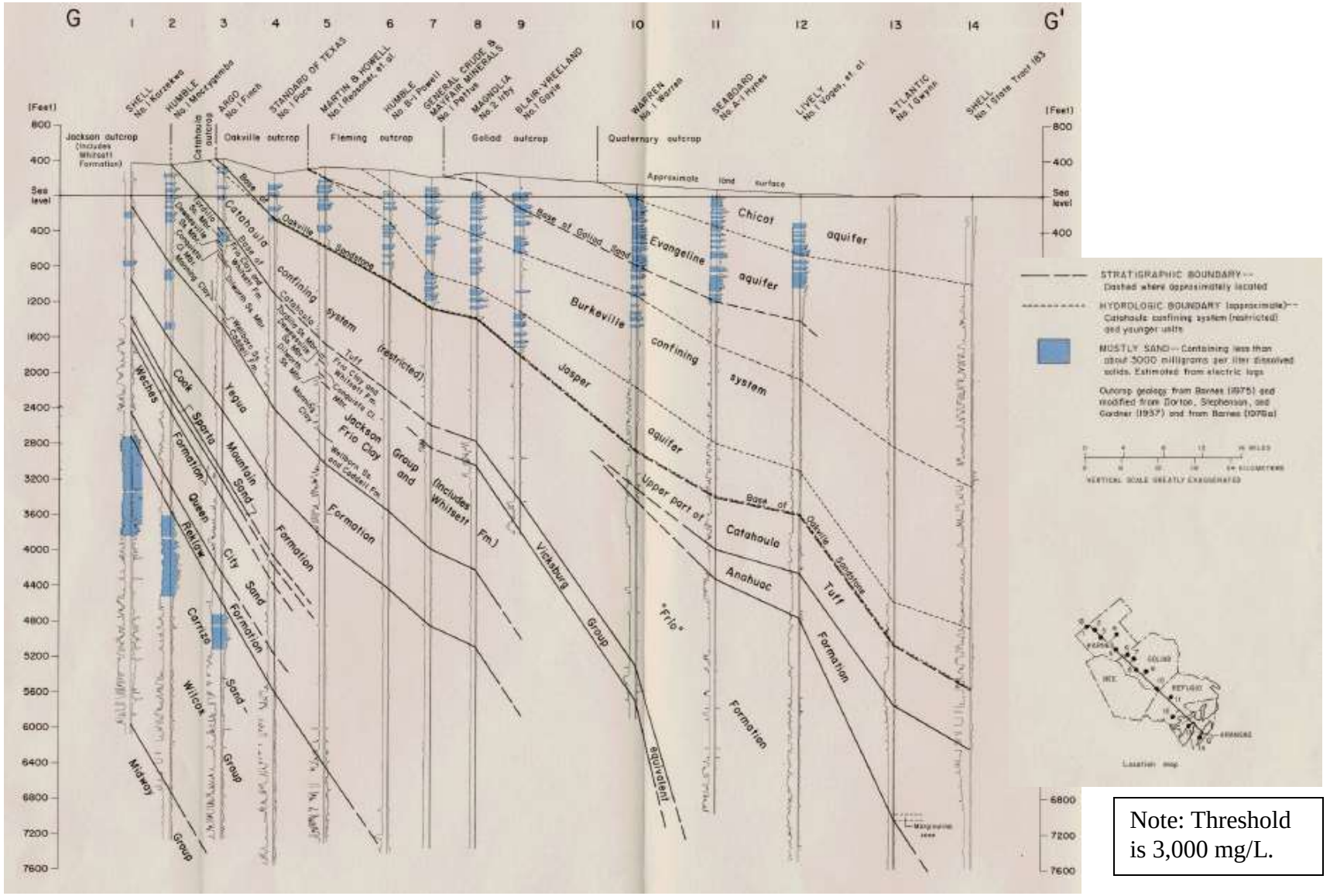

Note: Threshold is 3,000 mg/L.

Source: Baker (1979, Fig.8)

Figure 73. Stratigraphic and hydrogeologic cross section of Karnes County

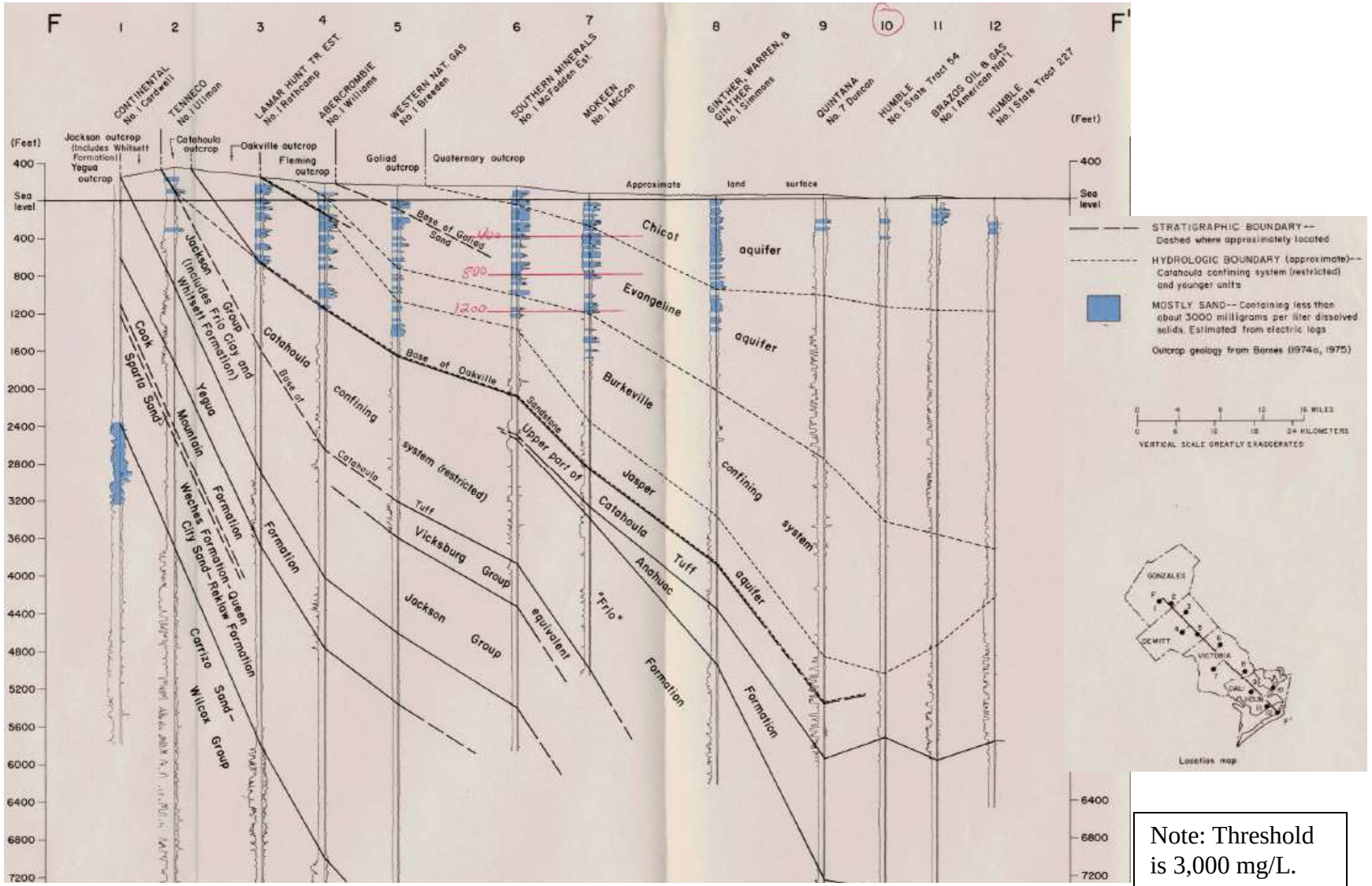

Note: Threshold is 3,000 mg/L.

Source: Baker (1979, Fig.7)

Figure 74. Stratigraphic and hydrogeologic cross section of Gonzales and De Witt Counties

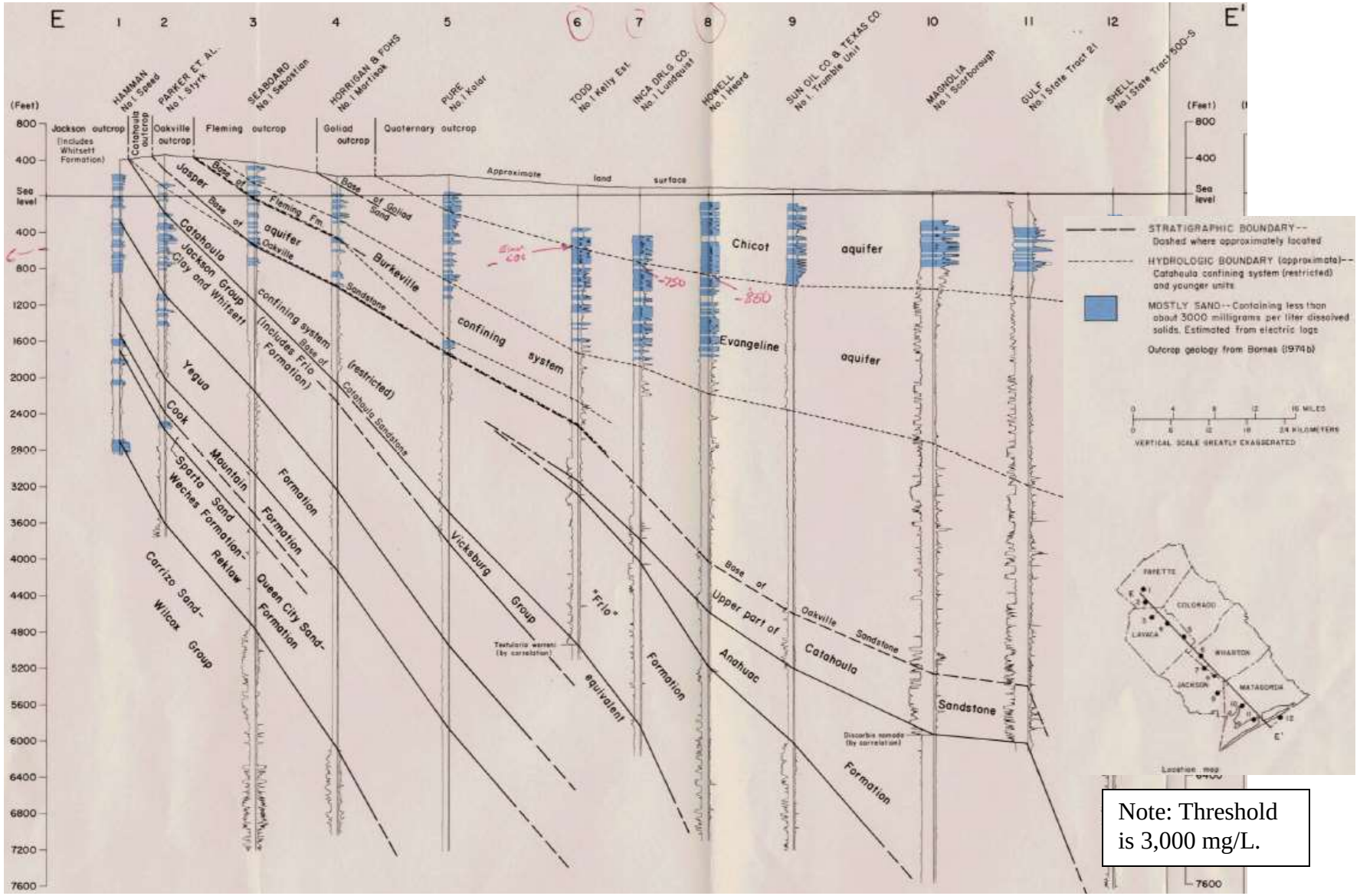

Source: Baker (1979, Fig.6)

Figure 75. Stratigraphic and hydrogeologic cross section of Fayette and Lavaca Counties

IV-2. Hydrogeochemistry

Fresh and brackish water aquifers can be characterized by two main parameters to which a third one can be added. The most important parameter is TDS / salinity. By definition a fresh water aquifer cannot have a TDS >1000 mg/L. The second important parameter is ionic make up. Major cations are Ca, Mg, and Na. Major anions are chloride, sulfate and bicarbonate. Water types are classified according to the various proportions of these dissolved constituents, typically by plotting them on the so-called Piper plot (see below). Redox conditions form the third parameter (for example, McMahon et al., 2009). They controlled amounts of minor constituents such as H_2S and Fe and trace elements such as As or B. A fourth parameter, pH, is also important but most natural waters fall into a relatively narrow range (pH of 6-8).

The TWDB sampling coverage of South Texas aquifers is good (Figure 76 and Figure 77) but focused on fresh water. Brackish water samples are also taken but not in a systematic way. In any case, South Texas does contain significant amount of brackish water (Figure 78). However, unlike fresh water aquifers, there are few publicly available studies of brackish aquifers in the state despite the strong interest displayed by both the State and municipalities to access the resource and desalinate it. The last comprehensive study of brackish resources in the state was done by LBG-Guyton (2003). Crude but informative sketches are presented in Figure 79 and Figure 80 for the Edwards, Carrizo-Wilcox, Gulf Coast, Queen City-Sparta and Yegua-Jackson aquifers. Similarly saline aquifers latest comprehensive study across the state was done by Core laboratories (1976).

Data used in the following analysis comes from the public domain TWDB groundwater database (http://www.twdb.state.tx.us/groundwater/data/gwdbrpt.asp). We used the most recent sample if several were taken at a given location and we performed additional QA. TDS was computed by adding concentrations of all dissolved species that were checked to be overall charge-balanced. A total of 8179 good samples were used. A total of 4287 samples were deleted: 2229 did not have enough information (i.e., no cation or anion info); 1841 failed the mass balance test; 104 failed the test for K<Na; and 113 failed the Mg/2<Ca test. Piper plots were constructed using the Aquachem software.

We plotted data for 18 aquifers or aquifer groups. From the youngest to the oldest they are: alluvium aquifers (non Brazos alluvium) (Figure 81), Brazos river alluvium aquifer (Figure 82), classified as a minor aquifer, Leona Fm. and Uvalde gravel group (Figure 83) in hydraulic communication with the Edwards aquifer, the three main aquifers of the Gulf Coast aquifer system: the Chicot aquifer (Figure 84), the Evangeline aquifer (Figure 85), and the Jasper aquifer (Figure 86), the Jackson aquifer (Figure 87), the Yegua aquifer (Figure 88), the Sparta aquifer (Figure 89), the Queen City aquifer (Figure 90), the Carrizo aquifer (Figure 91), the Wilcox (Figure 92) and Simsboro (Figure 93) aquifers, the Upper Cretaceous aquifers presented as carbonates (Figure 94) or clastics(Figure 95), the Edwards aquifer (Figure 96), and, on the west side of the Ouachita front, the Glenrose (Figure 97) and Trinity sands (Figure 98) component of the Trinity aquifer.

The plots show variable composition in alluvium aquifers (Figure 81), mostly because they represent different river basins. Brazos River alluvium (Figure 82), Leona Fm., Uvalde gravel group (Figure 83), and Upper Cretaceous carbonate aquifers (Figure 94) tend to be of a Ca-bicarbonate type as expected from a limestone matrix. The Edwards (Figure 96) and Glenrose

(Figure 97) aquifers show a strong dolomitic imprint and have Ca-Mg bicarbonate waters (with some sulfate for the Glenrose). The Chicot (Figure 84), Evangeline (Figure 85), and Jasper (Figure 86) aquifers present a mixed Ca-Na bicarbonate-chloride composition suggesting imprint of NaCl brines on a Ca-bicarbonate substrate. The Jackson (Figure 87) and Yegua (Figure 88) aquifers and Sparta aquifer (Figure 89) tend towards a mixed Na chloride-sulfate. The Queen City (Figure 90), Carrizo (Figure 91), Wilcox (Figure 92) and Simsboro (Figure 93) aquifers also tend to have mixed water dominated by Ca and bicarbonate.

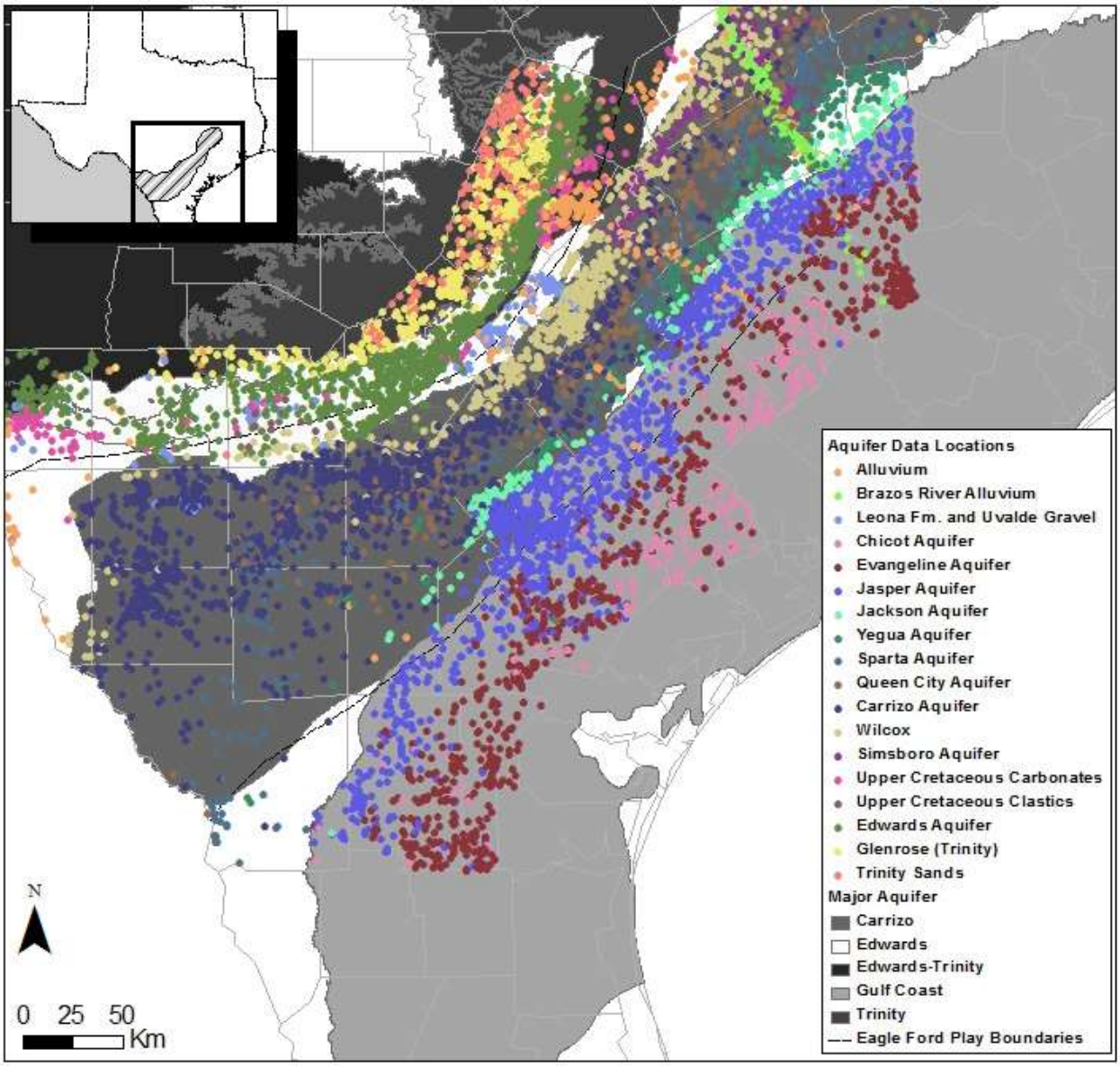

Source: TWDB groundwater database

Figure 76. Aquifer color-coded TWDB water samples and major aquifer footprints

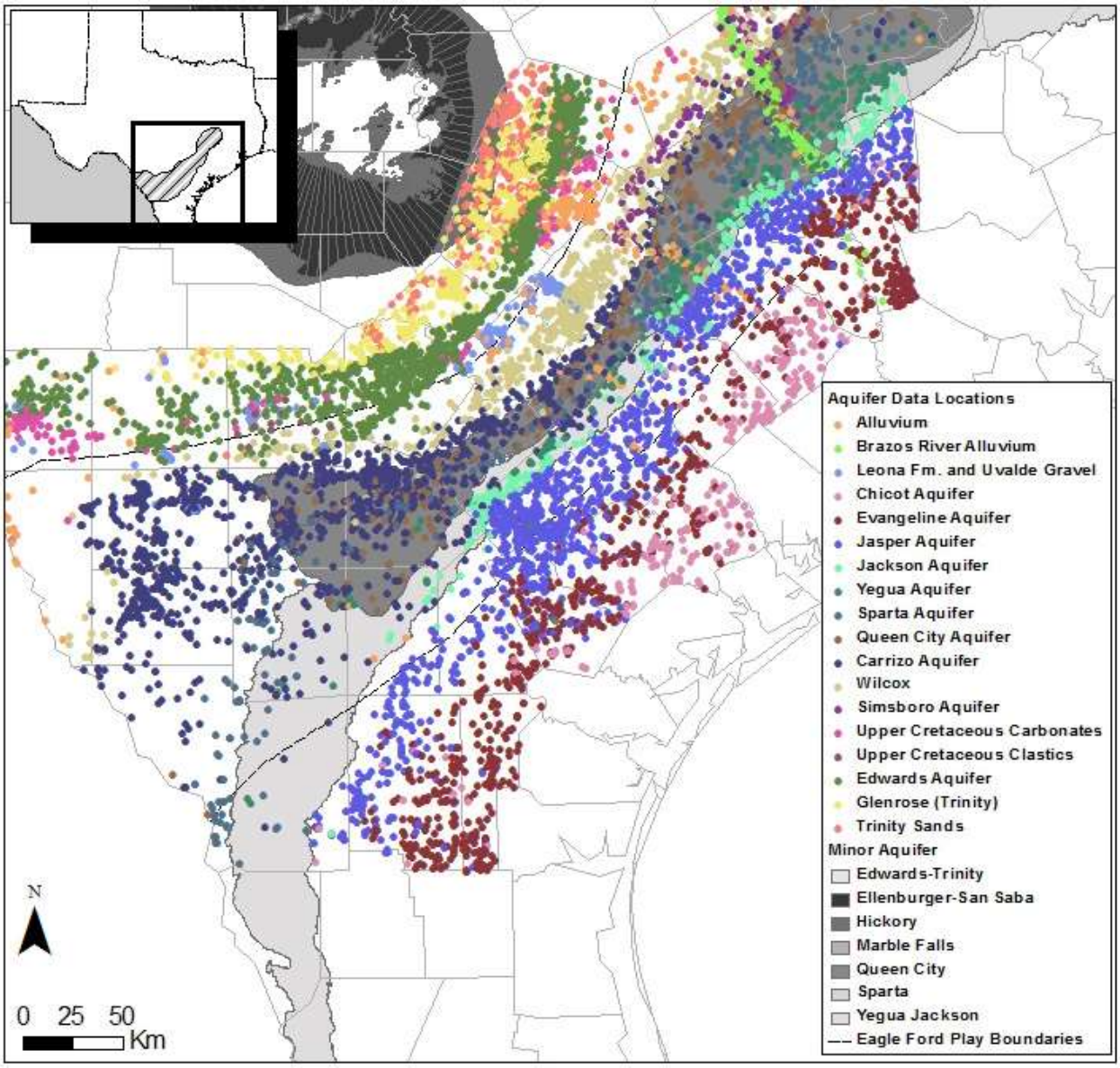

Source: TWDB groundwater database

Figure 77. Aquifer color-coded TWDB water samples and minor aquifer footprints

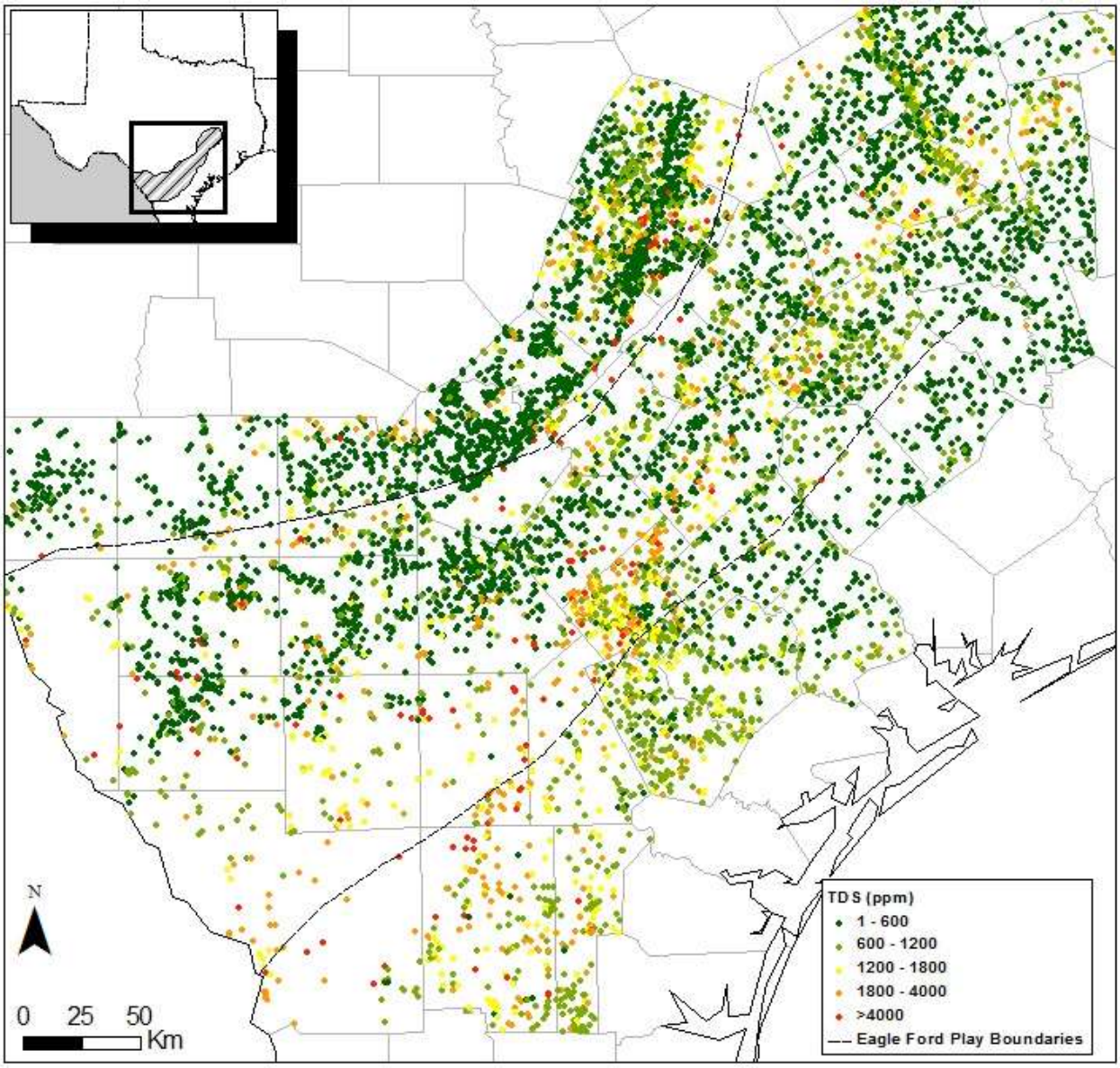

Source: TWDB groundwater database

Figure 78. TWDB water samples color-coded by TDS

Edwards Aquifer:

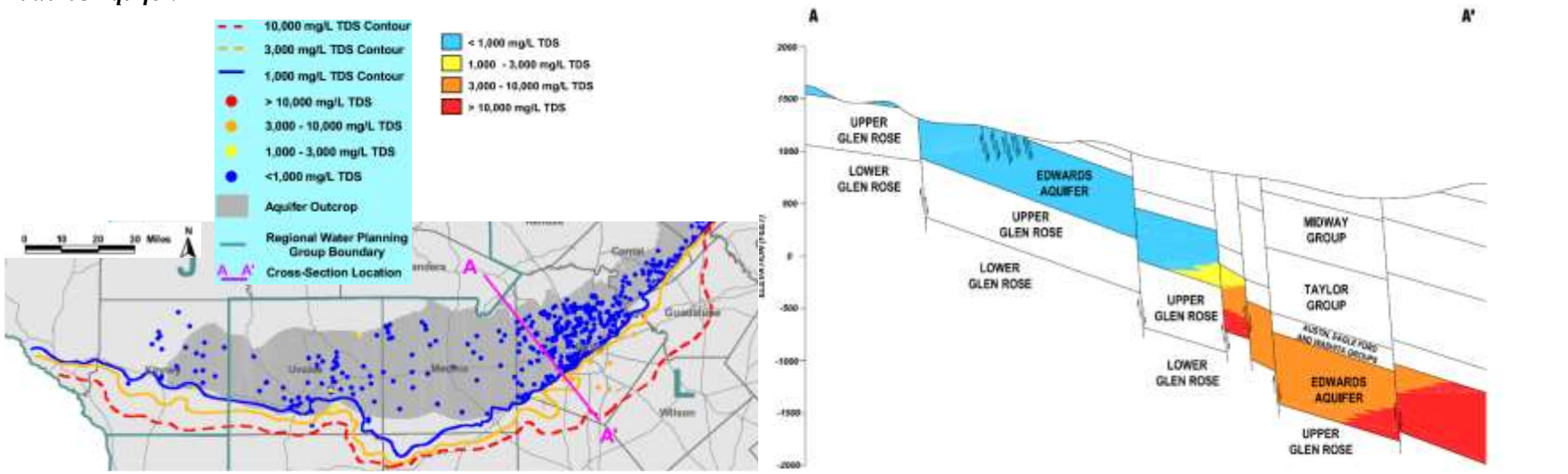

Carrizo-Wilcox Aquifer:

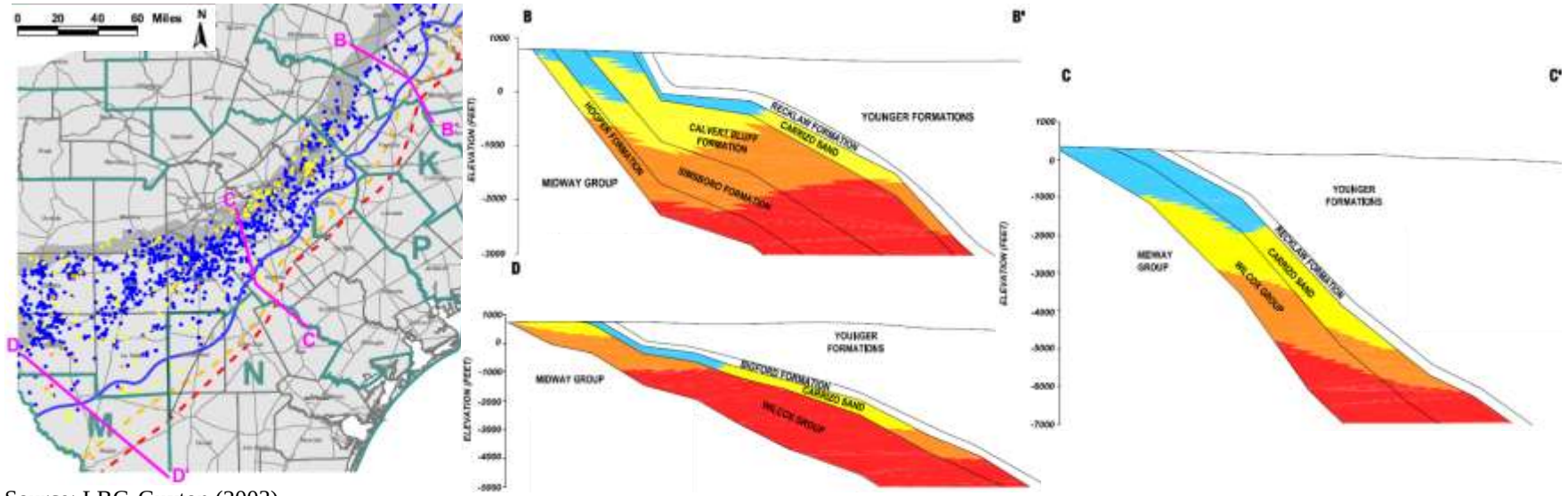

Source: LBG-Guyton (2003)

Figure 79. Rough sketches of Edwards and Carrizo-Wilcox aquifers brackish sections

Gulf Coast Aquifers

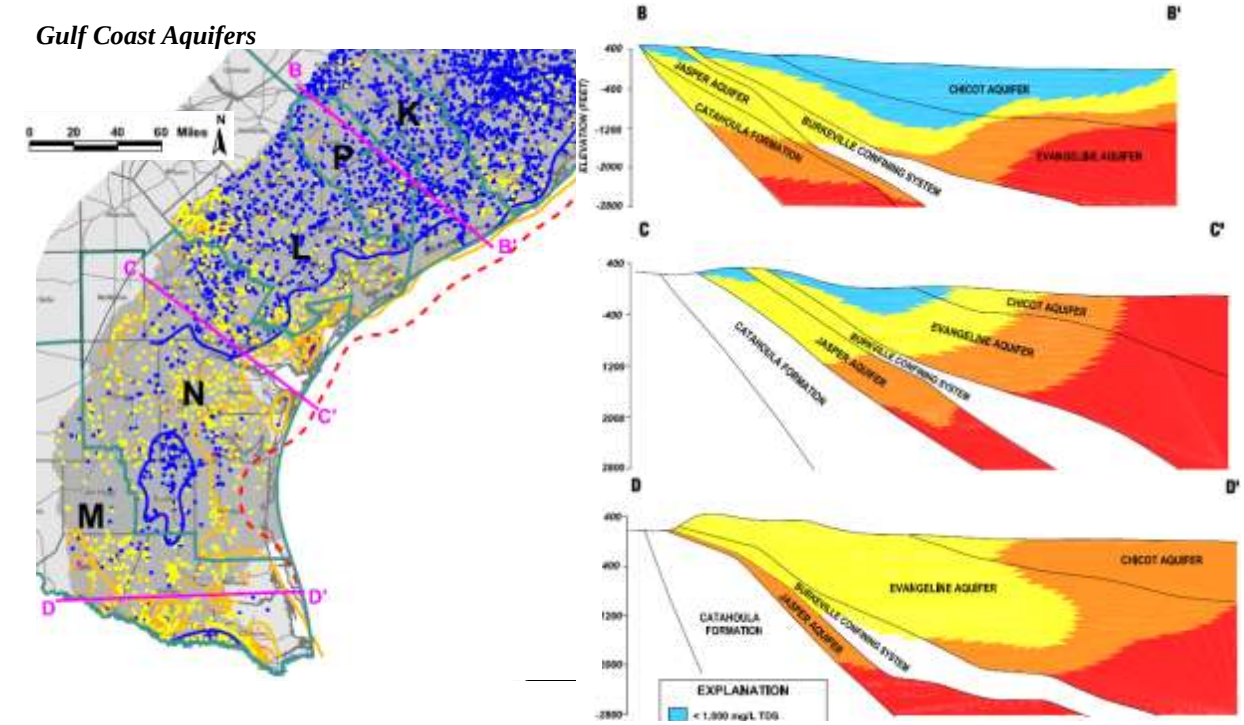

Queen City-Sparta Aquifers

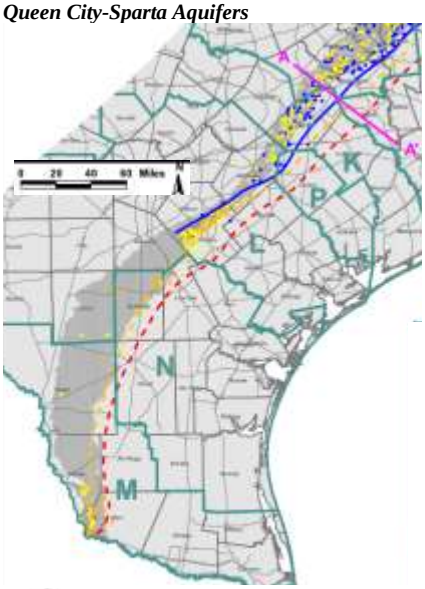

Yegua-Jackson Aquifer

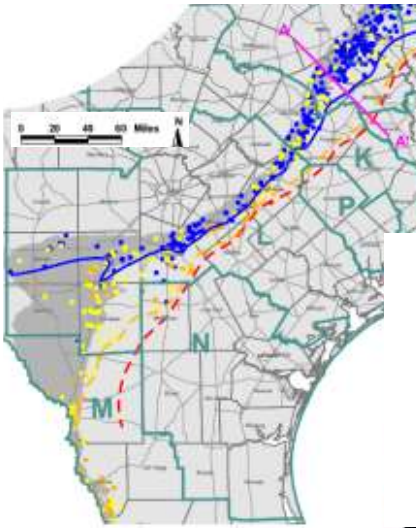

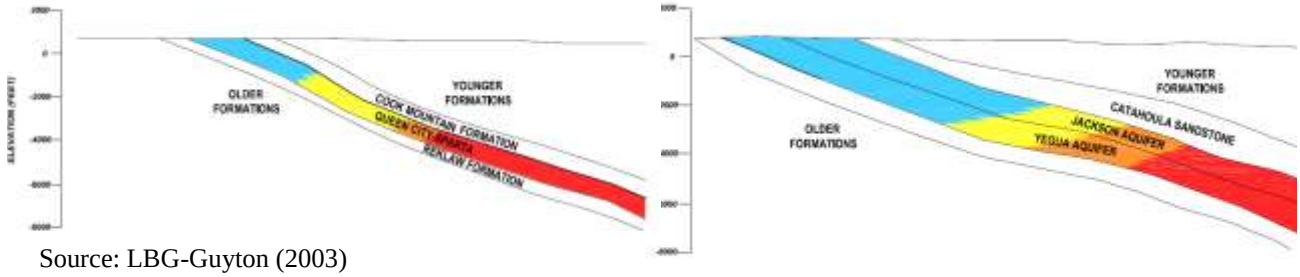

Source: LBG-Guyton (2003)

Figure 80. Rough sketches of Gulf Coast, Queen City-Sparta and Yegua-Jackson aquifers brackish sections

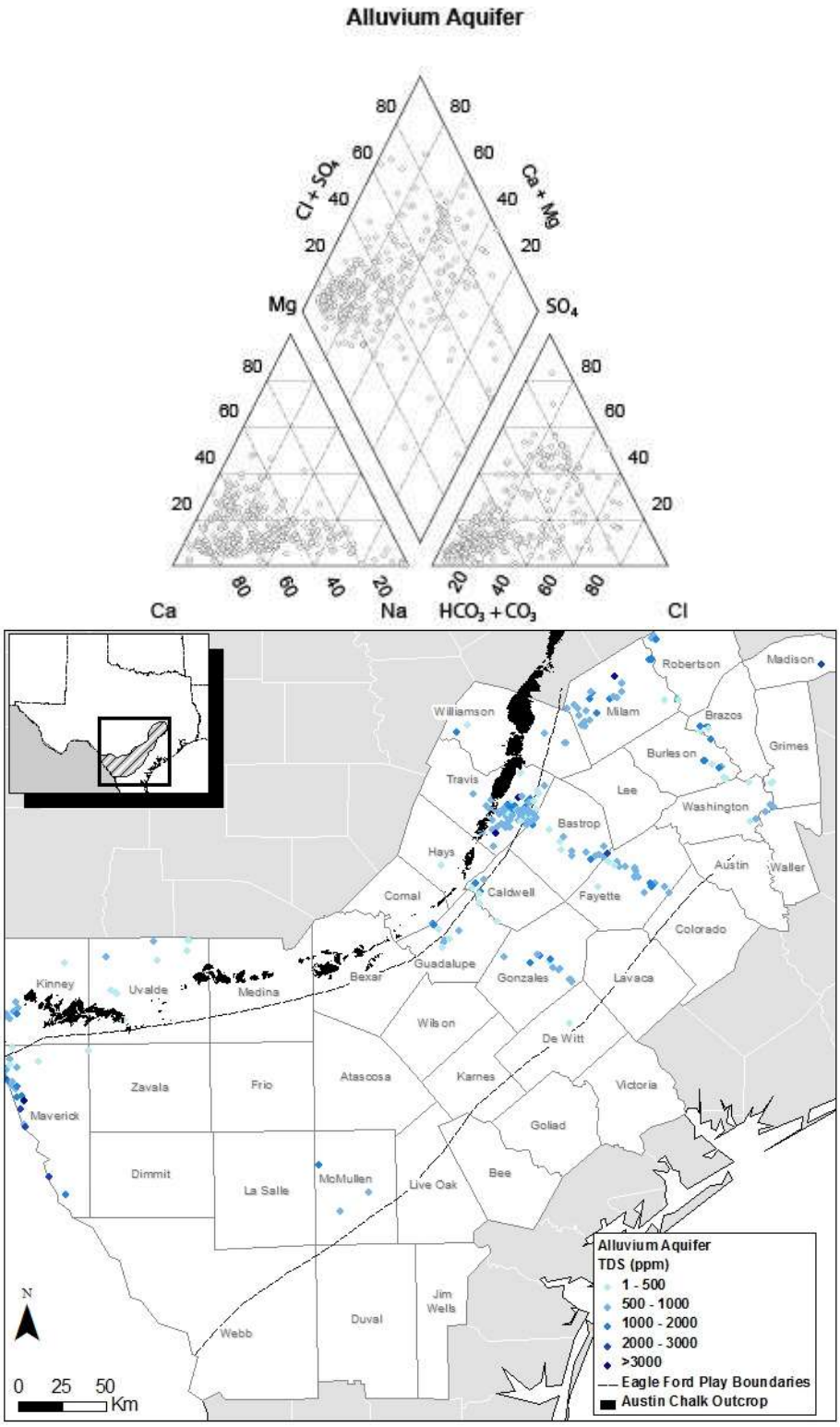

Source: TWBD, http://www.twdb.state.tx.us/groundwater/data/gwdbrpt.asp

Figure 81. Map and piper plot of Alluvium Aquifer group

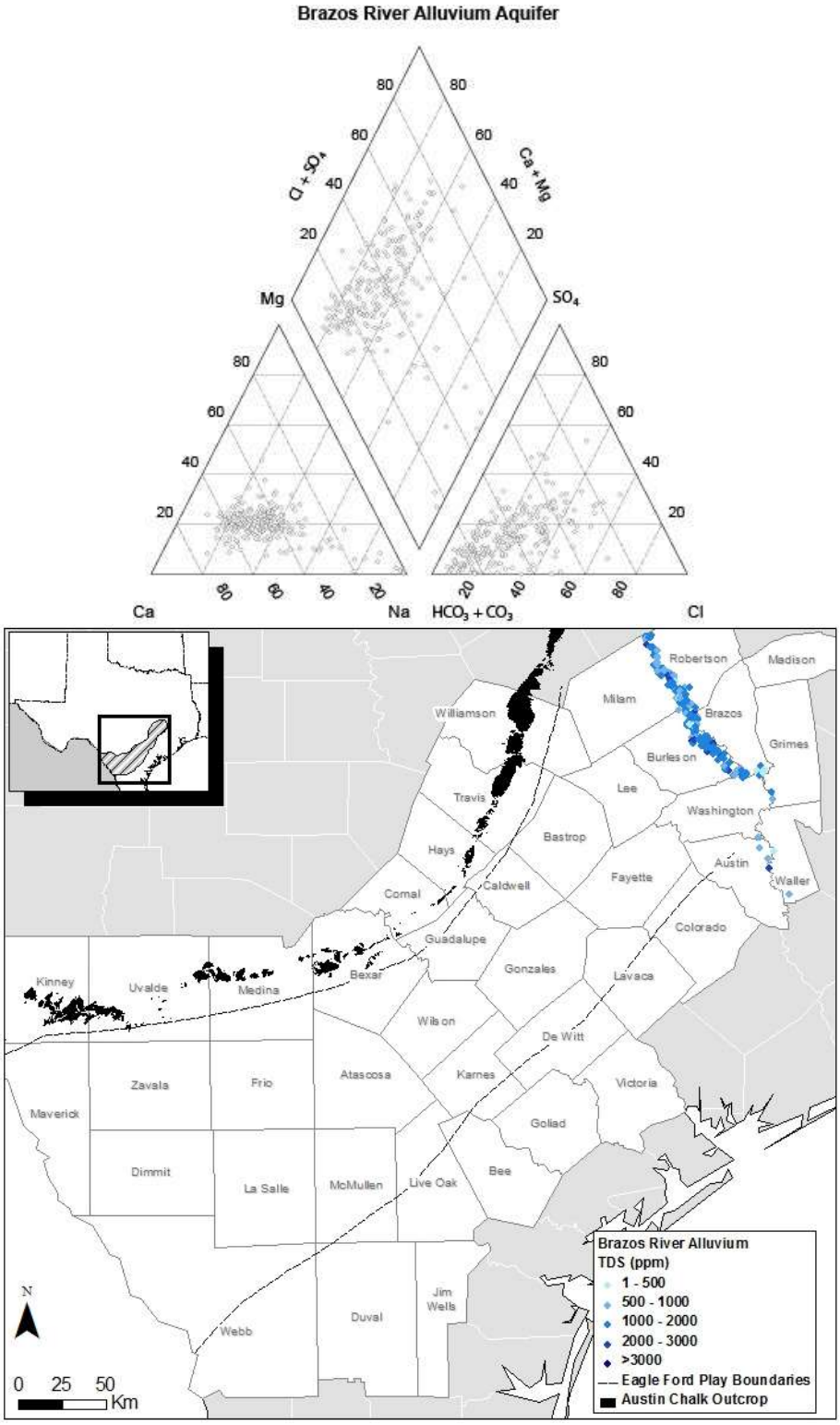

Source: TWBD, http://www.twdb.state.tx.us/groundwater/data/gwdbrpt.asp

Figure 82. Map and piper plot of Brazos River Alluvium Aquifer

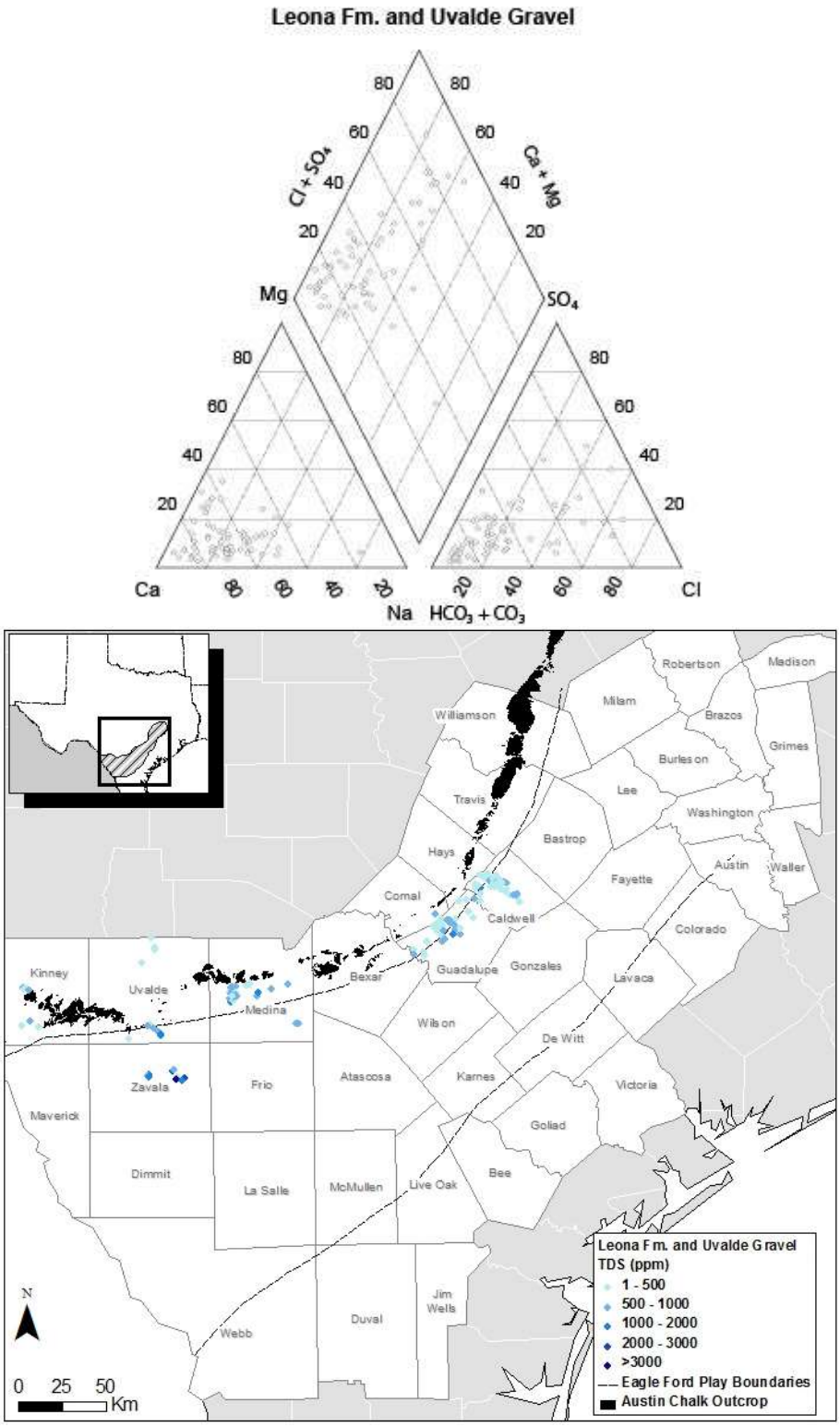

Source: TWBD, http://www.twdb.state.tx.us/groundwater/data/gwdbrpt.asp

Figure 83. Map and piper plot of Leona Formation and Uvalde Gravel group

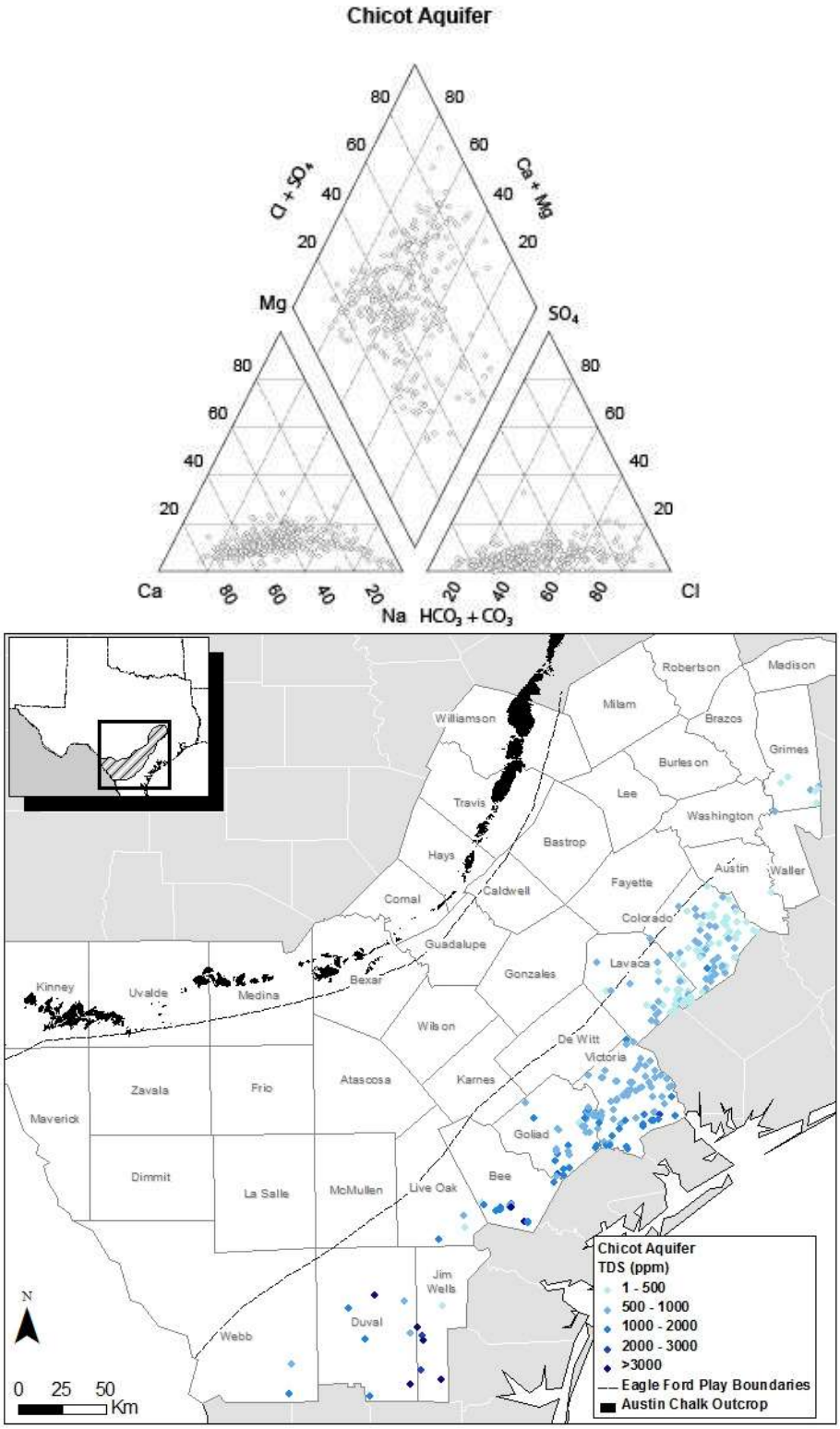

Source: TWBD, http://www.twdb.state.tx.us/groundwater/data/gwdbrpt.asp

Figure 84. Map and piper plot of Chicot Aquifer

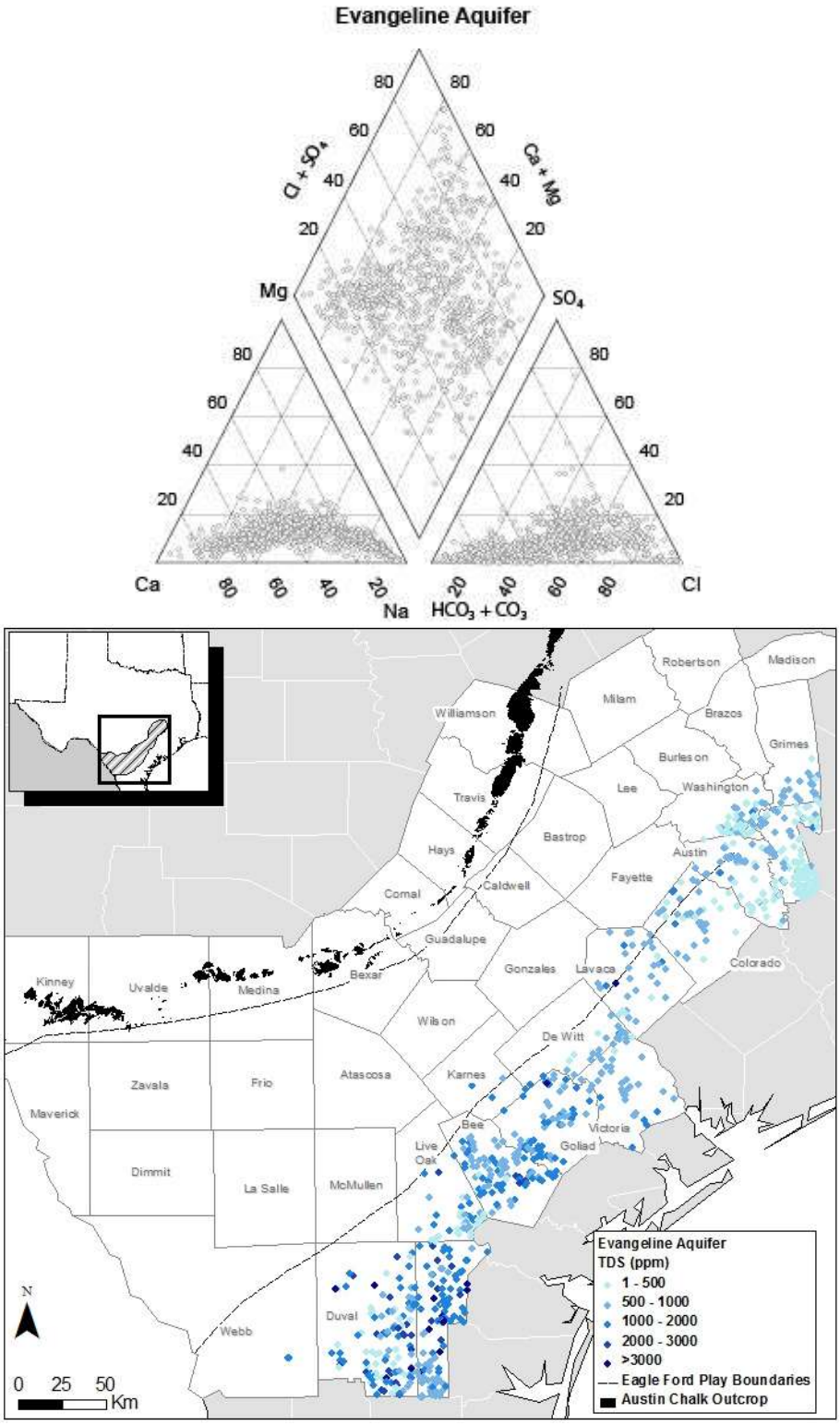

Source: TWBD, http://www.twdb.state.tx.us/groundwater/data/gwdbrpt.asp

Figure 85. Map and piper plot of Evangeline group

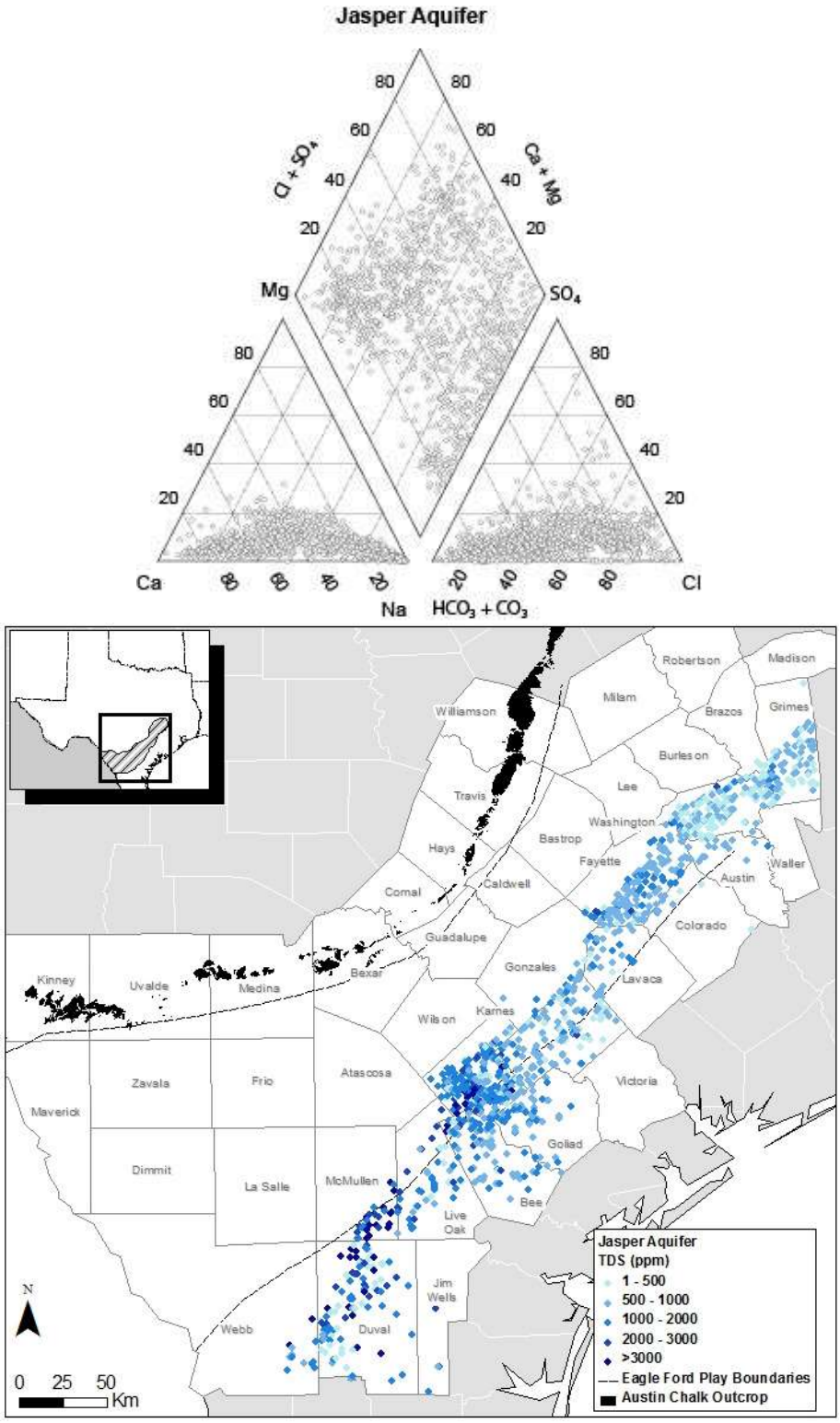

Source: TWBD, http://www.twdb.state.tx.us/groundwater/data/gwdbrpt.asp

Figure 86. Map and piper plot of Jasper Aquifer

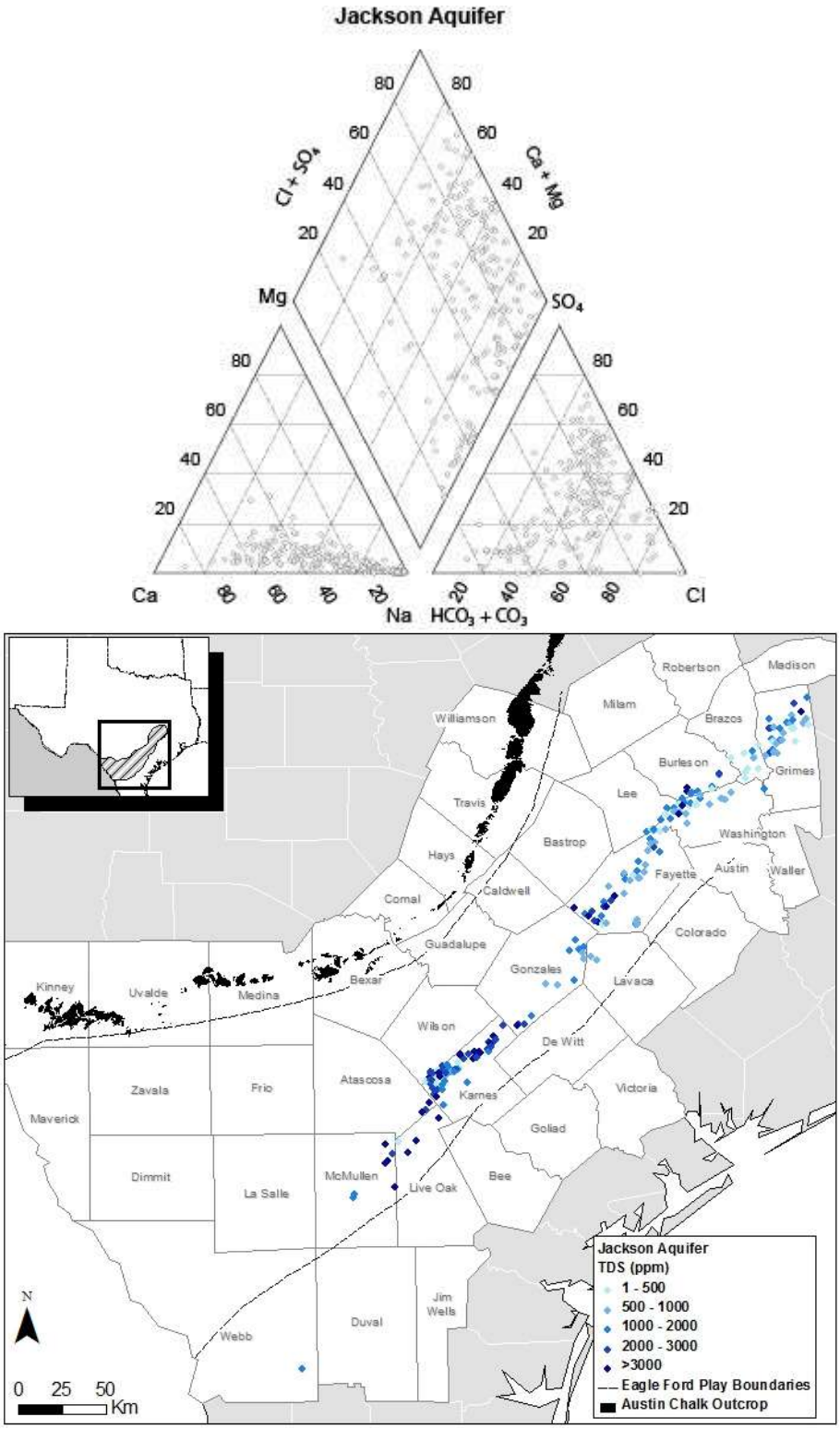

Source: TWBD, http://www.twdb.state.tx.us/groundwater/data/gwdbrpt.asp

Figure 87. Map and piper plot of Jackson Aquifer

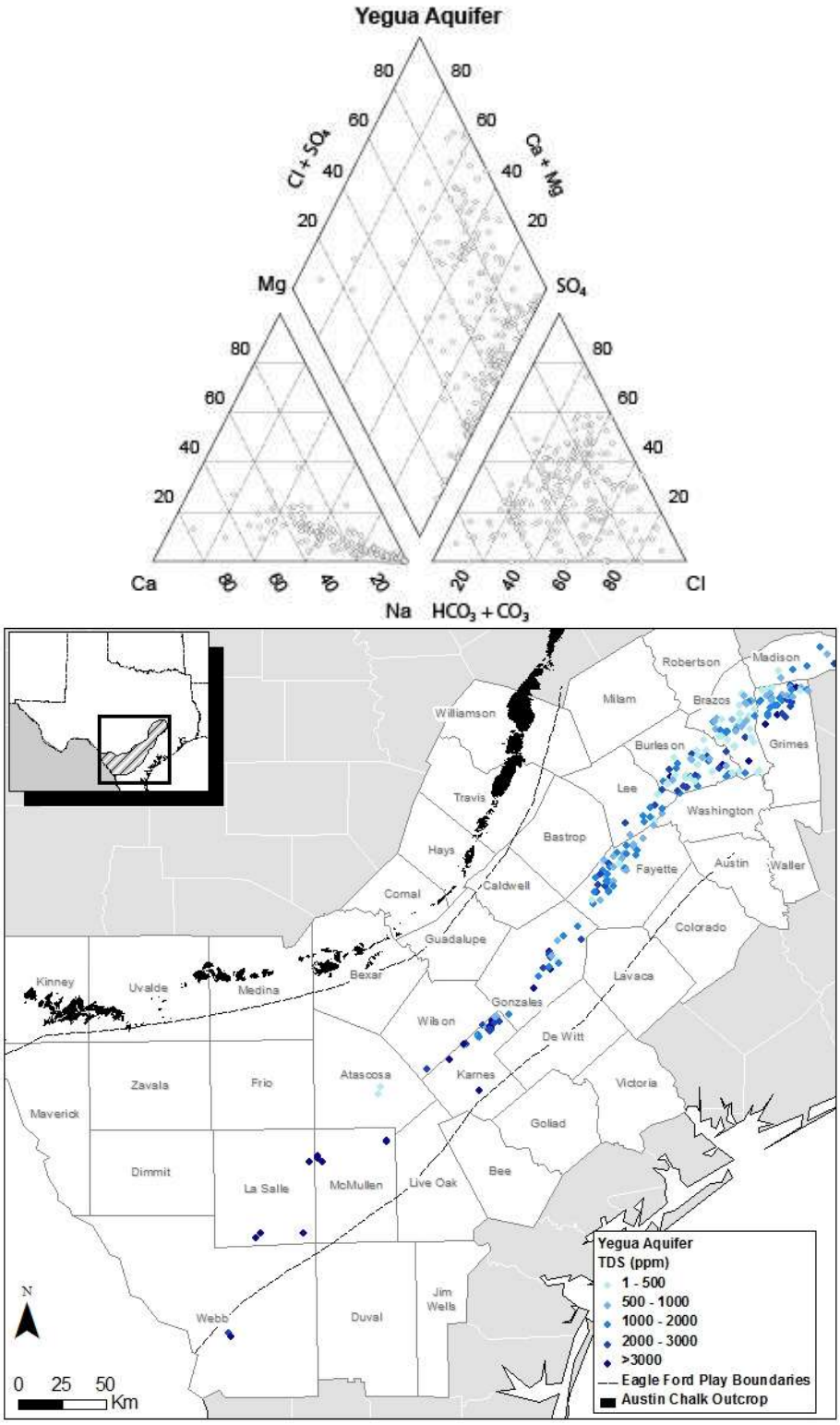

Source: TWBD, http://www.twdb.state.tx.us/groundwater/data/gwdbrpt.asp

Figure 88. Map and piper plot of Yegua Aquifer

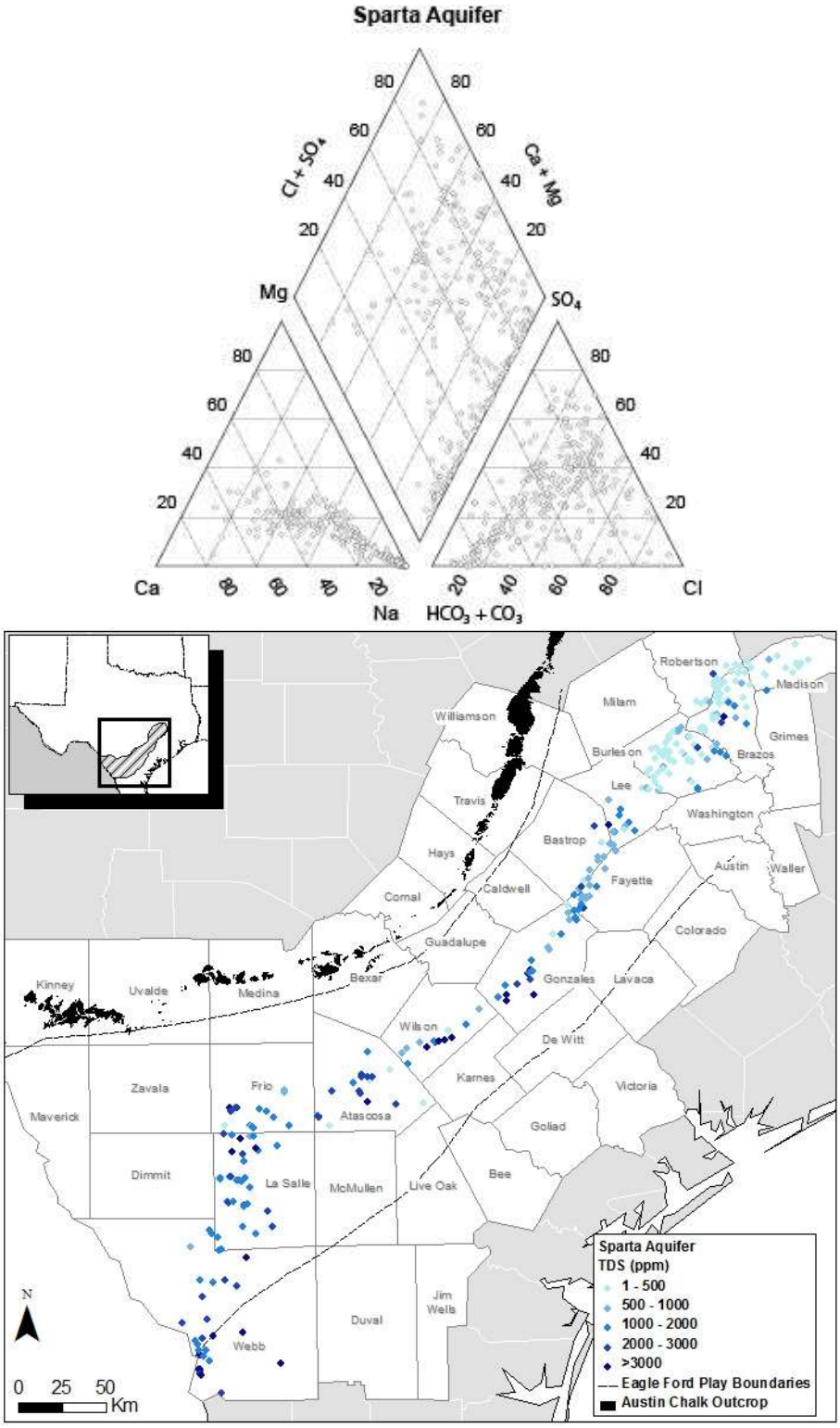

Source: TWBD, http://www.twdb.state.tx.us/groundwater/data/gwdbrpt.asp

Figure 89. Map and piper plot of Sparta Aquifer

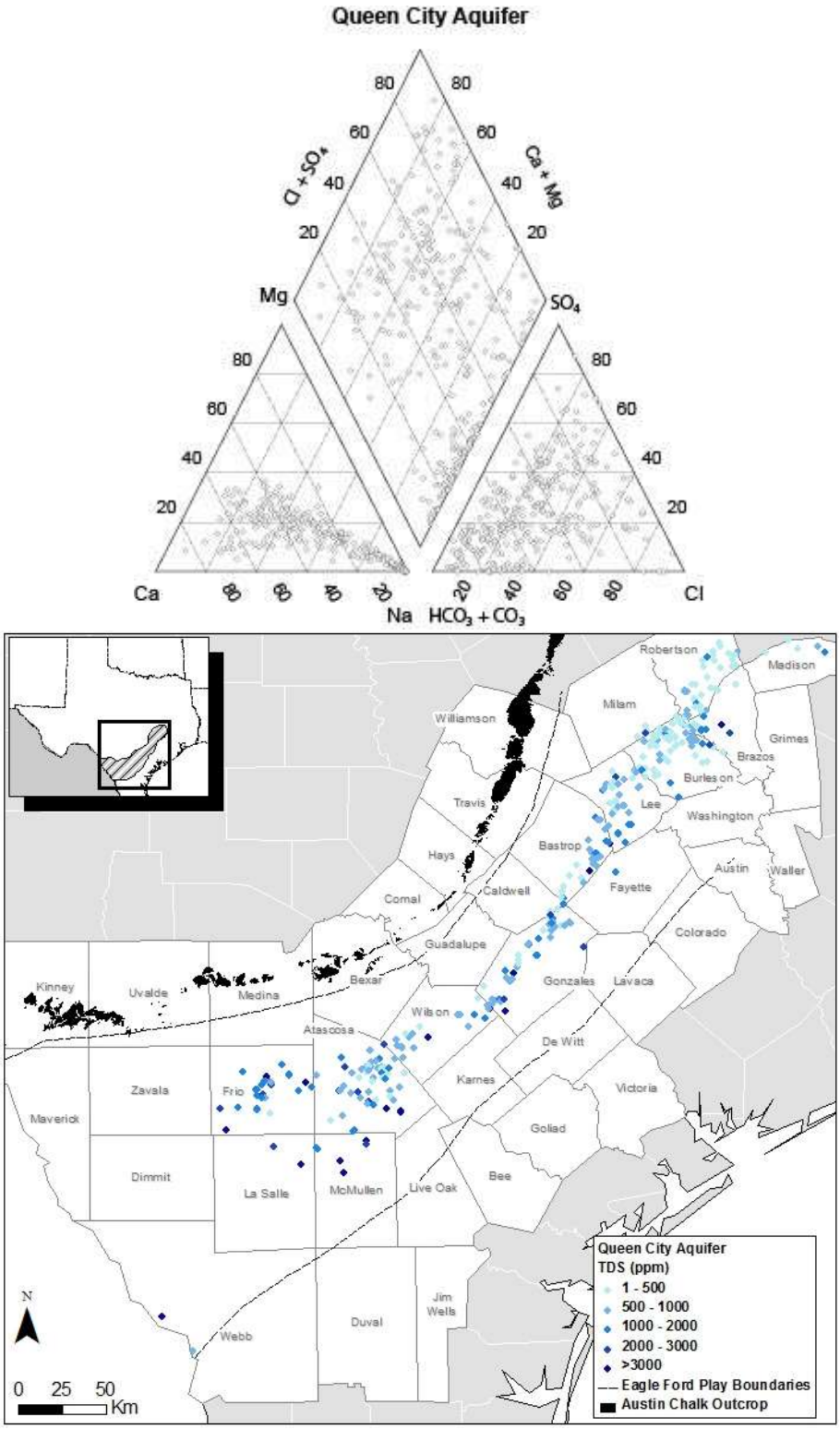

Source: TWBD, http://www.twdb.state.tx.us/groundwater/data/gwdbrpt.asp

Figure 90. Map and piper plot of Queen City Aquifer

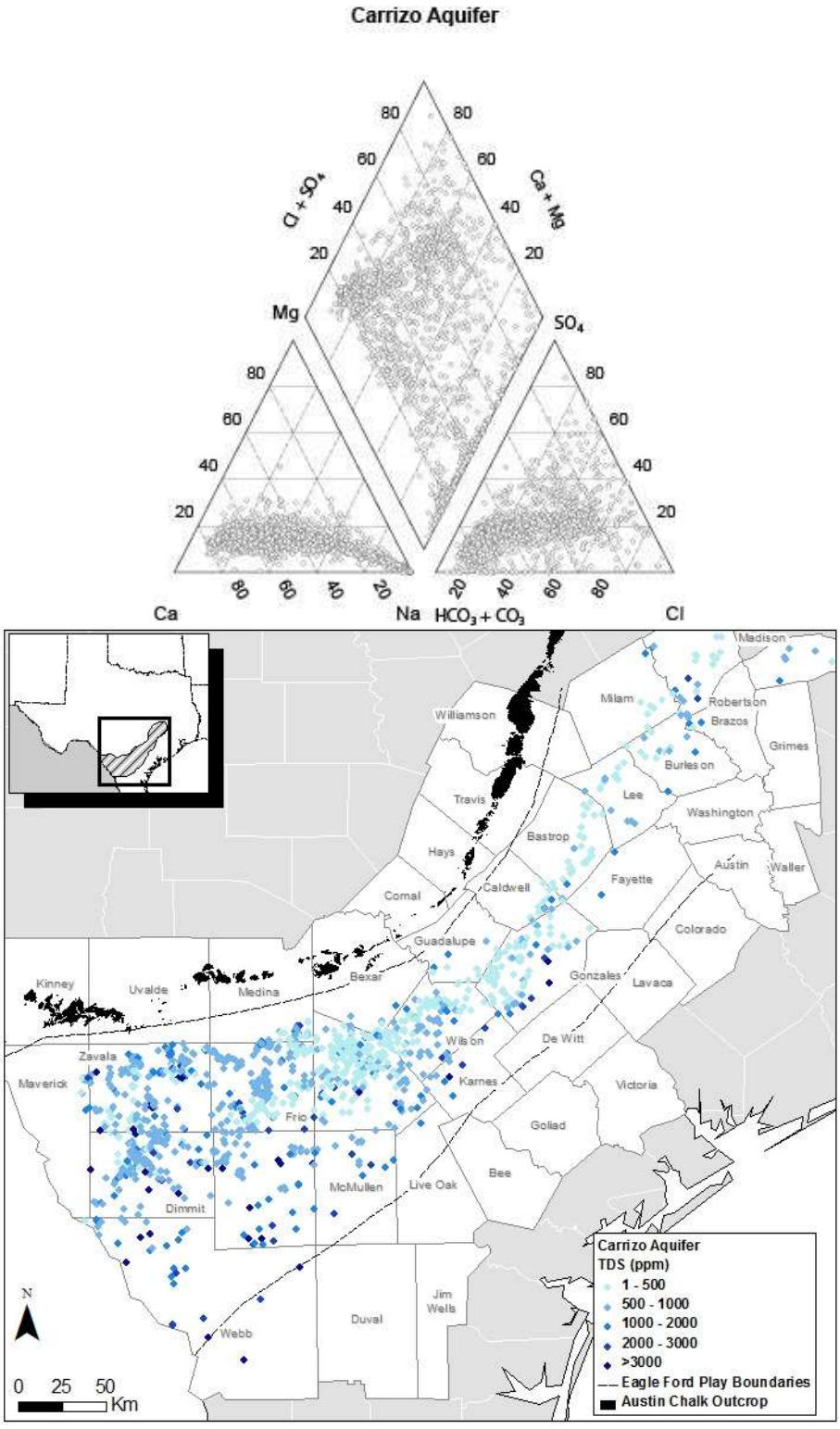

Source: TWBD, http://www.twdb.state.tx.us/groundwater/data/gwdbrpt.asp

Figure 91. Map and piper plot of Carrizo Aquifer

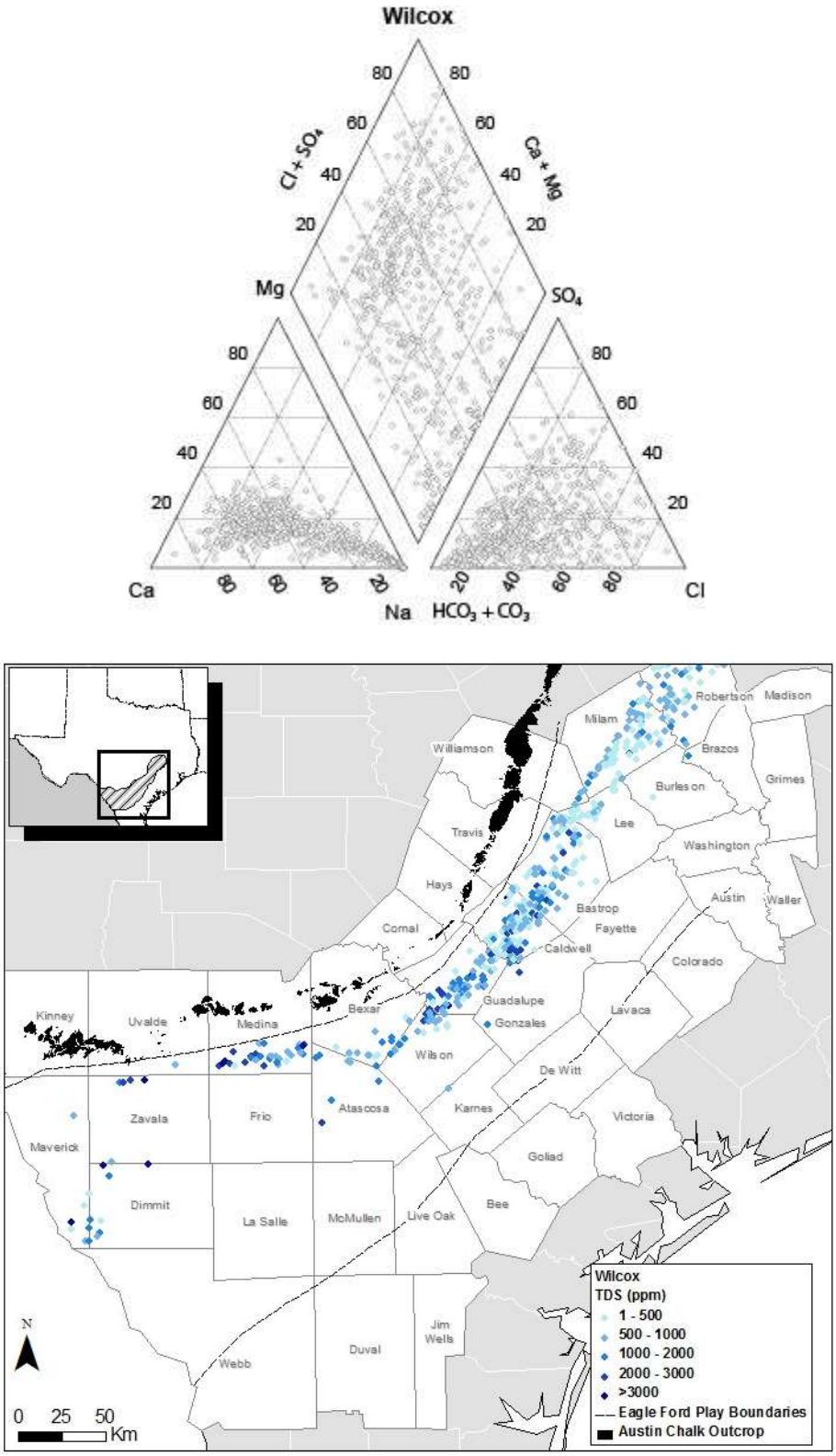

Source: TWBD, http://www.twdb.state.tx.us/groundwater/data/gwdbrpt.asp

Figure 92. Map and piper plot of Wilcox Aquifers (non Simsboro)

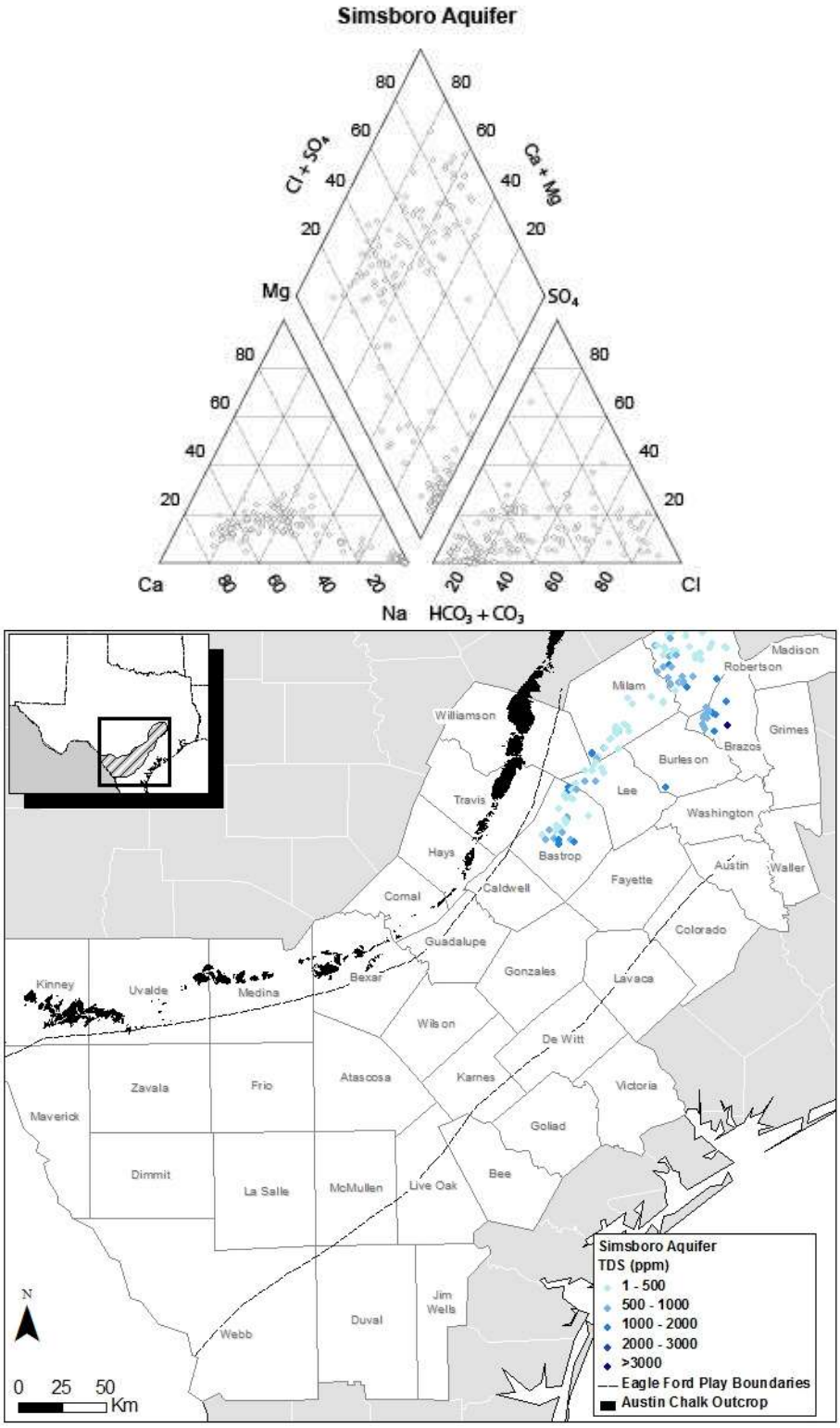

Source: TWBD, http://www.twdb.state.tx.us/groundwater/data/gwdbrpt.asp

Figure 93. Map and piper plot of Simsboro Aquifer

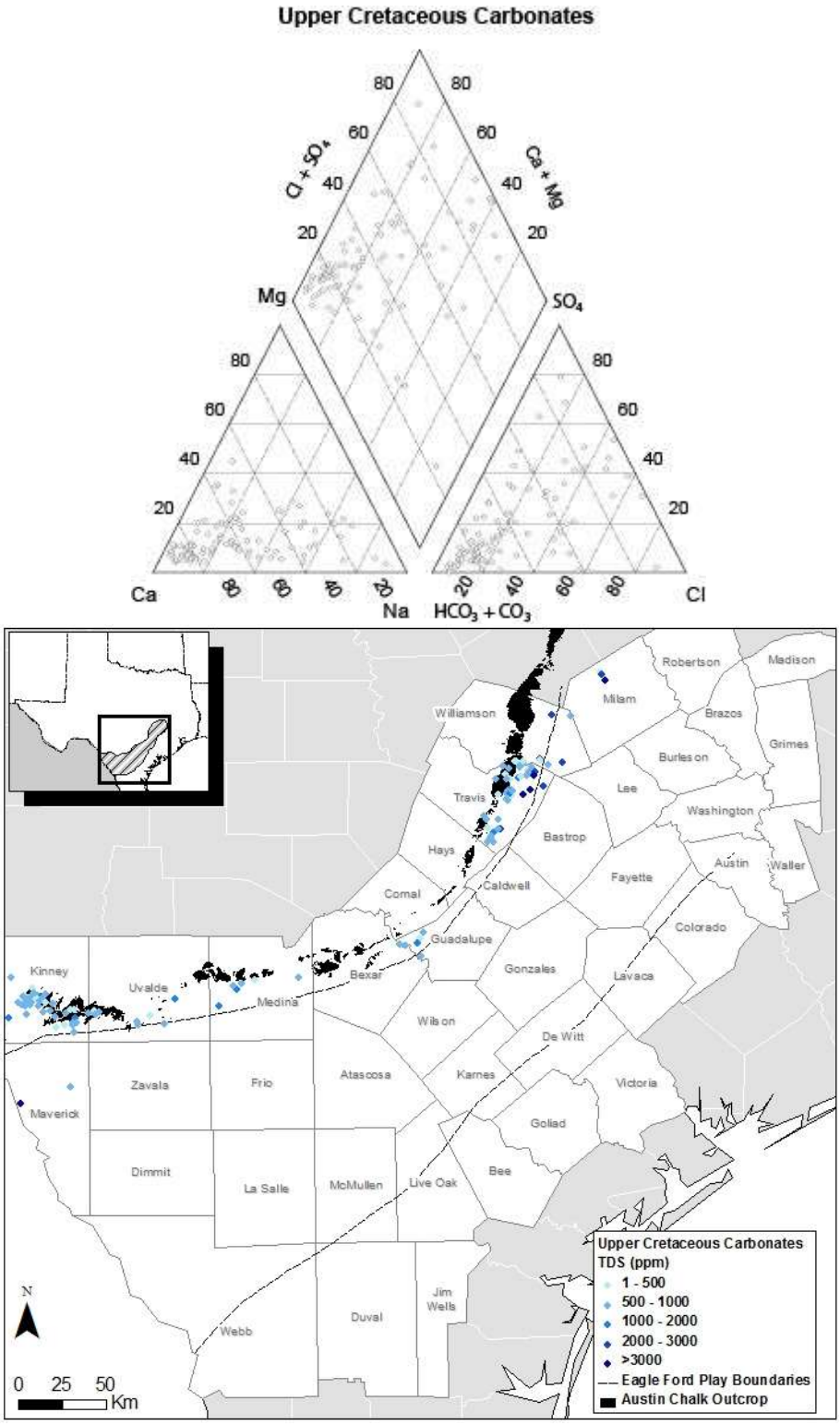

Source: TWBD, http://www.twdb.state.tx.us/groundwater/data/gwdbrpt.asp

Figure 94. Map and piper plot of Upper Cretaceous Carbonates group

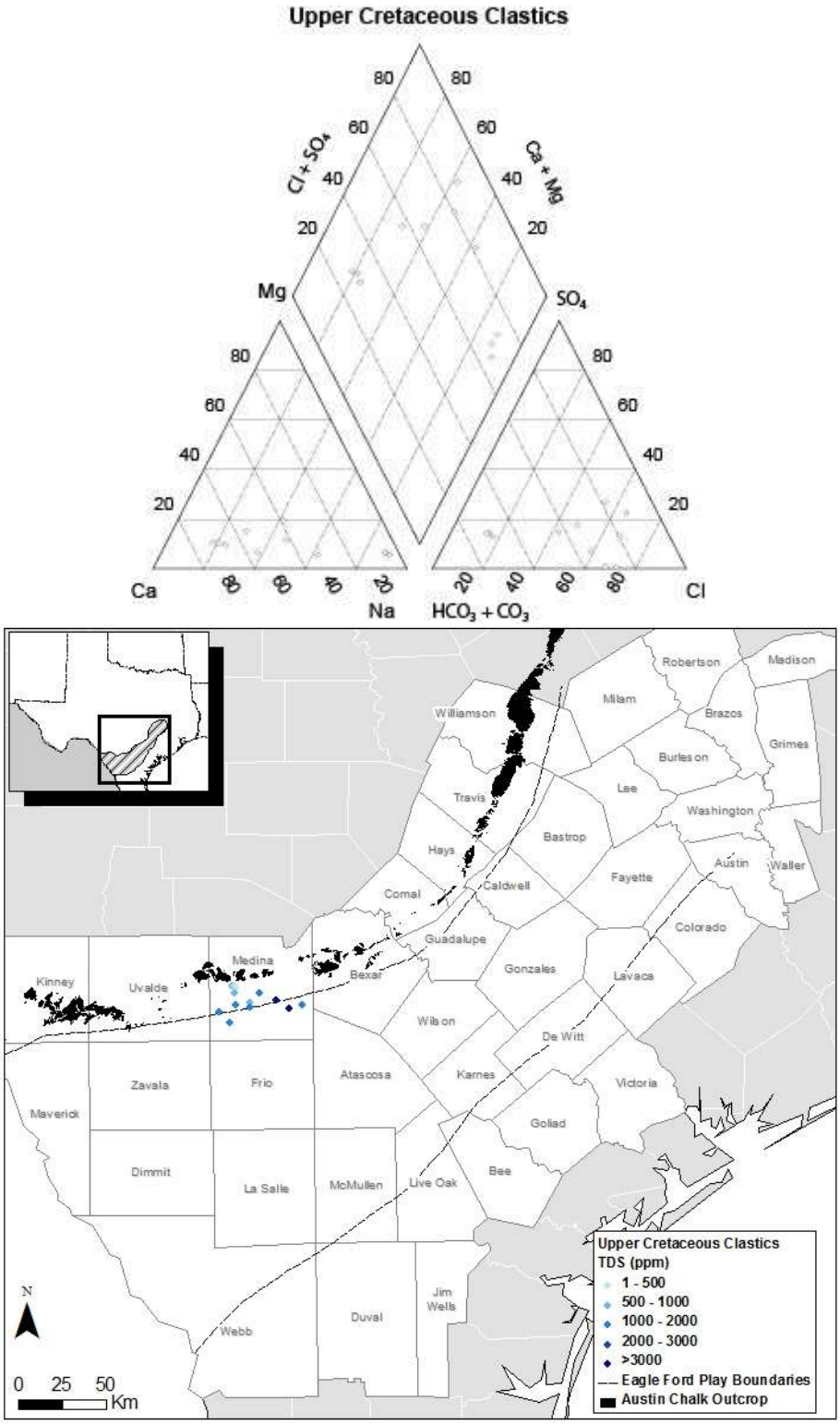

Source: TWBD, http://www.twdb.state.tx.us/groundwater/data/gwdbrpt.asp

Figure 95. Map and piper plot of Upper Cretaceous Clastics group

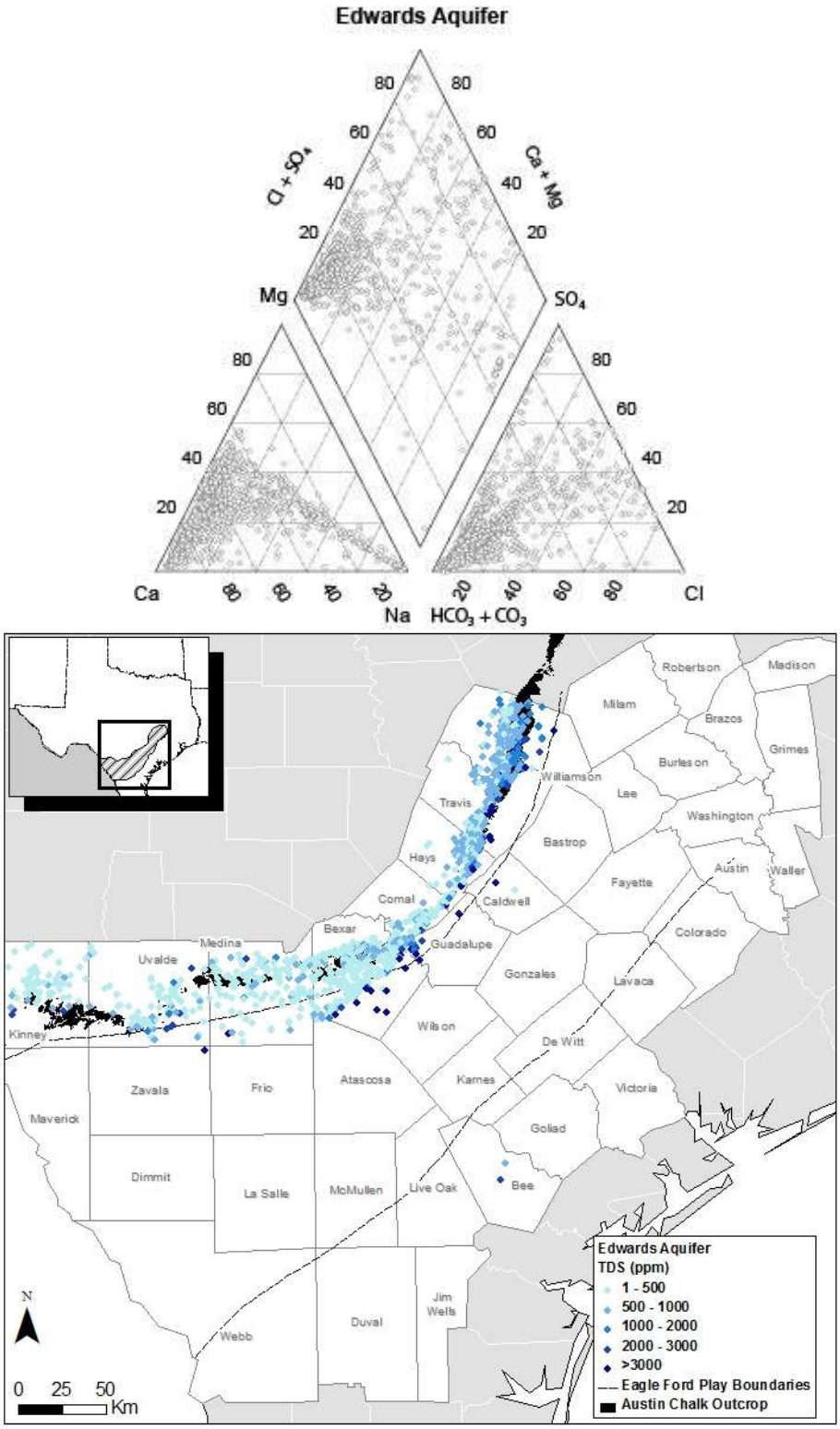

Source: TWBD, http://www.twdb.state.tx.us/groundwater/data/gwdbrpt.asp

Figure 96. Map and piper plot of Edwards Aquifer

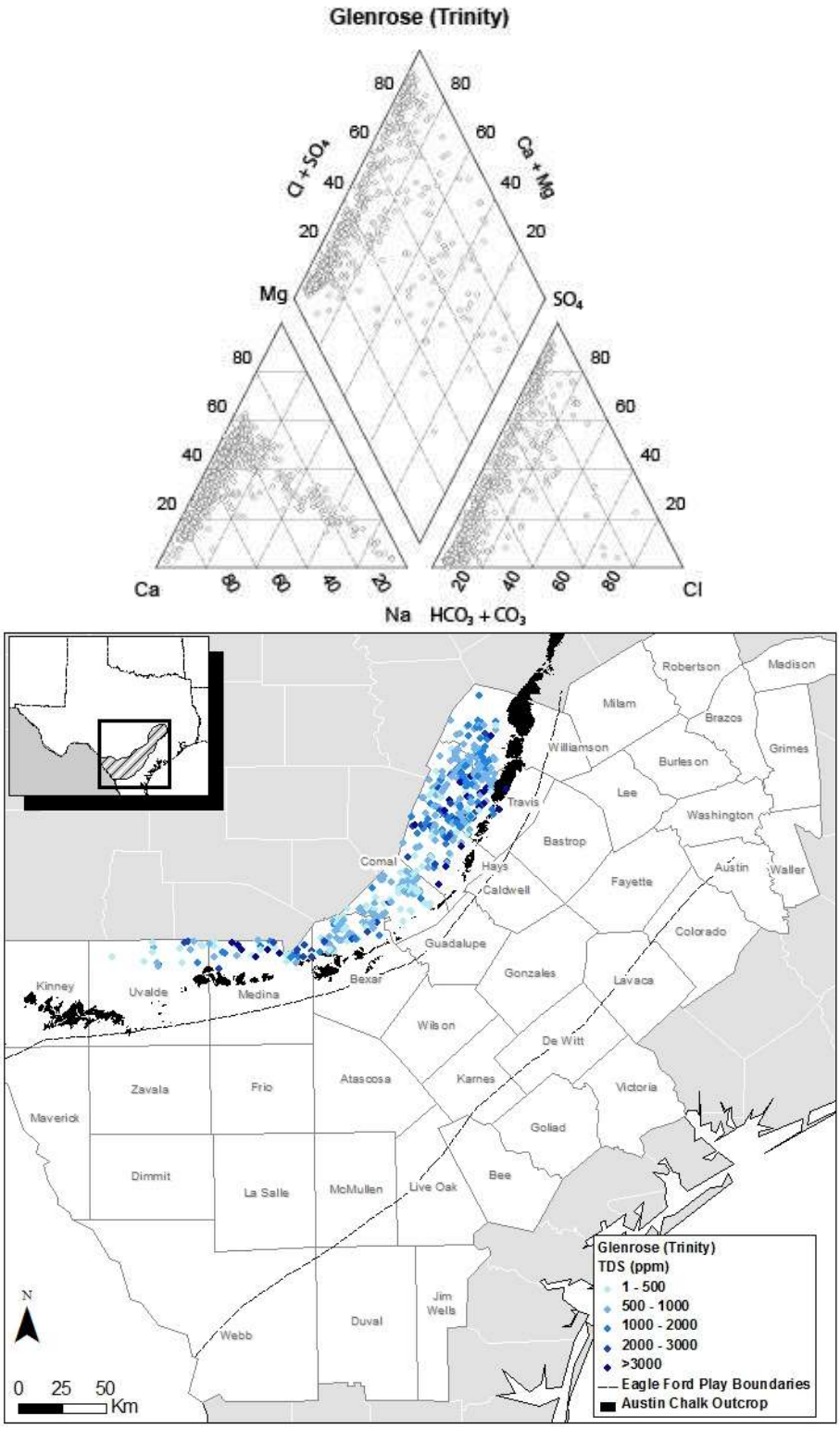

Source: TWBD, http://www.twdb.state.tx.us/groundwater/data/gwdbrpt.asp

Figure 97. Map and piper plot of Glenrose (Trinity) Aquifer

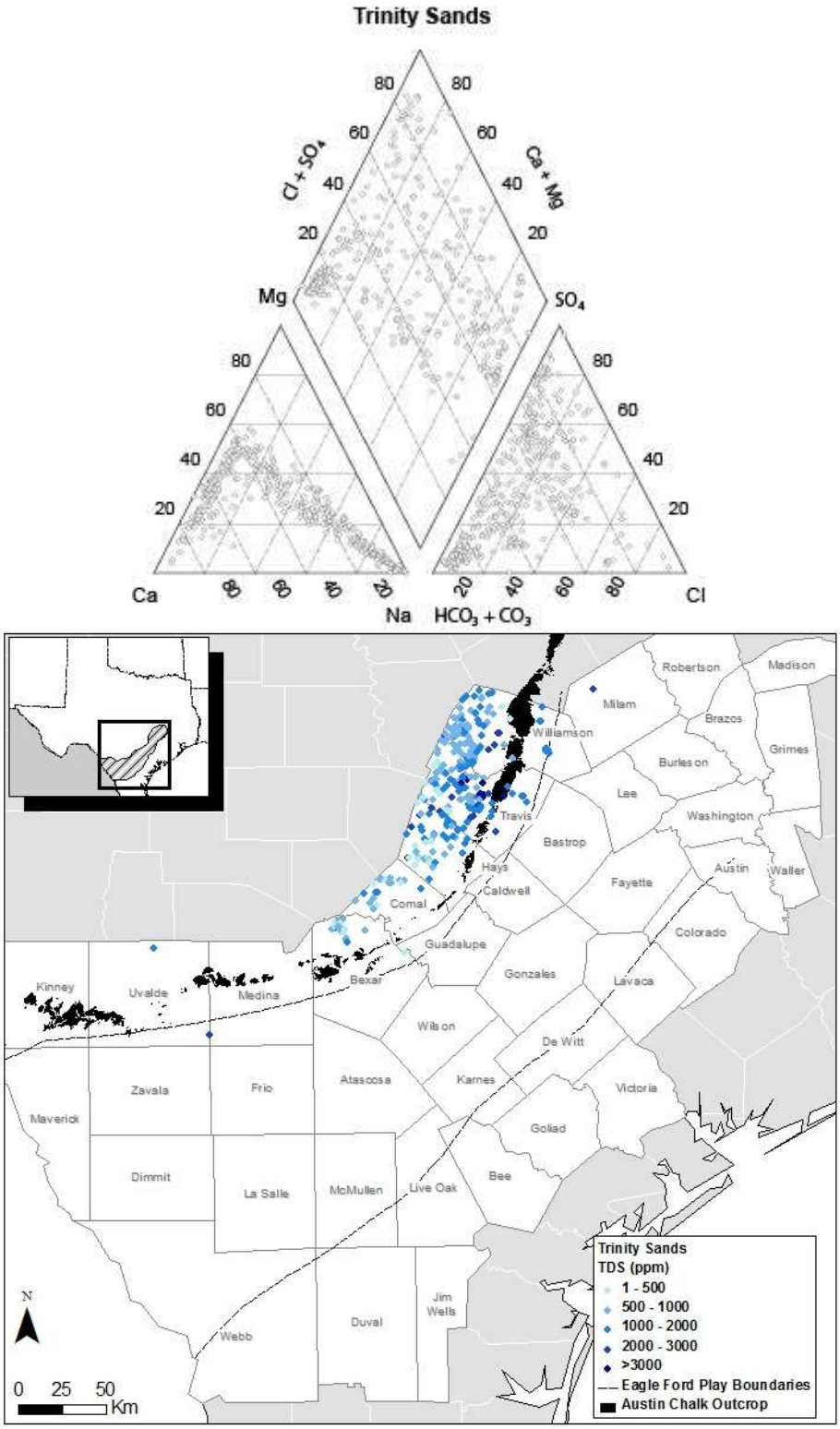

Source: TWBD, http://www.twdb.state.tx.us/groundwater/data/gwdbrpt.asp

Figure 98. Map and piper plot of Trinity Sands group

V. Oil and Gas Resources

In this section we develop an analysis based on 45 counties within or next to the EF footprint (Figure 99). South Texas has been an active hydrocarbon production area for decades and tens of thousands of non EF wells exist in the EF footprint (Figure 100 and Figure 101). We used the IHS database (IHS Enerdeq, http://www.ihs.com/) from which we queried and downloaded all wells in the entire database from those counties. We used the Status final code to determine if the wells had been active in the past and whether it is an oil or gas well. We used either producing formation or formation at TD from the well header to calculate statistics.

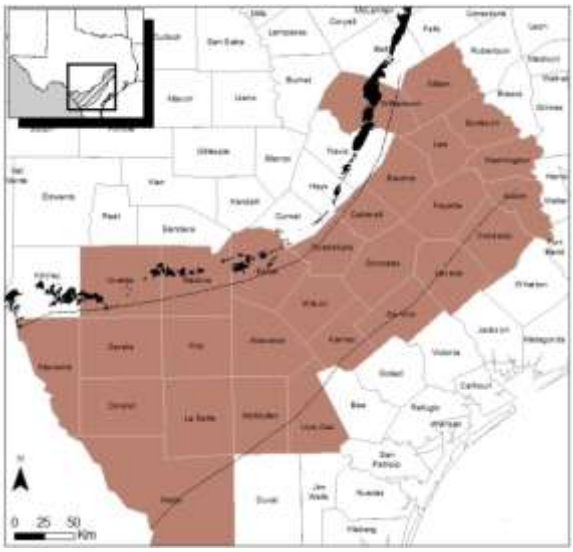

Figure 99. Counties included in the statistical analysis

Figure 102, Figure 103, and Figure 104 show all oil and gas, oil, and gas wells, respectively. Figure 105, Figure 106, and Figure 107 present the same information but only for active wells, excluding EF wells. Analysis of the well database indicates that 110,990 wells have been drilled in the EF area (Figure 99) but not producing from the EF between 1905 and 2012. Approximately 50% of the wells have information concerning the producing formation and ~66% of wells have information concerning the formation at Total Depth. Approximately 88,079 wells have been active or are active in the EF area (Figure 99) between 1902 and 2012 - ~62,300 produce or produced oil and ~25,592 produce or produced gas, and a few are both. About 82% of the wells producing oil have information concerning the producing formation and ~89% of wells producing gas have information concerning the producing formation. Table 4a illustrates the top producing formations in the Eagle Ford area. Alternatively, ~89% of gas and ~80% of oil wells have information concerning the formation at Total Depth. Table 4b illustrates the top formations at Total Depth.

Table 2 collects the top producing formations in the Eagle Ford area. They are the Austin Chalk (28% of total active wells), the Navarro and Taylor groups (a combined 42%), and the Wilcox Fm. (5%). They represent ~75% of the wells and those formations are all located above the EF. Table 3 presents similar information but focusing on formation at total depth rather than producing formation and Table 4 splits the information into gas and oil producing formations.

Note that the total, active, and inactive percent for an individual formation excludes wells that have an unknown producing or Total depth formations respectively.

Table 2. Top producing formations for the Eagle Ford area.

Rank	Group	Total	% of Total	Active	% of Active	Inactive	% of Inactive
1	Austin Chalk	15706	28	15698	28	8	32
2	Navarro	9810	18	9805	18	5	20
3	Olmos	9750	18	9749	18	1	4
4	San Miguel	3256	6	3252	6	4	16
5	Wilcox	2852	5	2852	5	0	0

Table 3. Top formations at Total Depth for Eagle Ford area.

Rank	Group	Total	% of Total	Active	% of Active	Inactive	% of Inactive
1	Navarro	11302	15	9720	18	1582	8
2	Austin Chalk	10912	15	8590	16	2322	12
3	Olmos	9592	13	8020	15	1572	8
4	Buda	6742	9	5696	11	1046	5
5	Wilcox	5729	8	3074	6	2655	13

Table 4. Top producing formations (a) and top formations at Total Depth (b) for the Eagle Ford area

Category	Rank	Group	%
Oil	1	Austin Chalk	32
	2	Navarro	19
	3	Olmos	11
	4	San Miguel	6
	5	Eagle Ford	5
	6	Edwards	3
Gas	1	Wilcox	30
	2	Olmos	18
	3	Eagle Ford	7
	4	Austin Chalk	6
	5	Lobo	6
	6	Frio	6

(a)

Category	Rank	Group	%
Oil	1	Navarro	19
	2	Austin Chalk	18
	3	Buda	12
	4	Olmos	9
	5	Eagle Ford	9
	6	Edwards	5
Gas	1	Wilcox	28
	2	Olmos	16
	3	Eagle Ford	7
	4	Austin Chalk	5
	5	Edwards	5
	6	Yegua	5

(b)

We are also interested in understanding how close other wells are from the EF. EF wells are wells above and below the EF are color-coded in Figure 108. Clearly many wells are above the EF and EF wells are not in areas of dense previous activity. Table 5 shows the statistics for the top producing formations as categorized by the distance above the Eagle Ford (Table 6 displays same information for wells below the EF). The Total % for an individual producing formation excludes wells that have an unknown producing formation. Figure 109 and Figure 110 illustrate the density of wells above and below, respectively, the EF as categorized by the distance above or below it. Most wells producing from above the EF will not intersect the EF whereas wells producing from formations below the EF will and come provide a leakage pathway, particularly active wells (Figure 111).

Table 5. Top Producing formations for distances above the Eagle Ford.

Ft above Barnett	% of Total	% of Active	Top Producing Formations			
			Rank	Group	Total	% of Known Total
			1	Austin Chalk	5698	38
1-1000	22	28	2	Olmos	4363	29
			3	Navarro	1808	12
			1	Navarro	6398	54
1000-2000	19	21	2	Olmos	2078	17
			3	San Miguel	1944	16
			1	Olmos	2817	43
2000-3000	11	11	2	Navarro	1506	23
			3	San Miguel	1958	30
			1	Wilcox	375	47
3000-4000	3	2	2	Olmos	171	21
			3	Navarro	30	4
			1	Wilcox	591	60
4000-5000	3	2	2	Carrizo	52	5
			3	Escondido	52	5
			1	Wilcox	164	20
5000-6000	3	2	2	Olmos	109	14
			3	Carrizo	105	13
			1	Queen City	131	15
6000-7000	3	2	2	Carrizo	119	13
			3	Wilcox	113	13
			1	Austin Chalk	160	45
7000-8000	2	1	2	Carrizo	26	7
			3	Yegua	19	5
			1	Austin Chalk	214	54
8000-9000	2	1	2	Mirando	42	11
			3	Jackson	26	7
			1	Austin Chalk	114	39
9000-10000	2	1	2	Miocene	33	11
			3	Oakville	21	7
			1	Jackson	152	26
10000-11000	3	2	2	Pettus	114	20
			3	Austin Chalk	90	16
			1	Austin Chalk	78	31
11000-12000	1	1	2	Pettus	55	22
			3	Government wells	28	11

Table 6. Top producing formations beyond the Eagle Ford.

Rank	Group	Total	% of Total	Active	% of Active
1	Edwards	2088	46	2086	43
2	Buda	958	21	956	20
3	Georgetown	487	11	487	10
4	Cretaceous	381	8	381	8
5	Glenrose	179	4	179	4
6	Serpentine	50	1	50	1

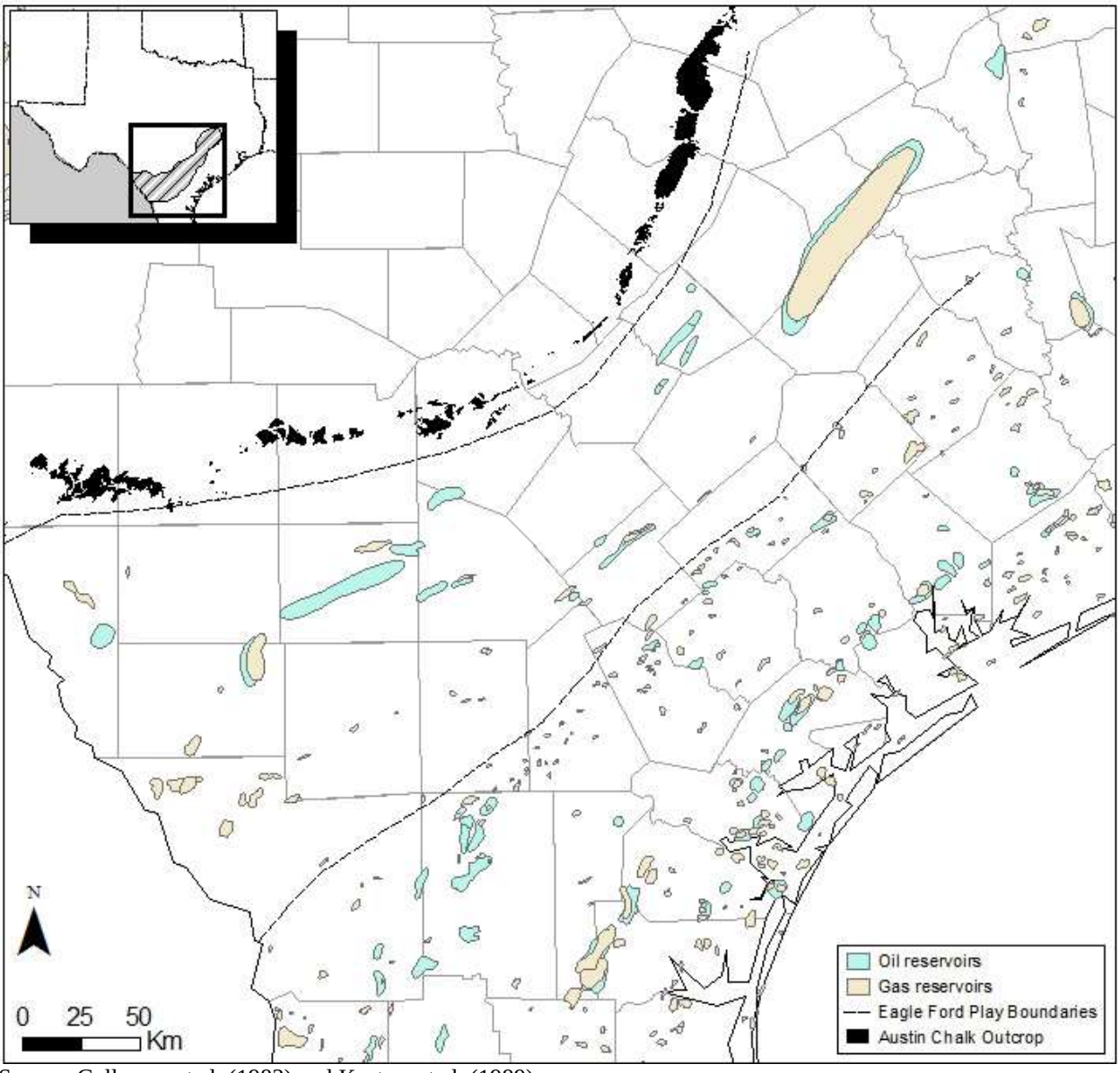

Source: Galloway et al. (1983) and Kosters et al. (1989)

Figure 100. Approximate location of major conventional oil and gas fields South and Central Texas

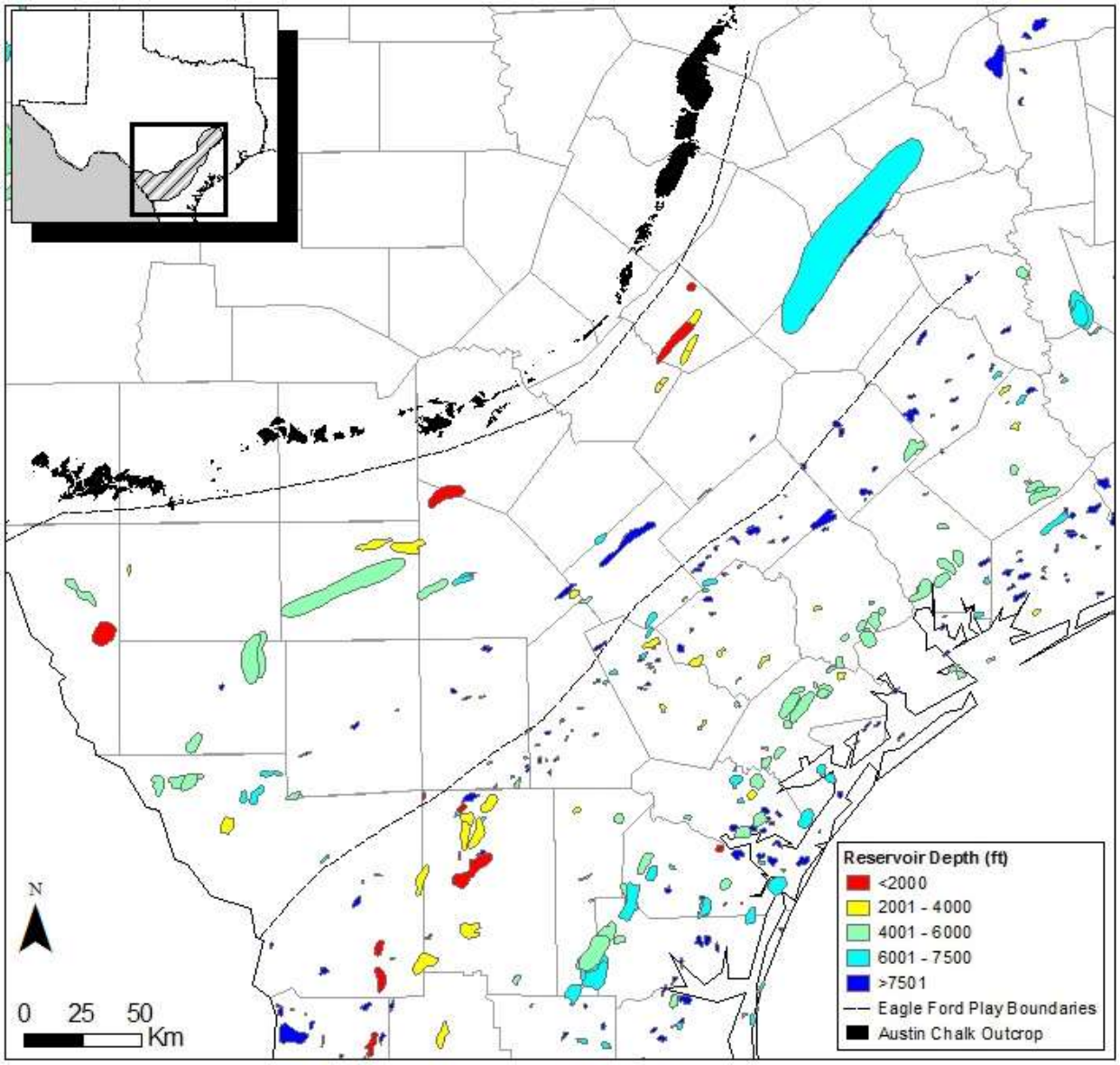

Source: Galloway et al. (1983) and Kosters et al. (1989)

Figure 101. Color-coded map of major conventional oil and gas reservoir depth South and Central Texas.

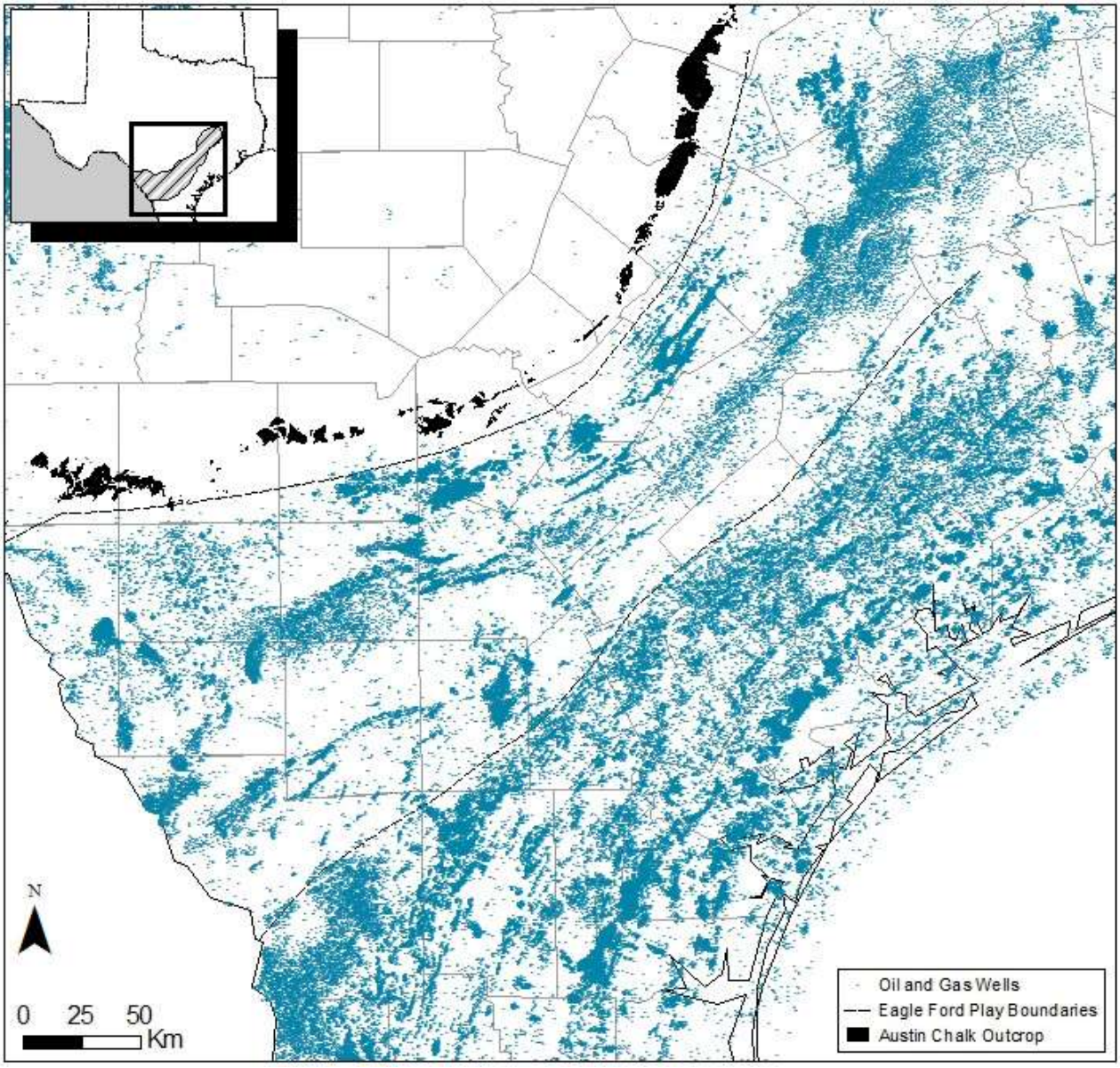

Source: IHS

Figure 102. Oil and gas wells in South and Central Texas

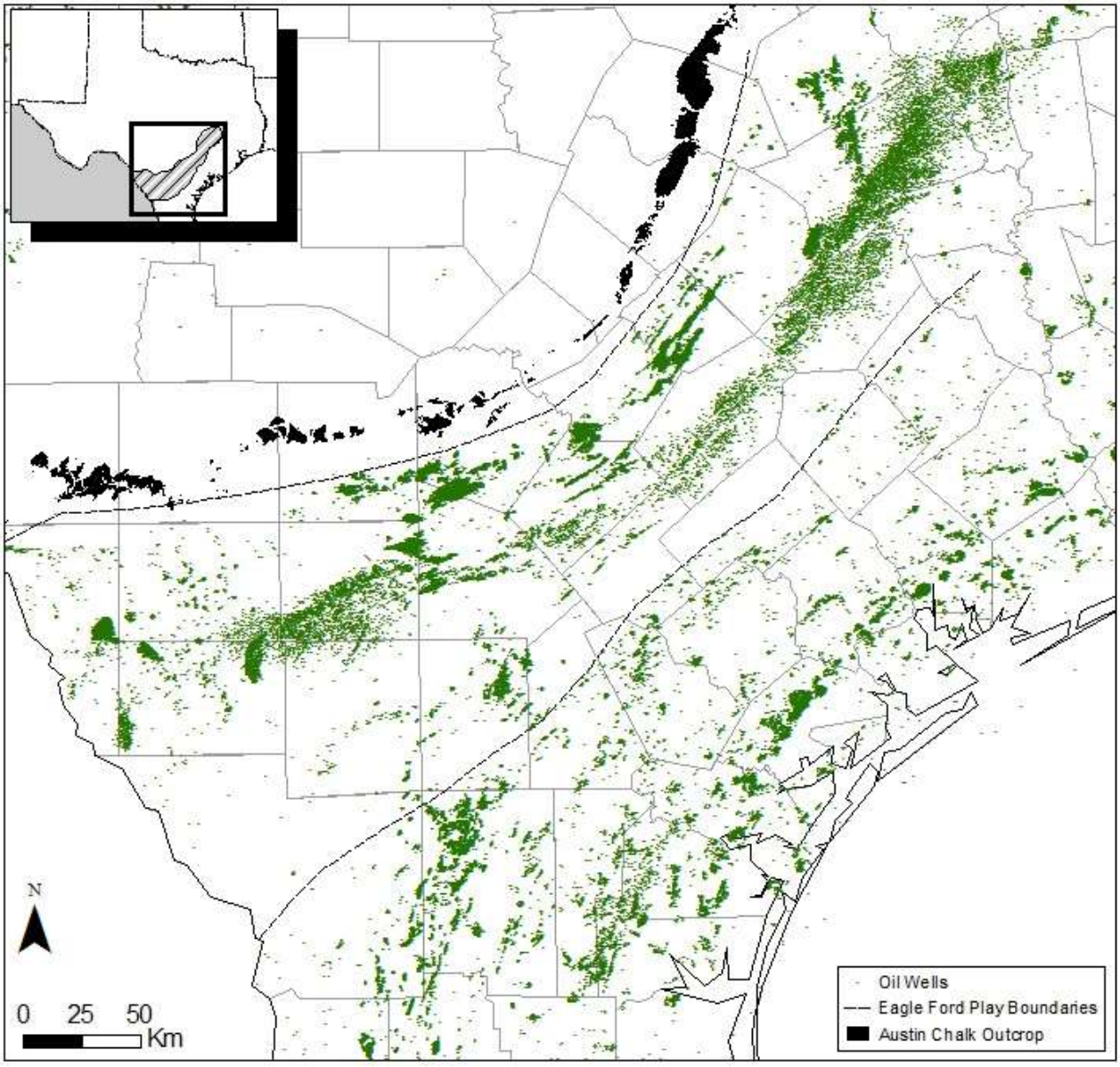

Source: IHS

Figure 103. Oil wells in South and Central Texas

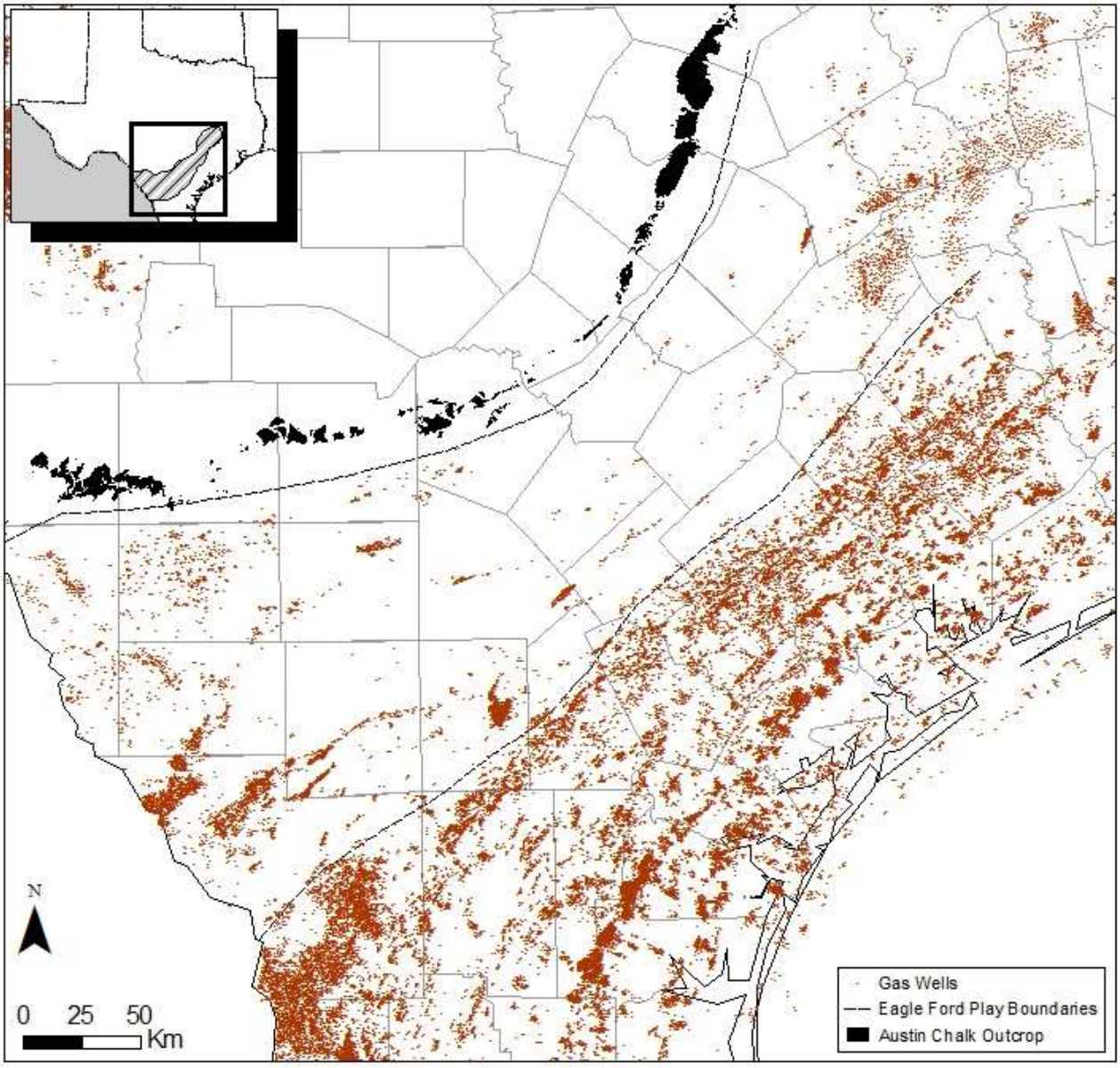

Source: IHS

Figure 104. Gas wells in South and Central Texas

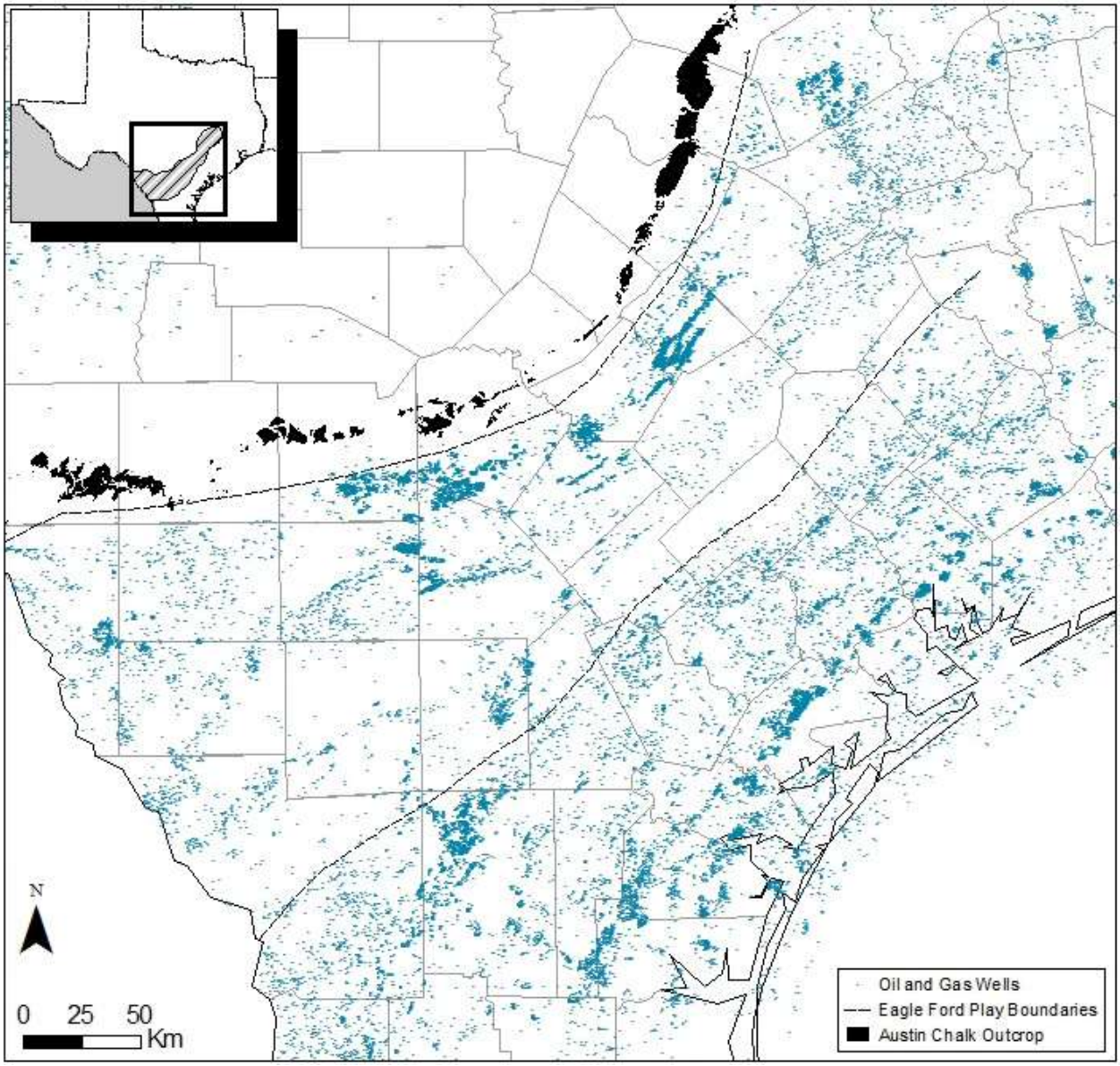

Source: IHS

Figure 105. Active oil and gas wells in South and Central Texas not producing from the Eagle Ford Formation

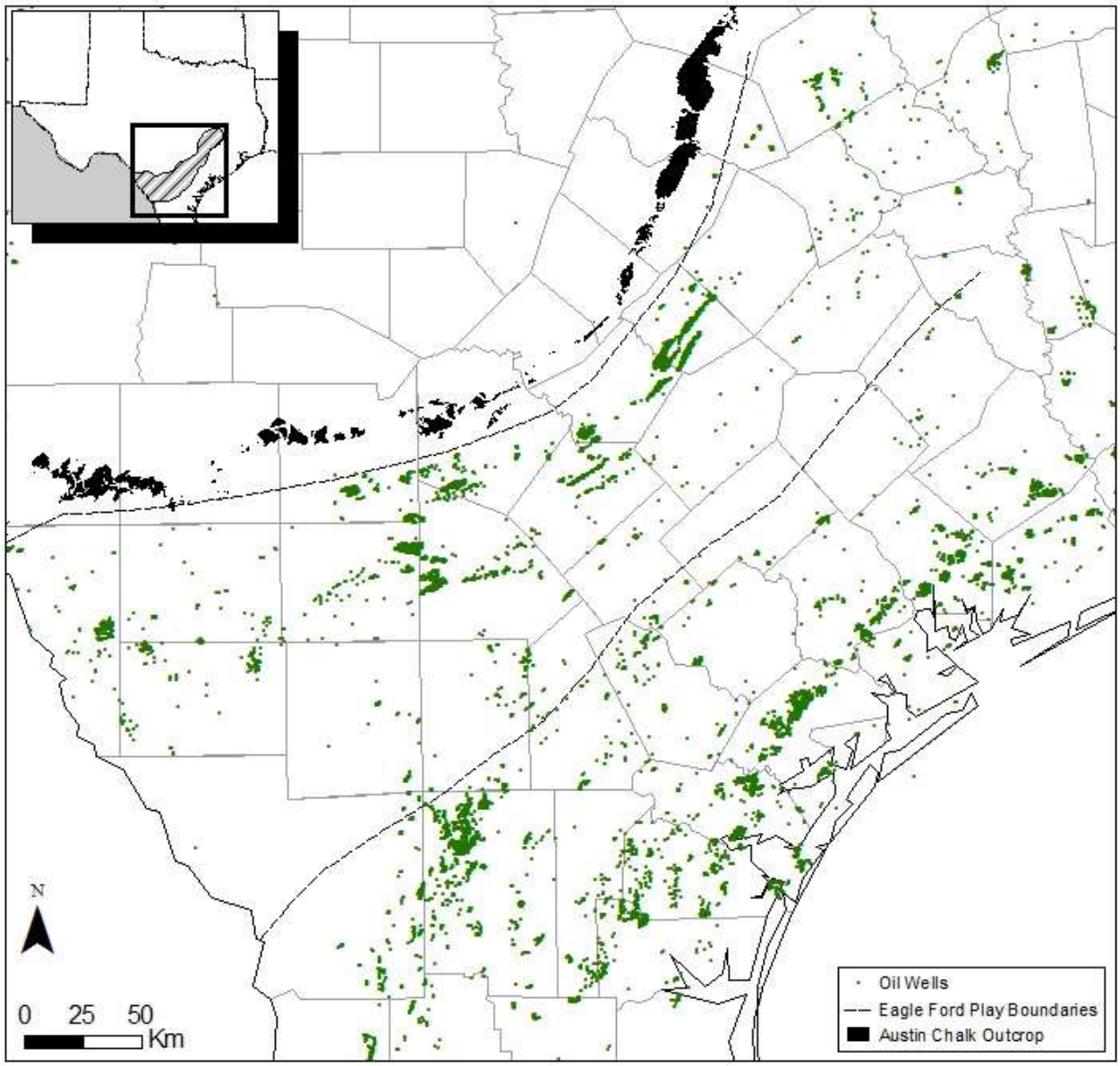

Source: IHS

Figure 106. Active oil wells in South and Central Texas not producing from the Eagle Ford Formation

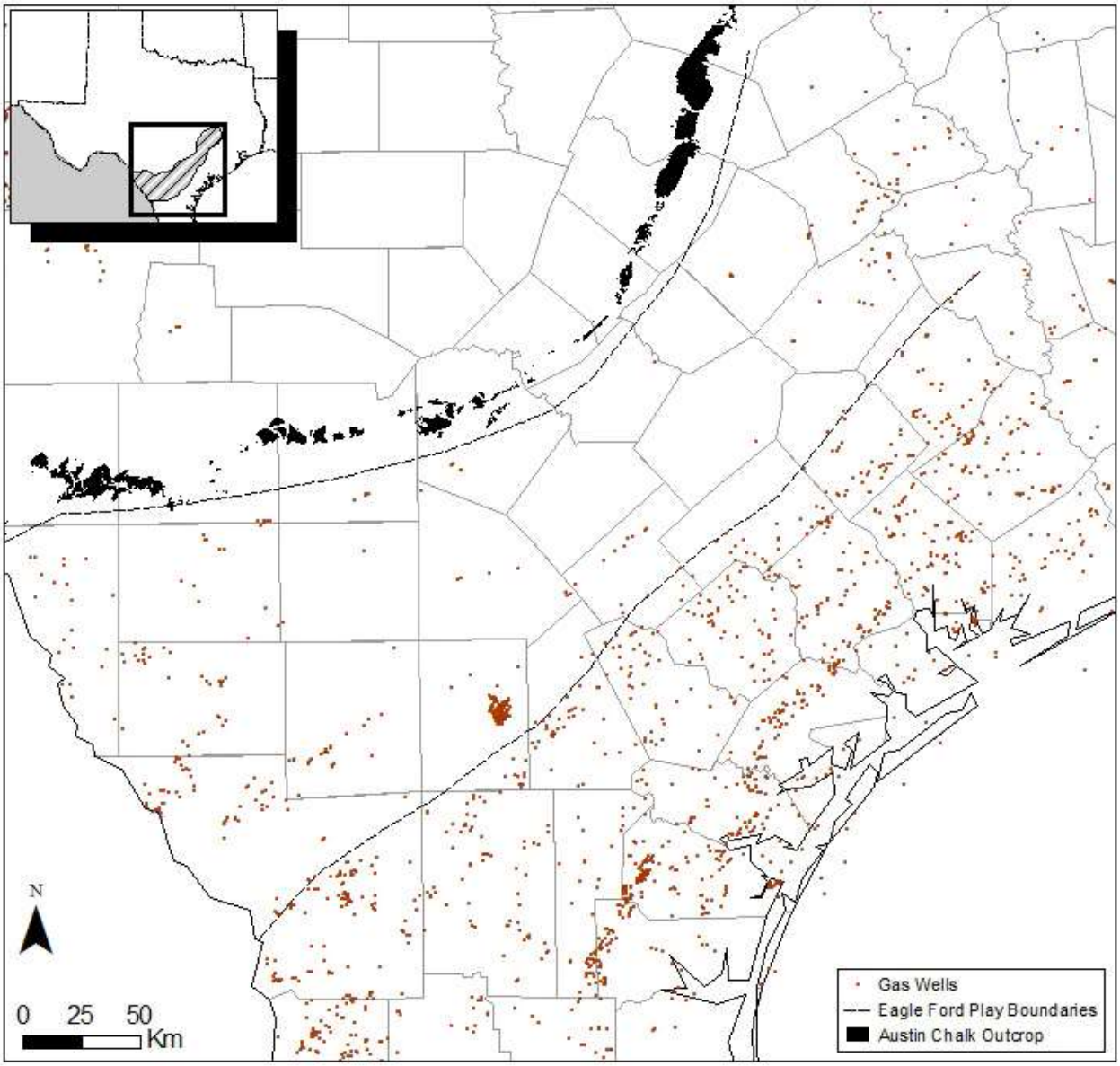

Source: IHS

Figure 107. Active gas wells South and Central Texas not producing from the Eagle Ford Formation

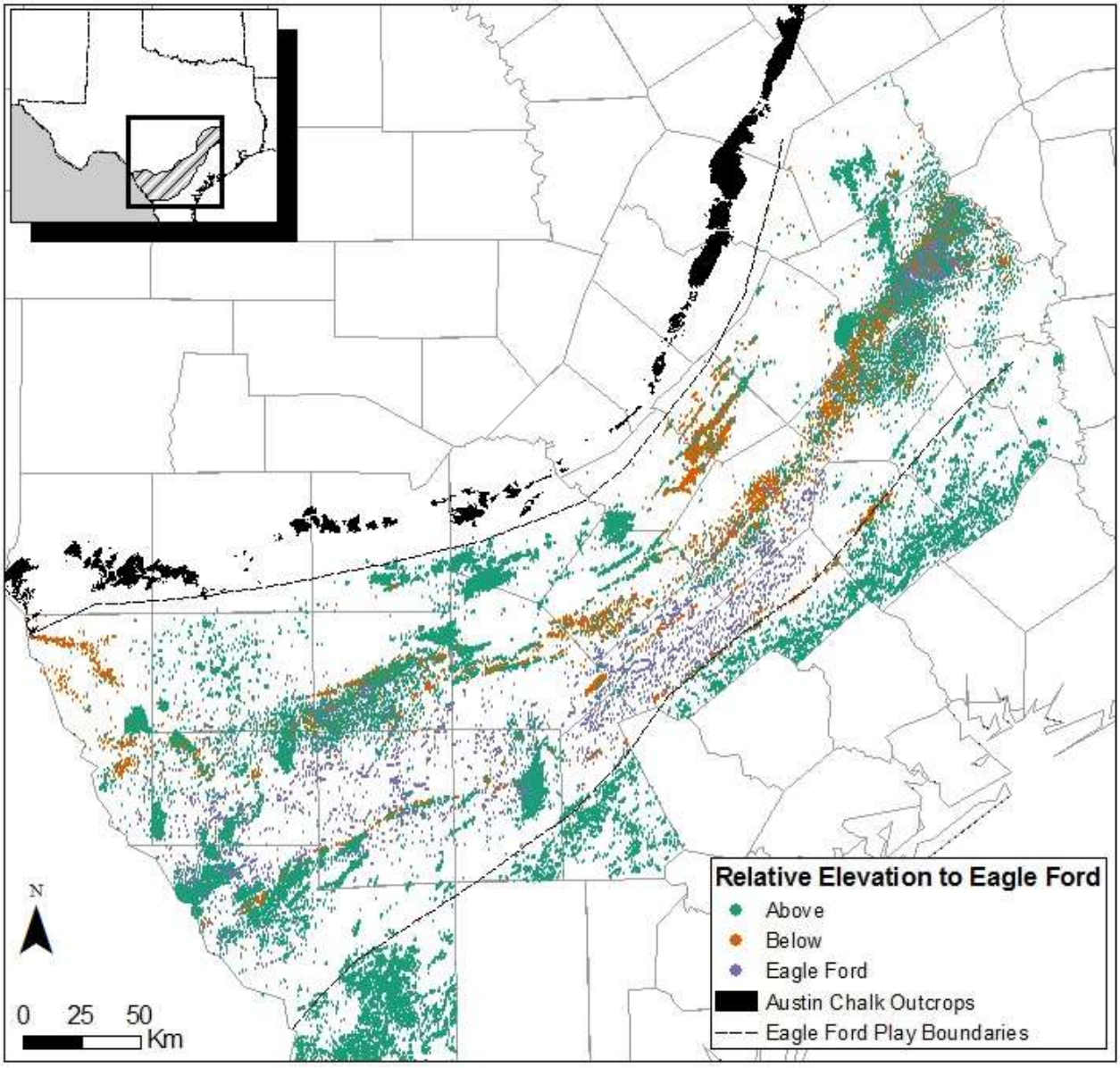

Source: IHS ; displayed locations represent ~80% of all wells of the database in the multi-county area but 96% of well for which formation at TD is given (the remainder being ambiguous names)

Figure 108. Oil and gas wells in South and Central Texas whose total depth is either above or below the Eagle Ford Formation

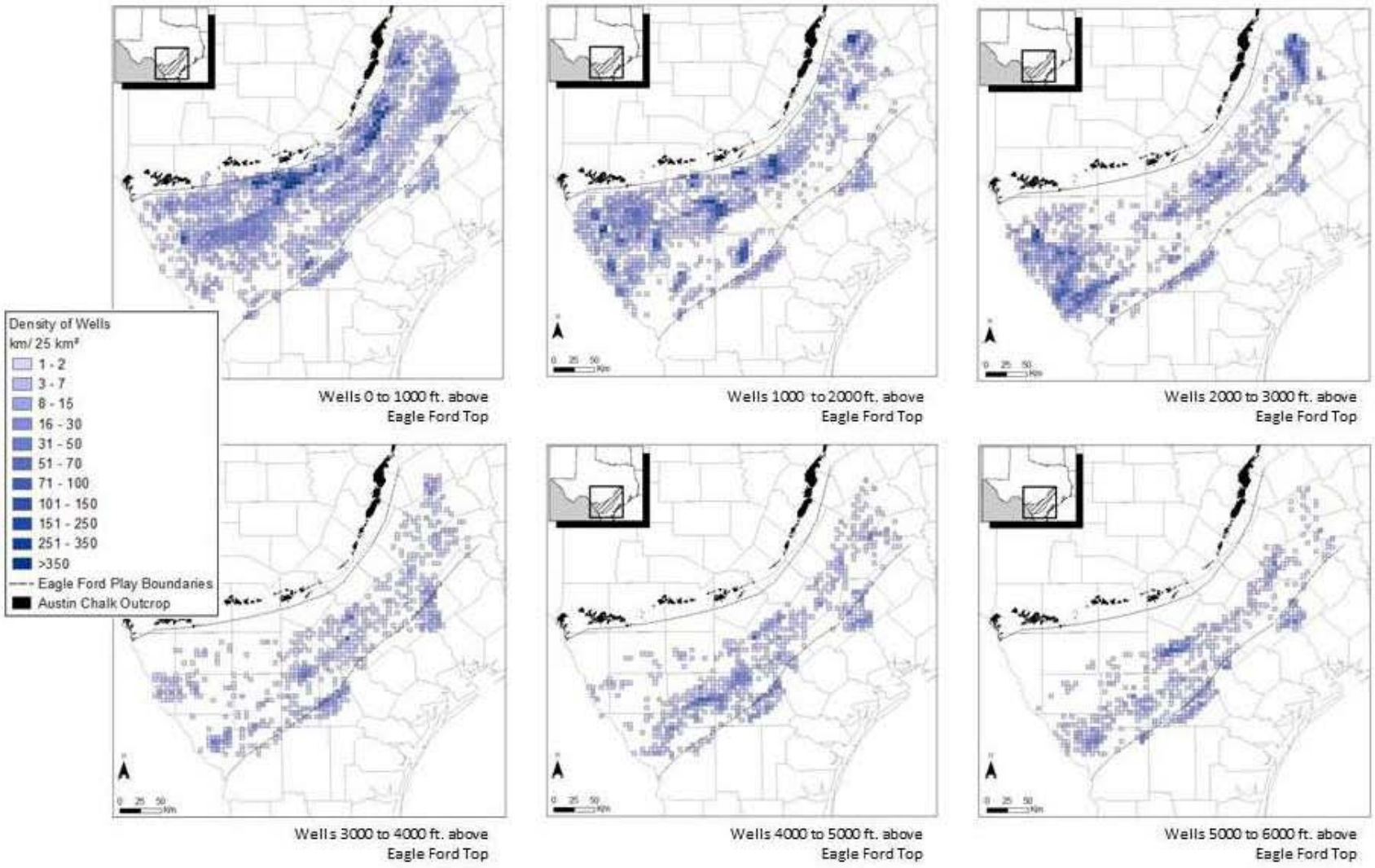

Source: IHS

Figure 109. Density maps of wells above the Eagle Ford

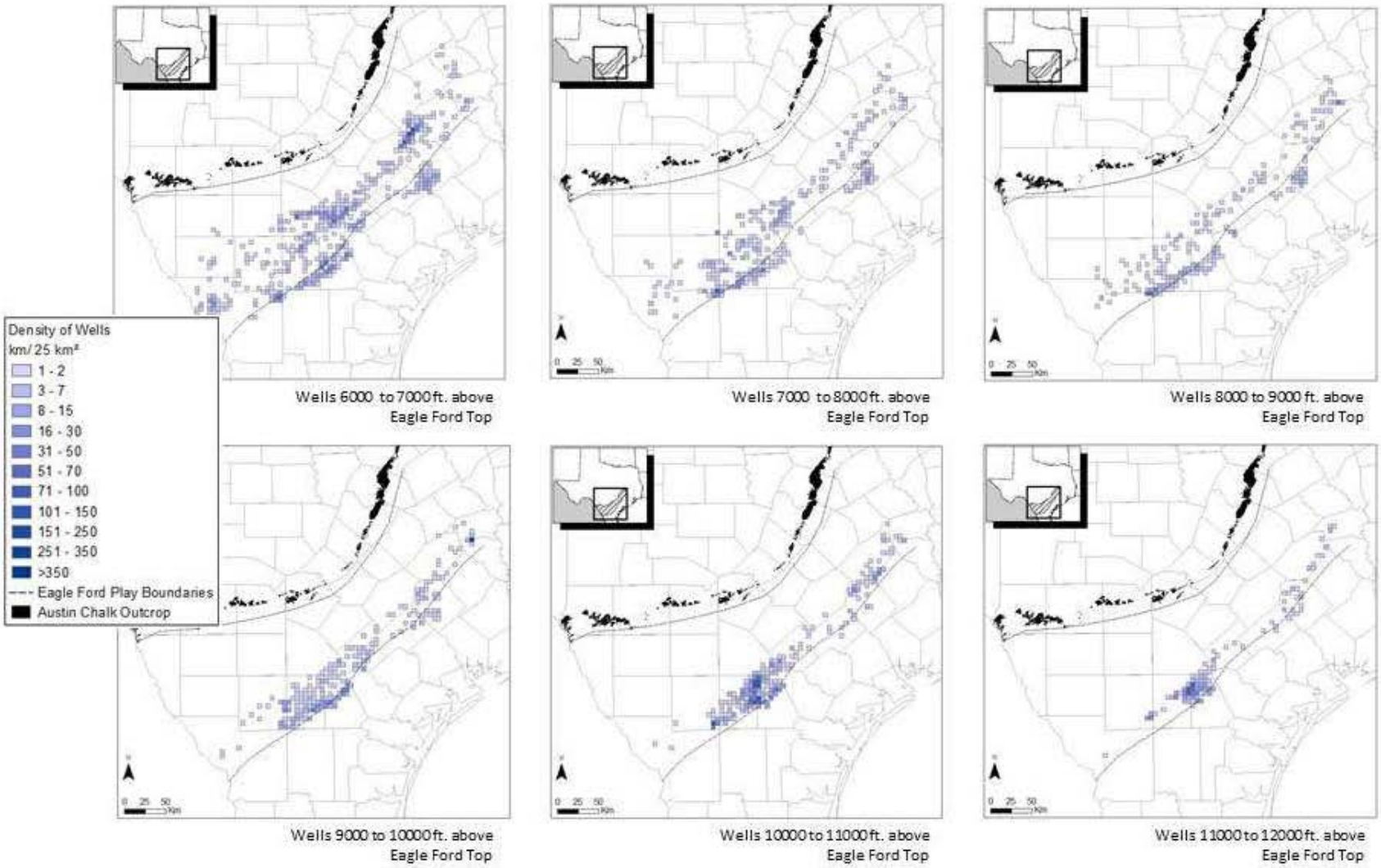

Source: IHS

Figure 109. Density maps of wells above the Eagle Ford (continued)

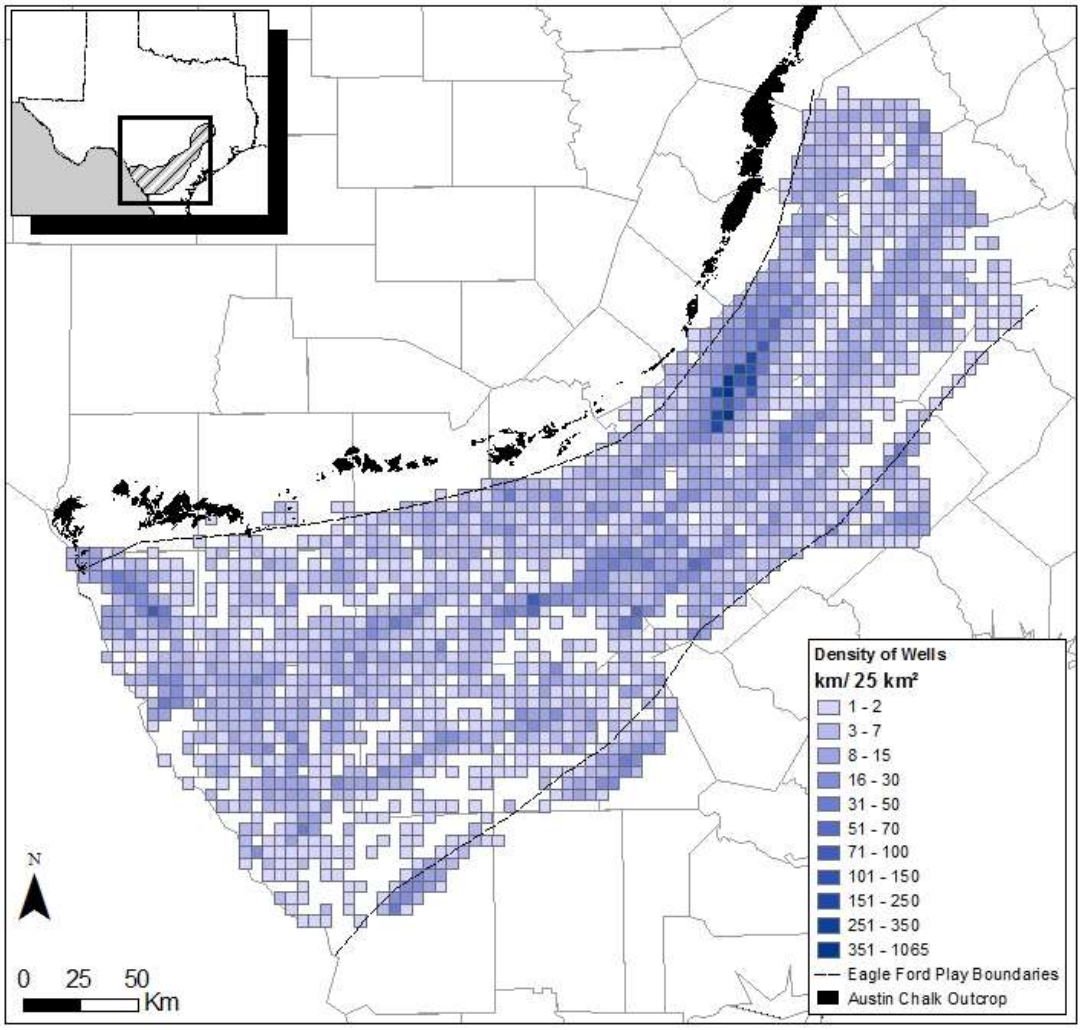

Source: IHS

Figure 110. All wells beyond the Eagle Ford

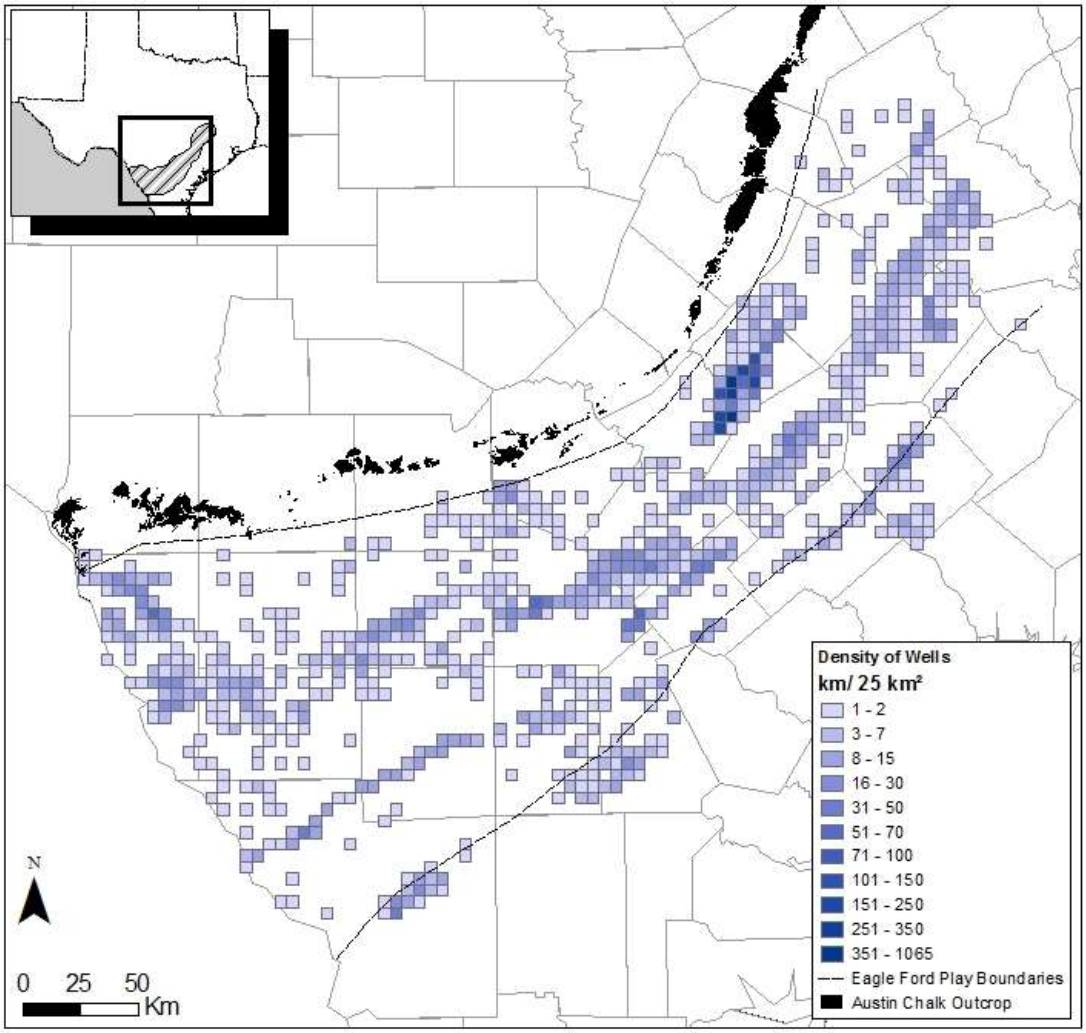

Source: IHS

Figure 111. Active wells beyond the Eagle Ford

VI. Quantifying Water Challenges in The Eagle Ford Shale

In this section, we examine HF water use and consumption and flow back and produced water volumes. We also investigated injection well locations and injected volumes.

VI-1. Water Use and Consumption for Hydraulic Fracturing

Several documents have been recently published on water use for hydraulic fracturing in the state of Texas (Nicot et al., 2011; Nicot et al., 2012; Nicot and Scanlon, 2012). Details on how the numbers were obtained are presented in these documents. The latest analysis was done is 2012 using the last year with full data (2011). The EF Shale play has seen tremendous development since 2008. The discovery well was drilled by Petrohawk in 2008 in La Salle County (Powell Barnett Shale newsletter- http://www.barnettshalenews.com/, Sept 20, 2010). The formation produces natural gas, condensate, and oil. Much earlier wells were vertical, located in Central Texas (Brazos, Burleson Counties), and looking for oil. Initially started as a new Barnett Shale, it quickly turned into a different type of play when the extent of the oil window became clear. In addition to the fast increase in wells completed (~1,400 in 2011) (Figure 112a) and the subsequent increase in water use at ~24 kAF in 2011 (~19 kAF of consumption), the EF Shale has the unique feature among all the plays examined in Nicot et al., 2012 to experience a sharp decrease in water intensity (Figure 112e) decreasing almost in half in 4 years to ~850 gal/ft in 2011. This is seemingly due to operational changes moving from high-volume slick water HF operations to gel fracs that can carry as much proppant with much less water. This decrease in water intensity combined with an increase in average lateral length (~5,000 ft, Figure 112c) still translates into a decrease in water use per well to ~5 million gallons/well (Figure 112d). Not surprisingly, the proppant loading has considerably increased to 1 lb/gal in 2011 (Figure 112f). The use of cross-link gels for oil production requires a higher proppant loading (Fan et al., 2011). The percentage of wells with complete and consistent data set (water, proppant, length) in year 2011 is only ~47%. The top HF users in the EF consist of Webb (4.6 kAF), Karnes (3.9 kAF), Dimmit (3.7 kAF), and La Salle (2.9 kAF) counties.

The cross-plots of water intensity vs. depth and thickness are inconclusive and even misleading (Figure 113a and b). They show no real trend except perhaps a decrease in water intensity with depth. However, Figure 114a clearly shows a higher water intensity in the down dip sections of the play, suggesting an intensity as high as 1400 gal/ft in the gas-rich area and 800 gal/ft in the oil-rich area. Densities of lateral (Figure 114b) and average lateral spacing (Figure 115, Table 7) suggest that the Eagle Ford Shale play has two cores: next to the Mexican border in Dimmit, LaSalle, McMullen, and Zavala Counties and south of San Antonio in Gonzales, Karnes and De Witt Counties. The average lateral spacing (>10,000 ft, that is, large spacing but low lateral density) suggests that many more wells will be drilled and completed there in the future. Bubble maps presentation water use evolution of the play through time are presented in Figure 116 (left-hand side maps include all wells including those with extrapolated information; right-hand side maps present maps with only those wells with full information).

Operators rely mostly on groundwater (estimated at 90% of “new” water, Nicot et al., 2012, Tab. 8) and there is a significant amount of brackish water being used (currently estimated at 20% but variable among operators, Nicot et al., 2012, Tab. 7). As seen in previous sections, several aquifers are brackish in the footprint of the play: the Gulf Coast aquifers and the Wilcox aquifers as well as the downdip section of the Carrizo aquifer.

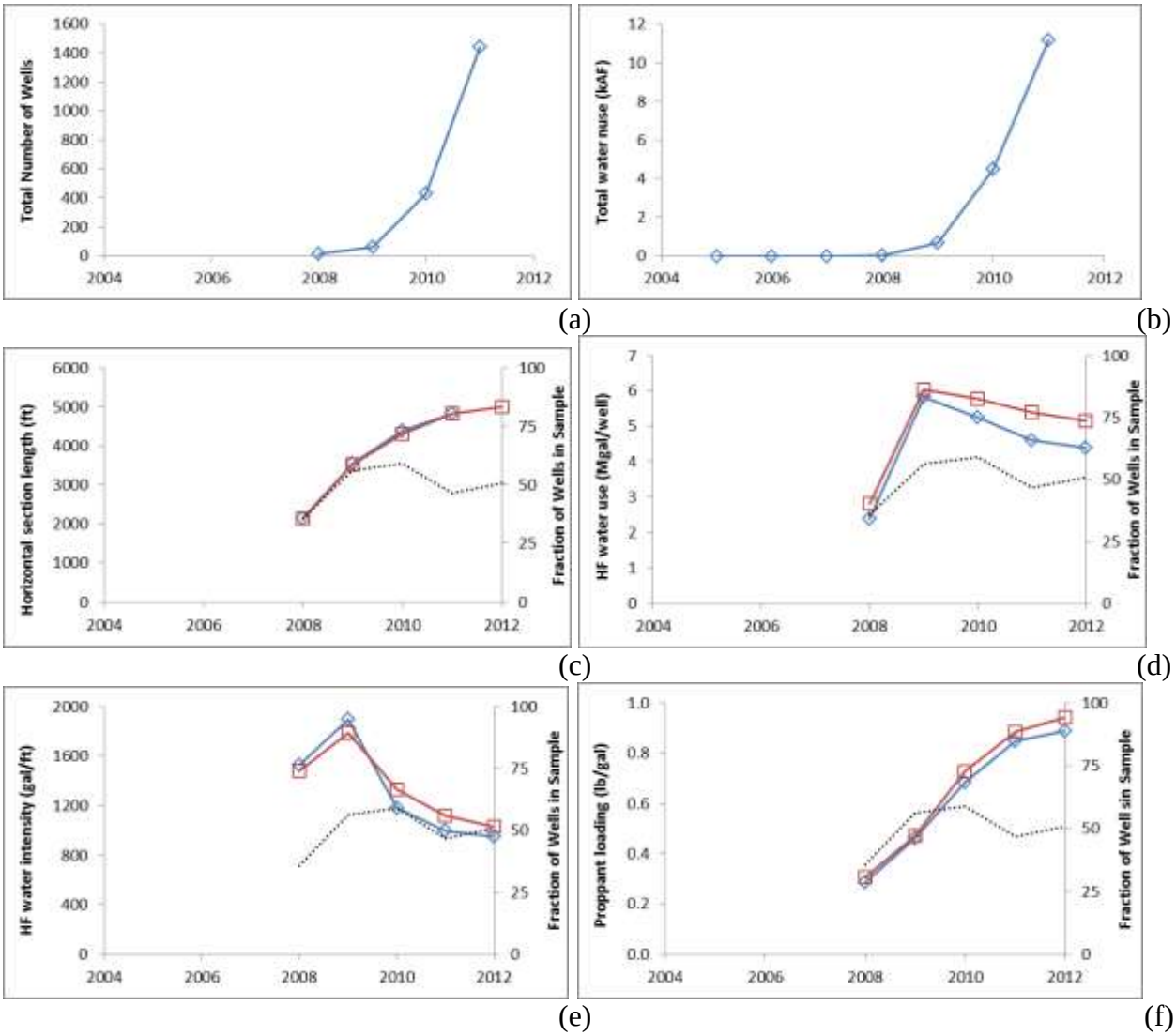

Source: Nicot et al. (2012)
Note: red squares represent average ; blue diamonds represent median; only partial data for 2012

Figure 112. Eagle Ford horizontals, various historical parameters and coefficients for reported and estimated water use as a function of time: (a) number of wells; (b) water use (for those wells with full information only); (c) average/median lateral length; (d) average/median water use per well; (e) average/median water use intensity; (f) average/median proppant loading.

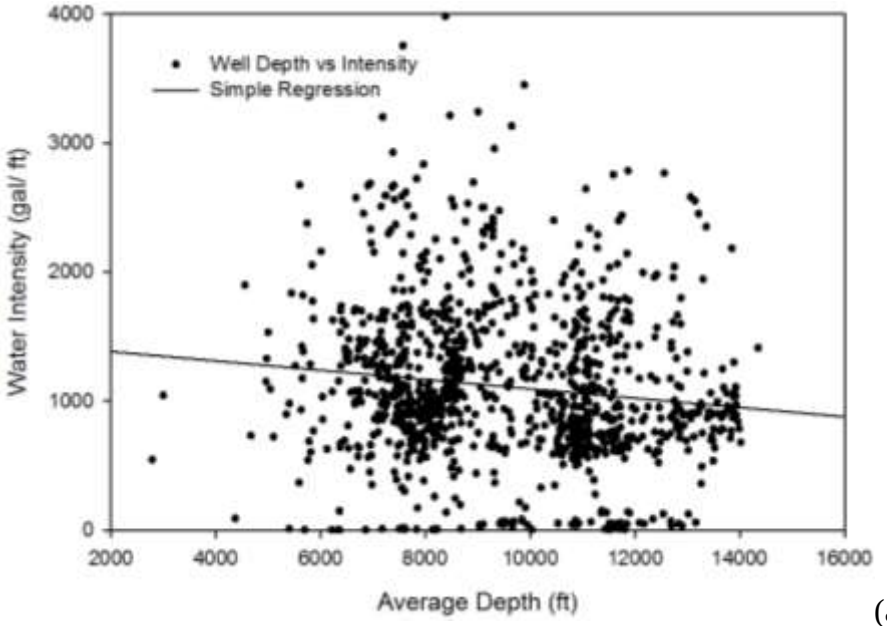

(a)

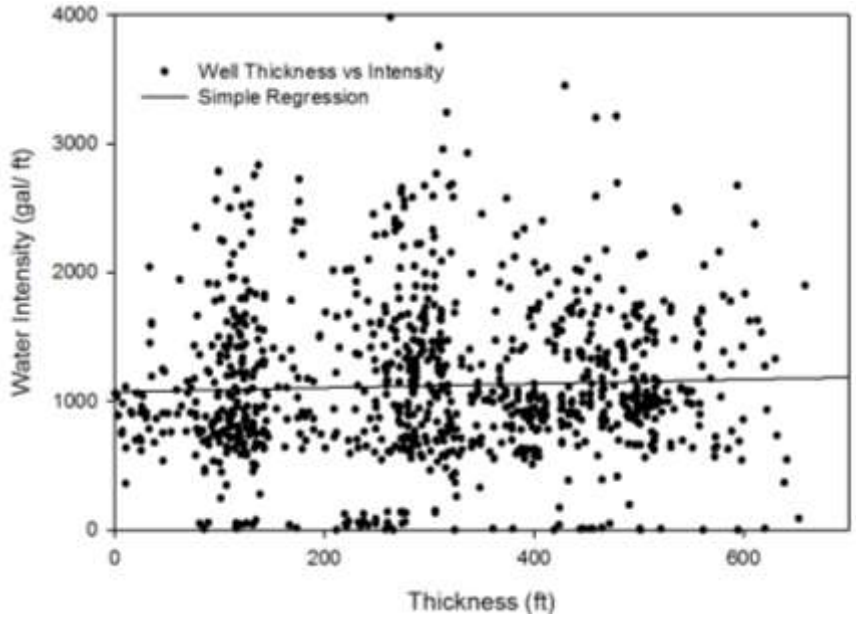

(b)

Source: Nicot et al. (2012)

Figure 113. Eagle Ford Shale horizontal wells' water use intensity as a function of (a) depth; and (b) formation thickness.

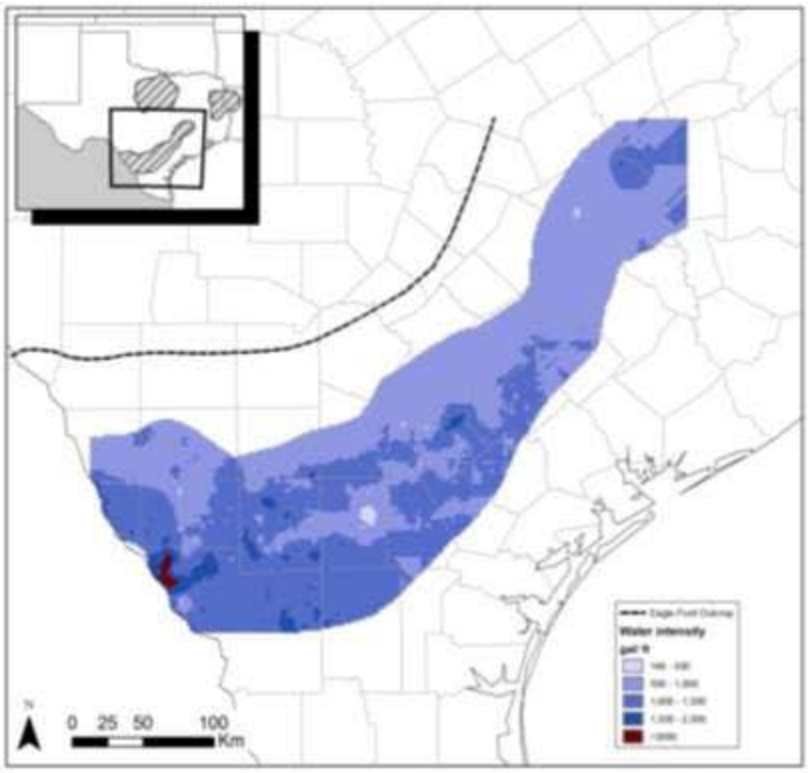

(a)

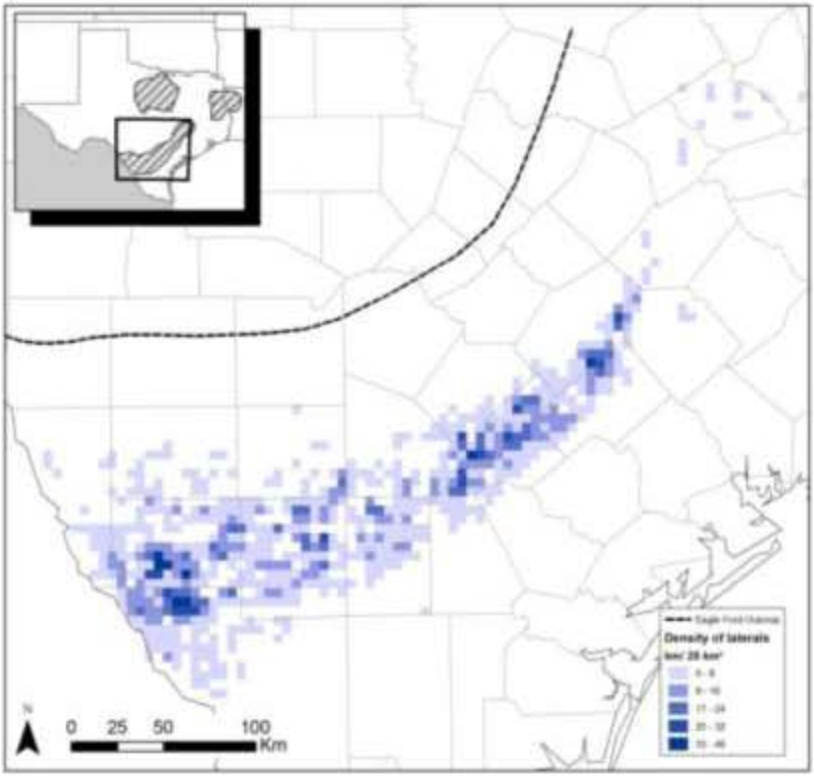

(b)

Source: Nicot et al. (2012)
Note: 25 km^2 = 154 × 40 acres, that is, 154 wells/25 km^2 = 1 well/40 acres

Figure 114. End of 2011 Eagle Ford Shale spatial distribution of (a) water intensity; and (b) density of lateral (cumulative length per area).

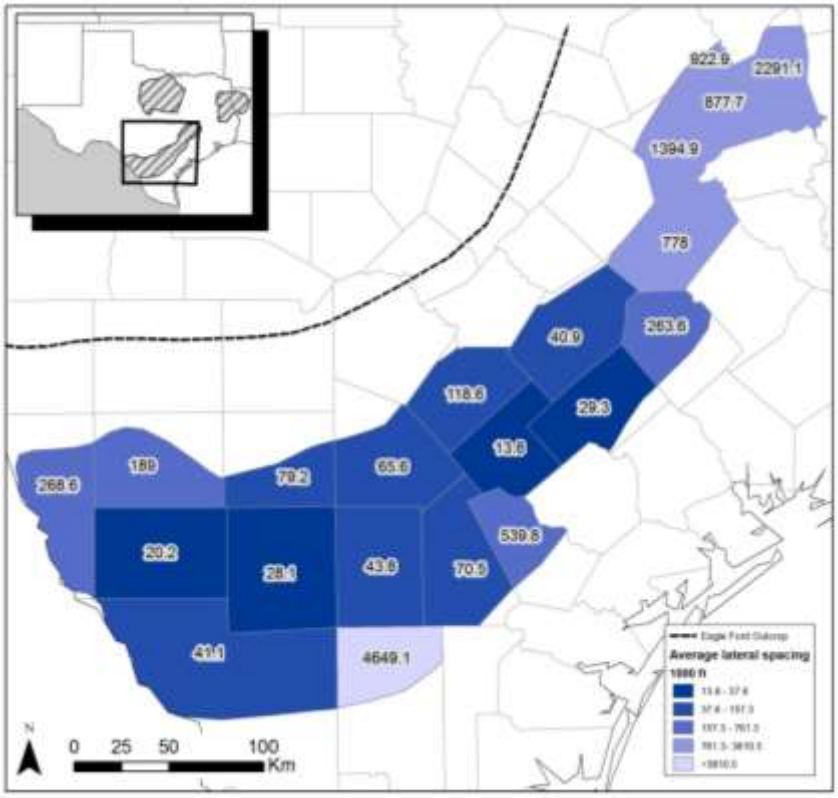

Source: Nicot et al. (2012)

Figure 115. End of 2011 Eagle Ford Shale county-level average lateral spacing.

Table 7. End of 2011 Eagle Ford Shale county-level average lateral spacing for top producing counties.

County Name	Sum lateral length / county area (km/km^2)	Average Lateral Spacing (1000 ft)
Karnes	0.236	13.93
Dimmit	0.162	20.30
La Salle	0.116	28.20
De Witt	0.111	29.63
Gonzales	0.080	41.01
McMullen	0.075	43.79
Webb	0.080	41.11

With extrapolated HF water use

Only those wells with direct data

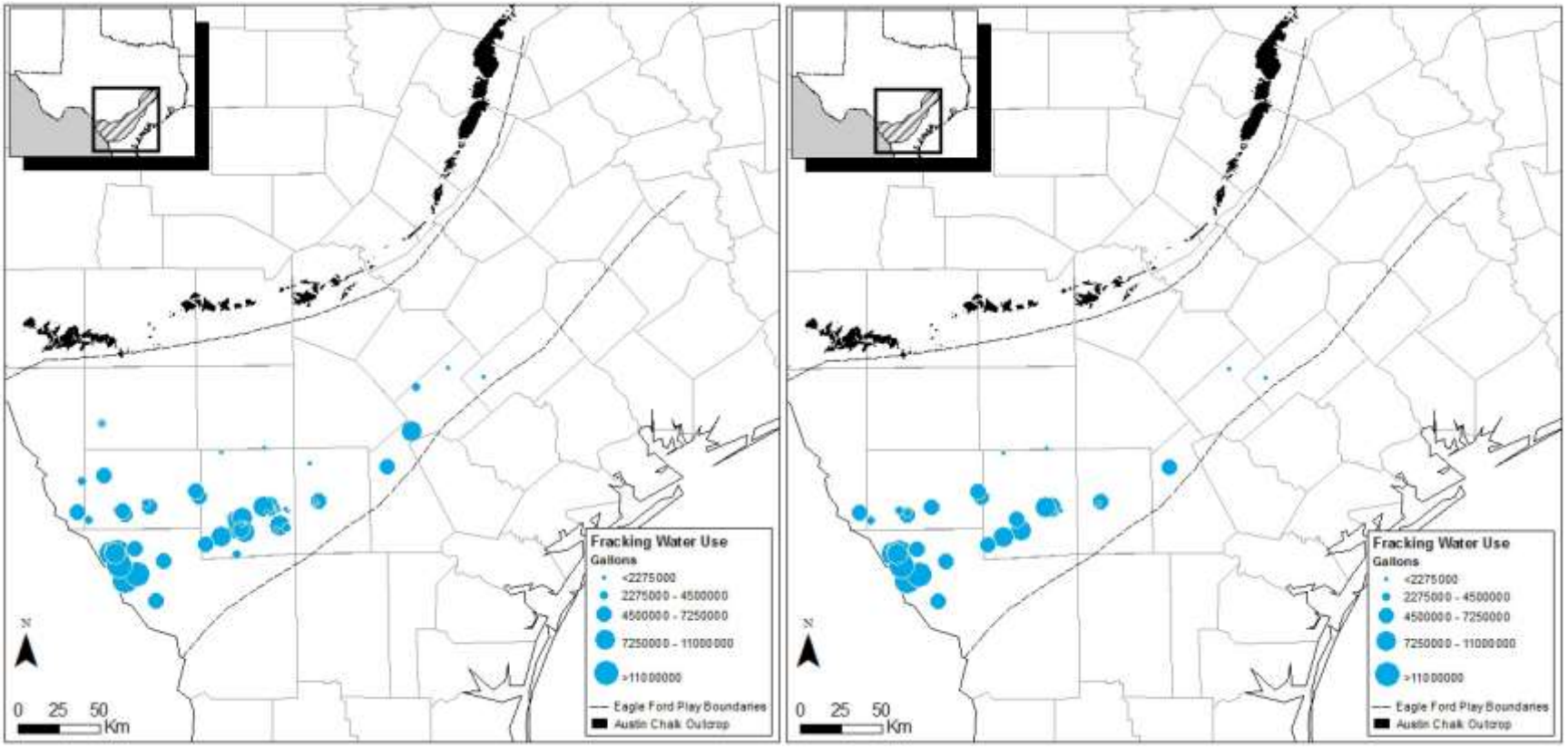

(56 wells)

(32 wells)

A = Year 2009

Figure 116. Annual and yearly bubble pot of HF water use

With extrapolated HF water use

Only those wells with direct data

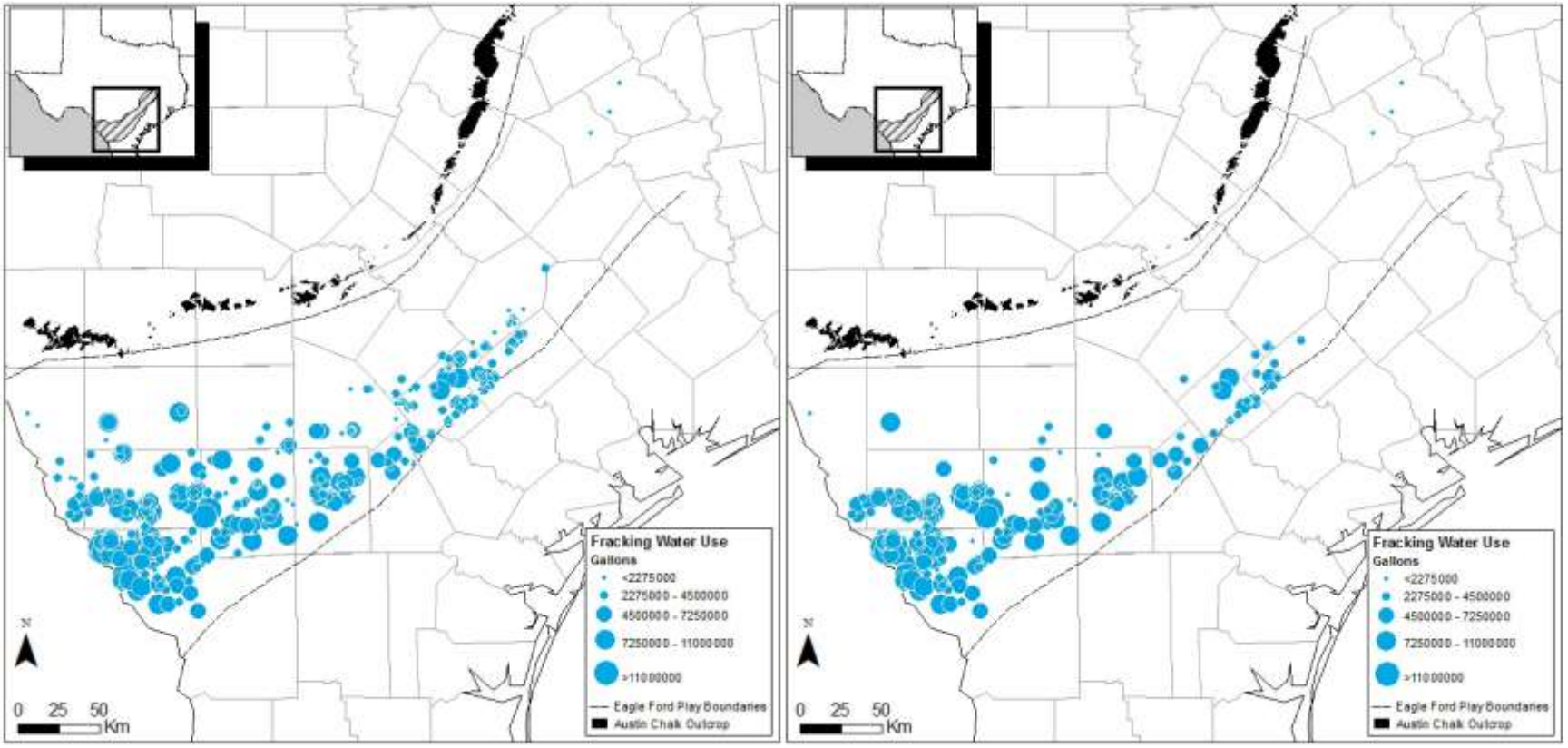

(398 wells)

(226 wells)

B = Year 2010

Figure 116. Annual and yearly bubble pot of HF water use (continued)

With extrapolated HF water use

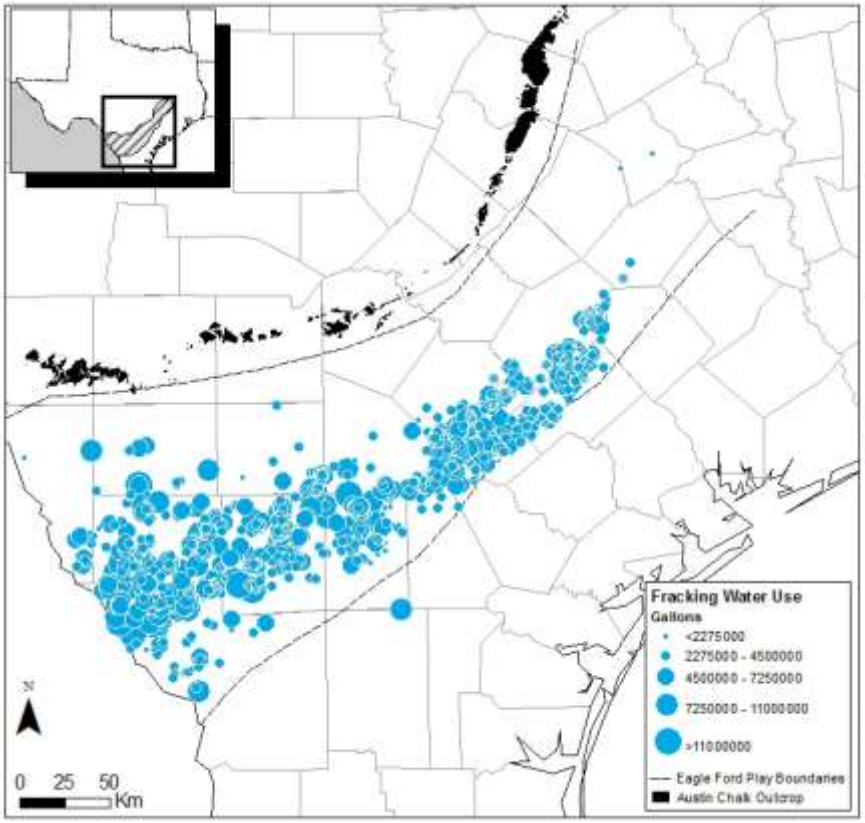

(1204 wells)

Only those wells with direct data

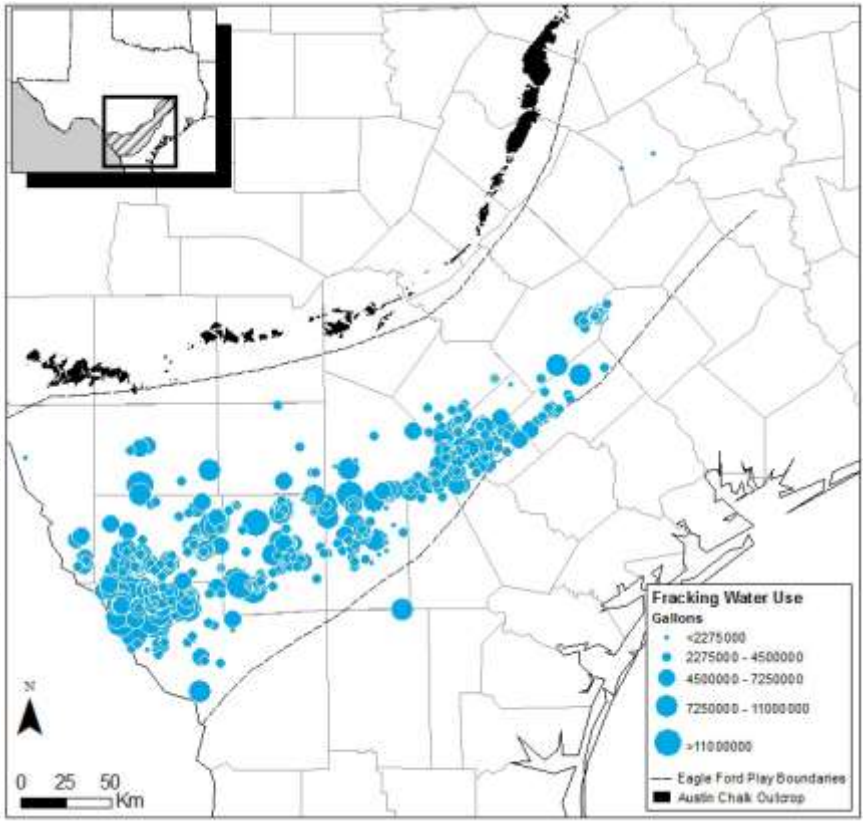

(611 wells)

C = Year 2011

Figure 116. Annual and yearly bubble pot of HF water use (continued)

With extrapolated HF water use

Only those wells with direct data

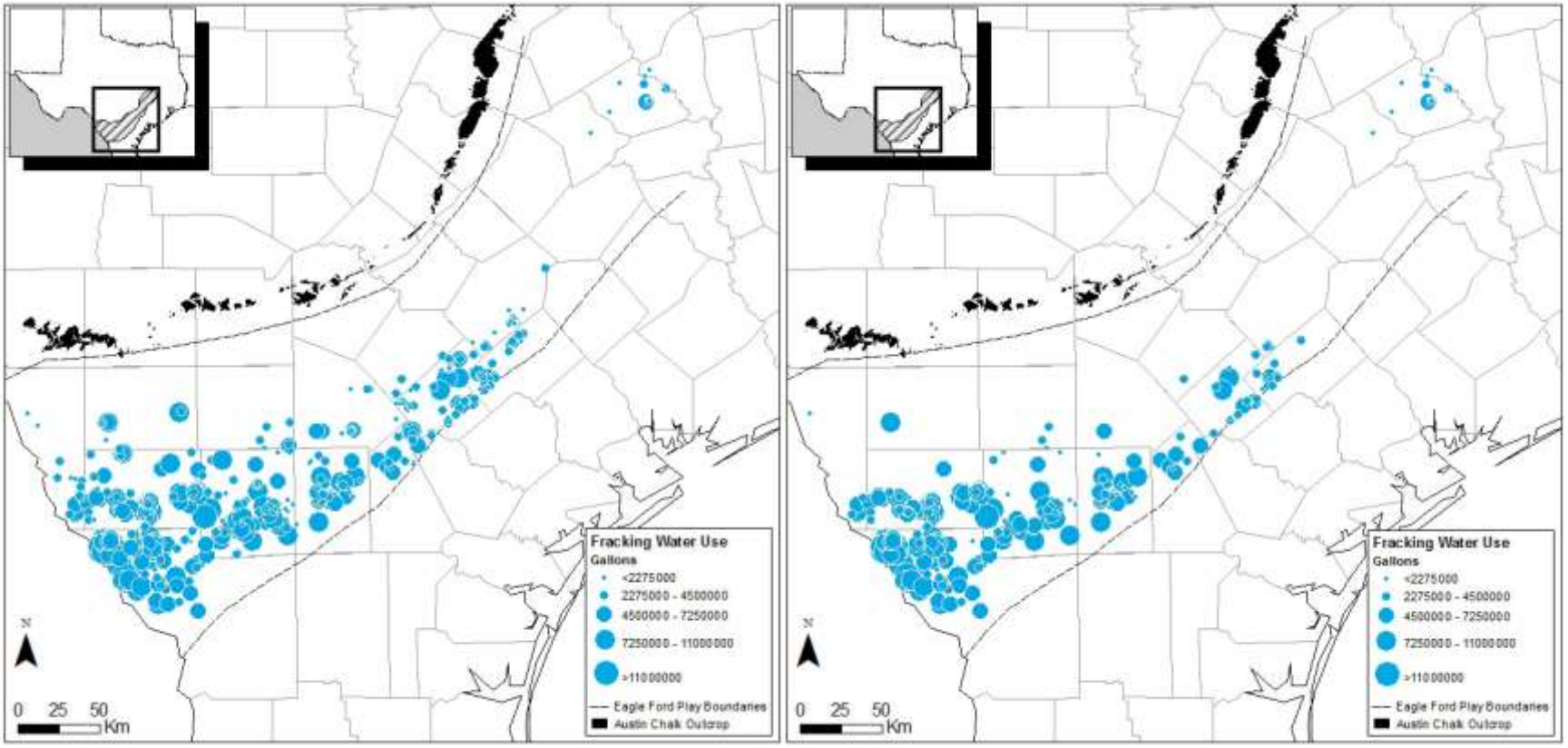

(466 wells)

(270 wells)

D = Cumulative 2008 – 2010

Figure 116. Annual and yearly bubble pot of HF water use (continued)

With extrapolated HF water use

Only those wells with direct data

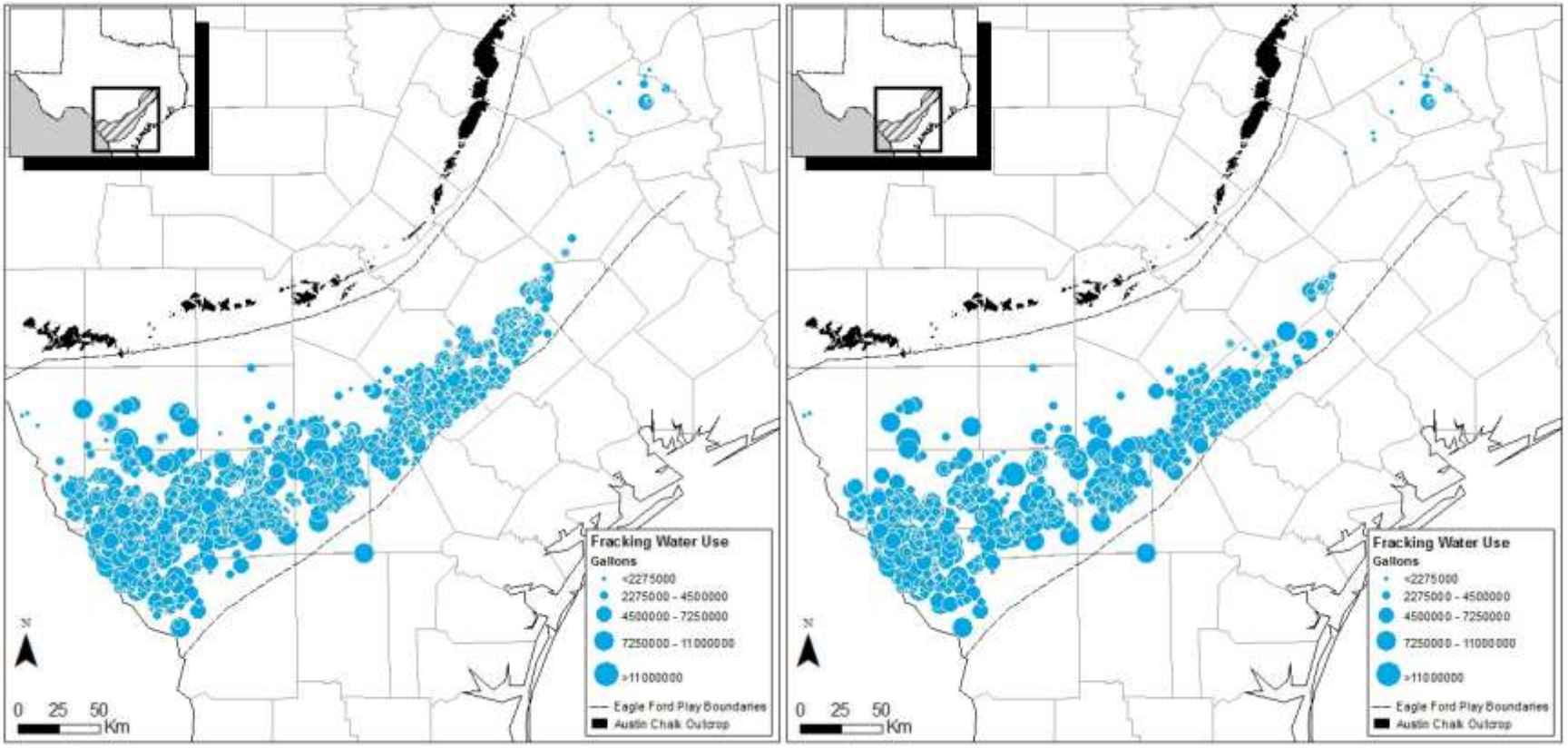

(1670 wells)

(984 wells)

E = Cumulative 2008 - 2011

Figure 116. Annual and yearly bubble pot of HF water use (continued)

The following paragraphs address HF water use projection issues. Figure 117 displays water use and fresh water consumption in the high, low, and most likely scenarios. Low and high scenarios were derived by varying two factors: (1) the prospectivity factor, which encapsulates future hydrocarbon production and consequently provides an estimate of the ultimate amount of HF water use, (2) coefficients for recycling/reuse and brackish water use (Table 8). Projections suggest a slow increase in water for the next 10 years with a broad peak at ~35kAF and a slow decrease beyond 2060. Unlike the Barnett with a clearly delimited core, we assumed that most counties in the Eagle Ford are highly prospective and thus there is not much variation between high and low scenario projections except when recycling/reuse and use of brackish water are included (Figure 117).

Table 8. Coefficients (%) to compute water consumption to be applied to future total water use.

Play / Region		High Water Use	Most Likely	Low Water Use
Eagle Ford Shale	**Recycling**			
	2011	0	0	0
	2020	0	10	10
	2060	0	10	10
	Brackish			
	2011	20	20	20
	2020	20	40	50
	2060	20	50	50

Source: Nicot et al. (2012)

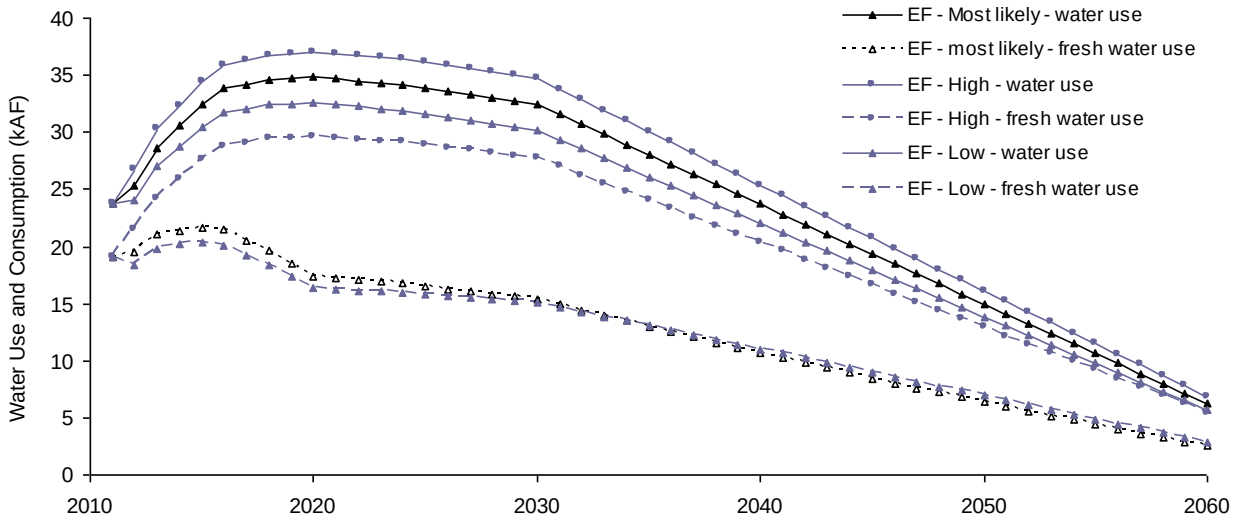

Source: Nicot et al. (2012)

Figure 117. Eagle Ford Shale water use and consumption projections under three scenarios.

VI-2. Water Use History

County-level and city-level water use history collected by the TWDB can be found at http://www.twdb.state.tx.us/waterplanning/waterusesurvey/estimates/2009/index.asp.

VI-3. Analysis of Flowback and Produced Water

Volumes and amount of flowback and produced water vary from well to well and from play to play. Nicot et al. (2012, Tab. 14) reported that a few EF operators estimated that approximately 20% of the injected volume flows back throughout the life of the well. This is comparable to what has been reported for the Haynesville and Marcellus shales but smaller than reported values for the Barnett Shale and much smaller than volumes reported for tight formations such as those in East Texas, the Permian Basin, or the Anadarko Basin (Nicot et al. (2012).

We again used the IHS Enerdeq database and extracted information about monthly production of oil, gas, and water. Water production is then plotted monthly with initial time is end of completion. It is understood that some operators do not flow the water back immediately , however we assumed they all do. Percentiles of flowback / produced water (5^{th}, 30^{th}, median, 70^{th}, and 90^{th}) show a sharp decrease through time (Figure 118 and Figure 119 without the 90^{th} for clarity). Note that we also included the number of wells used to derive the percentiles (right-hand side y-axis), it also decreases quickly as expected because few wells are more than a few years old. A given percentile curve does not represent a single well but rather the value meeting the desired percentile for every month regardless of the well record it is taken from. The median flowback after a month is approximately 4500 bbls or ~190,000 gal but some wells show much higher flow back at <1 million gal. The same information can also be plotted with cumulative volumes (Figure 120) with a long-term volume of ~50,000 bbls, that is, ~2 million gallons. This number is much higher than that commonly reported in the play and could be attributed to the limited number of wells included in the analysis after 2 or 3 years. It could also be related to oil vs. gas well differences. We did not perform that analysis. Note the wiggliness of the percentile curves suggesting that the sampling size is insufficient after a few months / years. In addition, those percentiles were obtained without accounting for the amount of water injected so we derived another parameter: fraction of injected volume recovered through time (Figure 121 and Figure 122 without the 90^{th} for clarity). The median flowback curve stabilizes around a year at approximately 40% of the volume injected but could be <20% of volume injected for 30% of the wells and >80% for 30% of the wells at the other end of the range. The same information can be plotted in visually different fashion with crossplots (Figure 123 and following figures). If a dot is above the 1:1 line, more water has been produced than injected. In agreement with Figure 122, Figure 123 shows that 1 month after HF, only a small fraction have flowed back. After 3 months (Figure 124a), the ratio has increased but still clearly <1. After 1 year and beyond (Figure 124b, c, and d), the spread increasing considerably and the number of dots as well, denoting the recent development of the play. In order to detect spatial patterns, we also drew maps with the same information (Figure 125). To better understand what the median well means, we analyzed the composite median which is obtained as explained above by taking the median value for each month regardless of the well it is associated with (Figure 126). The plots display actual data from the four wells that are the closest in some sense to the composite median at that particular time. They were chosen by doing the sum of the absolute values of the difference over the number of months scaled by the median value for that month [|general median-well data|/general median]. The wells with the smallest sums are displayed.

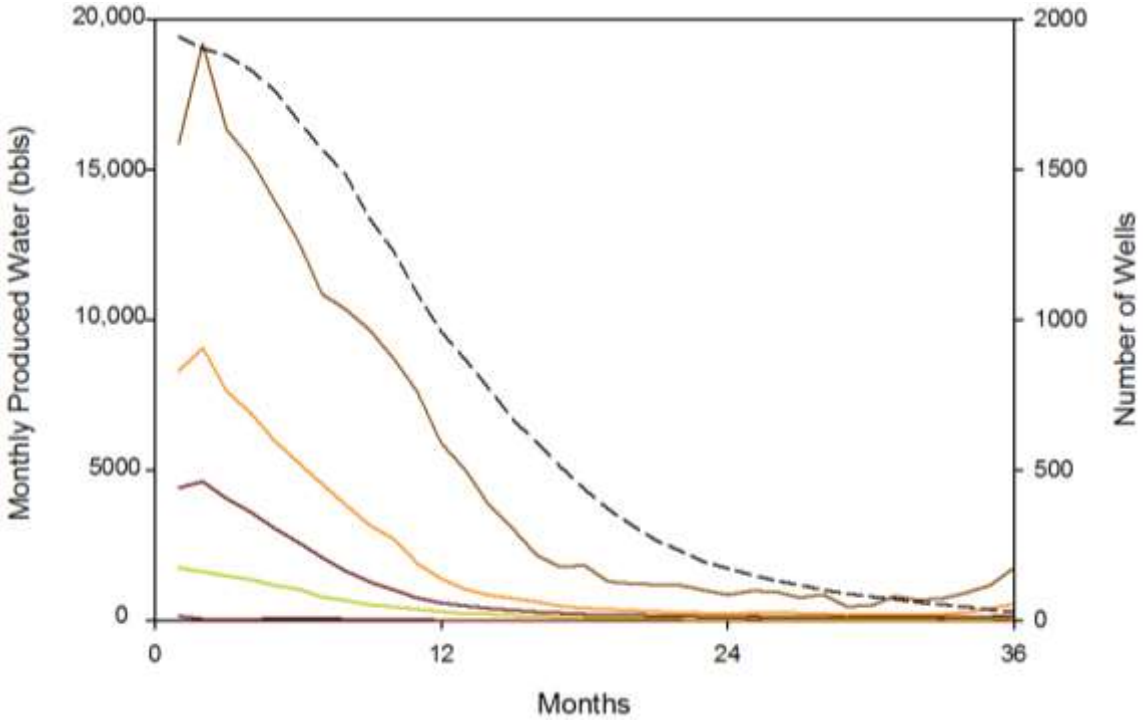

Source: IHS database

Figure 118. Monthly water production percentiles (5th, 30th, 50th, 70th, and 90th) and number of wells (dotted line).

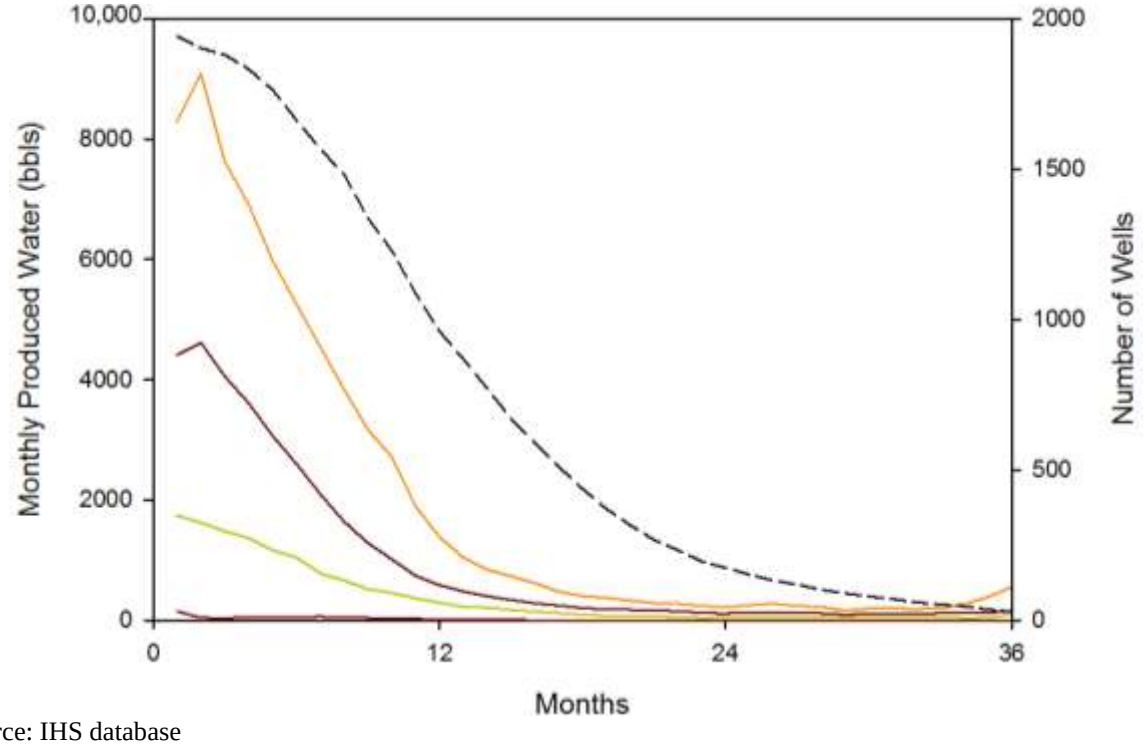

Source: IHS database

Figure 119. Monthly water production percentiles (5th, 30th, 50th, and 70th) and number of wells (dotted line).

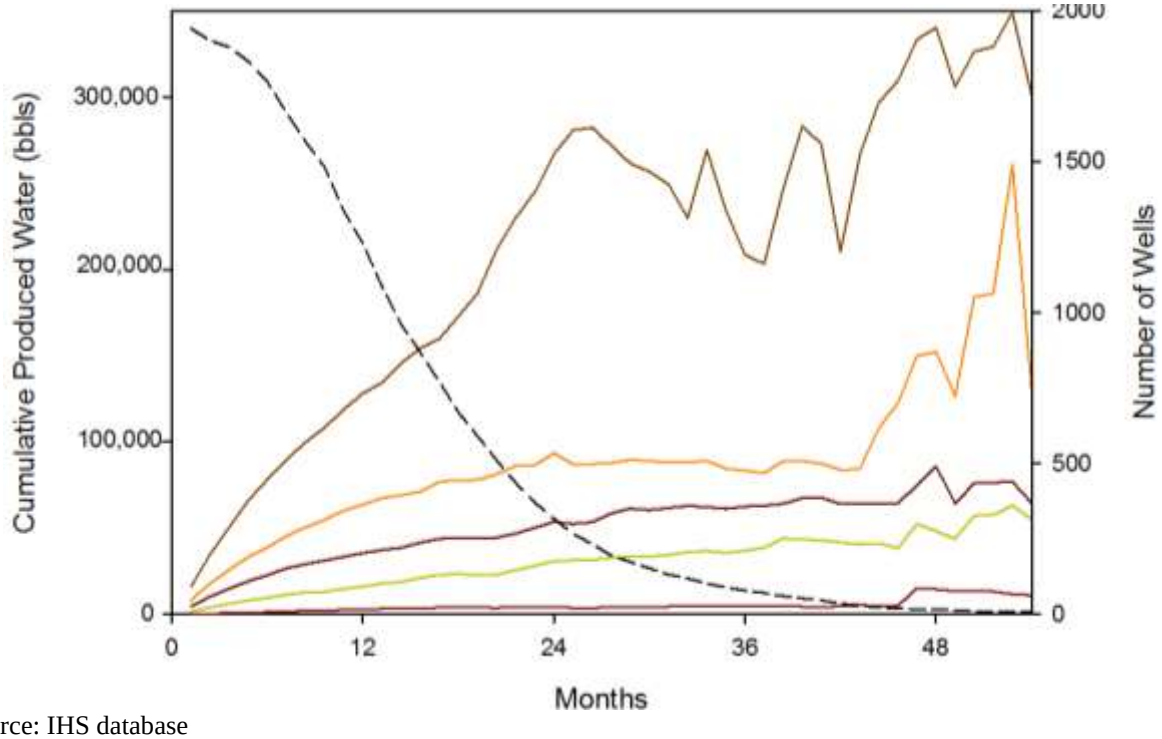

Source: IHS database

Figure 120. Cumulative water production percentiles (5th, 30th, 50th, 70th, and 90th) and number of wells (dotted line).

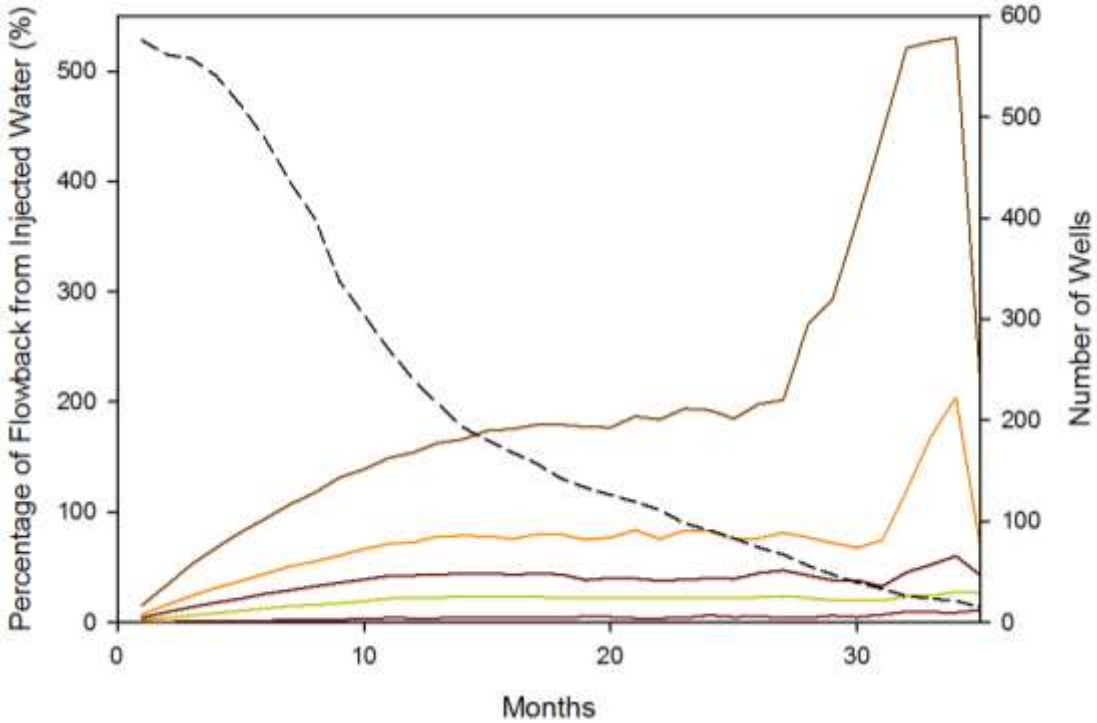

Source: IHS database; Note: see number of wells axis, only those wells with full information (water, proppant, length) are used

Figure 121. Ratio of flowback / produced water to HF water through time (5th, 30th, 50th, 70th, and 90th percentiles) and number of wells (dotted line).

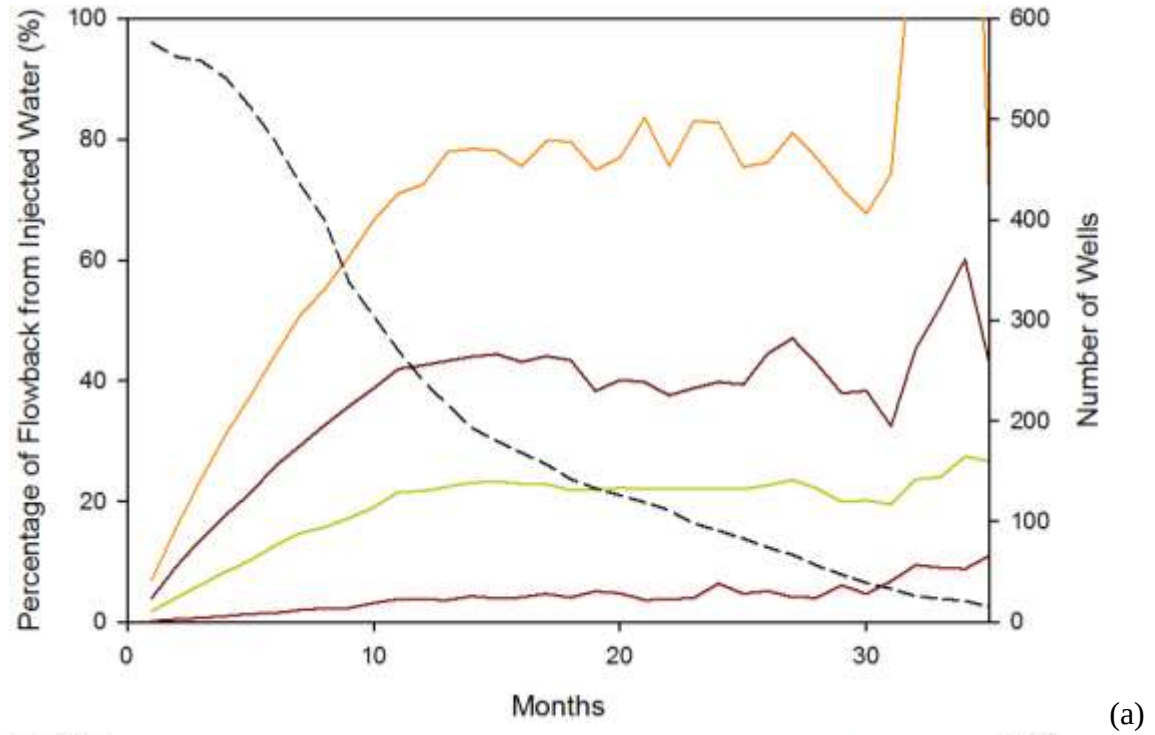

(a)

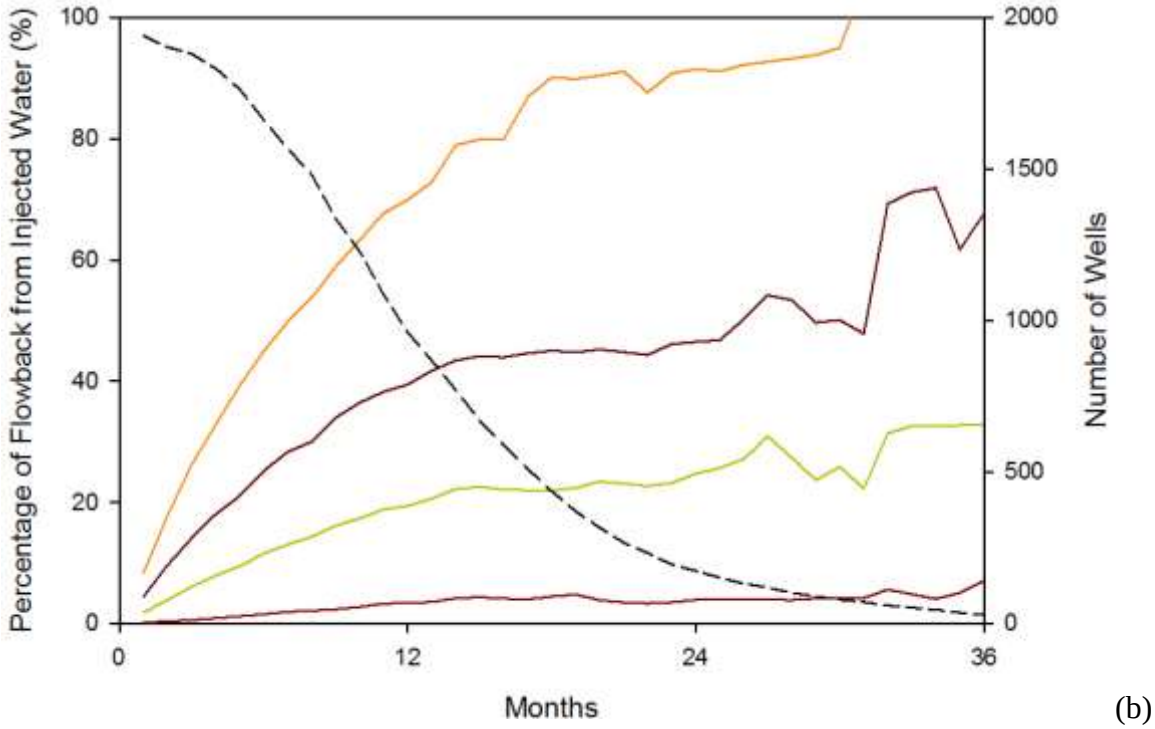

(b)

Source: IHS database

Note: see number of wells axis, only those wells with full information (water, proppant, length) are used in plot (a) whereas plot (b) also include wells with estimated volumes of HF ("injected") water

Figure 122. Ratio of flowback / produced water to HF water through time (5^{th}, 30^{th}, 50^{th}, and 70^{th} percentiles) and number of wells (dotted line).

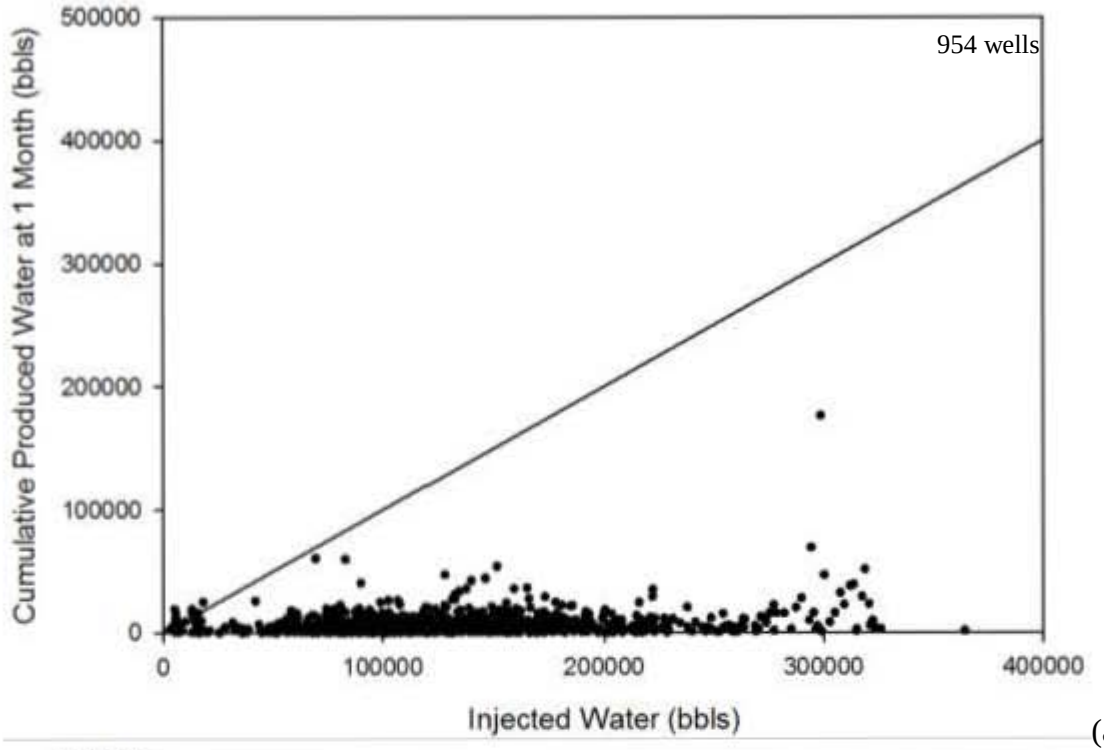

(a)

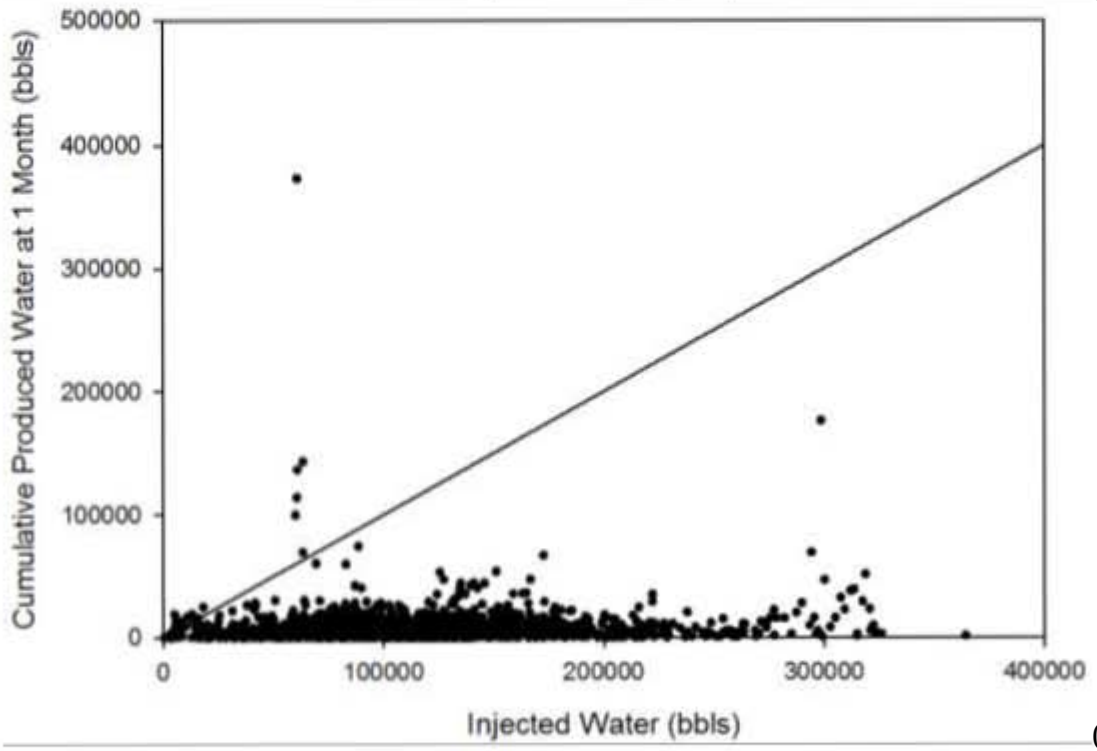

(b)

Source: IHS database

Note: see number of wells axis, only those wells with full information (water, proppant, length) are used in plot (a) whereas plot (b) also include wells with estimated volumes of HF ("injected") water

Figure 123. Crossplot of flowback / produced water vs. HF water at month 1.

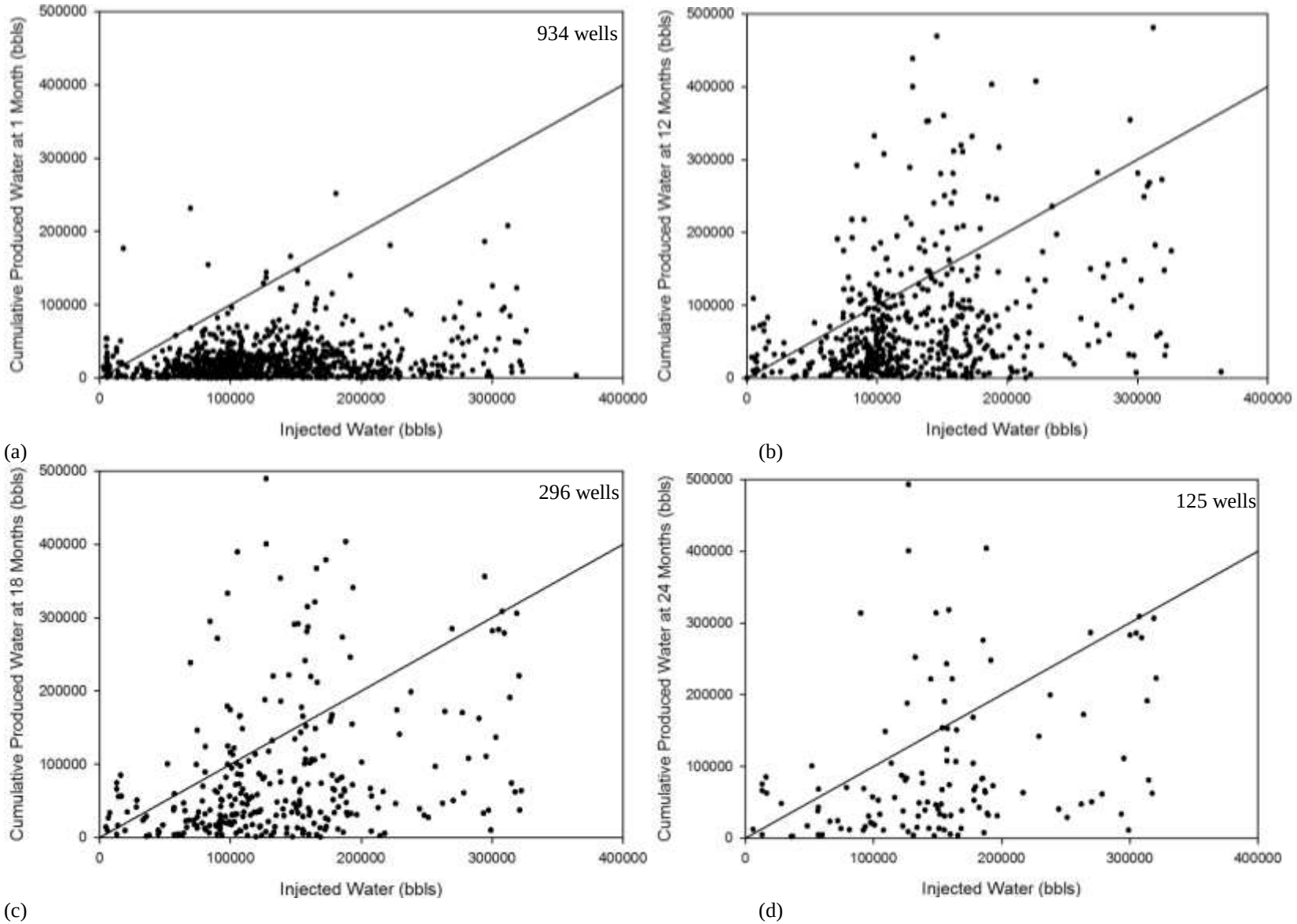

Source: IHS database; Note: see number of wells axis, only those wells with full information (water, proppant, length) are used

Figure 124. Crossplot of flowback / produced water vs. HF water at (a) month 3, (b) month 12, (c) month 18, and (d) month 24.

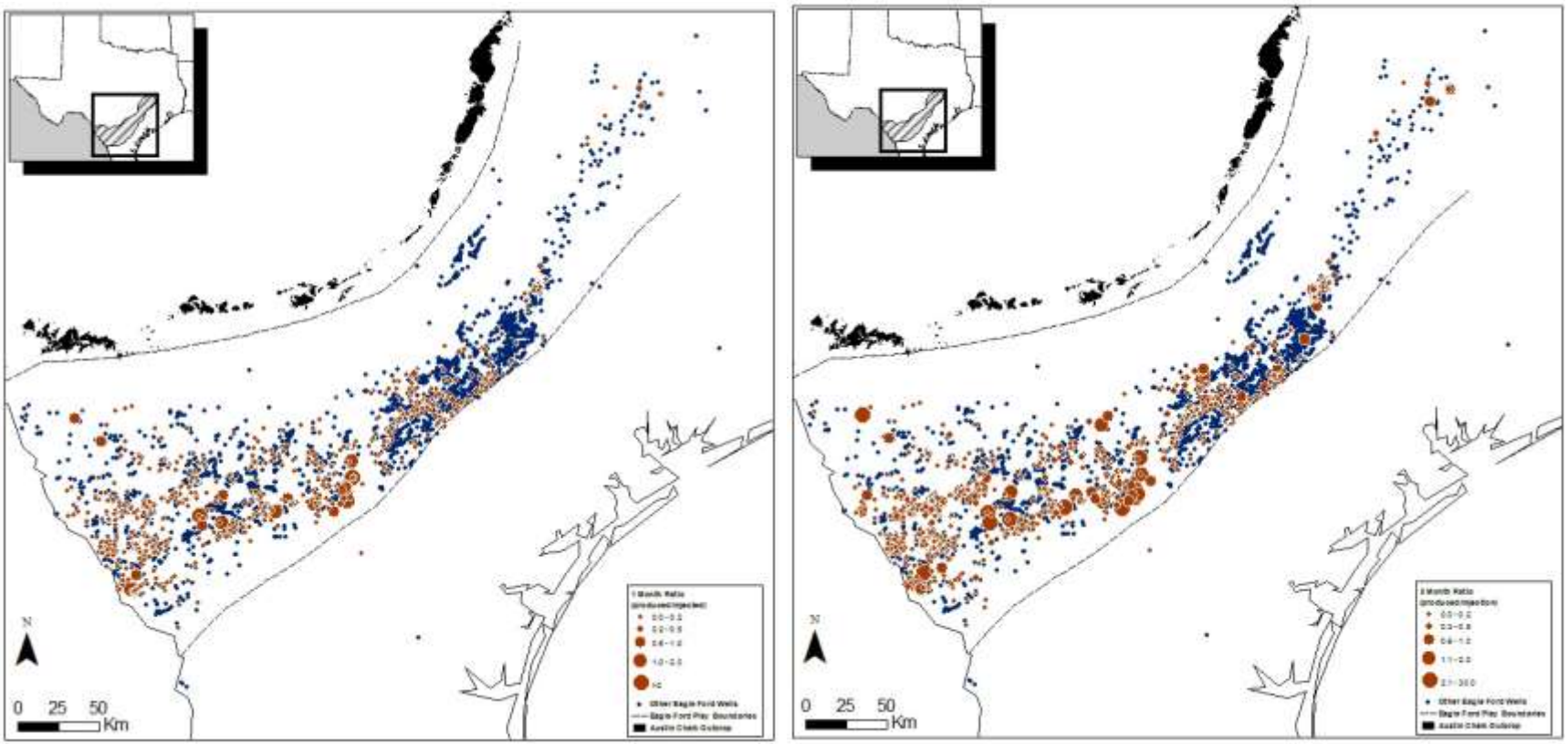

(a) (b)

Note: only those wells with full information (water, proppant, length) are plotted

Figure 125. Maps of flow back / HF volume ratio at (a) 1 month, (b) 3 months, (c) 12 months, (d) 18 months, and (e) 24 months

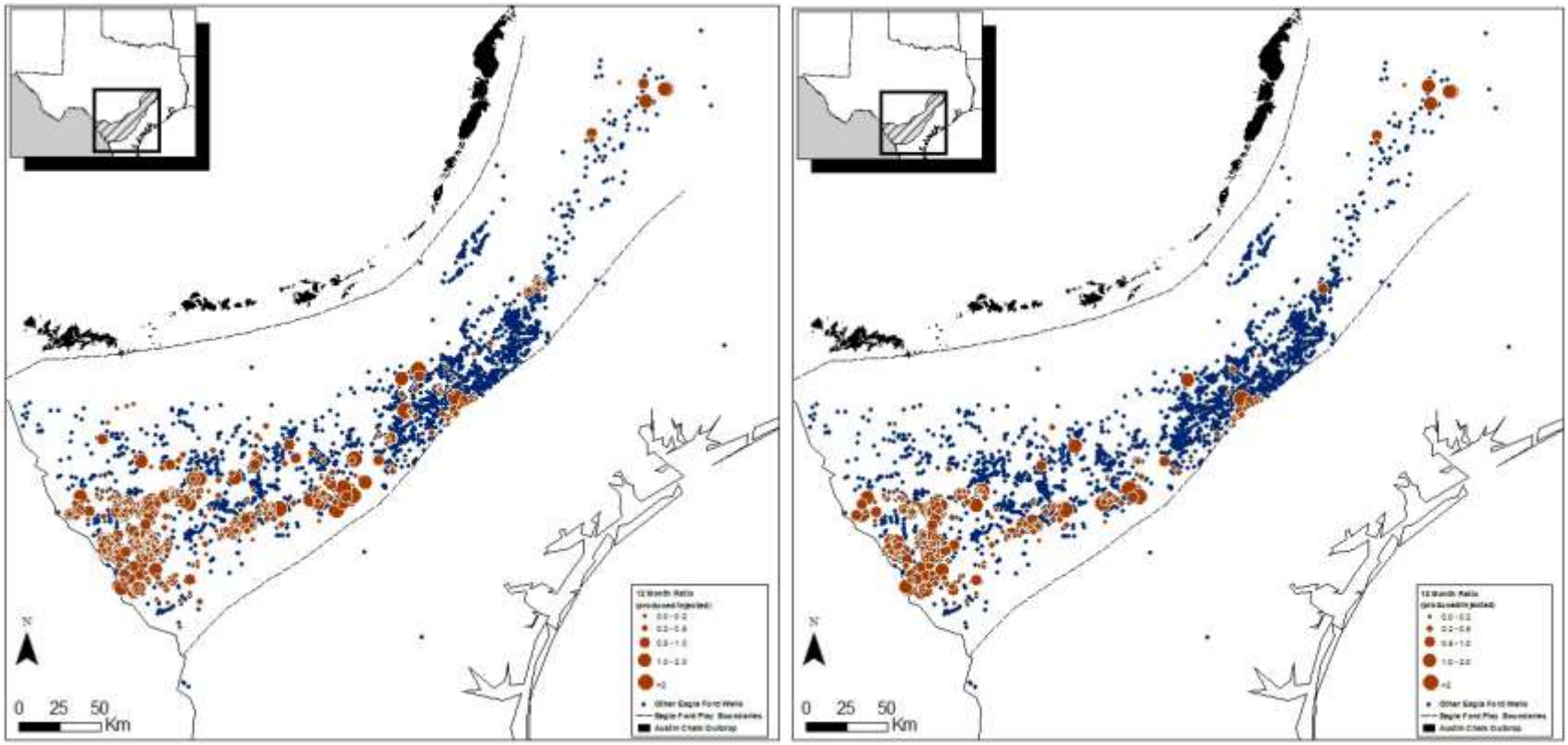

(b) (d)

Note: only those wells with full information (water, proppant, length) are plotted

Figure 125. Maps of flow back / HF volume ratio at (a) 1 month, (b) 3 months, (c) 12 months, (d) 18 months, and (e) 24 months (continued)

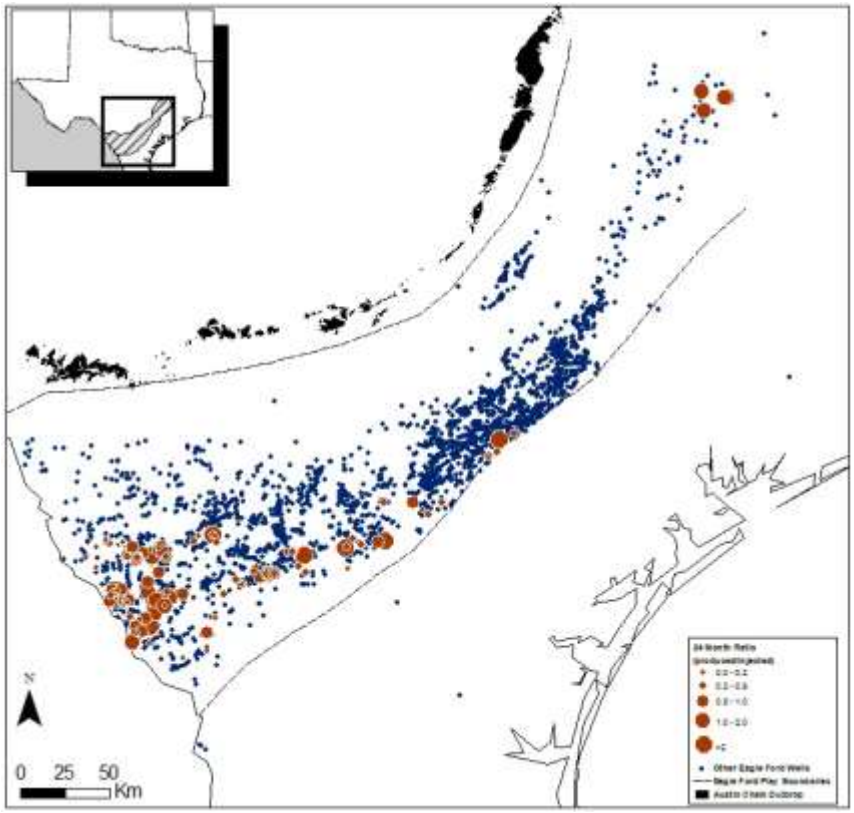

(e)

Note: only those wells with full information (water, proppant, length) are plotted

Figure 125. Maps of flow back / HF volume ratio at (a) 1 month, (b) 3 months, (c) 12 months, (d) 18 months, and (e) 24 months (continued)

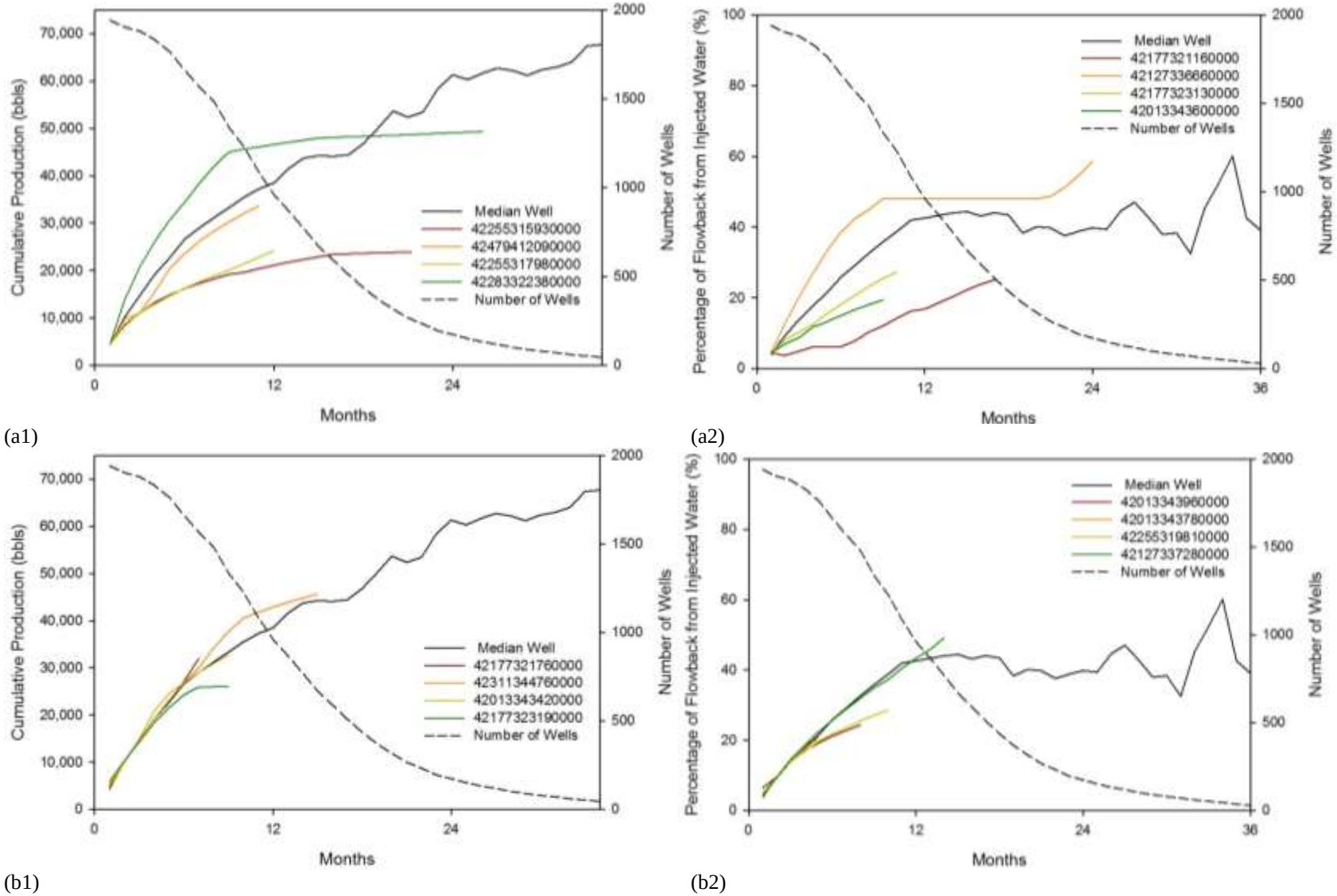

Note: all wells (with full information and estimated) are included

Figure 126. Behavior of synthetic median at (1) 1 month, (b) 3 months, (c) 12 months, (d) 18 months, and (e) 24 months for cumulative production (_1) and fraction of flowback vs. HF (_2). Wells closest to the median at given time also shown.

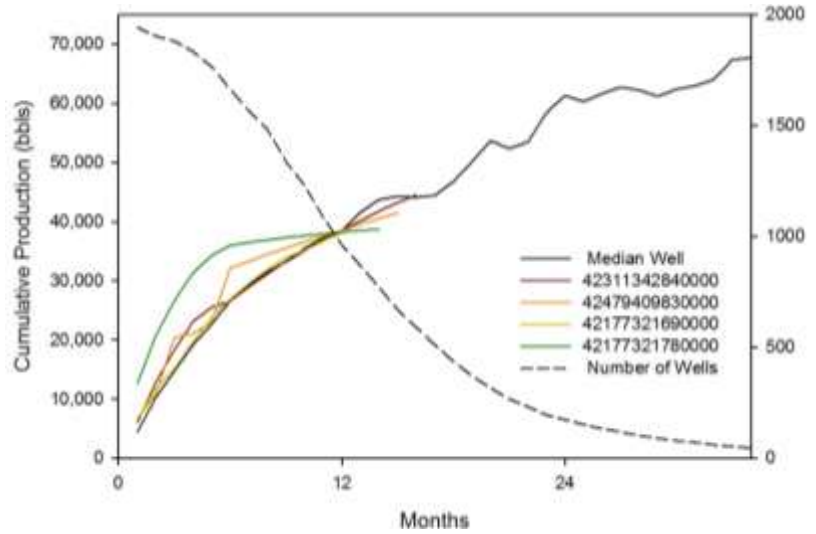

(c1)

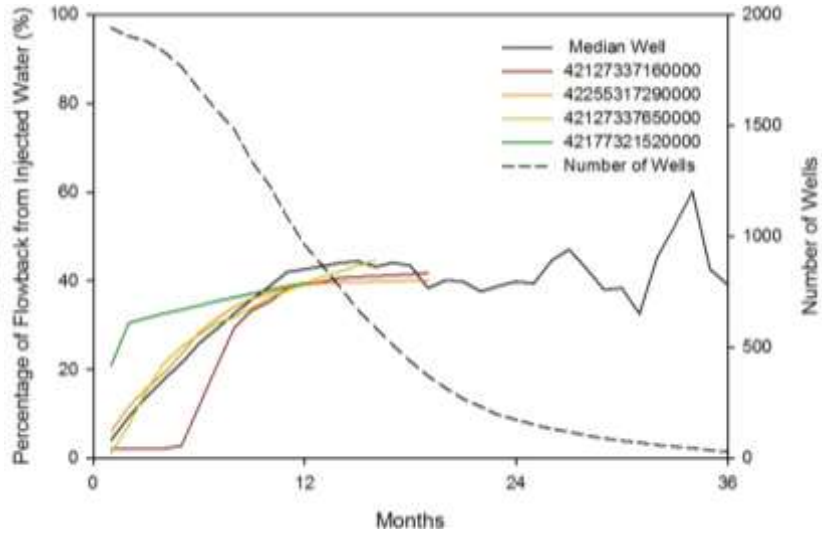

(c2)

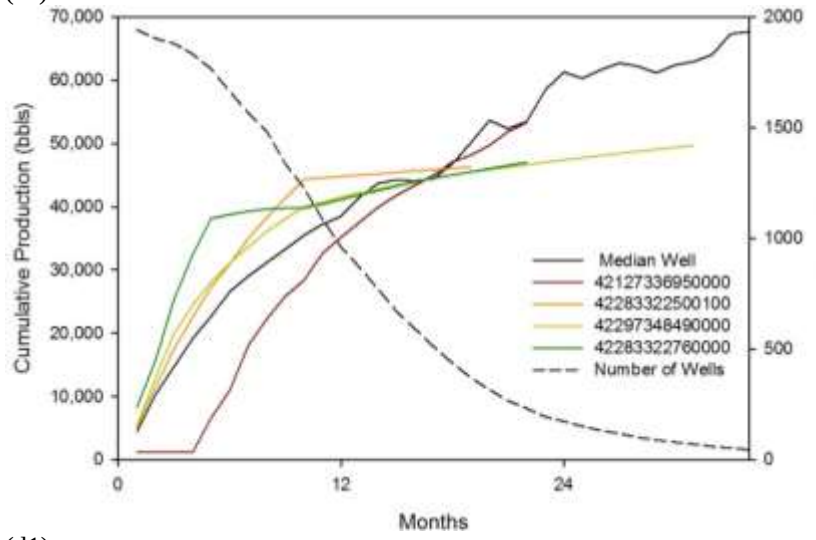

(d1)

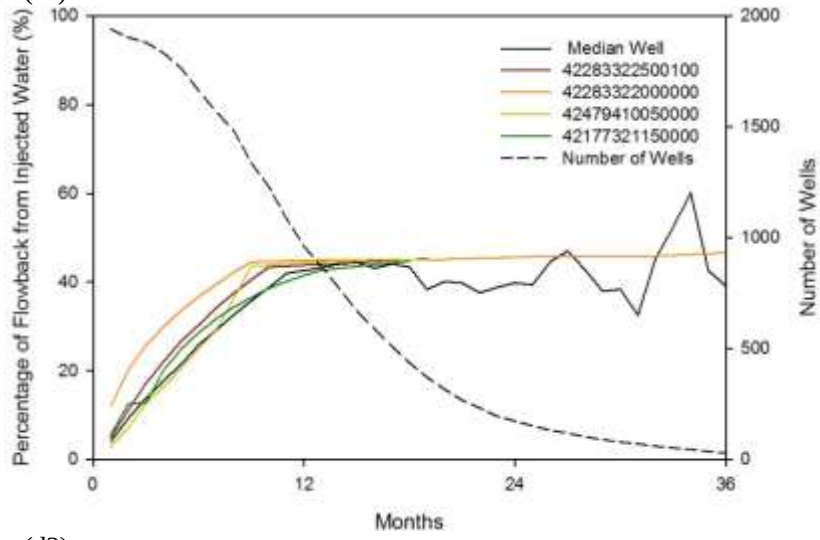

(d2)

Note: all wells (with full information and estimated) are included

Figure 126. Behavior of synthetic median at (1) 1 month, (b) 3 months, (c) 12 months, (d) 18 months, and (e) 24 months for cumulative production (_1) and fraction of flowback vs. HF (_2). Wells closest to the median at given time also shown. (continued)

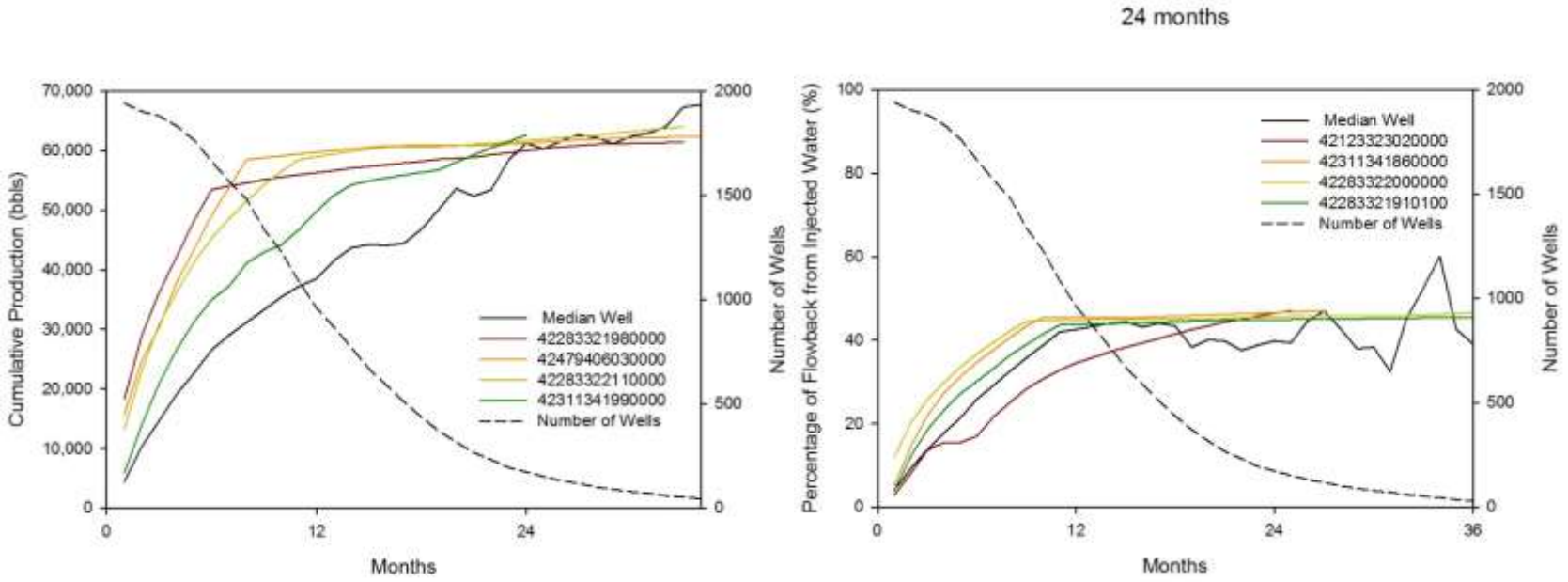

(e1) (e2)

Note: all wells (with full information and estimated) are included

Figure 126. Behavior of synthetic median at (1) 1 month, (b) 3 months, (c) 12 months, (d) 18 months, and (e) 24 months for cumulative production (_1) and fraction of flowback vs. HF (_2). Wells closest to the median at given time also shown. (continued)

VI-4. Analysis of Injection Wells

Analysis of HF water disposal has recently begun to be possible thanks to a change in reporting operator data from RRC; we also made use of IHS database. Injection data can be binned into two binary sets: (1) reservoir productive of oil and/or gas (RRC form H-1) or formation non-productive of oil and gas (RRC form W-14), performed by (2) an oil and gas operator or a commercial disposal operation. All disposal operations must report annual volumes injected (RRC form H-10). The RRC website provide a query tool to access injection and disposal wells (http://webapps2.rrc.state.tx.us/EWA/uicQueryAction.do). Some of the information is also available from IHS. Aggregated injection volume and other parameters are also provided by the RRC at http://webapps.rrc.state.tx.us/H10/h10PublicMain.do. We retrieved data at the county level. Injection volumes are available for commercial operations injection either in productive or non-productive interval and for oil and gas operators. Nature of the injected fluid is also available. The relevant categories are "salt water" and, available starting end of 2011, "fracture water flow back". Queries of the database do not allow for a finer resolution such as flowback water injected into commercial wells. Because of the one-year reporting rule, data submitted after February 2012 cannot be consider complete, that leaves only a few months of HF injection data which is more than one year old and may not represent current trends. In addition, we downloaded the data at the county level.

The State of Texas has historically generated large volumes of produced water. Veil and Clark (2010) reported that Texas generated 7.38×10^9 bbl of produced water, ~1/3rd of the total US volume in 2007 that was reported by them at 20.26×10^9 bbl. Currently there are 2541 injection wells in the mapped area (Figure 127); database labels included "Injection-Active", "Injection-Shut-in", "Waste Disposal", and "Salt water disposal". Approximately 1600 have been active since 2008. Most of the state produced water is generated in the Permian Basin in RRC districts 8, 8A, and 7C. To put things in perspective, state-wide HF consumption in 2011 was ~65 thousand AF or 0.50×10^9 bbl. Assuming 100% of the injected water is produced back, it would account for only 2.5% of all injections. EF area consumed 18,810 AF (0.146×10^9 bbl) for HF in 2011 (but used / injected 23,760 AF for HF). RRC has released and posted on the web injection volumes for many years but has just recently started also providing information about the nature of the fluids. It started in October 2011. However mandatory report of injection volume is done on an annual basis (RRC from H-10) and therefore only volumes up to January 2012 can be considered final. To assess the general consistency of our datasets, we use three months (November and December 2011 and January 2012). In 2012 (that is, still incomplete reporting), a total volume of 0.54×10^9 bbl was injected in EF footprint counties. HF accounted for 2.0% of that volume. It is unclear how much HF flowback / produced water is disposed of in commercial wells but over the same footprint, Caldwell and Guadalupe Counties, somewhat outside of the EF footprint, report very high injection volumes with no recorded HF injection. Removing them from the computation gives 0.14×10^9 bbl and 7.5% of the HF water use consumption volume. In terms of volume, they are followed by Victoria and Duval Counties, both also outside of the EF footprint.

If the number of injection wells is large, the number of active injection wells is much smaller and many are injected limited volumes for waterflooding purposes (Figure 129). The locations of the injection wells active in the past 5 years (2008-2012 or the actual number of active years if not active one or more years) have not change much (Figure 130, Figure 131, Figure 132, and Figure 133).

The injection formation is also accessible (Figure 134). A count is presented in Table 9 (it includes wells active at least one year since 2008 as well as shut-in wells). Note that the injection interval is not always provided in the database when the same well has been a producer. We assumed that injection and production intervals are the same. The Navarro-Taylor groups in far south Texas are the most abundant in terms of well count (42% of active wells). Other important injection formations are the Edwards Fm. (Figure 135) with high-volume wells in Caldwell and Guadalupe Counties. The Woodbine Fm. (Figure 136) Austin Chalk wells (Figure 137) are towards the north of the EF footprint. Figure 138 confirms that Navarro-Taylor injection wells are abundant in South Texas. A narrow interval in the Midway Fm. is sandy but it is unclear if the injection interval of these wells that initially produced from the Poth sands injected fluids into the same interval (Figure 139). Most Wilcox (Figure 140) and Yegua-Jackson wells (Figure 141) are somewhat outside of the EF footprint but sufficiently close to it to receive flowback water. Frio (Figure 142) and Miocene (Figure 143) wells are likely to far from the EF footprint to receive much flowback.

It is not possible to exactly determine which interval flowback / produced water from HF operations are injected into but it is relatively easy to determine the fraction of HF out of the entire injected volume by county (Table 10). These values were computed using the 3 months of available complete flowback data (Q4 of 2011) extrapolated to 1 year by multiplying the result by 4 and compared to average annual injection volumes. Actual monthly data are shown in Figure 144. Karnes and Dimmit county HF had the highest disposal volumes at the beginning of year 2012. Data are presented in bar plots in Figure 145. Figure 146 illustrates the value used to derive Table 10. In terms of flowback fraction relative to total injection volumes, the following counties are noticeable: Dimmit (23.1%), Jim Wells (21.9%), Gonzales (16.2%), Atascosa (15.0%), Madison (13.2%), Goliad (11.2%), and La Salle (10.8%). Not coincidently, the same counties also score high in terms of total volume injected (Figure 146). The calculation of flowback relative to the injected HF volume is harder to compute at the county level because disposal is clearly done in counties outside of the EF play (for example, Victoria, Goliad, Bee, Duval, and Jim Wells counties to the SE of the play) (Table 11). These recently available figures from the RRC suggest that <10% (8.7%) of the water used for HF is disposed of. The discrepancy with data presented in Section VI-3 is unexplained so far but may be related to the average age of the wells.

The formations of choice for disposal are within the Navarro-Taylor group below the Midway (Olmos, San Miguel Fms). They offer good porosity and permeability and transition to shaley facies in the updip direction. They also shale out in the downdip direction and do not exist much towards the north of the EF footprint. In that case the deep Edwards (also below the Midway) can be used (for example, Atascosa or McMullen County or Central Texas) if the Lower Wilcox is protected. The Lower Wilcox is above the Midway and could be a good choice if the injectivity is sufficient. In some counties of Central Texas the Carrizo is not protected because the 10,000 ppm contour line is close to the outcrop (DeWitt) and could be used as injection interval. This is also true for the Yegua-Jackson and underlying Sparta that can become brackish quickly at shallow depths. Ideally strike-oriented sand with a 50,000 ppm TDS are ideal candidate for disposal when they are bounded by low-permeability facies in the updip direction, by more sand facies in the downdip direction, and by faults laterally (or mud facies).

Table 9. Active injection interval count (well with data only)

Formation	Count	Percent
San Miguel	587	22.6%
Jackson	347	13.3%
Olmos	328	12.6%
Frio-Vicksburg	250	9.6%
Austin Chalk	219	8.4%
Wilcox	210	8.1%
Navarro	173	6.6%
Edwards, Buda, Georgetown	106	4.1%
Woodbine	91	3.5%
Poth (Midway)	56	2.2%
Yegua	64	2.5%
Miocene	37	1.4%
Queen City	28	1.1%
Catahoula	24	0.9%
Sum	2511	96.8%

Source: IHS

InjectionEF2_JP.xls

Table 10. Fraction of HF disposal in all disposal and injection for waterflood.

County		County		County		County	
Atascosa	15.0%	Dimmit	23.1%	Kinney	n/a	Travis	0.0%
Austin	0.0%	Duval	0.6%	La Salle	10.8%	Uvalde	n/a
Bastrop	0.0%	Fayette	0.0%	Lavaca	1.4%	Victoria	0.4%
Bee	5.5%	Frio	3.4%	Lee	0.0%	Waller	0.0%
Bexar	0.0%	Goliad	11.2%	Live Oak	8.6%	Washington	0.0%
Brazos	1.8%	Gonzales	16.2%	Madison	13.2%	Webb	0.0%
Burleson	0.0%	Grimes	0.0%	Maverick	0.0%	Williamson	n/a
Caldwell	0.0%	Guadalupe	0.0%	McMullen	3.1%	Wilson	6.9%
Colorado	2.8%	Hays	n/a	Medina	0.0%	Zavala	0.0%
Comal	n/a	Jim Wells	21.9%	Milam	4.6%		
De Witt	0.0%	Karnes	10.9%	Robertson	4.4%		

Note: n/a = no injection taking place in this county

RRCstuff_JP.xls

Note: county is highlighted if HF fluid disposal accounts for >10% of total fluid injection in the county

Table 11. County level flowback disposal vs. HF volumes in 2011

County	HF volumes (AF)[&]	Volumes of HF flowback disposed of (AF)*	Volumes of HF flowback disposed of (AF)*	County-level flowback / HF ratio
EF counties				
Atascosa	1009	184		18%
Bee	66	42		64%
Brazos	0	19		
Burleson	0	0		
Dewitt	2151	0		0%
Dimmit	3512	384		11%
Fayette	61	0		0%
Frio	487	48		10%
Gonzales	2164	201		9%
Karnes	3861	275		7%
La Salle	2847	196		7%
Lavaca	117	6		5%
Lee	0	0		
Leon	0	0		
Live oak	971	112		12%
Maverick	170	0		0%
McMullen	1636	49		3%
Milam	0	6		
Webb	4038	0		0%
Wilson	417	51		12%
Zavala	249	0		0%
TOTAL	23,754	1574		
Counties with no or little overlap with EF footprint				
Colorado			11	
Duval			43	
Goliad			155	
Jim Wells			149	
Madison			75	
Robertson			39	
Victoria			15	
TOTAL			487	
GRAND TOTAL	23,754	2061		8.7%

Source: http://webapps.rrc.state.tx.us/H10/h10PublicMain.do ("fluid type" query)
Note: & = Nicot et al. (2012); * = estimated for the year – see Figure 146 RRCstuff_JP.xls

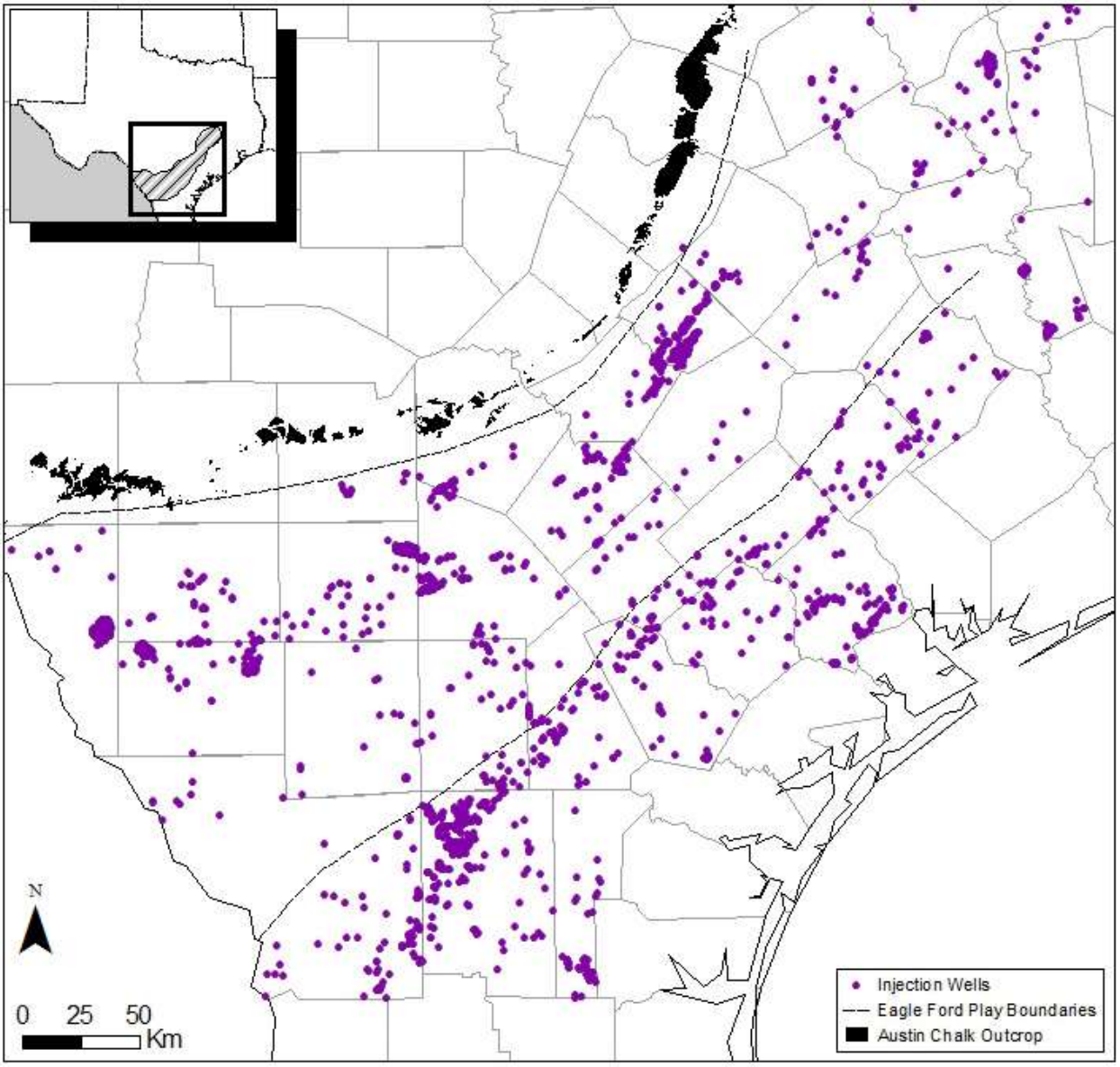

Source: IHS Enerdeq database

Figure 127. Injections wells in the Eagle Ford area

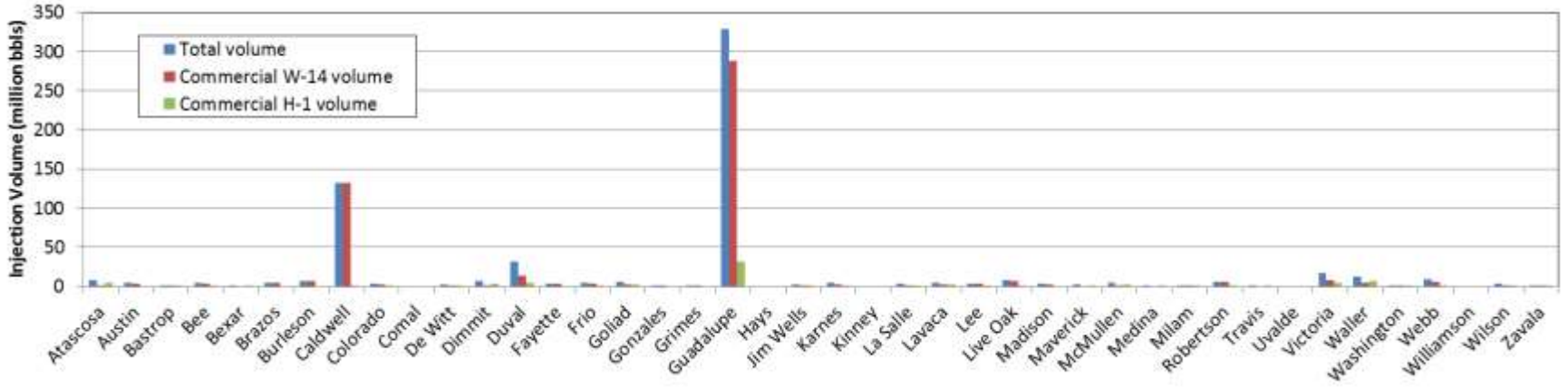

(a)

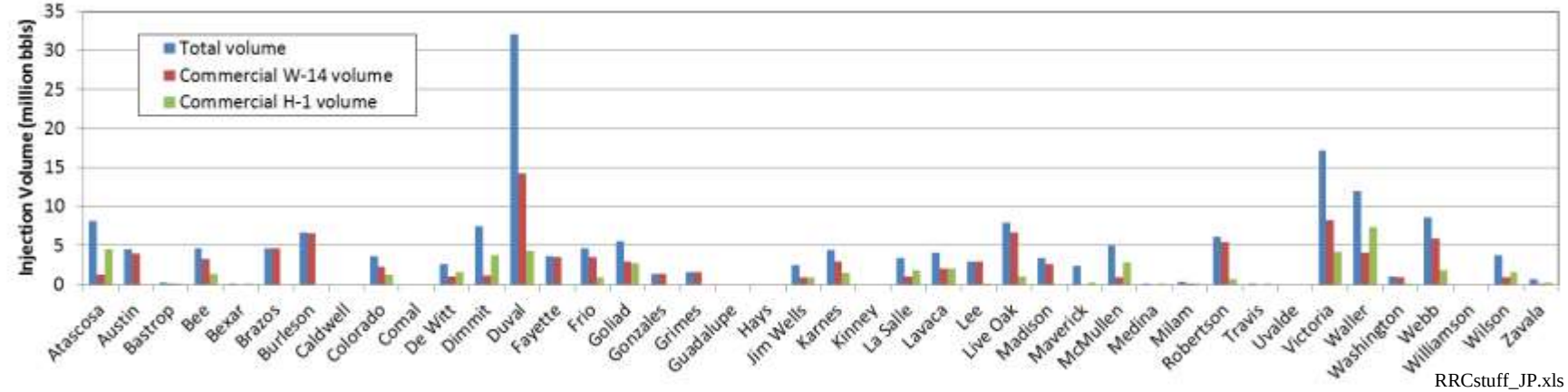

(b)

Source: RRC website

Figure 128. County-level annual injection volume (a) all EF counties and (b) without Caldwell and Guadalupe counties

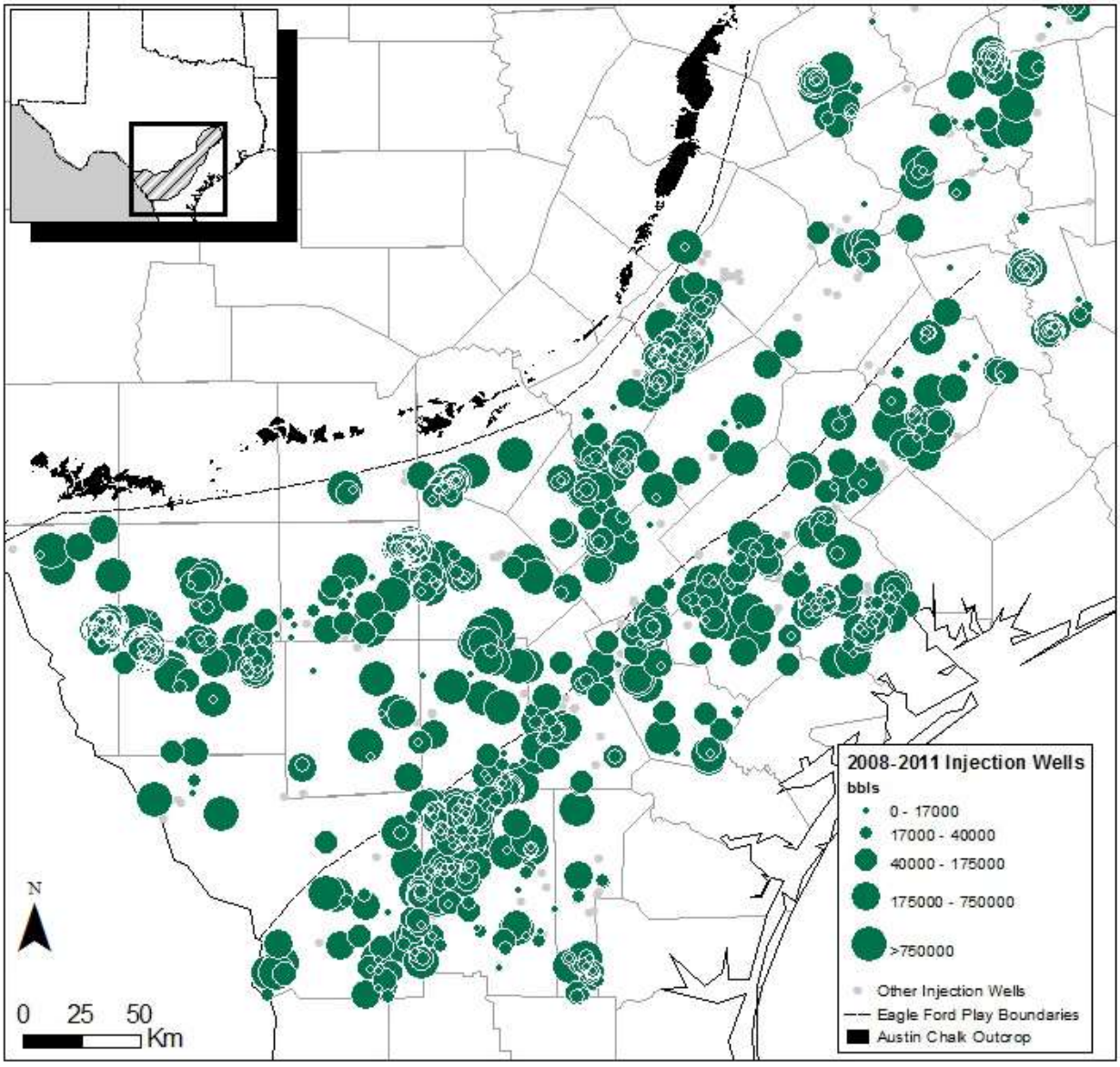

Source: IHS Enerdeq database

Figure 129. Active injections wells in the Eagle Ford area and injected volume (2008-2011)

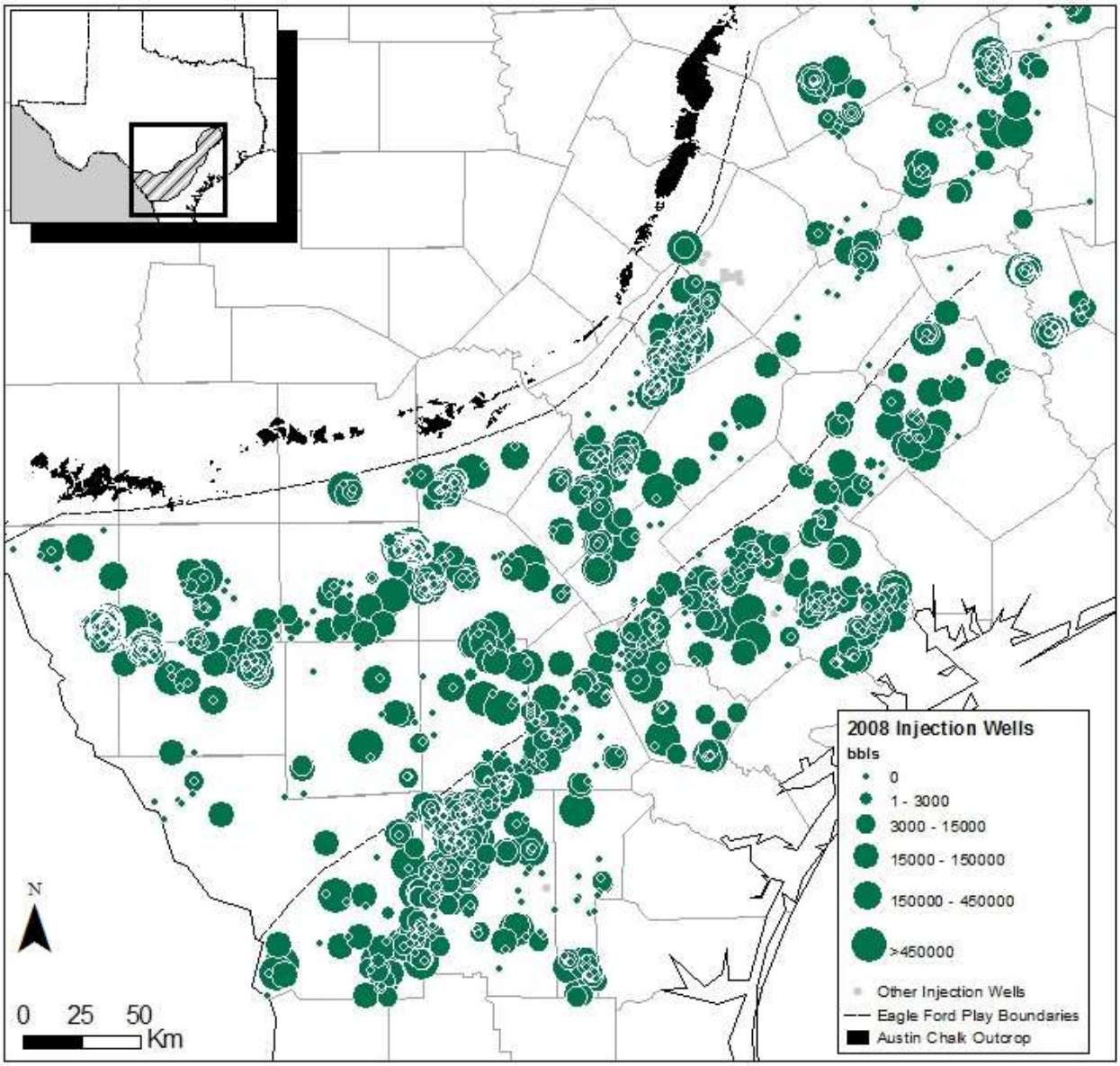

Source: IHS Enerdeq database

Figure 130. Active injections wells in the Eagle Ford area and injected volume (2008)

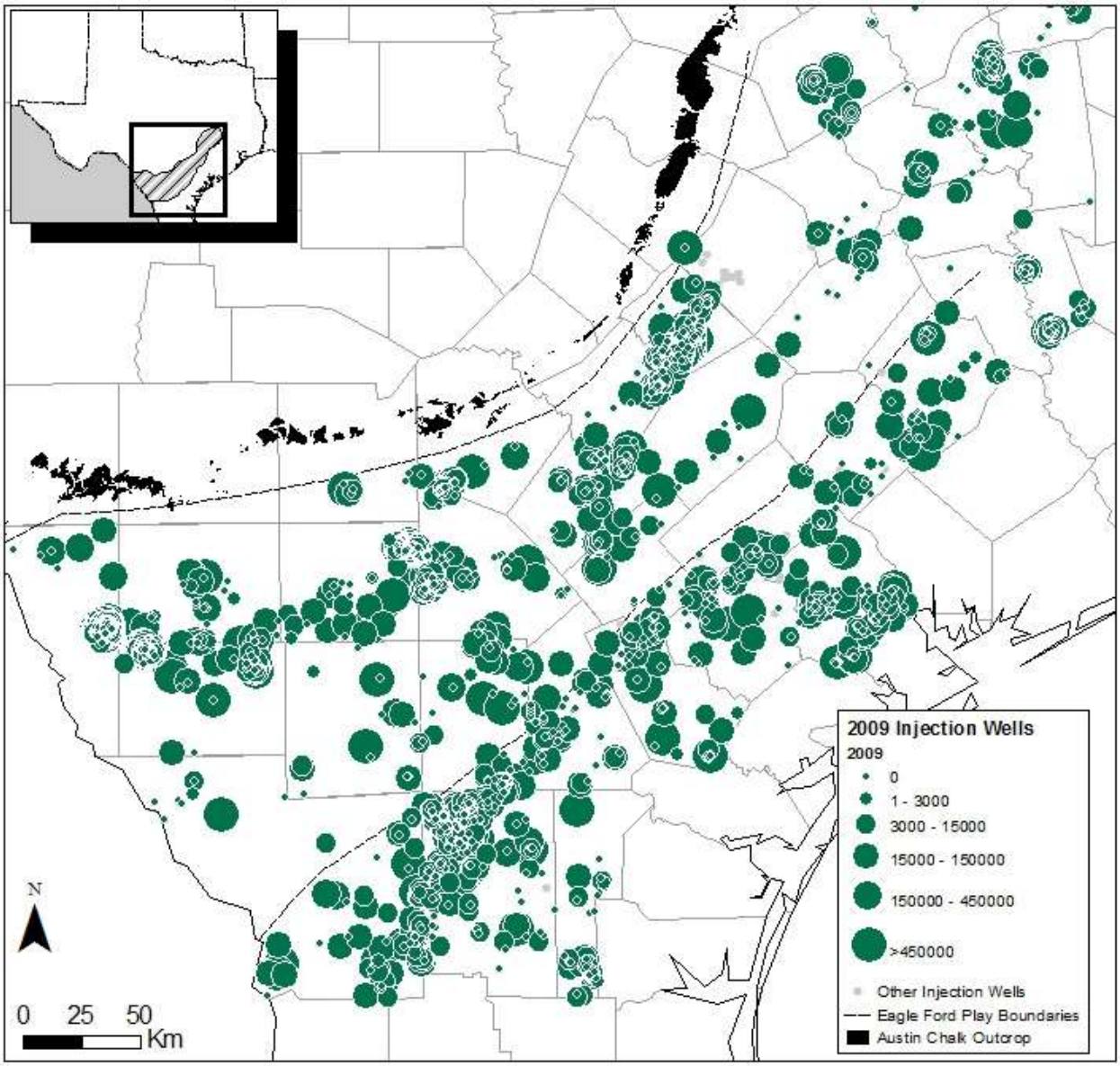

Source: IHS Enerdeq database

Figure 131. Active injections wells in the Eagle Ford area and injected volume (2009)

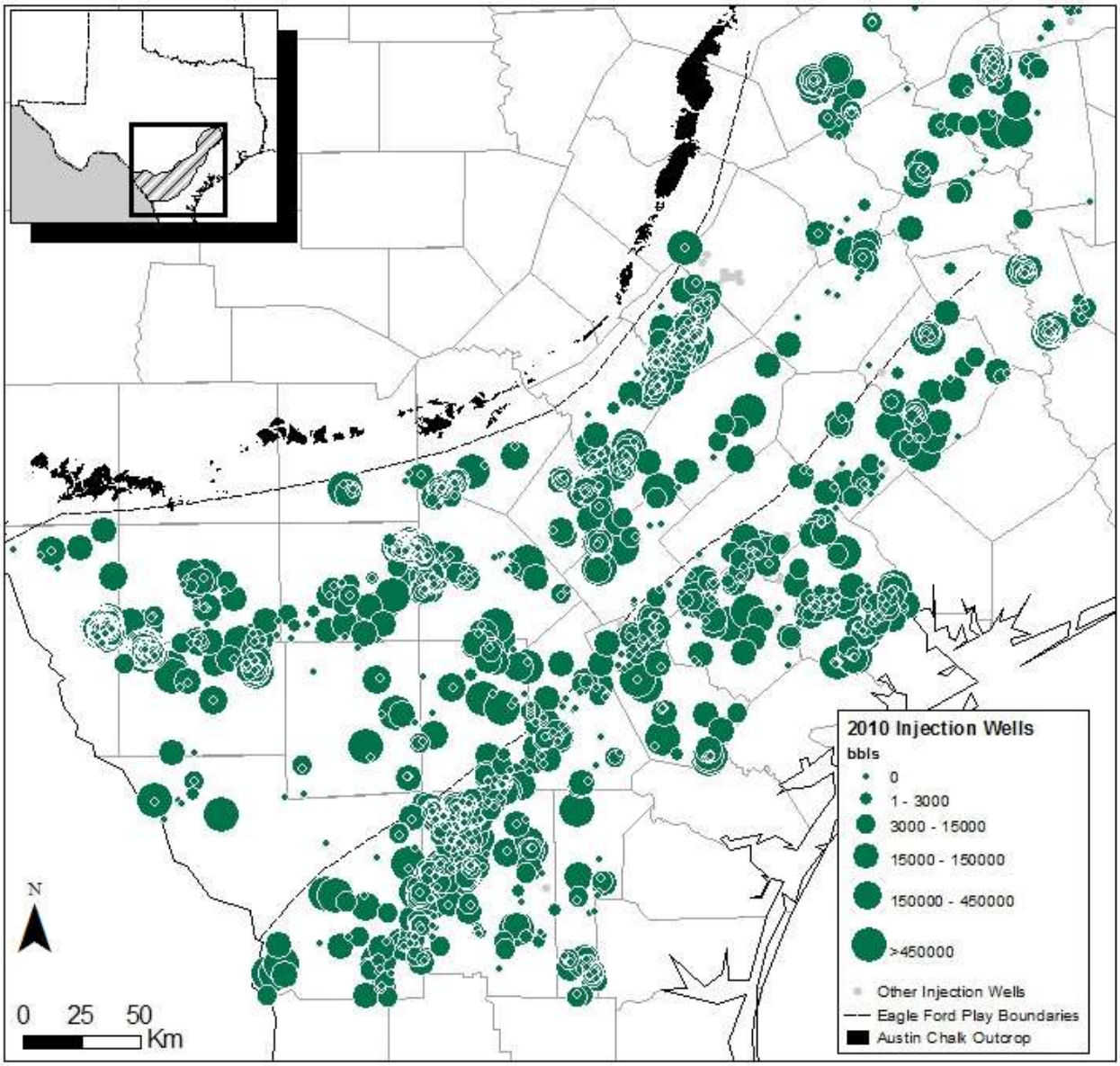

Source: IHS Enerdeq database

Figure 132. Active injections wells in the Eagle Ford area and injected volume (2010)

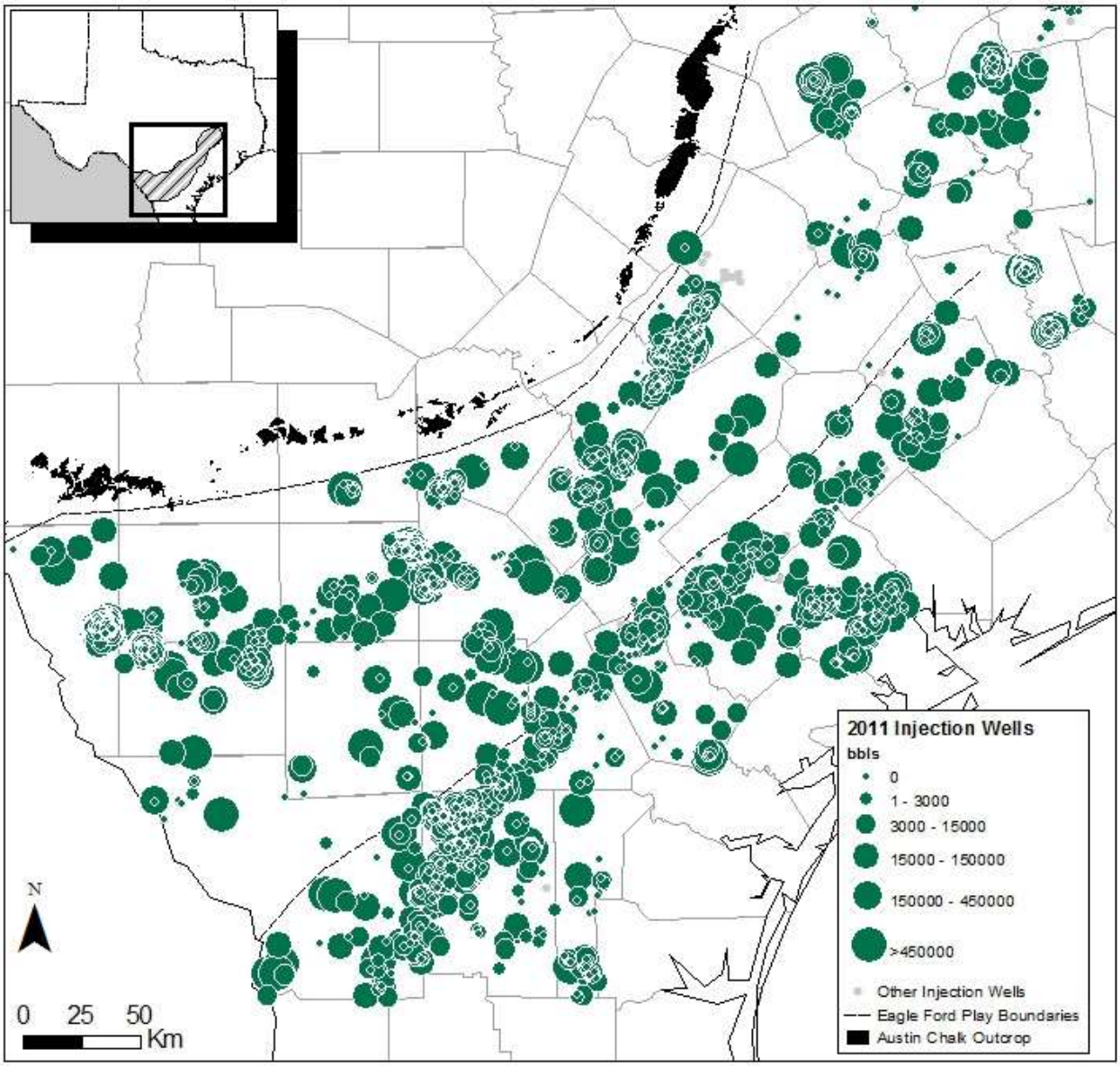

Source: IHS Enerdeq database

Figure 133. Active injections wells in the Eagle Ford area and injected volume (2011)

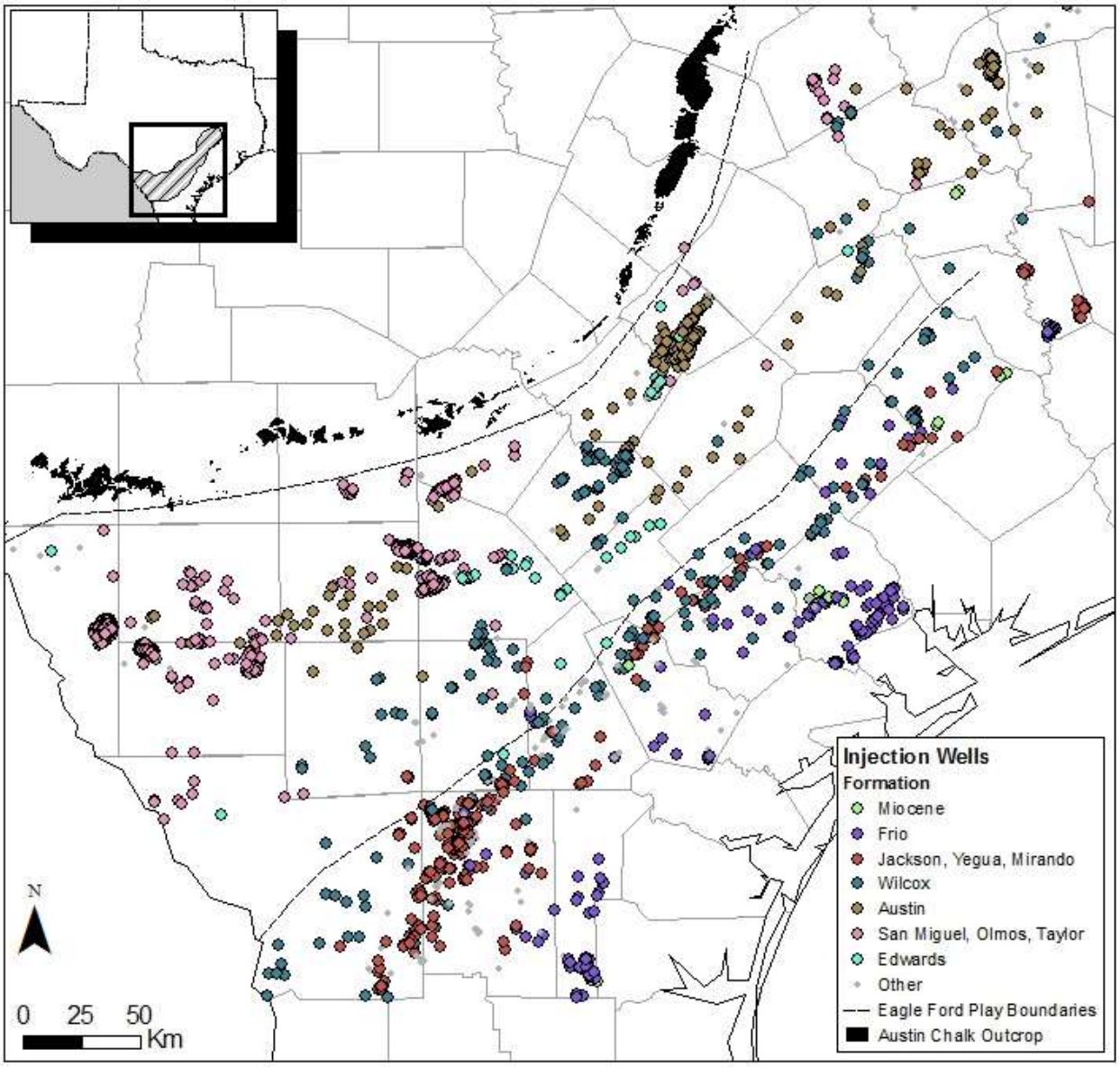

Source: IHS Enerdeq database

Figure 134. Injections wells in the Eagle Ford area color-coded by injection formation.

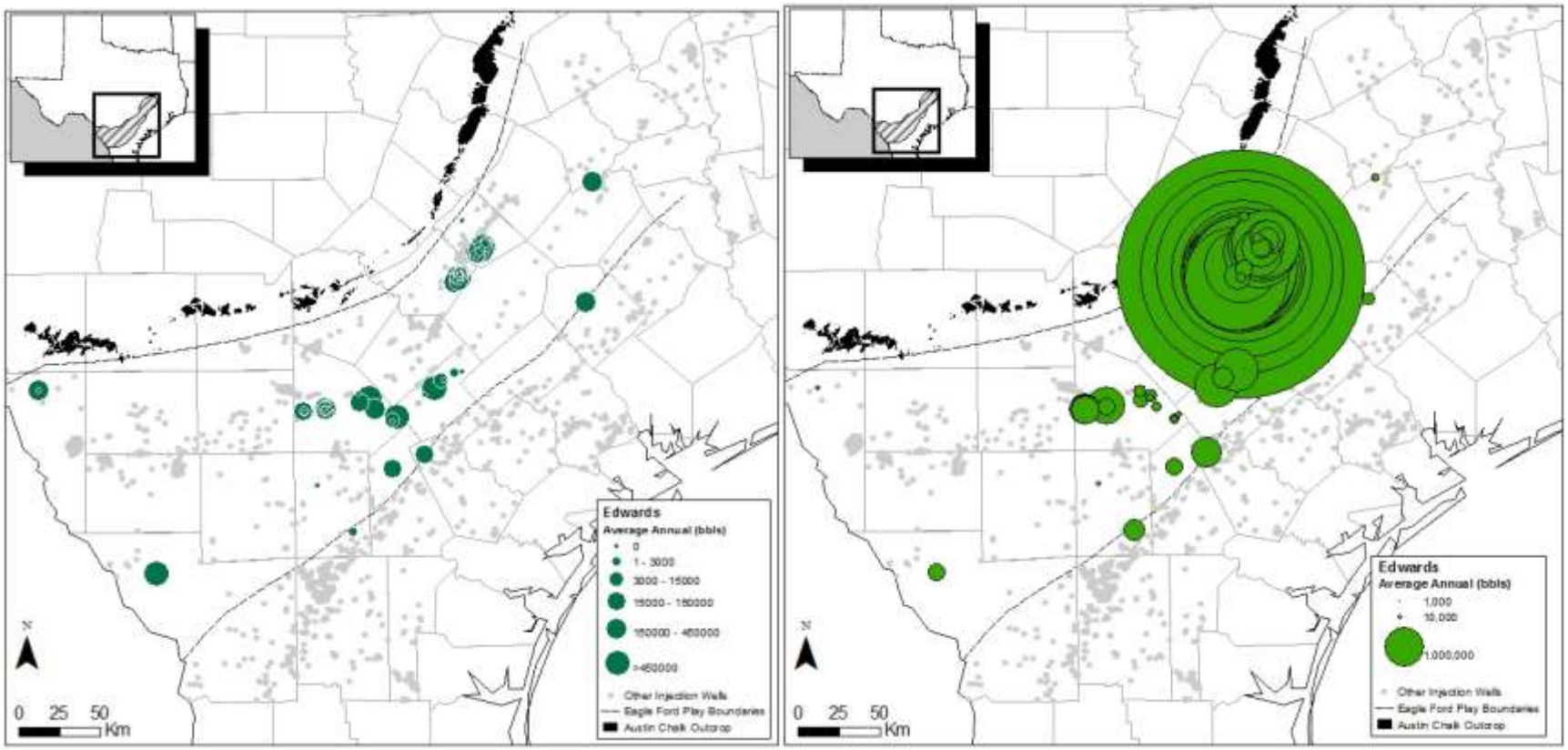

Source: IHS Enerdeq database
Note: LHS map uses ~even-sized bins; symbol size on RHS map is an approximate function of average volume injected

Figure 135. Active injections wells in the Eagle Ford area and injected volume (2008-2011 average – Edwards Fm.)

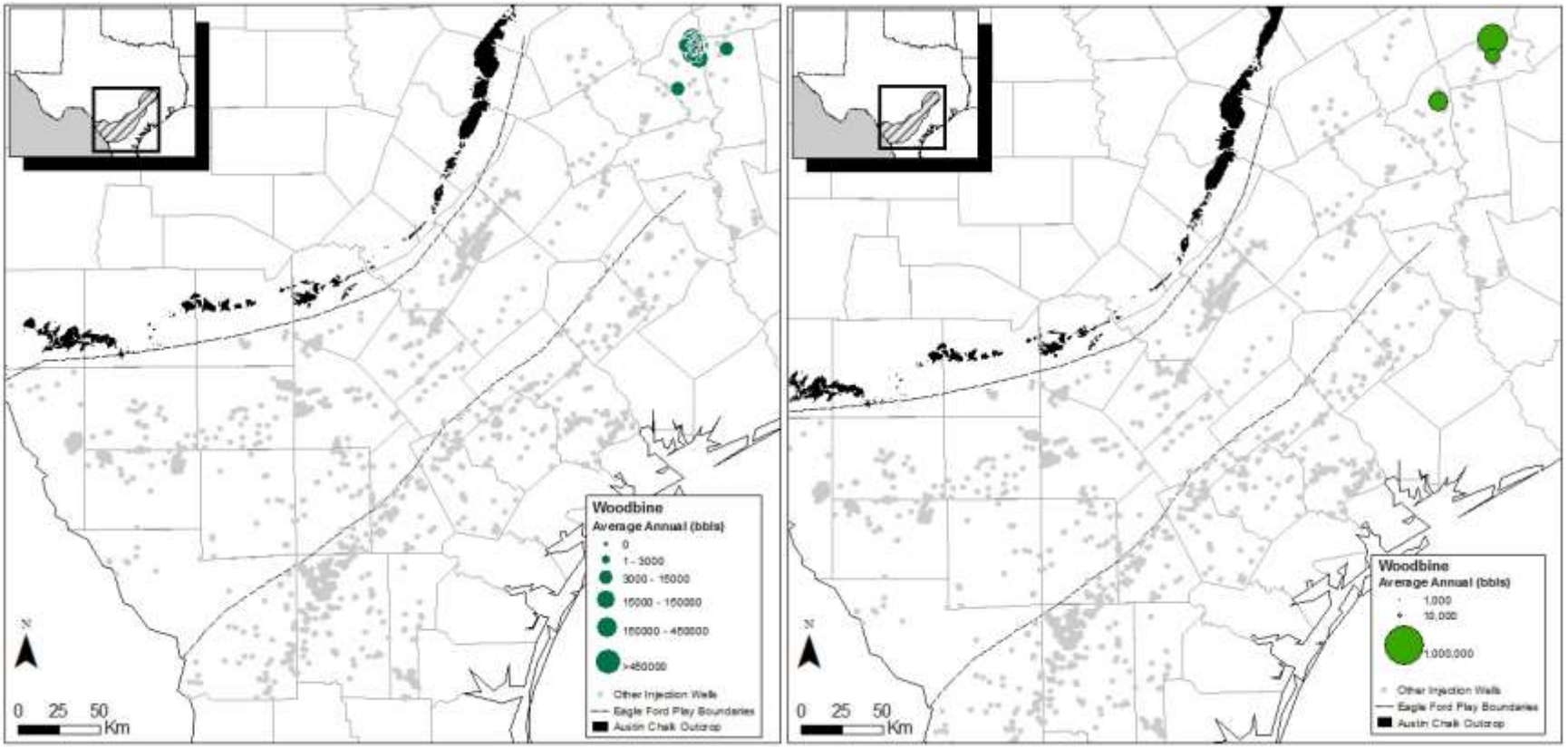

Source: IHS Enerdeq database
Note: LHS map uses ~even-sized bins; symbol size on RHS map is an approximate function of average volume injected

Figure 136. Active injections wells in the Eagle Ford area and injected volume (2008-2011 average – Woodbine)

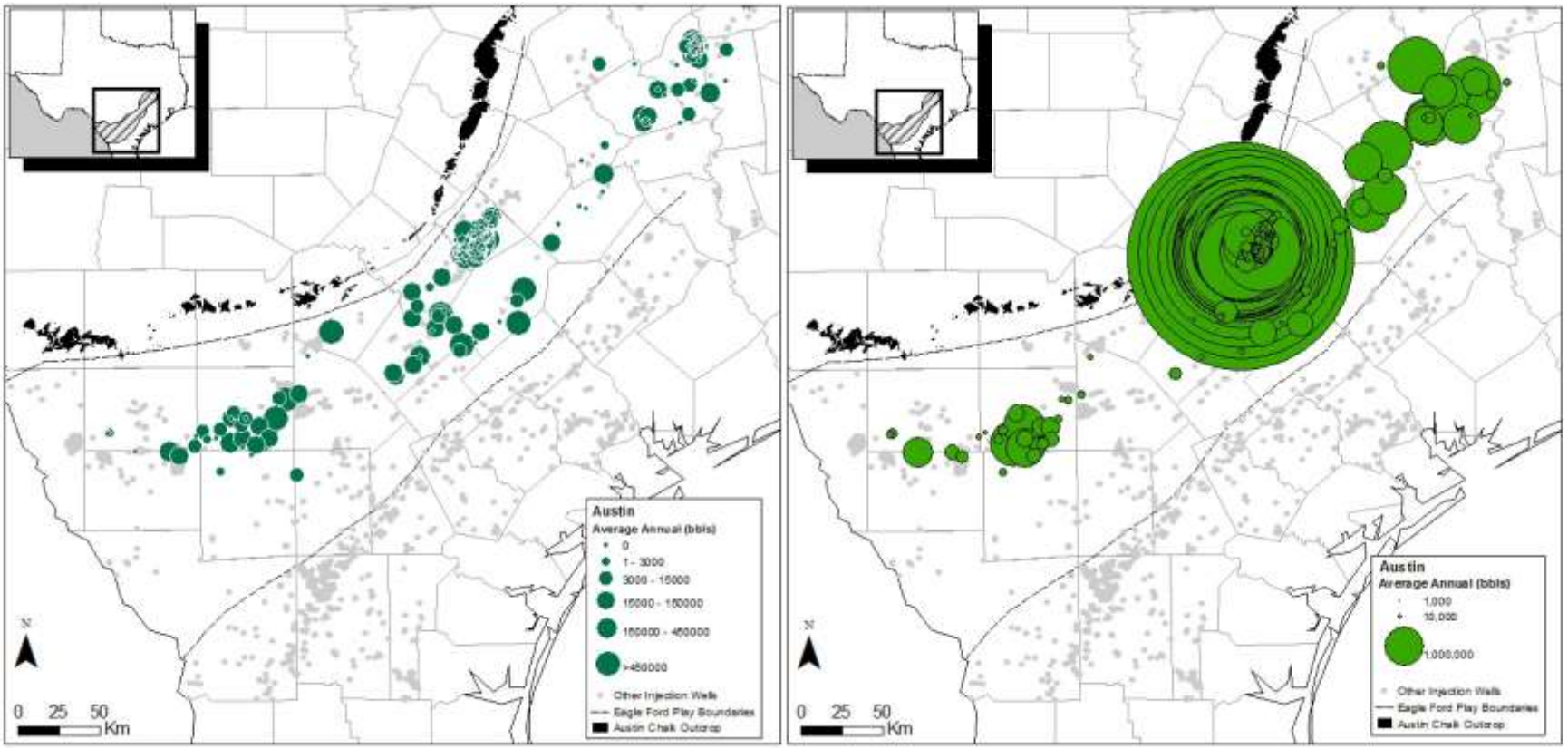

Source: IHS Enerdeq database
Note: LHS map uses ~even-sized bins; symbol size on RHS map is an approximate function of average volume injected

Figure 137. Active injections wells in the Eagle Ford area and injected volume (2008-2011 average – Austin Chalk)

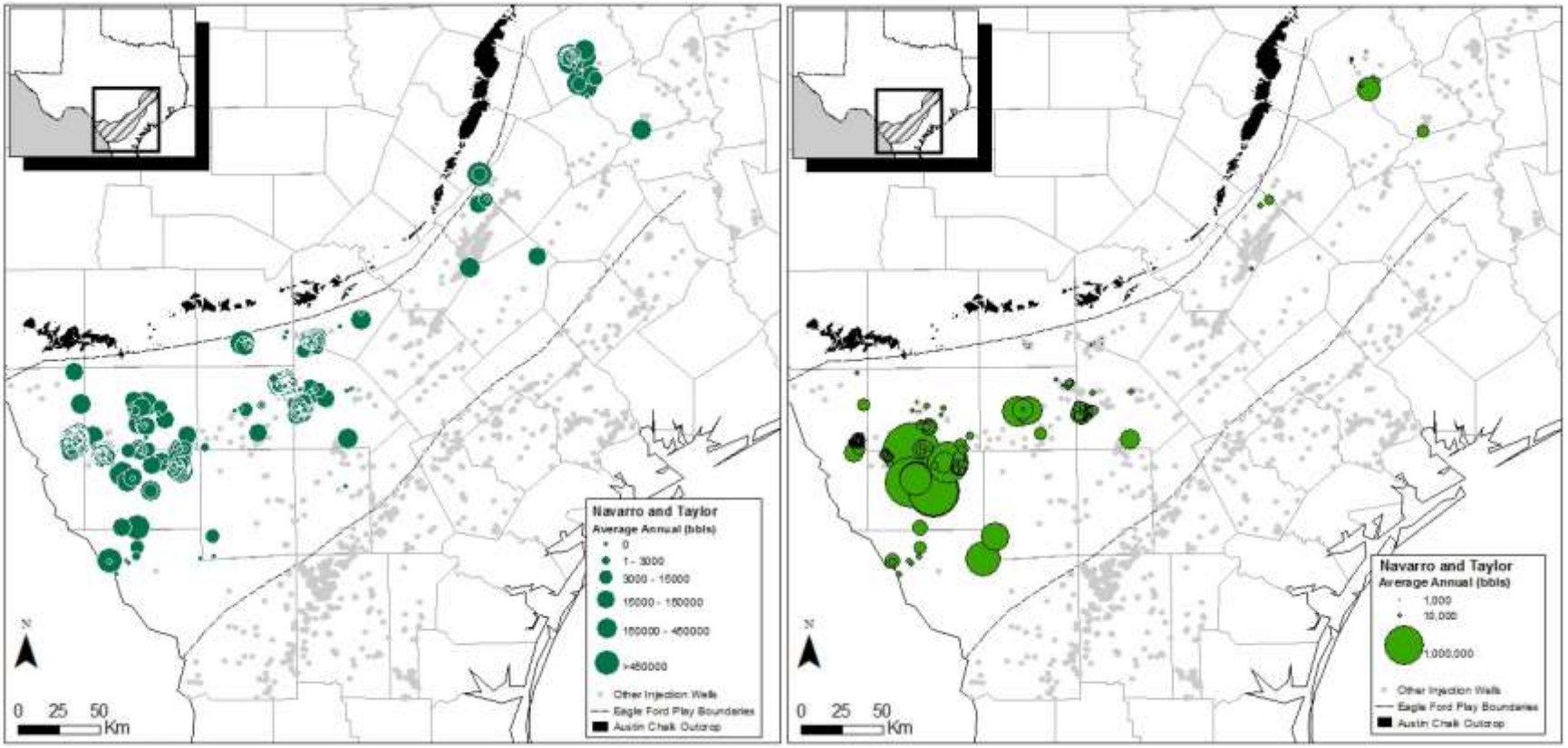

Source: IHS Enerdeq database
Note: LHS map uses ~even-sized bins; symbol size on RHS map is an approximate function of average volume injected

Figure 138. Active injections wells in the Eagle Ford area and injected volume (2008-2011 average – Navarro and Taylor groups)

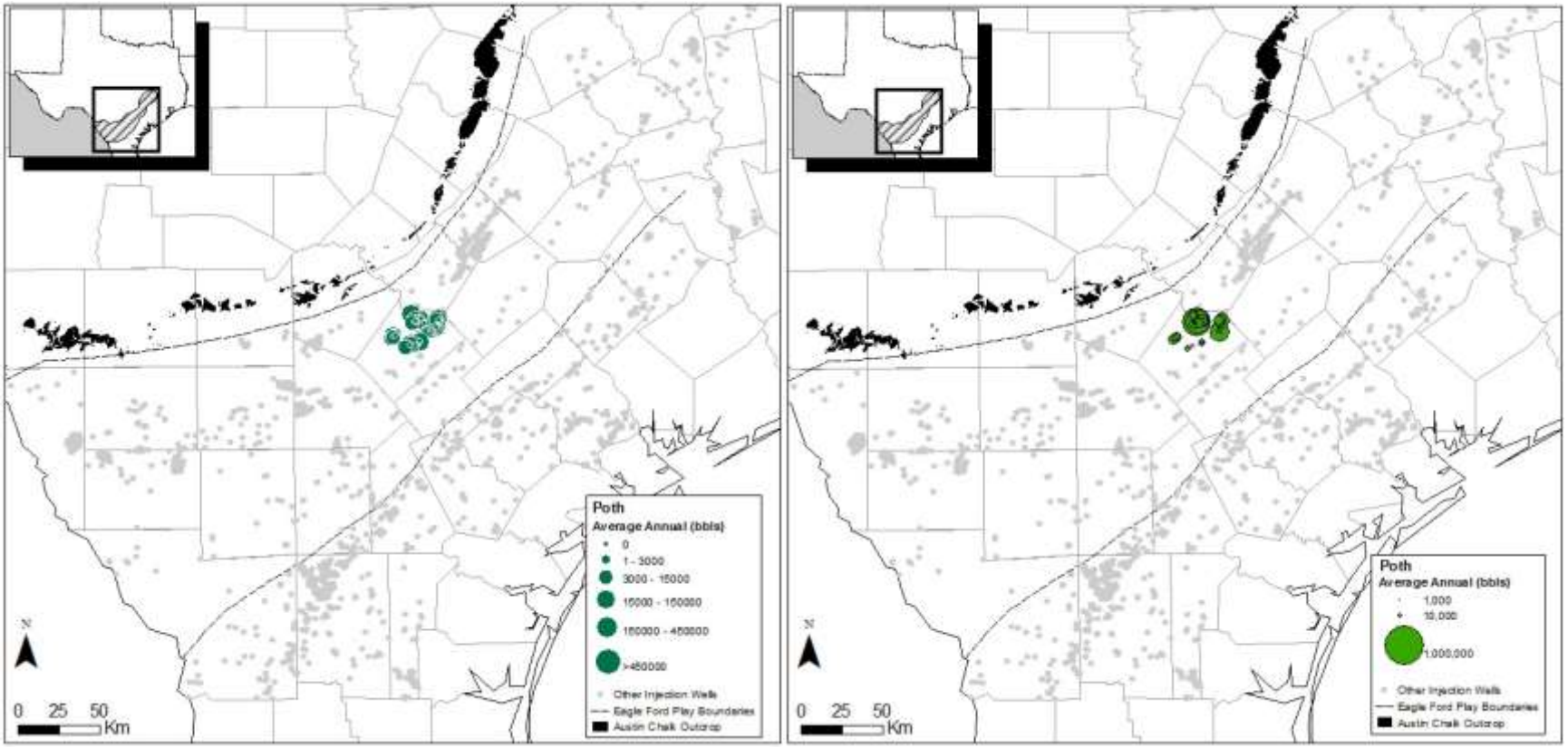

Source: IHS Enerdeq database
Note: LHS map uses ~even-sized bins; symbol size on RHS map is an approximate function of average volume injected

Figure 139. Active injections wells in the Eagle Ford area and injected volume (2008-2011 average – Poth sands -Midway Fm.)

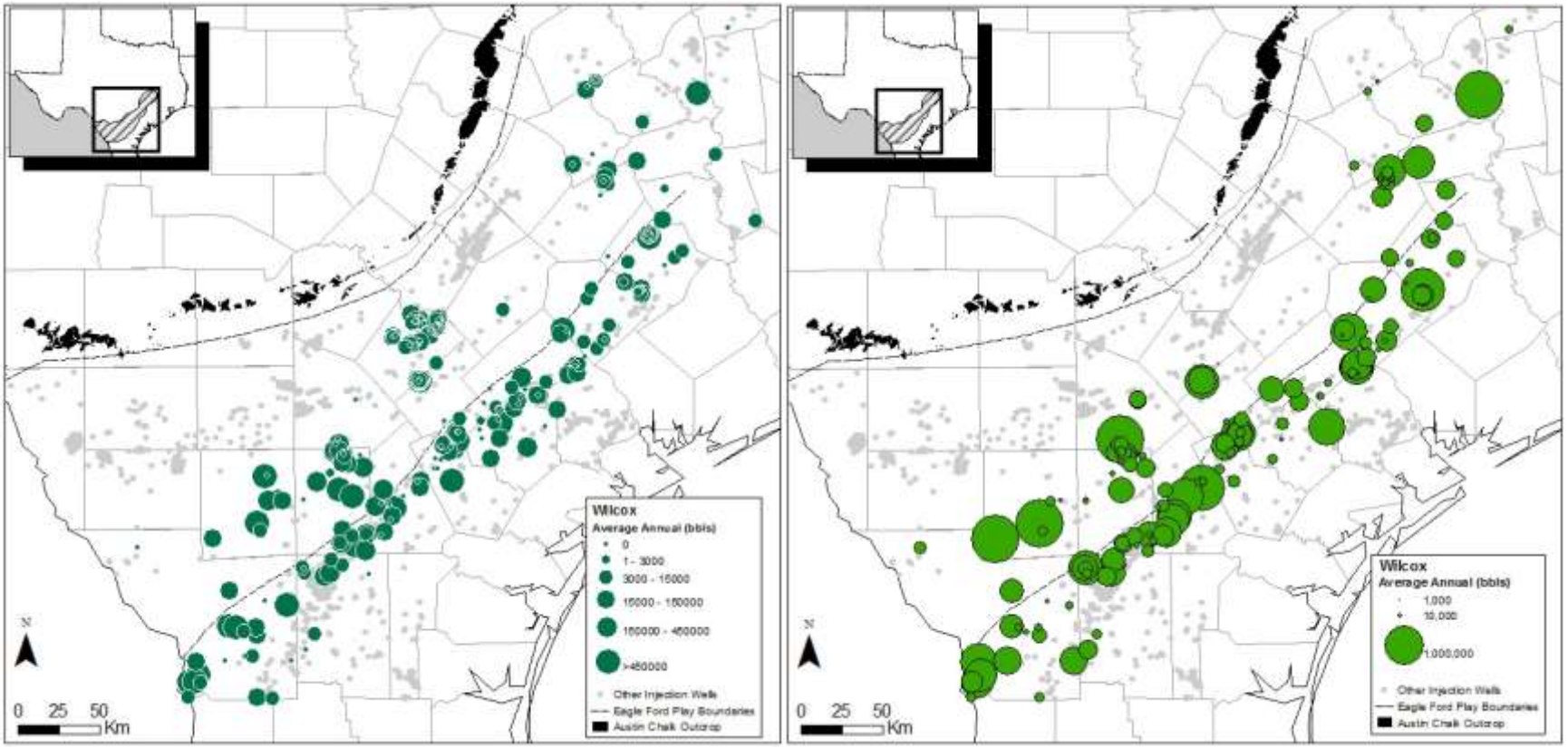

Source: IHS Enerdeq database
Note: LHS map uses ~even-sized bins; symbol size on RHS map is an approximate function of average volume injected

Figure 140. Active injections wells in the Eagle Ford area and injected volume (2008-2011 average – Wilcox Fm.)

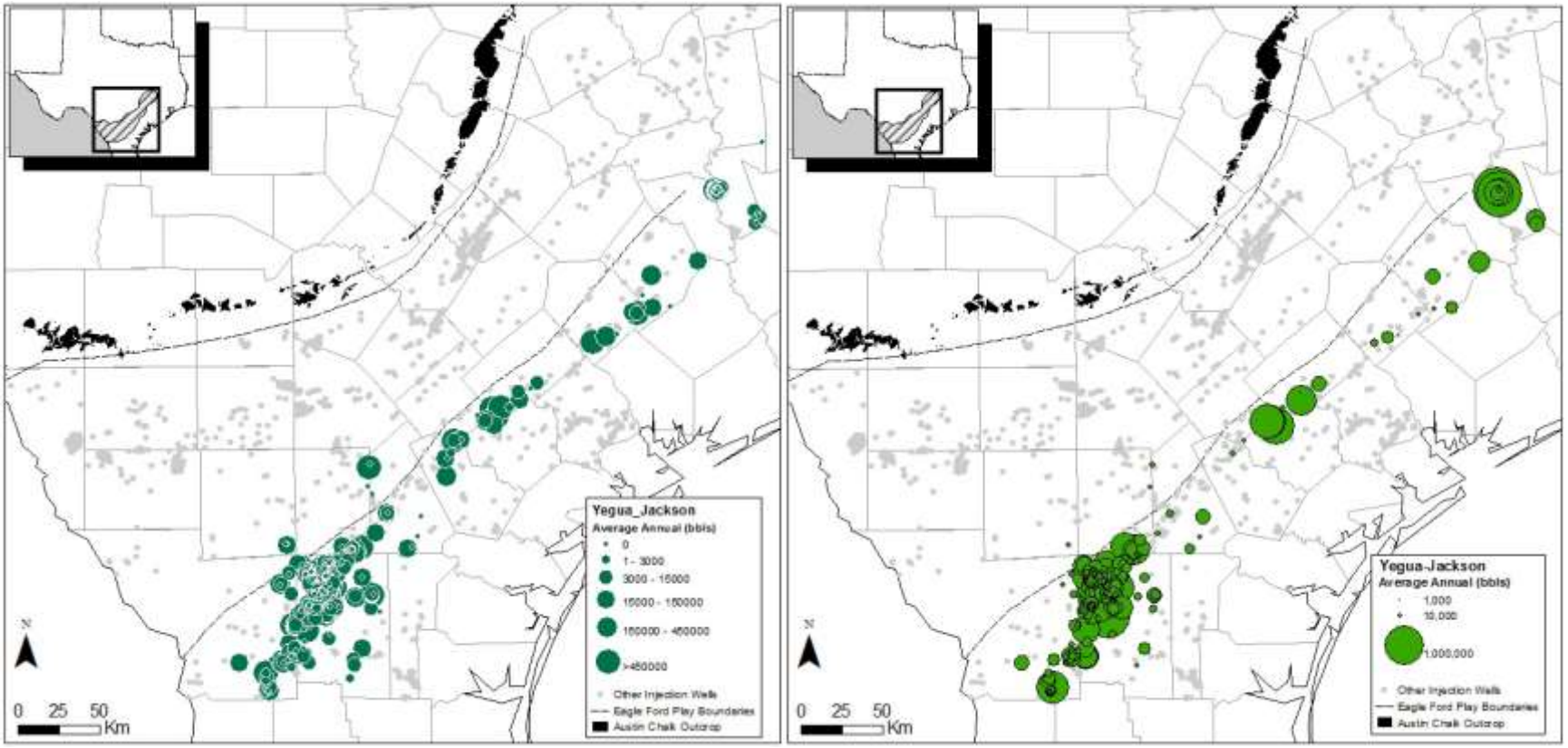

Source: IHS Enerdeq database
Note: LHS map uses ~even-sized bins; symbol size on RHS map is an approximate function of average volume injected

Figure 141. Active injections wells in the Eagle Ford area and injected volume (2008-2011 average – Jackson Group and Yegua Fm.)

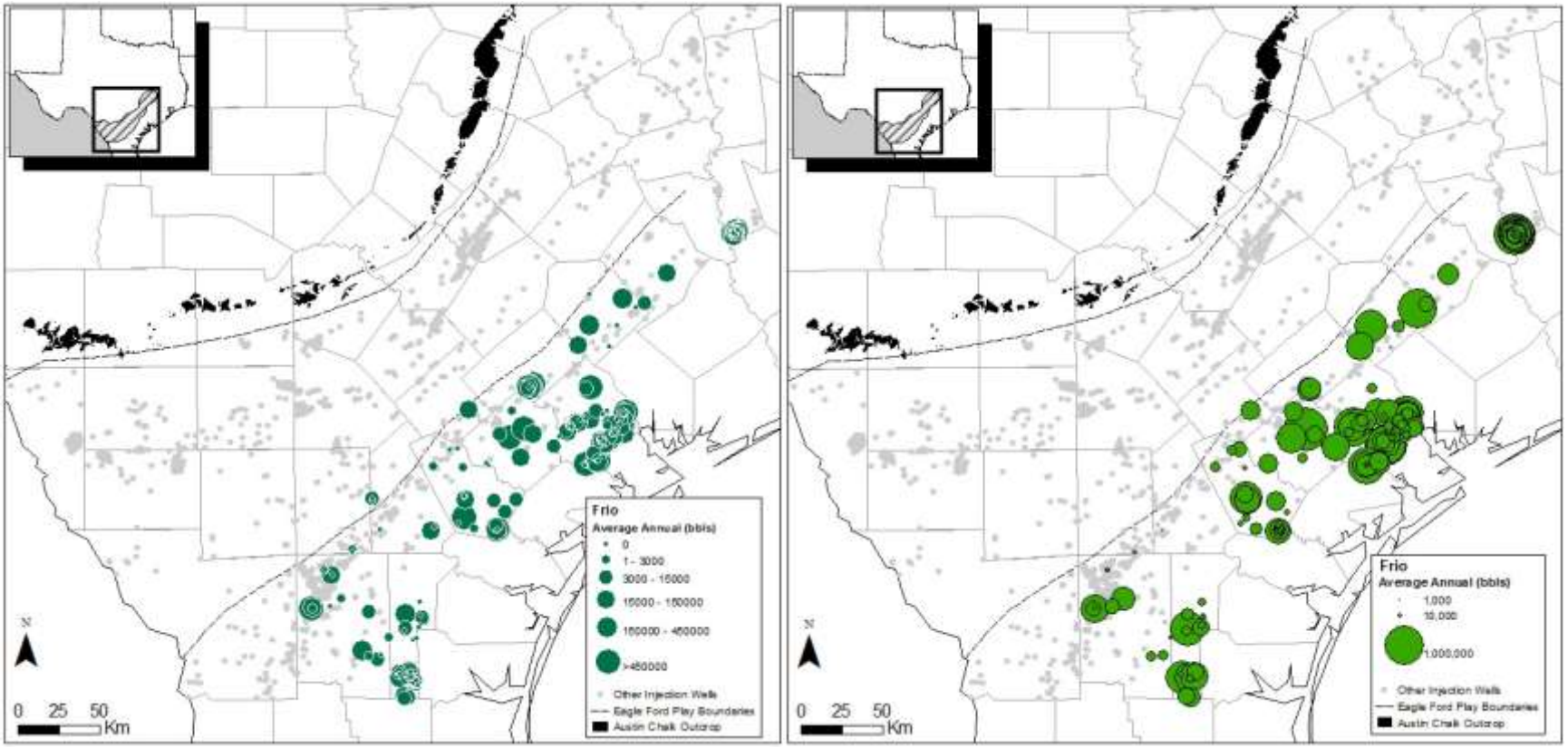

Source: IHS Enerdeq database
Note: LHS map uses ~even-sized bins; symbol size on RHS map is an approximate function of average volume injected

Figure 142. Active injections wells in the Eagle Ford area and injected volume (2008-2011 average – Frio Fm.)

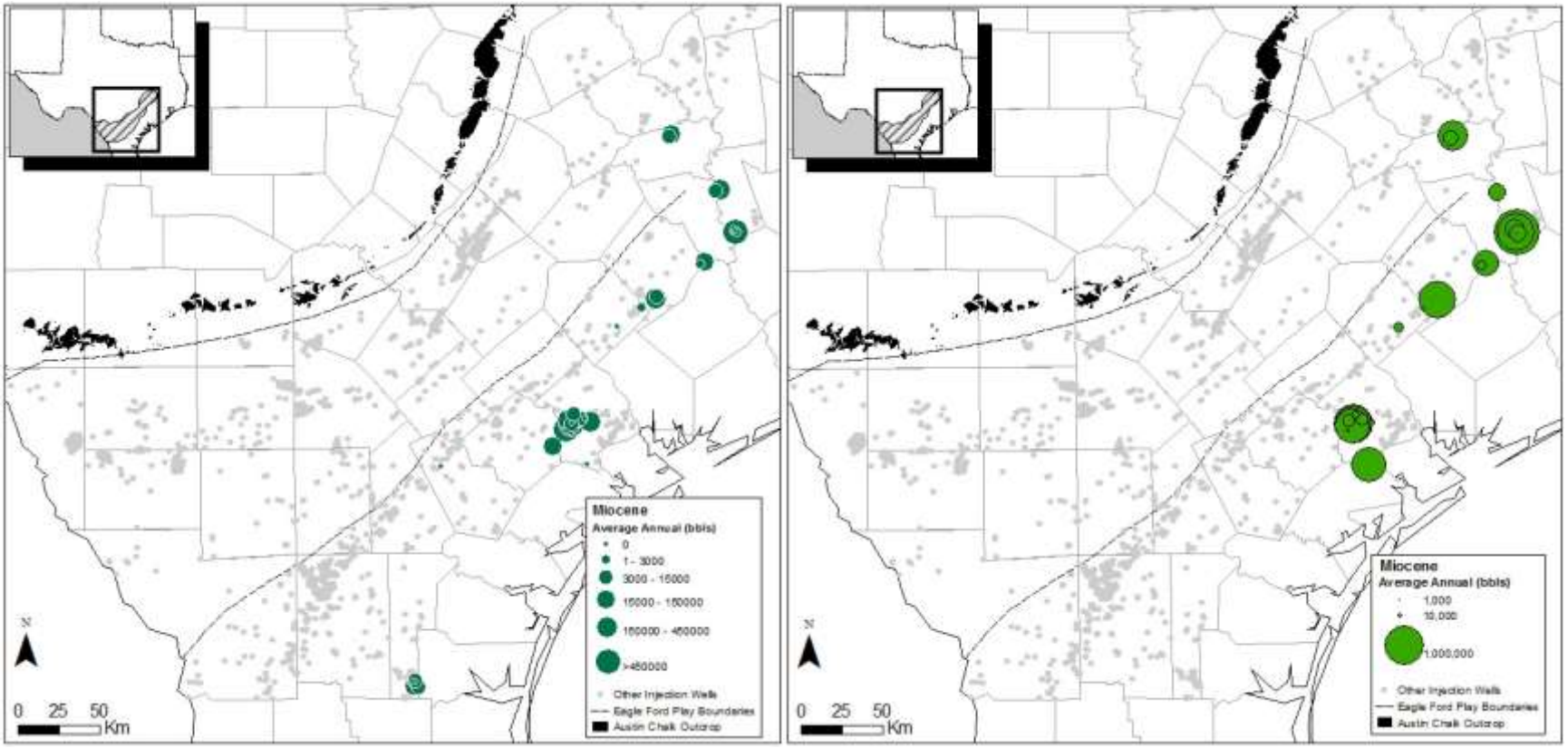

Source: IHS Enerdeq database
Note: LHS map uses ~even-sized bins; symbol size on RHS map is an approximate function of average volume injected

Figure 143. Active injections wells in the Eagle Ford area and injected volume (2008-2011 average – Miocene Fms.)

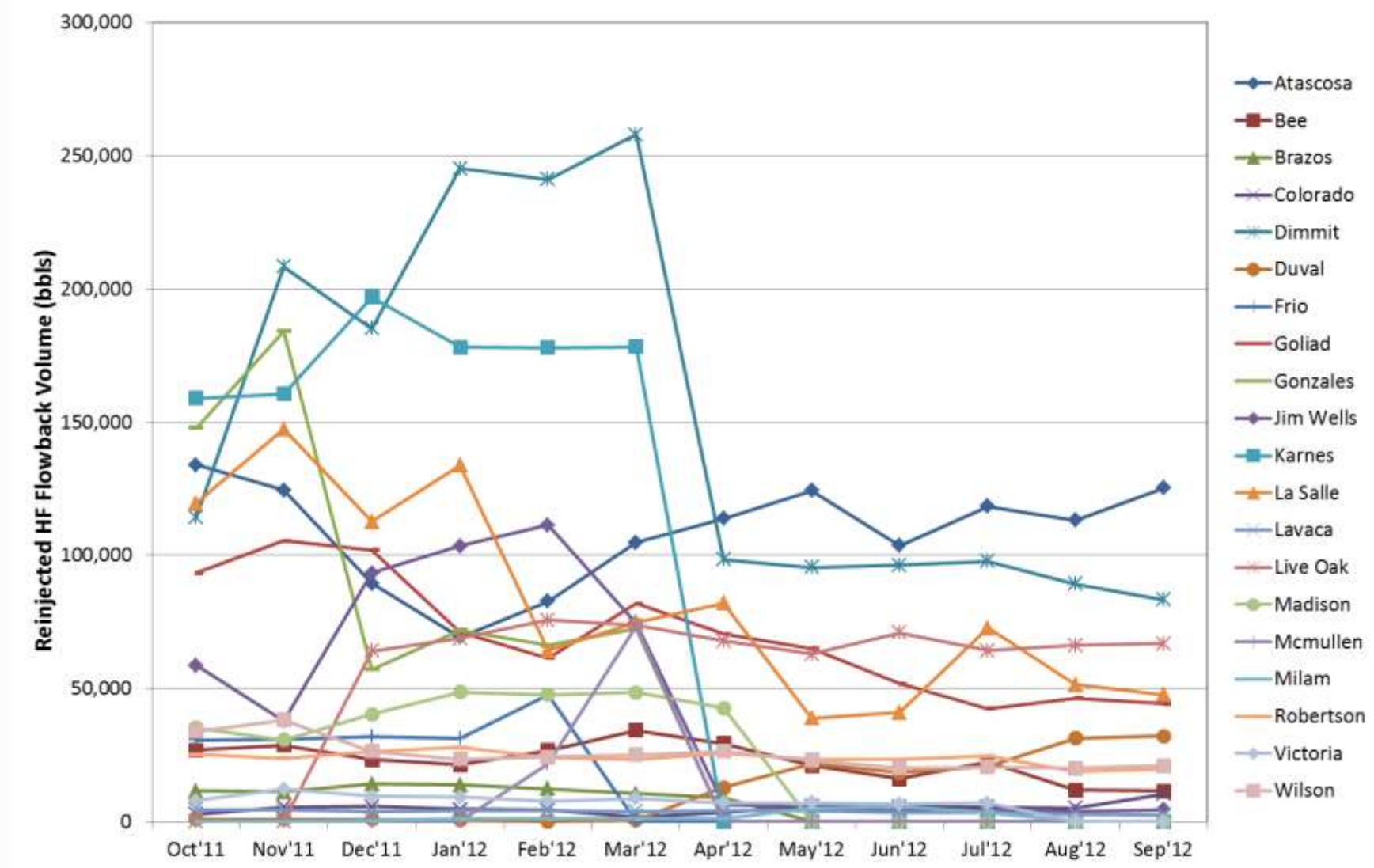

Source: RRC website (February 2013)
Note: 1 AF = 7758 bbls

RRCstuff_JP.xls

Figure 144. Reported county-level monthly HF flowback injected for disposal

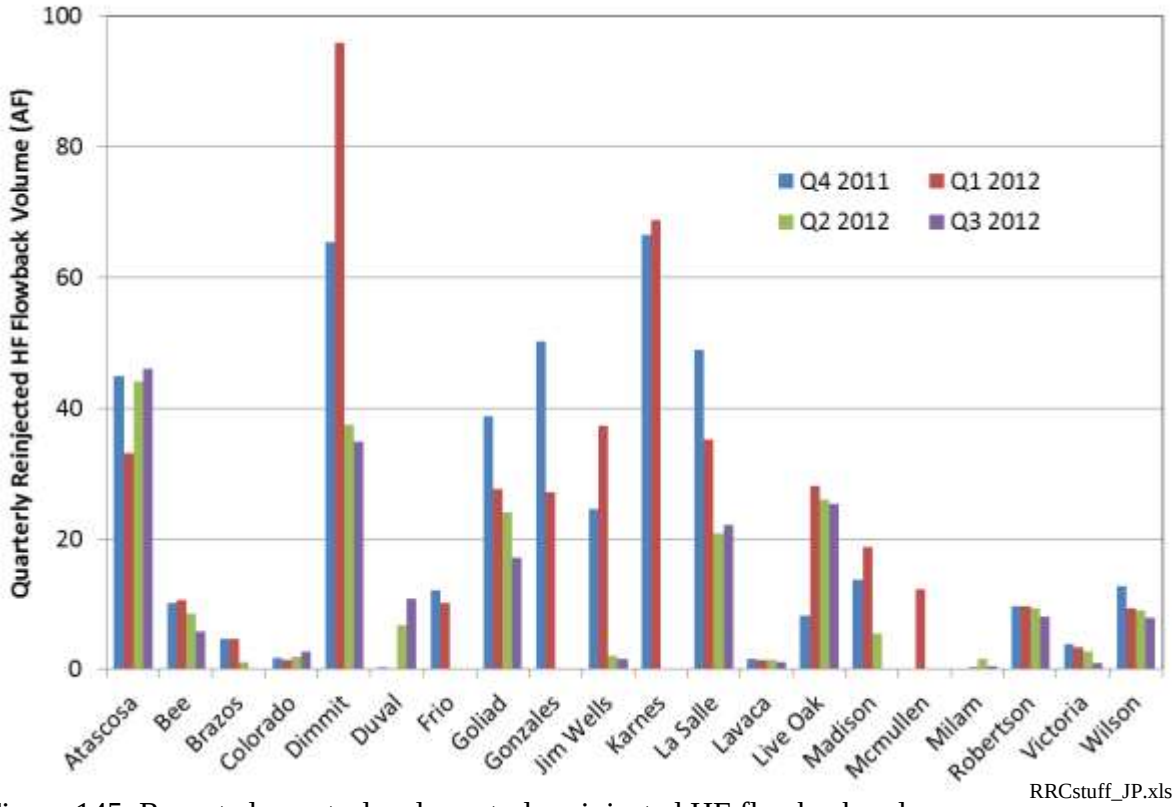

Figure 145. Reported county-level quarterly reinjected HF flowback volume

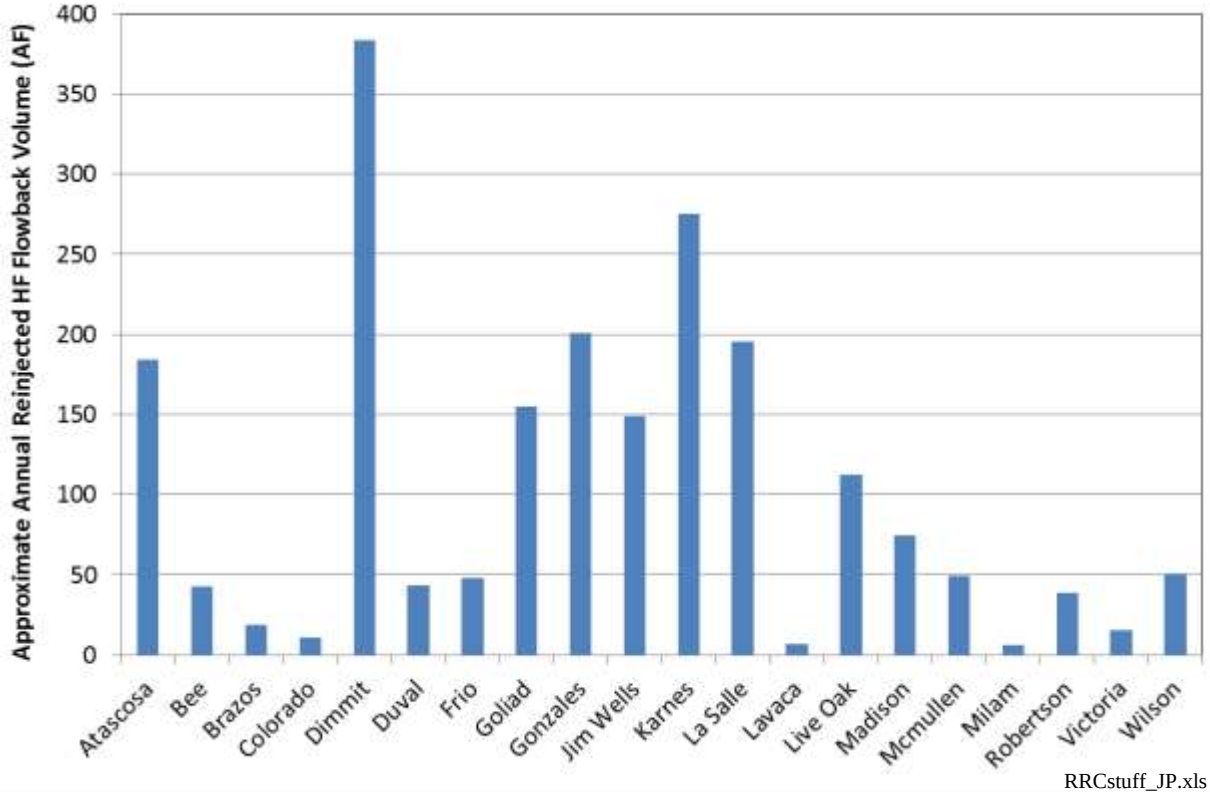

Figure 146. Approximate county-level annual reinjected HF flowback volume

VII. References

Ambrose, W. A., C. Breton, S. D. Hovorka, I. J. Duncan, G. Gülen, M. H. Holtz, and V. Núñez-López, 2010, Geologic and infrastructure factors for delineating areas for clean coal: examples in Texas, USA: Environmental Earth Sciences, 63(3), p.513-532

Ashworth, J.B. and J. Hopkins, 1995, Aquifers of Texas, Texas Water Development Board report #345.

Asquith, W. H., and M. C. Roussel, 2004, Atlas of depth-duration frequency of precipitation annual maxima for Texas: U.S. Geological Survey Scientific Investigation Report 2004-5041, 114 p.

Ayers, W.B., Jr., and Lewis, A.H., 1985, The Wilcox Group and Carrizo Sand (Paleogene) in east-central Texas: depositional systems and deep-basin lignite: The University of Texas at Austin, Bureau of Economic Geology Special Publication, 19 p., 30 plates

Baker, E. T., 1979, Stratigraphic and hydrogeologic framework of part of the Coastal Plain of Texas: Texas Department of Water Resources, Austin, Texas Report No. 236, 43 p.

Baker, E. T., Jr., 1986, Hydrology of the Jasper aquifer in the southeast Texas Coastal Plain: Texas Water Development Board, Austin, Texas Report 295, 64 p.

Baker, E. T., Jr., 1995, Stratigraphic nomenclature and geologic sections of the gulf coastal plain of Texas: U.S. Geological Survey Open-File Report 94-461, 34 p.

Bebout, D.G. and R.G. Loucks, 1974, Stuart City trend, Lower Cretaceous, south Texas: University of Texas at Austin, Bureau of Economic Geology, Report of Investigations #78.

Bebout, D.G., D.A. Budd, and R.A. Schatzinger, 1981, Depositional and diagenetic history of the Sligo and Hosston Formations (Lower Cretaceous) in South Texas, The University of Texas at Austin Bureau of Economic Geology Report of Investigations #109, 70p.

Bebout, D.G., B.R. Weise, A.R. Gregory, and M.B. Edwards, 1982. Wilcox Sandstone reservoirs in the deep subsurface along the Texas Gulf Coast; their potential for production of geopressured geothermal energy: The University of Texas at Austin, Bureau of Economic Geology Report of Investigations No. 117, 125 p.

Bornhauser, M. A., 1979, Subsurface Stratigraphy of the Midway-Wilcox, Zapata County, Texas, Gulf Coast Association of Geological Societies Transactions, 29, p.29-34.

Budd, D. A. and R. G. Loucks, 1982, Smackover and Lower Buckner Formations South Texas: Depositional Systems on a Jurassic Carbonate Ramp, The University of Texas at Austin Bureau of Economic Geology Report of Investigations #112, 38p.

Byerly, G. R., 1991, Nature of igneous activity, *in* A. Salvador, editor, The Gulf of Mexico basin: Boulder, Colorado, The Geology of North America, Geological Society of America, v. J., p. 91-108.

Chowdhury, A. H., S. Wade, R. E. Mace, and C. Ridgeway, 2004, Groundwater Availability Model of the Central Gulf Coast Aquifer System: Numerical Simulations through 1999, Texas Water Development Board, Austin, TX, 108p.

Chowdhury, A. H., and M. J. Turco, 2006, Geology of the Gulf Coast aquifer, Texas, *in* R. E. Mace, S. C. Davidson, E. S. Angle, and W. F. Mullican (eds.), Aquifers of the gulf coast of Texas: Texas Water Development Board, Report 365, p. 23-50.

Core Laboratories Inc.,1972, A survey of the subsurface saline water of Texas. Texas Water Development Board Report 157.

Cusack, C., J. Beeson, D. Stoneburner, and G. Robertson, 2010, The discovery, reservoir attributes, and significance of the Hawkville Field and Eagle Ford Shale trend, Texas: Gulf Coast Association of Geological Societies Transactions, v. 60, p. 165-179.

Deeds, E., V. Kelley, D. Fryar, T. Jones, A. J. Whallon, and K. E. Dean, 2003, Groundwater Availability Model for the Southern Carrizo-Wilcox Aquifer: Intera, Austin, TX, final report prepared for the Texas Water Development Board, variously paginated

Dutton, A. R., Harden, R., Nicot, J.-P., and O'Rourke, D., 2003, Groundwater availability model for the central part of the Carrizo-Wilcox aquifer in Texas: The University of Texas at Austin, Bureau of Economic Geology, final technical report prepared for Texas Water Development Board, under contract no. 2001-483-378, 295 p. + apps.

Dutton, A. R., Nicot, J.-P., and Kier, K. S., 2006, Hydrologic convergence of hydropressured and geopressured zones, Central Texas, Gulf of Mexico Basin, USA: Hydrogeology Journal, v. 14, p. 859–867.

Dutton, S. P., S. J. Clift, D. S. Hamilton, H. S. Hamlin, T. F. Hentz, W. E. Howard, M. S. Akhter, and S. E. Laubach, 1993, Major low-permeability sandstone gas reservoirs in the continental United States, The University of Texas at Austin Bureau of Economic Geology Report of Investigations No. 211, 221p.

EIA (Energy Information Administration), 1993, Drilling Sideways -- A Review of Horizontal Well Technology and Its Domestic Application, DOE/EIA-TR-0565, 24p.

Enomoto, C. B., K. R. Scott, B. Valentine, P. C. Hackley, K. Dennen, and C. Lohr, 2012, Preliminary evaluation of the shale gas prospectivity of the Lower Cretaceous Pearsall Formation in the onshore Gulf Coast region, United States: Gulf Coast Association of Geological Societies Transactions, v. 62, p. 93–115.

Ewing, T. E., 1991, The tectonic framework of Texas: The University of Texas at Austin. Bureau of Economic Geology, 36 p.

Ewing, T. E., 2010, Pre-Pearsall geology and exploration plays in South Texas: Gulf Coast Association of Geological Societies Transactions, v. 60, p. 241-260.

Fan, L., R. Martin, J. Thompson, K. Atwood, J. Robinson, and G. Lindsay, 2011, An Integrated Approach for Understanding Oil and Gas Reserves Potential in Eagle Ford Shale Formation: SPE 148751.

Fisher, W. L., 1969, Facies Characterization of Gulf Coast Basin Delta Systems, with Some Holocene Analogues, Gulf Coast Association of Geological Societies Transactions, Vol.19, p.239-261

Fisher, W. L. and J. H. McGowen, 1967, Depositional systems of the Wilcox Group of Texas and their relationship to occurrence of oil and gas: Gulf Coast Association of Geological Societies Transactions, 17, p. 105-125.

Fisher, W. L., C. V. Proctor, W. E. Galloway, and J. S. Nagle, 1970, Depositional systems in the Jackson Group of Texas-Their relationship to oil, gas, and uranium: Gulf Coast Association of Geological Societies Transactions, 20, p. 234-261.

Galloway, W. E., 1977, Catahoula Formation of the Texas coastal plain: depositional systems, composition, structural development, ground-water flow history, and uranium deposition: The University of Texas at Austin, Bureau of Economic Geology Report of Investigations No. 87, 59p.

Galloway, W. E., 1982a. Epigenetic zonation and fluid flow history of uranium-bearing fluvial aquifer systems, south Texas uranium province: The University of Texas at Austin, Bureau of Economic Geology Report of Investigations No. 119, 31 p.

Galloway, W. E., C. D. Henry, and G. E. Smith, 1982a, Depositional framework, hydrostratigraphy, and uranium mineralization of the Oakville sandstone (Miocene), Texas coastal plain: The University of Texas at Austin, Bureau of Economic Geology Report of Investigations No. 113, 51 p.

Galloway, W. E., 1982b, Depositional architecture of Cenozoic Gulf Coastal Plain fluvial systems: The University of Texas at Austin, Bureau of Economic Geology, Geological Circular 82-5, 29 p. Reprinted from SEPM Special Publications 31, *Recent and ancient non-marine depositional environments: Models for exploration,* August 1981.

Galloway, W. E., D. K. Hobday, and K. Magara, 1982c, Frio Formation of Texas Gulf Coastal-Plain—Depositional systems, structural framework, and hydrocarbon distribution: AAPG Bulletin, 66, p. 649-688.

Galloway, W. E., Ewing, T. E., Garrett C. M., Jr., Tyler N., and Bebout, D. G., 1983, Atlas of Major Texas Oil Reservoirs: The University of Texas at Austin, Bureau of Economic Geology, 139 p.

Galloway, W. E., and D. K. Hobday, 1996, Terrigenous clastic depositional systems: Springer, 2nd edition, 489 p.

Galloway, W. E., P. E. Ganey-Curry, X. Li, and R. T. Buffler, 2000, Cenozoic depositional history of the Gulf of Mexico basin: AAPG Bulletin, 84, p. 1743-1774.

George, P.G., R.E. Mace, and R. Petrossian, 2011, Aquifers of Texas, Texas Water Development Board report #380, 172p.

Griffith, G.E., Bryce, S.A., Omernik, J.M., Comstock, J.A., Rogers, A.C., Harrison, B., Hatch, S.L., and Bezanson, D., 2004, Ecoregions of Texas (color poster with map, descriptive text, and photographs): Reston, Virginia, U.S. Geological Survey (map scale 1:2,500,000).

Guevara, E.H., and R. Garcia, 1972. "Depositional systems and oil-gas reservoirs in the Queen City Formation (Eocene), Texas". Gulf Coast Association of Geological Societies Transactions, Volume 22.

Hamlin, H. S., 1988, Depositional and Ground-Water Flow Systems of the Carrizo-Upper Wilcox, South Texas, The University of Texas at Austin Bureau of Economic Geology Report of Investigations #175, 61p.

Harbor, R. L., 2011, Facies Characterization and Stratigraphic Architecture of Organic-Rich Mudrocks, Upper Cretaceous Eagle Ford Formation, South Texas; M.S. Thesis, University of Texas at Austin, Austin, TX, 184p.

Harden, R.W. & Associates, 2004, Northern Trinity / Woodbine Aquifer Groundwater Availability Model: report prepared for the Texas Water Development Board, variously paginated. & Associates, 2004, Northern Trinity / Woodbine Aquifer Groundwater Availability Model: report prepared for the Texas Water Development Board, variously paginated.

Hentz, T. F., and S. C. Ruppel, 2010, Regional lithostratigraphy of the Eagle Ford Shale: Maverick Basin to East Texas Basin: Gulf Coast Association of Geological Societies Transactions, v. 60, p. 325-337

Hershfield, D. M., 1961, Rainfall frequency atlas of the United States for durations from 30 minutes to 24 hours and return periods from 1 to 100 years: Weather Bureau, U.S. Department of Commerce, Technical Paper 40, 61p., http://hdsc.nws.noaa.gov/hdsc/pfds/other/tx_pfds.html, last accessed April 2009.

Hovorka, S.D., A.R. Dutton, S.C. Ruppel, and J.S. Yeh, 1996, Edwards Aquifer Ground-Water Resources: Geologic Controls on Porosity Development in Platform Carbonates, South Texas, The University of Texas at Austin Bureau of Economic Geology Report of Investigations #238, 75p.

Hovorka, S. D., R. E. Mace, and E. W. Collins, 1998, Permeability Structure of the Edwards Aquifer, South Texas—Implications for aquifer management, The University of Texas at Austin Bureau of Economic Geology Report of Investigations #250, 55p.

Hosman, R. L., and Weiss, J. S., 1991, Geohydrologic units of the Mississippi Embayment and Texas Coastal uplands aquifer systems, South-Central United States—regional aquifer system analysis—Gulf Coastal Plain: U.S. Geological Survey Professional Paper 1416-B, 19 p.

Huang, Y., Scanlon, B. R., Nicot, J.-P., Reedy, R. C., Dutton, A. R., Kelley, V. A., and Deeds, Neil, 2012, Sources of groundwater pumpage in a layered aquifer system in the Upper Gulf Coastal Plain, USA: Hydrology Journal, v. 20, p. 783–796.

Hull, D.C., 2011, Stratigraphic Architecture, Depositional Systems, and Reservoir Characteristics of the Pearsall Shale-Gas System, Lower Cretaceous, South Texas, M.S. Thesis, The University of Texas at Austin, 192p.

Jones, I. C., 2003, Groundwater Availability Modeling: Northern Segment of the Edwards Aquifer, Texas, Texas Water Development Board Report #358, 75p.

Kelley, V. A., Deeds, N. E., Fryar, D. G., and Nicot, J.-P., 2004, Groundwater availability model for the Queen City and Sparta aquifers: final report prepared for the Texas Water Development Board: INTERA, Inc., Austin, Texas, final report prepared for the Texas Water Development Board, variously paginated

Knox, P. R., V. A. Kelley, A. Vreugdenhil, N. Deeds, and S. Seni, 2007, Structure of the Yegua-Jackson aquifer of the Texas Gulf Coast Plain: Intera, Inc., Austin, Texas, report prepared for the Texas Water Development Board, variously paginated.

Kosters, E. C., Bebout, D. G., Seni, S. J., Garrett, C. M. Jr., Brown, L. F. Jr., Hamlin, H. S., Dutton, S. P., Ruppel, S. C., Finley, R. J., and Tyler, N., 1989. Atlas of Major Texas Gas Reservoirs. University of Texas at Austin, Bureau of Economic Geology Atlas AT0001, 161p.

Kreitler, C.W., 1989. Hydrogeology of sedimentary basins. Journal of Hydrology, 106, p.29-53.

Lanning-Rush, J., W. H. Asquith, and R. M. Slade, Jr., 1998, Extreme precipitation depths for Texas, excluding the Trans-Pecos region: U.S. Geological Survey Water Resources Investigation Report 98-4099, 38 p.

Larkin, T.J., Bomar, G.W., 1983, Climatic Atlas of Texas, Texas Department of Water Resources, pp. 151.

LBG-Guyton & Associates, 2003, Brackish groundwater manual for Texas Regional Water Planning Groups: Report prepared for the Texas Water Development Board, Austin, Texas, 188 p.

Loucks, R.G., 1977, Porosity development and distribution in shoal-water carbonate complexes – Subsurface Pearsall Formation (Lower Cretaceous), South Texas, *in* Cretaceous Carbonates of Texas and Mexico: Applications to Subsurface Exploration D. G. Bebout and R. G. Loucks Editors, The University of Texas at Austin Bureau of Economic Geology Report of Investigations #89, 322 p.

Loucks, R. G., 2002, Controls on Reservoir Quality in Platform-Interior Limestones Around the Gulf of Mexico: Example from the Lower Cretaceous Pearsall Formation in South Texas, Gulf Coast Association of Geological Societies Transactions (GCAGS), 52, p.659-672.

Lindgren, R.J., A.R. Dutton, S.D. Hovorka, S.R.H. Worthington, and Scott Painter, 2004, Conceptualization and Simulation of the Edwards Aquifer, San Antonio Region, Texas, U.S. Geological Survey Scientific Investigations Report 2004–5277, 143p. + plates

Mace, R. E., A. H. Chowdhury, R. Anaya, and S.-C. Way, 2000, Groundwater Availability of the Trinity Aquifer, Hill Country Area, Texas: Numerical Simulations through 2050, Texas Water Development Board, Asuti, TX Report #353, 117p.

McCoy, T. W., 1990, Evaluation of groundwater resources in the Lower Rio Grande Valley, Texas: Texas Water Development Board, Report 316, 47 p.

McMahon, P.B., T.K. Cowdery, F.H. Chapelle, and B.C. Jurgens, 2009, Redox Conditions in Selected Principal Aquifers of the United States, National Water-Quality Assessment Program, U.S. Geological Survey Fact sheet 2009–3041, 6p.

Meckel, III, L.D., and Galloway, W.E., 1996, Formation of high-frequency sequences and their bounding surfaces; Case study of the Eocene Yegua Formation, Texas Gulf Coast, USA: Sedimentary Geology, v. 102, p. 155-187

Mullen, J., 2010. Petrophysical characterization of the Eagle Ford Shale in South Texas, SPE #138145, 19p.

NCDC (National Climatic Data Center, operated by NOAA), 2009, Heavy rainfall frequencies for the U.S., http://www.ncdc.noaa.gov/oa/documentlibrary/rainfall.html, last accessed February 2010.

Nicot, J.-P., Scanlon, B. R., Yang, C., and Gates, J., 2010, Geological and geographical attributes of the South Texas Uranium Province: The University of Texas at Austin, Bureau of Economic Geology, contract report prepared for the Texas Commission on Environmental Quality, 156 p.

Nicot, J.-P., Hebel, A. K., Ritter, S. M., Walden, S., Baier, R., Galusky, P., Beach, J. A., Kyle, R., Symank, L., and Breton, C., 2011, Current and projected water use in the Texas mining and oil and gas industry: The University of Texas at Austin, Bureau of Economic Geology, Contract Report prepared for Texas Water Development Board, 357 p. https://www.twdb.texas.gov/publications/reports/contracted_reports/doc/0904830939_MiningWaterUse.pdf

Nicot, J.-P., and Duncan, I. J., 2012, Common attributes of hydraulically fractured oil and gas production and CO_2 geological sequestration: Greenhouse Gases Science and Technology, v. 2, p. 352–368.

Nicot, J.-P. and B. R. Scanlon, 2012, Water Use for Shale-Gas Production in Texas, U.S., Environmental Science & Technology, 46 (6), p.3580-3586

Nicot, J.-P., R. C. Reedy, R. A. Costley, and Y. Huang, 2012, Oil & Gas Water Use in Texas: Update to the 2011 Mining Water Use Report: Bureau of Economic Geology, Contract Report to Texas Oil and Gas Association, Austin, TX, September 2012, 97p. http://www.twdb.texas.gov/waterplanning/rwp/planningdocu/2016/doc/current_docs/project_docs/201209FinalReport__O&GWaterUse.pdf

Nicot, J.-P., 2012, Current and Future Water Demand of the Texas Oil and Gas and Mining Sectors and Potential Impact on Aquifers, GCAGS Journal,1, p.145-161

Nicot, J.-P., 2013, Hydraulic fracturing and water resources: a Texas study, Gulf Coast Association of Geological Societies Transactions, 63

Pollastro, R.M., R.J. Hill, D.M. Jarvie, and M.E. Henry, 2003, Assessing undiscovered resources of the Barnett-Paleozoic Total Petroleum System, Bend Arch-Fort Worth Province, Texas, in AAPG Southwest Section Convention, Fort Worth, Texas, March 1–5.

Reedy, R. C., Nicot, J. -P., Scanlon, B. R., Deeds, N. E., Kelley, V. A., and Mace, R. E., 2009, Chapter 11. Groundwater recharge in the Carrizo-Wilcox aquifer, in Aquifers of the upper coastal plains of Texas: Texas Water Development Board Report 374, p. 185–203.

Ricoy, J.U., and L.F. Brown, Jr., 1977. Depositional Systems in the Sparta Formation (Eocene) Gulf Coast Basin of Texas. Gulf Coast Association of Geological Societies Transactions, Volume 27, p. 139-154.

Roy, E. C., 1984, Stratigraphy and Sedimentology of the Kincaid Formation, Midway Group (Paleocene), Upper Rio Grande Embayment, Texas, Gulf Coast Association of Geological Societies Transactions, 34, p.211-216

Ryder, P. D. and Ardis, A. F., 1991, Hydrology of the Texas Gulf Coast aquifer systems, U.S. Geological Survey Open-File Report: 91-64, 147p.

Ryder, P. D., and A. F. Ardis, 2002, Hydrology of the Texas gulf coast aquifer systems: U.S. Geological Survey Professional Paper 1416-E, 77 p.

Scanlon, B.R., R. E. Mace*, B. Smith**, S. Hovorka, A.R. Dutton, and R.t Reedy, 2001, Groundwater availability of the Barton Springs segment of the Edwards aquifer, Texas:

numerical simulations through 2050: University of Texas at Austin, Bureau of Economic Geology, prepared for Lower Colorado River Authority, 36p. appendices

Scott, R. J., 1977, The Austin Chalk-Buda Trend of South Texas, Gulf Coast Association of Geological Societies Transactions, 27, p. 164-168

Scott, R. J., 2004, The Maverick Basin: New Technology - New Success, Gulf Coast Association of Geological Societies Transactions (GCAGS), 54, p.603-620.

Senger, R. K. and C. W. Kreitler, 1984, Hydrogeology of the Edwards Aquifer, Austin Area, Central Texas, The University of Texas at Austin Bureau of Economic Geology Report of Investigations #141, 35p.

Smith, R.,2004, Paleozoic aquifers of the Llano Uplift, *in* Aquifers of the Edwards Plateau, edited by R. E. Mace, E. S. Angle and W. F. Mullican, 366p., Texas Water Development Board, Austin, Texas, Report #360, p181-200.

TPWD (Texas Parks and Wildlife Department), Plant guidance by ecoregions: Ecoregion 6, http://www.tpwd.state.tx.us/huntwild/wild/wildscapes/guidance/plants/ecoregions/ecoregion_6.phtml, last accessed February 2010.

Tyler, N. and W.A. Ambrose, 1986, Depositional systems and oil and gas plays in the Cretaceous Olmos Formation, South Texas, The University of Texas at Austin Bureau of Economic Geology Report of Investigations #152, 42p.

Vassilellis, G. D., C. Li, R. Seager, and D. Moos, 2010, Investigating the expected long-term performance of shale reservoirs: Society of Petroleum Engineers, SPE paper #138134.

Veil, J. A. and C.E. Clark, 2010, Produced Water Volume Estimates and Management Practices, SPE #125999, 8p.

Weise, B.R., 1980, Wave-dominated delta systems of the Upper Cretaceous San Miguel Formation, Maverick Basin, South Texas, The University of Texas at Austin Bureau of Economic Geology Report of Investigations #107, 39p.

Williamson, A. K., and Grubb, H. F., 2001, Groundwater flow in the Gulf Coast aquifer systems, Regional aquifer system analysis—Gulf Coastal Plain: U.S. Geological Survey Professional Paper 1416-F, 173 p.

Xue, L., and Galloway, W. E., 1995, High-resolution depositional framework of the Paleocene middle Wilcox strata, Texas coastal plain: American Association of Petroleum Geologists Bulletin, v. 79, no. 2, p. 205–230.

VIII. Appendix A: Dataset

Many of the figures presented in this document were created in an ArcGIS software environment. We provide alongside this report a data set with the following geodatabase contents:

1. Aquifer_Major_TWDB - The 21 minor aquifers of Texas as defined by the TWDB, Updated December 2006 (Figure 67)
2. Aquifer_Minor_TWDB - The 21 minor aquifers of Texas as defined by the TWDB, Updated December 2006 (Figure 68)
3. Austin_Chalk_Outcrop- The Austin Chalk outcrop extracted from the Geologic Atlas of Texas (Figure 2 and many others)
4. EagleFordBase - Eagle Ford base elevation in feet (Figure 62)
5. EagleFordBoundaries - An estimate of the Eagle Ford Play boundaries (Figure 2 and many others)
6. EagleFordOGWells - Eagle Ford Producing Oil and Gas wells (Figure 65 and Figure 66)
7. EagleFordOutcrop- The Eagle Ford outcrop extracted from the Geologic Atlas of Texas (Figure 2 and many others)
8. EagleFordTopcontours- Eagle Ford top elevation in feet (Figure 61)
9. EF_Thickness_ft – Eagle Ford thickness in feet (Figure 60)
10. Eftwdbwells- Water Wells in Study Area (Figure 76, Figure 77, Figure 78)
11. FaultTraces- Approximate location of fault zones (not necessarily all faults) in south and central Texas (Figure 63)
12. GasReservoirs-Major Gas Reservoirs (Figure 100 and Figure 101)
13. GATeagleFord – The Geology of the Eagle Ford area extracted from Geologic Atlas of Texas (Figure 29)
14. Gross_Lake_Annual_Evaporation- This dataset contains the Gross and Net Annual Evaporation of Texas in inches (Figure 19 and Figure 20)
15. Groundwater_Conservation_District-Texas Groundwater Conservation Districts (Figure 5)
16. Groundwater_mgmt_areas- Texas Groundwater Management Areas (Figure 7)
17. InjectionWellslocation- Injection Wells in the study area (Figure 127 and Figure 129 to Figure 143)
18. Natural_Regions- Generalized locations of the natural regions of Texas (Figure 21)
19. NonEFwellsinstudyarea - Non-Eagle Ford Oil and Gas wells (Figure 102, Figure 103, Figure 104, Figure 105, Figure 106, Figure 107, and Figure 108)
20. OilReservoirs – Major Oil Reservoirs (Figure 100 and Figure 101)
21. Population_2010- Population Density for Census Tracks in Texas (Figure 3)

22. Regional_Water_Planning_Groups - The 16 Water Planning Regions in Texas, as created by TWDB, updated March 2008 (Figure 6)
23. River_Basins- This dataset represents the boundaries for the river basins of Texas (Figure 11)
24. Rivers- Major Rivers for the National Hydrography Dataset (Figure 11)
25. Tx_eco_I3- Texas Ecoregions. At Level III, the continental United States contains 105 regions (Figure 22)
26. Tx_eco_I4- Texas Ecoregions. Level IV ecoregions are further subdivisions of Level III ecoregions (Figure 22)
27. TxDot_Roadways_State- TxDOT's GIS linework for State Maintained Highways, County Roads and Functionally Classified City Streets (Figure 4)
28. US_Counties_Generalized – US counties (Figure 2 and many others)
29. US_States_Generalized – US states (Figure 2 and many others)
30. Weather_Stations - Weather Stations of South Texas from the National Center for Atmospheric Research (Figure 12)
31. yr_1h_rainfall - Max Precipitation contour line 1 hr rainfall (Figure 15)
32. yr_24h_rainfall - Max Precipitation contour line 24 hr rainfall (Figure 15)
33. yr_2h_rainfall - Max Precipitation contour line 2 hr rainfall (Figure 15)
34. yr_30min_rainfall - Max Precipitation contour line 30 min rainfall (Figure 15)
35. yr_6h_rainfall - Max Precipitation contour line 6 hr rainfall (Figure 15)

We did not provide DEM/elevation coverage (Figure 9 and Figure 10), precipitation and temperature coverages (Figure 13, Figure 14, Figure 16, Figure 17, and Figure 18), and land use coverage (Figure 23). Their size is prohibitively large. However links to the source is provided in the caption of the figures. We also limited chemical information on water wells to the TDS and did not include ionic make up (Figure 80 to Figure 98). Links to the TWDB database are provided.

Relative to Eagle Ford wells, all other oil and gas wells, and injection wells, we provided only locations and not the individual data presented on the various plots and figures. Most of the information, although in the public domain but hard to collect, came from the private IHS database and cannot be released as such.